San Bernardino County Museum Association
Special Publication
Volume 93-1, MDQRC 1993

Ashes, Faults and Basins

San Bernardino County Museum Association 93-1
prepared in conjunction with the
1993 Desert Research Symposium
May 21-24, 1993

REYNOLDS, R.E. & J. REYNOLDS (EDITORS).
ASHES, FAULTS AND BASINS.
SPECIAL PUBLICATION 93-1, MDQRC 1993

2024 ORANGE TREE LANE, REDLANDS CA 92374

Cover photograph: Native palm trees at Willis Palms Oasis. Mt. San Jacinto is barely visible in distance, its snow-capped peak dimmed by wind-blown sand in San Gorgonio Pass. Palms are growing along the trace of the Banning fault, where water rises near the surface. photograph by jennifer reynolds.
PHOTOGRAPHS IN THIS VOLUME ARE BY THE RESPECTIVE AUTHORS, UNLESS OTHERWISE NOTED.

Ashes, Faults and Basins

San Bernardino County Museum Association Special Publication 93-1
Robert E. Reynolds & Jennifer Reynolds, editors

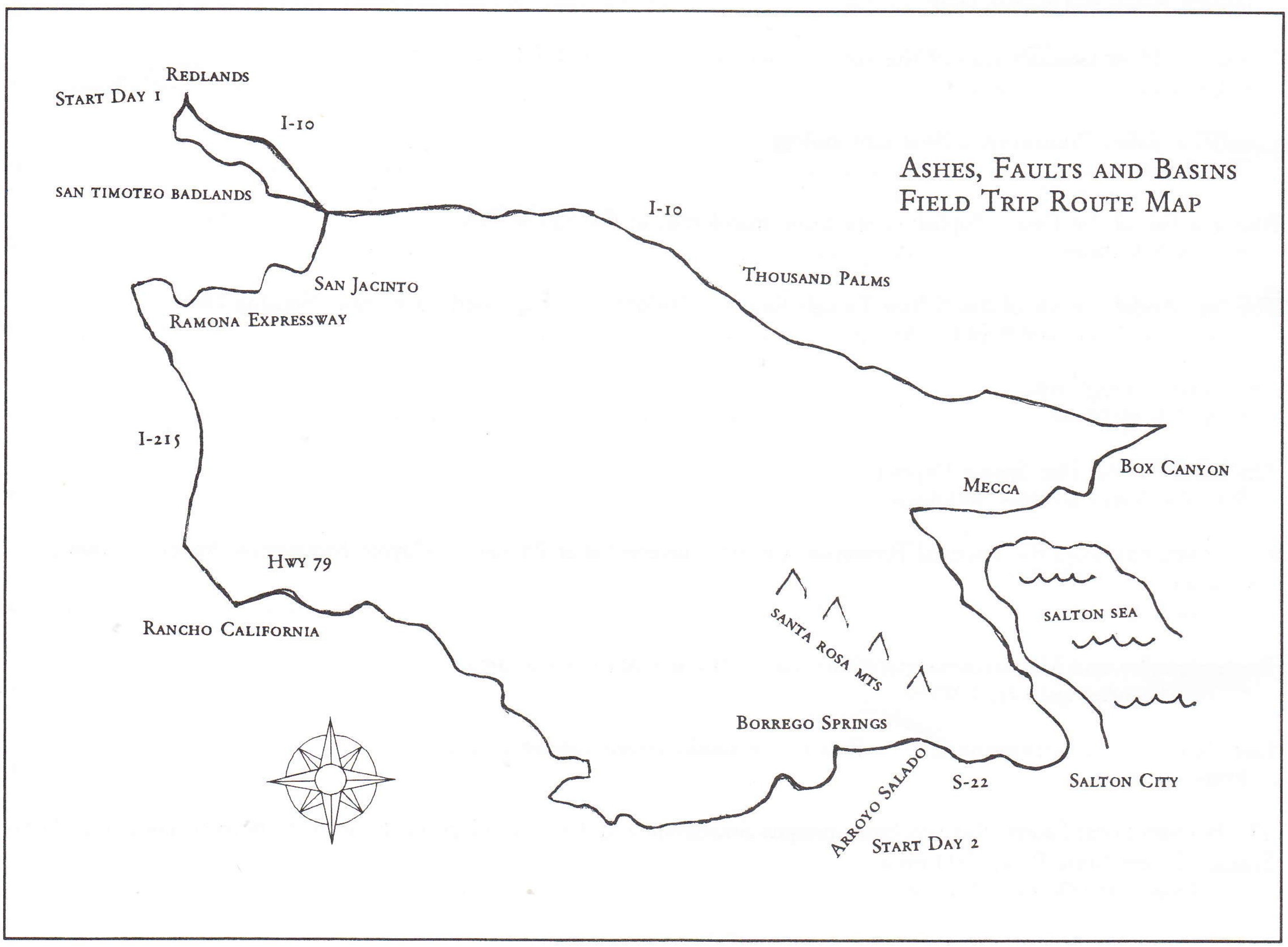
Ashes, Faults and Basins
Field Trip Route Map
Redlands
Start Day 1
I-10
San Timoteo Badlands
I-10
Thousand Palms
San Jacinto
Ramona Expressway
I-215
Box Canyon
Mecca
Hwy 79
Rancho California
Santa Rosa Mts
Salton Sea
Borrego Springs
Arroyo Salado
S-22
Salton City
Start Day 2

ASHES, FAULTS AND BASINS

The 1993 Mojave Desert Quaternary Research Center Field Trip

ROBERT E. REYNOLDS *San Bernardino County Museum, Redlands CA 92374;*
PAUL REMEIKA *Anza-Borrego State Park, Borrego Springs CA 92004*

This trip will take us from the San Bernardino Valley east and south to both sides of the Salton Trough, then west through Anza-Borrego Desert State Park and over the Santa Rosa Mountains to the Murrieta area, then north through the San Timoteo Badlands and back into the San Bernardino Valley. We will explore basins between three of the major fault zones in southern California. We will see how tectonic activity has affected the geographic and ecologic evolution of these basins and their surrounding mountain ranges. We will see how the dates of sedimentary deposition in the basins can be determined by stratigraphic occurrences of the Bishop Ash and by Plio-Pleistocene faunas.

DAY 1

0.0 (0.0) START at the San Bernardino County Museum, 2024 Orange Tree Lane, Redlands. TURN RIGHT from parking lot entrance onto Orange Tree Lane and proceed to California Street.

0.2 (0.2) TURN LEFT at the stop sign onto California Street.

San Andreas Fault Segment

This portion of the San Andreas fault system marks the boundary between the Transverse Range Province and the Peninsular Range Province. The right lateral San Andreas fault system is joined by the San Jacinto fault to the south. These faults control the local geography and topography. We will be driving parallel to various components of the San Andreas system as we go southeast toward Palm Springs and Indio (Crowell, 1975, 1992; Matti and others, 1992; Sieh and Matti, 1992).

0.4 (0.2) TURN LEFT onto Interstate 10 East, heading east toward Yucaipa and Palm Springs. Ahead you can see Yucaipa Ridge and San Bernardino Peak (elevation 10,525'). Yucaipa Ridge sits between the north branch (Mill Creek strand) and south branch (San Bernardino strand) of the San Andreas fault. The Wilson Creek fault (Matti and others, 1983 and 1985) crosses Yucaipa Ridge and separates the San Gabriel basement from basement rocks typical of the San Bernardino Mountains.

San Bernardino Peak and Mt. San Gorgonio are part of a complex of Precambrian biotite gneiss and schist, and granitoid gneiss intruded by Mesozoic quartz monzonite and granodiorite (Morton and others, 1980b). The massif was glaciated during the Pleistocene (Sharp and others, 1959; Dibblee, 1964).

2.3 (1.9) Holocene alluvium is on both sides of the freeway. To the right at about 2:00, Smiley Heights is on a Pleistocene alluvial surface with a Pleistocene soil (Reynolds and Reeder, 1986). This Pleistocene surface will be encountered repeatedly between Yucaipa and Banning.

6.1 (3.8) Reservoir Canyon. Cross the trace of the Crafton fault (Reservoir Canyon fault) offsetting Quaternary alluvium and uplifting Precambrian metamorphic and igneous basement rocks (Rogers, 1967). The Crafton Hills are a faulted complex of upper and lower plate rocks divided by the Vincent Thrust (Morton, pers. comm. to Reynolds, 1986).

6.4 (0.3) Upper plate gneissic quartz diorite exposed in these road cuts, is separated from lower plate Pelona Schist by the Vincent Thrust (Morton, pers. comm. to Reynolds, 1986). On the left, these exposures of the upper plate gneisses include Permo-Triassic Lowe Granodiorite and cataclasites. Pelona Schist is exposed in the road cuts to the left near the top of Reservoir Canyon.

6.8 (0.4) Marked by trees and bushes to the right, Crystal Springs comes to the surface at the fault trace. These springs supported a small bottled water industry in the past. Much of the Yucaipa area was drained through Reservoir Canyon in late Pleistocene times; the drainage was later captured through Live Oak Canyon (Dutcher and Burnham, 1960).

8.1 (1.3) Cross the Western Heights fault, cutting Pleistocene alluvium. This fault, which bounds the Crafton Hills on the southeast, is subparallel to the Redlands fault.

8.6 (0.5) Mount San Jacinto is seen ahead at 12:00; Pisgah Peak (elevation 5,480') is at 10:30. Pisgah Peak is south of the south branch of the San Andreas fault and consists of upper plate granitic and granitoid gneissic rocks overlying the Vincent Thrust. Wilson Creek, northeast of Yucaipa, is the site of studies by Hardin and Matti (1992) that showed offset rates on the San Andreas fault of 9-13 mm/yr.

9.8 (1.2) To the right is deep dissection in the Holocene alluvium overlying eroded Quaternary old alluvium of Live Oak Canyon. The dissection of these recent sediments has occurred since the start of agricultural development in the area, no more than 130 years ago (D. Morton, pers. comm. 1986).

11.2 (1.4) At County Line Road off ramp, we have returned to the Pleistocene surface. Fossiliferous Pleistocene sediments of the San Timoteo formation beneath the Pleistocene surface are located between this off ramp and Calimesa Blvd. off ramp (Dibblee, 1981; Reynolds and Reeder, 1986 and 1991).

14.2 (3.0) Terraces to the right are developed on Pleistocene and Holocene alluvium. The badlands topography is developed in the Plio-Pleistocene San Timoteo formation (Reynolds and Kooser, 1986; Reynolds and Reeder, 1986, 1991).

17.8 (3.6) CONTINUE on Interstate 10. Offramp to I-60 West is on the right.

18.9 (1.1) Beaumont Avenue/Highway 79 exit. Continue on I-10 East.

19.7 (0.8) San Gorgonio Pass is the lowest topographic break in southern California through the mountains to the inland deserts, separating Mt. San Gorgonio (11,502') and Mt. San Jacinto (10,804'), the two highest mountains in southern California. The crest of the pass, although broad and ill-defined, is the complicated junction of three major drainage basins: the interior-draining Whitewater River-Salton Trough to the east via Smith Creek; the generally interior-draining San Jacinto basin to the south via Potrero Creek; and the Santa Ana basin to the west via San Timoteo Canyon.

We leave the Santa Ana basin and cross eastward to the San Jacinto basin. Through rapid headward erosion, Potrero Creek (to the right at 3:00) has progressed northward, extending the northward limit of the

Table I. Sedimentary deposition in four fault zones along the Ashes, Faults & Basins field trip route. Age in millions of years.

ELSINORE FAULT ZONE	N. SAN JACINTO F. Z.	S. SAN JACINTO F.Z.	SAN ANDREAS F.Z.I	AGE
Pauba fm (Kennedy 77)	Qoa (Dibblee 68)	Fonts Pt Sandstone		
			Ocotillo Conglomerate	0.5
x x x x x x x x x x x x	*no deposition*	? ? ? ? ? ? ? ? ? ? ? ?	x Borrego x x x x x	Bishop Ash
				1.0
		Ocotillo fm (Remeika & Jefferson, this volume)		
			Palm Spring fm (Rymer 91, Dibblee 54)	1.5
unnamed sandstone (Kennedy 77, Reynolds et al 91)	San Timoteo fm (Reynolds & Reeder 91; Albright & Woodburne 93)	Palm Spring fm		2.0
		Borrego fm		2.5
				3.0
		Diablo fm		3.5
Temecula Arkose (Mann 55, Reynolds & Reynolds, this volume)			no deposition	
				4.0
	Mt. Eden fm (May & Repenning 82)	Imperial Fm (Remeika & Jefferson, this volume)		
no deposition				
			Painted Hill fm (Matti et al 85)	5.0
				6.0
	no deposition			
Puente fm (Durham & Yerkes 1964, Pajak et al. 1991)			Imperial fm (Murphy 86, Allen 57)	7.0
	? Imperial fm (Reynolds & Reeder, 91)			
				8.0
				9.0
			Coachella Fanglomerate (Allen 57, Peterson 75)	10.0

San Jacinto basin along the crest of the alluvial fan complex essentially to Highland Springs, 2.5 miles north of Interstate 10.

20.5 (0.8) At Highland Springs Avenue we leave the San Jacinto basin and cross eastward into the Whitewater River drainage. The San Bernardino Mountains are on the north and the San Jacinto Mountains of the northern Peninsular Range (Dibblee, 1981) are on the south. The Peninsular Range batholith was emplaced in Cretaceous times over a 40 million year period (Hill, 1981).

21.0 (0.5) At 10:00, the Banning Bench is bounded on the south by an unnamed thrust fault, and capped by the Heights Fanglomerate of Allen (1957). *Bison* remains recovered from the Heights Fanglomerate (Jefferson, 1986) indicate that it is less than 500,000 ybp (Savage and Russell, 1983). From this point eastward to Whitewater, we enter an area dominated by compressional features.

26.4 (5.4) The houses straight ahead are built on a surface cut by dissected thrust fault scarps (Bortugno and Spittler, 1986; Dibblee, 1982). In the hills to the left, the Banning fault has thrust basement rocks over sandstone of the Hathaway formation. In Lion Canyon, the Hathaway fm is conformably overlain by the marine Imperial formation which is in turn conformably overlain by the nonmarine Painted Hill formation. These three formations, Miocene and Pliocene in age, are caught up between thrust faults along the base of the mountain front from this point to Stubbe Canyon (Allen, 1957; Dibblee, 1982).

27.0 (0.6) The Quaternary Cabezon Fanglomerate (lower hills straight ahead) has been anticlinally folded and cut by thrust faults.

27.6 (0.6) To the left, beneath the water tank, is the most youthful thrust fault scarp in this area related to compression associated with activity along the Banning fault. At this point, the scarp changes orientation from a northwest strike to a northeast strike.

28.3 (0.7) Major fans are being shed southward from the San Bernardino Mountains across the Banning fault. These slope south and end at the San Gorgonio River. Only small fans are being shed north in the canyons of the San Jacinto Mountains. Even though Mt. San Jacinto (elevation 10,804') and Mt. San Gorgonio (elevation 11,502') are approximately the same height, the major fans from the north suggest that the San Bernardino Mountains are rising at a more rapid rate than the San Jacintos, although the San Jacinto Mountains have a more precipitous face. Geochemistry of the Peninsular Range pluton is discussed by Gastil and others (1991).

To the left in Millard Canyon; a fault scarp crosses the alluvial fan near the canyon mouth. The debris of the Millard Canyon fan overwhelms debris from Mt. San Jacinto. Drainage to the base of Mt. San Jacinto is thus forced eastward from this point to the Whitewater River.

28.9 (0.6) Cabezon exit. Continue along freeway. To the right, the steep escarpment of the San Jacinto Mountains is interpreted to be the result of uplift on the postulated South Pass fault (Allen, 1957).

31.5 (2.6) Good exposures of the Cabezon Fanglomerate are to the left. Hathaway, Imperial and Painted Hill sediments are thrust over the Cabezon Fanglomerate and are in turn overthrust by the San Gabriel igneous-metamorphic complex. At 11:00, Lion Canyon is bounded on the east by a large landslide. The upper "boundary" of this landslide is in the Cabezon Fanglomerate and, as shown by Allen (1957), is convex and points to the south. This is contrary to a landslide headscarp and, because pressure ridges are also apparent within the landslide, suggests that the feature is the result of "bulldozing" by a larger mass to the north and not simply a slope failure (Matti and others, 1992; Morton and others, 1992). Willingham (1981) discusses thrust relationships of the Banning fault in this area.

32.4 (0.9) To the left at 10:00 at Stubbe Canyon, a thrust in the basement rocks is seen where pink piemontite-bearing rocks are thrust over green epidote-bearing rocks. The distinctive piemontite-bearing gneisses are found as clasts in sediments north and south of the Banning fault. Since the source area is of limited extent, this has proven useful in estimating fault offset as well as identifying source areas and transport directions (Allen, 1957).

34.3 (1.9) Based on geophysical evidence, the ridge of metamorphic rocks (ahead at 12:00 extending from Mt. San Jacinto) continues beneath the alluvium to a point north of the freeway and northward of the southernmost thrusts characteristic of the San Bernardino Mountains' side of the pass. This ridge reduces the energy of the strong winds which are regularly funneled through San Gorgonio Pass, and dune sands are deposited against it (Fig. 1).

36.0 (1.7) Verbenia exit; continue on Interstate 10.

The Banning fault, to the north, is characterized by compressional oblique slip movement and is the site of very deep seismic activity (Morton and others, 1992).

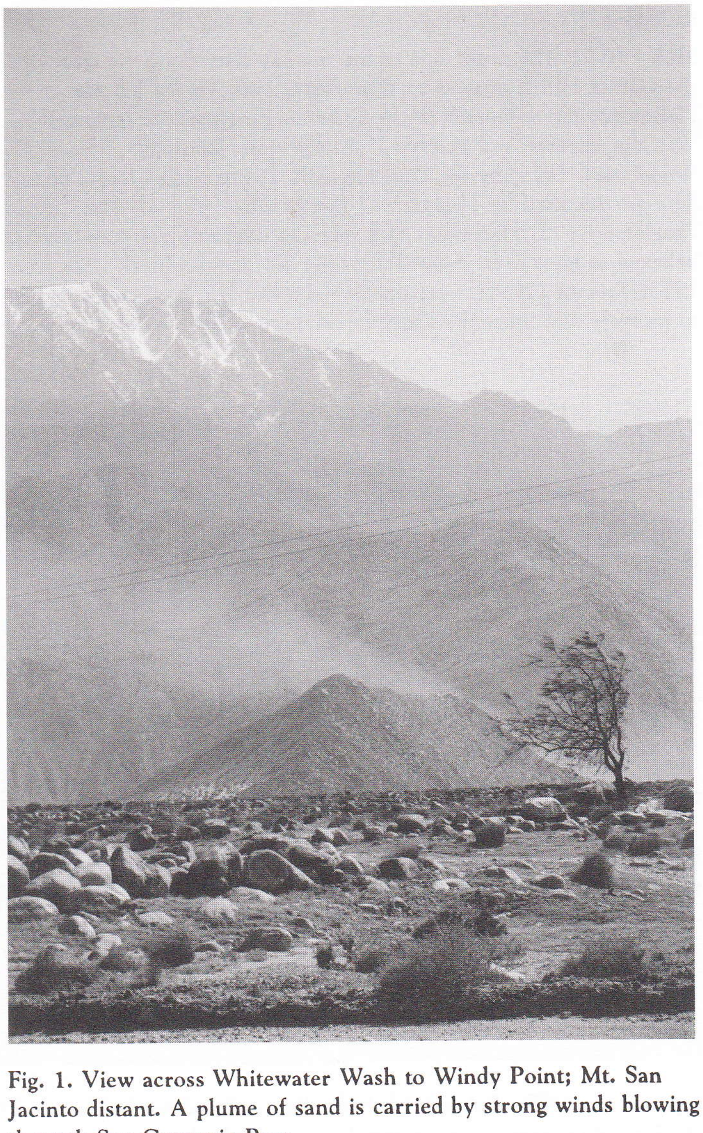

Fig. 1. View across Whitewater Wash to Windy Point; Mt. San Jacinto distant. A plume of sand is carried by strong winds blowing through San Gorgonio Pass.

36.7 (0.7) Highway 111 to Palm Springs passes through the old Whitewater Ranch property. Do not exit. Landslide deposits are to the left.

37.0 (0.3) To the left, the Garnet Hill fault disrupts alluvium 2/3 of the way from the freeway to the base of the hills. The fault runs across the mouth of Whitewater Canyon where it is visible at 9:00. The fault trace is exposed only west of Whitewater River. Based on trenching between Cottonwood and Whitewater Canyons, there is no evidence for Holocene activity on the Garnet Hill fault (Reeder, p.c. 1986, cited in Reynolds and Kooser, 1986). The Garnet Hill fault displaces Pleistocene-age Whitewater gravels of Windmill Hill (Allen, 1957). To the east, its trace is covered by alluvium and the main evidence for its existence within the Coachella Valley is a strong gravity anomaly. Gravity low contours define a trough which is almost as well delineated as the gravity troughs associated with the Banning and Mission Creek faults (Proctor, 1968). Proctor suggests that the Garnet Hill fault may be an ancestral branch of the San Andreas fault.

39.3 (2.3) Cross the Whitewater River. Upstream are exposures of the Coachella Fanglomerate (Peterson, 1975) which underlies the marine Imperial formation. It contains andesite dated at 10 Ma and clasts suggesting a source in the Cargo Muchacho Mountains, about 214 km distant to the southeast. The Coachella Fanglomerate is the oldest sedimentary unit in the Banning portion of the San Andreas fault zone.

39.8 (0.5) The north side of the freeway runs along the trace of the Garnet Hill fault next to Whitewater Hill. To the left are Pleistocene fan sediments of the Cabezon Fanglomerate separated from the Imperial and Painted Hill formations (Murphy, 1986; Woodburne, 1975) by the Banning fault. Fossils whales found near here are discussed by Thomas and Barnes (this volume). The Cabezon Fanglomerate of Whitewater Hill includes a lens of limestone breccia believed to have been derived from the San Jacinto block (Allen, 1957). Proctor (1968) notes that Whitewater Hill has been uplifted so recently that relict drainages exposed on its surface do not conform to its current topography. Paleogeographic reconstructions have been done by Dibblee (1977) and Fritsche (1977a, 1977b).

We are entering the Coachella and Imperial valleys (Elders, 1979, 1985) comprising the Salton trough. The trough is a product of oceanic spreading centers acting on a continental plate (Elders and others, 1970; and see McKibben, this volume). The Salton trough is apparently the northern extension of the East Pacific Rise (Meidav and Rex, 1970), characterized by abnormally high heat flow and earthquake activity (Biehler and Rex, 1971; Grannell, 1985; McKibben, 1991; Meidav and Rex, 1970; Morton and Gray, 1971; Sheehan, 1986).

40.8 (1.0) Pass exit to Morongo Valley, Highway 62. Ground water in the Mission Creek subbasin to the north is discussed by Slade (1981).

42.9 (2.1) Ahead at 1:00, the freeway passes on the north side of Garnet Hill; the Garnet Hill fault passes on the south side of Garnet Hill.

44.5 (1.6) Indian Avenue, North Palm Springs Blvd. Garnet Hill is on the right. Note Palm Canyon fault due south. This linear feature runs NNW-SSE. View south of major peak, San Jacinto Mountains, and other rocks.

47.4 (2.9) Continue past Palm Drive and Gene Autry Trail.

49.4 (2.0) Flat Top Mountain is north of the freeway at 9:00. The Garnet Hill fault is north of the freeway at the base of Flat Top Mountain. The Banning fault is out of sight behind Edom Hill at 10:00.

54.5 (5.1) EXIT at Ramon Road (Bob Hope Drive). Stay in left lane for Thousand Palms.

54.8 (0.3) Stop light. TURN LEFT and continue east along Ramon Road.

54.9 (0.1) Stop sign at off ramp. Continue on Ramon Road.

55.0 (0.1) Stop light at Varner. Continue east on Ramon Road.

55.8 (0.8) Stop sign at Monterey. Continue on Ramon Road.

56.9 (1.1) View north 10:00 of dissected gravels in the Indio Hills on the north side of the Banning fault. Note alignments of palms and mesquite along fault trace.

59.2 (2.3) TURN LEFT at Thousand Palms Canyon Road, and northeast to the base of the hills. Willis Palms oasis is on the left at 10:00. Tan siltstones of the Imperial formation west of palms that contrast with the gray gravels of the Ocotillo Conglomerate (Fig. 2).

59.7 (0.5) Cross the Banning fault at the base of the hills.

59.9 (0.2) STOP 1. Pull right to edge of road. View or walk east across Thousand Palms Wash. The Bishop Ash is exposed in the northeast-dipping gravels at the tip of the hill north of the Banning fault. A varnished, south-sloping fan erosional surface is at 10:00 on the left (west) at an elevation higher than inset terraced canyon gravels adjacent to the road.

61.2 (1.3) TURN LEFT into Thousand Palms Natural Area of the Coachella Valley Preserve.

Fig. 2. Near Willis Palms (right), the light-colored marine Imperial fm is interbedded with the Ocotillo Conglomerate along the Banning fault.

Fig. 3. View from Willis Palms toward Indio Hills (mid ground) and San Bernardino Mountains (snow-capped peaks, distant).

61.3 (0.1) STOP 2. Park in parking lot. This area is under the protection of the Nature Conservency, the Bureau of Land Management, and the Department of Fish and Wildlife. Sediments to the east dip northerly; sediments to the west are flat lying. We are on the trace of the Mission Creek fault. Mesquite mounds, smoke trees, creosote, and willows can be seen around the *Washingtonia* palm oasis and a large dune stabilized by mesquite can be seen to the west. Indian, Horseshoe, Pushawalla and Hidden Palms oases are to the east (Cornett, this volume). RETRACE to pavement.

61.4 (0.1) TURN RIGHT and proceed south on Thousand Palms Road.

63.0 (1.6) STOP 3. Pull over to the right shoulder for a view stop. View toward the San Jacinto Mountains (Dibblee, 1981) to the west and south from the Banning fault. Banning Pass is due west, Edom Hill at 2:00 below Mt. San Gorgonio. Mt. San Jacinto is at 1:00; Chino Canyon Fan and aerial tram is on the north side of Mt. San Jacinto. View at 12:30 towards Cathedral City; note terraces developed at low elevations in range. At 11:00, above Rancho Mirage, Magnesia Canyon runs upslope to a broad surface. Palm Desert is at 11:00. East (left) of Palm Desert is a prominent surface cut by Sheep Canyon and Deep Canyon. On skyline at 11:00 are Santa Rosa Mountain (elevation 8046') and Toro Peak (elevation 8716'). Martinez Mountain (elevation 6548') is at 2:00.

63.4 (0.4) TURN LEFT at stop sign at Thousand Palms Road and Ramon and proceed east on Ramon.

64.9 (1.5) Ramon bends southerly and turns into Washington Street.

66.7 (1.8) Sand dune area.

67.7 (1.0) Stop sign at Dell Webb Boulevard.

68.3 (0.6) Stop, do not enter freeway. TURN LEFT on Varner Road. To the north, note multiple palm oases on the south side of the Indio Hills marking the Banning fault zone aquifer.

70.2 (1.9) Jefferson offramp of freeway. Proceed .1 mile on Varner Road.

70.3 (0.1) TURN LEFT (north) onto Jefferson.

70.8 (0.5) Stop sign at 40th St. Continue on Jefferson.

71.8 (1.0) Stop at 38th Street, TURN RIGHT.

72.8 (1.0) **STOP 4.** Junction of Madison and 38th Street. Refer to discussion by Wells, Connell and Martin (this volume). Hike northeast to top of flood control berm. Look northeast towards fresh cuts at the west end of gravel operation. Note upper terrace developed on alluvial fan that has been uplifted along the Banning fault. Below the terrace is a fan with a varnished surface and no apparent source. Very recent fans in the foreground are unvarnished and bar and rill microtopography has not been deflated. Return to vehicles and proceed south (right) on Madison.

73.8 (1.0) Stop at 40th Street; TURN LEFT (east).

74.8 (1.0) Stop at Monroe; TURN RIGHT (south).

75.8 (1.0) Cross over freeway

76.0 (0.2) TURN LEFT and enter I-10.

77.9 (1.9) Pass junction with Highway 111 (86), continue on I-10.

78.7 (0.8) Continue along freeway, passing the first of two exits to Dillon Road.

79.8 (1.1) The second exit to Dillon Road has gas stations if you need fuel. Continue on I-10.

81.6 (1.8) We are crossing the Banning/Mission Creek fault along the All-American Canal. On the north side (left) of the freeway, in road cuts, see the grey fine-grained sands of the Palm Spring formation. To the northeast is the overlying gray conglomerate of the Ocotillo formation.

84.0 (2.4) At the bridge, notice steeply dipping sediments along the trace of the Mecca Hills fault on the north side of the freeway.

86.0 (2.0) We are on a large dissected fan emanating from Little San Bernardino Mountains to the north. The surface of the fan is very mature, evidencing no bar and rill.

87.9 (1.9) Note pedogenic carbonate in sediments near crest of fan.

88.6 (0.7) Cross Thermal Canyon Wash; note coarse Ocotillo Conglomerate and pedogenic carbonates in cuts along wash banks, lush with smoke tree, palo verde, and ocotillo.

90.2 (1.6) At Front Hill, enter granitic bedrock (Powell, 1982).

92.1 (1.9) Cactus City rest area. To the south is a well-varnished, mature pavement, lacking bar and rill, developed on the Ocotillo Conglomerate of the Mecca Hills. View of Orocopia Mountains at 1:00. Note graben of terraced old alluvium at east end of the mountains.

93.5 (1.4) Cross Pinkham Wash and trace of Hidden Springs fault; enter Shavers Valley.

98.1 (4.6) Buried Mountain at 2:00 is located in the center of the valley. Its east side is surrounded by mature pavement on fans (Fig. 4).

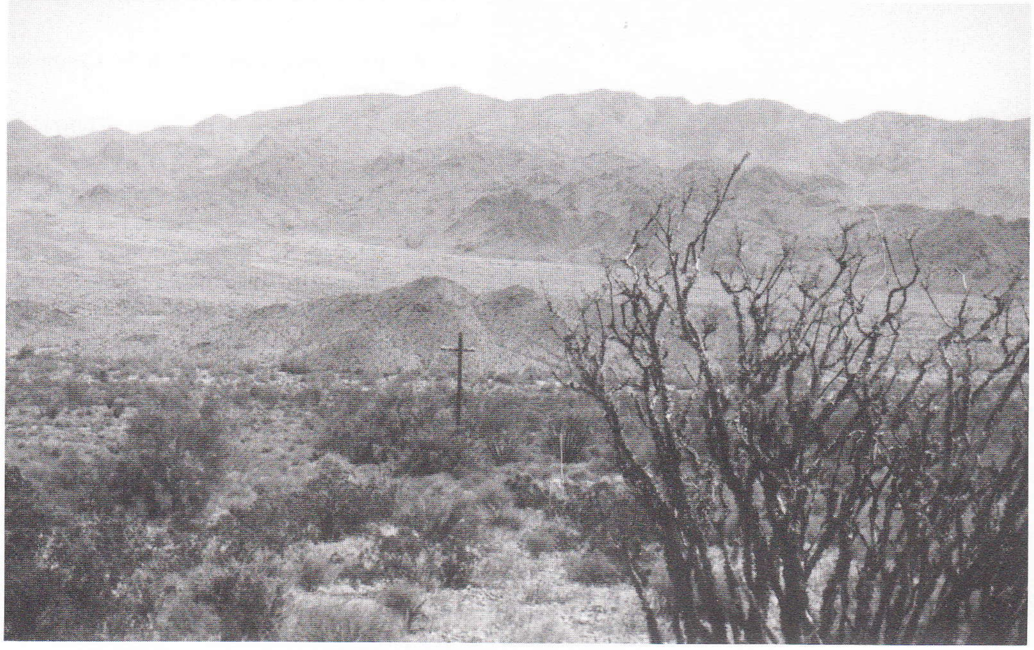

Fig. 4. Buried Mountain (center); Orocopia Mountains (distant).

101.5 (3.4) EXIT at off ramp to Mecca/Twentynine Palms.

101.8 (0.3) Stop sign. TURN RIGHT onto Box Canyon Road. Cottonwood Springs Road leads left (north) into southerly Joshua Tree National Monument. Near the monument boundary is a relatively recent Indian camp (see Schneider, this volume). Pinto Basin, to the north, has surface association of Pinto artifacts and Pleistocene mammals. We are continuing south on Box Canyon Road.

102.1 (0.3) Westerly bend in Box Canyon Road.

104.4 (2.3) View of Buried Mountain at 2:00, an outcrop of granitic rocks with Eocene marine sediments of the Maniobra formation on the east side (Fig. 4) (Crowell, 1975; Howell, 1975). The Maniobra fm may be right-laterally offset by 260 km (Howell, 1975). Exotic clasts are found in the Diligencia sediments in the Orocopia Mountains (Bohannon 1975). The Orocopia Mountains to the east-southeast contain a late Arikareean, early Miocene oreodont (Woodburne and Whistler (1973) in sediments that overlie the Eocene Maniobra formation. These Tertiary sediments are separated from the Orocopia Schist by the northwest-trending Clemens Wells fault and the Orocopia Thrust. The Orocopia Schist has been correlated with the Pelona Schist (Dibblee, 1977). At 2:00, note light granitic rocks and dark metamorphic rocks in the Little San Bernardino Mountains north of I-10.

107.2 (2.8) Note north-dipping surface developed on Ocotillo Conglomerate at 12:00. Surfaces of fans developed later dip south towards Shavers Well. Fanglomerates contain clasts from the Little San Bernardino Mountains and the Cottonwood Mountains to the northwest (Sylvester and Smith, 1991).

108.8 (1.6) SLOW, TURN LEFT and proceed up wash. Follow signs for Route SR1 through incised Ocotillo Conglomerate.

109.5 (0.7) Ascend terrace , turn left towards well casing to the north. **STOP 5. SHAVERS VALLEY PLAYA/LACUSTRINE SEDIMENTS** Cross the trace of the Clemens Well fault and enter Pleistocene playa sediments (Bridges and Meek, this volume). Examine the tan sediments with efflorescent salts which are draped by deflated gravels of Orocopia Schist. Return to vehicles and proceed southeast along jeep track to dry lake.

109.9 (0.4) Cross southernmost outcrop of tan playa sediments. Proceed south through Orocopia Schist and over saddle.

110.2 (0.3) TURN AROUND on the west side of "dry lake," a closed basin along the trace of the Hidden Springs fault. Note large green creosote and mesquite trees near the basin center indicating near-surface ground water. Deposition in this closed basin may be similar to that at Stop 2 prior to incision by the Box Canyon drainage. RETRACE to pavement.

111.6 (1.4) TURN LEFT onto pavement. Note joint sets dipping west and east in fanglomerate on south side of road. The Mecca Hills uplift is bounded by the San Andreas fault on the southwest and the Hidden Springs fault on the northeast, and is cut longitudinally by the Painted Canyon and Eagle Canyon faults (see Fig. 4 in Corona, this volume). These faults form prominent canyons or valleys in the Mecca Hills or control right-slip offsets along major drainage courses.

Fig. 5. The Ocotillo Conglomerate overlies fine-grained Palm Spring fm in Box Canyon.

The more northerly Painted Canyon, Eagle Canyon, and Hidden Springs faults are normal-oblique, right-slip structures splayed off the northwest-trending San Andreas fault (Corona, this volume).

111.9 (0.3) Site of Shaver Well, along the trace of the Hidden Spring fault. Green and black Orocopia Schist overlain by Ocotillo Conglomerate (Sylvester and Smith, 1991).

114.0 (2.1) White to gray-green fine-grained Palm Spring formation interfingers with the Ocotillo Conglomerate (Fig. 5).

114.5 (0.5) We are in deformed sediments near the junction of the Eagle Canyon fault zone and the Painted Canyon fault as we cross the Painted Canyon fault (Fig. 6). The Pliocene Palm Spring formation is uplifted on the west against the Ocotillo Conglomerate on the east. The flat-lying Palm Spring formation on the right side of the road; steeply-dipping beds of the south side of road mark transition across the Painted Canyon fault. Note pairs of anticlines and synclines.

Fig. 6. Deformed sediments near the Eagle Canyon fault zone and the Painted Canyon fault.

116.7 (2.2) Stop. TURN RIGHT (north) into Eagle Canyon. Proceed north to trace of Painted Canyon fault.

116.8 (0.1) BEAR LEFT up west branch of wash.

117.0 (0.2) At oxbow in wash, gravels are perched on terraces around the oxbow.

117.5 (0.5) STOP 6. Hike to a high point for the view along the Painted Canyon fault. Note joint sets, drag folds, and plastic deformation, and overall flower structure (Sylvester, 1991; Sylvester and Smith, 1975, 1991). RETRACE route to pavement.

118.0 (0.5) At pavement, TURN RIGHT.

118.7 (0.7) Road makes sharp bend south within Box Canyon.

119.5 (0.8) Vertical sediments mark the Banning branch of the San Andreas fault zone (Fig. 7). We have passed through Skeleton Canyon fault zone and the "flower" or "palm tree" structures described by Sylvester (1991) between Shavers Well and Painted Canyon Road.

120.4 (0.9) Painted Canyon Road. We are crossing the shoreline of ancient Lake Cahuilla above elevation 93'. Shorelines are higher than average in this area, and aboriginal stone rings or hearths were offset by the San Andreas fault within the last 1100 years (Shifflett and others, 1986).

121.1 (0.7) Cross Coachella Canal; proceed to Mecca.

124.6 (3.5) We are on 66th Avenue in Mecca.

125.5 (0.9) Road bends right, past Mecca Mall. Gas available. Proceed north to left turn to Highway 111.

125.6 (0.1) TURN LEFT onto cross road to Highway 111. The Bishop Ash (0.74 Ma) in the Mecca Hills was deposited near the top of the upper Palm Spring fm which is overlain by the Ocotillo Conglomerate (see Table I). It is described in detail by Rymer (1991) in the Thermal Canyon area. To reach Thermal Canyon, drive north on Highway 111, then east on Airport Boulevard and cross the Coachella Canal.

125.7 (0.1) Stop at Highway 111. TURN LEFT onto highway and prepare to bear right (west) onto Highway 195.

Fig. 7. Vertical beds at the trace of the Banning fault near Painted Canyon Road.

Fig. 8. The shoreline of ancient Lake Cahuilla at the fish traps area.

125.8 (0.1) BEAR RIGHT as Highway 195 becomes 66th Street.

127.7 (1.9) Stop sign. Proceed west on 66th Street. At this intersection, Highway 195 turns south.

131.7 (4.0) Stop sign. Highway 86 at Valerie Jean.

Proceed west across Highway 86 and continue on 66th St.

133.5 (1.8) 66th Street turns north and becomes Jackson.

133.9 (0.4) STOP 7, on the right side of the road, out of the way of traffic. View westerly of Lake Cahuilla shoreline (Fig. 8). Grey, angular, slightly varnished granitic rocks below the shoreline have been covered with varnished tufa. This cove of Lake Cahuilla contained aboriginal fish traps situated on the fluctuating shoreline (Wilke, 1978; Pallette, this volume). The Holocene history of filling and coastal land forms associated with Lake Cahuilla is summarized by Maloney (1986). The Martinez Mountain landslide, 3 miles west, is the largest in North America (Baldwin, 1986). RETRACE to Valerie Jean and Highway 86.

136.1 (2.2) Highway 86. **TURN RIGHT** (south) onto Highway 86.

138.2 (2.1) 70th St. View of Martinez Canyon and large fan due west.

138.8 (0.6) Polk Street. At 2:00, view of Pliocene gravels of the Canebrake Conglomerate capped by rolling erosional surface below Rabbit Peak (Fig. 9). Note several levels of terraced fans to south.

142.7 (3.9) Highway 86 joins Highway 195.

143.5 (0.8) Cross Kings Road. Pupfish in this area are discussed by Schoenherr (this volume).

145.4 (1.9) Notice the different ages of dissection on the fans to the west (3:00).

148.9 (3.5) Avenue 86. Travertine Rock is on the right at 2:00.

149.8 (0.9) Turn off Highway 86 onto dirt road. Go sharp right, northwesterly, paralleling Hwy 86 back to Travertine Point.

150.4 (0.6) STOP 8. Travertine Rock. CAUTION: *it is easy to get stuck in windblown sand here.* Early Holocene shoreline tufa was incised prehistorically with petroglyph carvings. Repeated deposition of tufa layers (Fig. 10) was so regular that the designs were transmitted to the most recent surface. Seven radiocarbon dates on tufa layers indicate that tufa deposition at Travertine Point began at 17,590±280 ybp and ended about 7,205±120 ybp. Petroglyphs were apparently carved in layers that date to approximately 9000 ybp (Reynolds and Turner, 1971; Turner and Reynolds, 1977).

Travertine Point, part of the metasedimentary/crystalline basement rock of the Peninsular Range Province, was a nearshore island during the highest stand of ancient Lake Cahuilla (Fig. 11). To paraphrase from Gath and others (1986), waves refracted around the island, promoted sand deposition in the lee of the island that would link to the mainland as a sand isthmus or tombolo. Later, as water levels receded, a headland was developed with remnant recessional strandlines.

Dark-stained subaqueous deposits of calcareous tufa mark the highwater level of ancient Lake Cahuilla at an elevation of 44 feet above sea level. During the Quaternary, many freshwater lakes repeatedly occupied the low-lying Salton Trough structural

Fig. 9. The Canebrake Conglomerate is marked by a flat erosional surface running across the center of this view.

Fig. 10. Thick tufa at Travertine Point was deposited in sunlit shallow waters of Lake Cahuilla. Modern graffiti is carved into the tufa, as were petroglyphs 9000 years ago.

depression. Pleistocene lakebed sediments have been dated at nearly 40 ky (Maloney, 1986). Younger lakes existed during the last few thousand years and may be as recent as 400 years old, with three previous fillings in the past 1,100 years (Maloney, 1986). Collectively they are known as Lake Cahuilla, named by William Phipps Blake in 1909. He first visited this area in 1853, serving as a geologist with the government Railroad Survey Party.

At its maximum extent, Lake Cahuilla was 160 km long by 56 km wide and about 100 m deep. The lake derived much of its water from distributary drainage of the Colorado River during periods of high meltwater flow, coinciding with glacial-interglacial epochs of the Ice Ages. On the west side of the Salton Trough, wave action left behind a wide variety of fossil shoreline features. These include barrier beaches, recessional shorelines, high water marks, spits and tombolos (Maloney, 1986). In places, freshwater mollusks of the planispiral snail *Planorbella* sp. and hydrobiid snails *Fontelicella (?Fontelicella)* sp. (dextral-coiled) and *Tryonia* sp. cf. *T. protea* (long-spiralled) litter the desert floor below remnant shorelines. Today, clays from Lake Cahuilla are fired to make common brick and drain tiles (Morton, 1977).

Dig yourself out of the soft sand and RETRACE route back to Highway 86.

151.1 (0.7) Stop sign at Highway 86. TURN RIGHT (south)

151.9 (0.8) Desert Shores Drive.

154.3 (2.4) TURN RIGHT on Brawley Avenue.

155.2 (0.9) Wonderstone Wash is on the right. Pull over and STOP before aggregate plant. Look westward to Rainbow Rock, a hot springs sinter deposit with gold values (Hillemeyer and others, 1991, 1992; Van Buskirk and McKibben, this volume). Varicolored felsitic rock of the Pliocene Truckhaven Rhyolite (Dibblee, 1954) is exposed along an east-west fracture zone in the basement terrane. Note thick section of Canebrake Conglomerate on south side of the Santa Rosa Mountains. These dip south and east into the Colorado River Group sequence. RETRACE ROUTE to Highway 86.

156.1 (0.9) Stop. TURN RIGHT on Highway 86 and proceed south.

156.5 (0.4) On the left is the Salton Sea. In 1905 the Colorado River was accidentally diverted from its normal channel into the irrigation canals of the Imperial Valley. For two years, river waters flowed unimpeded into the area. As a result, the Salton Sea—a man-made feature—is the largest lake in California. It is 33 miles long by 6 to 13 miles wide, covering over 400 square miles. Its present water surface lies about 235 feet below sea level.

The Salton Trough–Gulf of California structural depression is a true rift valley, an elongated, down-dropped block of the earth's crust that separates two major plate-tectonic boundaries. Movements are splitting sialic crust apart, with Baja California rafting away from mainland Mexico along active transform segments of the San Andreas fault zone. North of the International Border this vast fragmentary boundary, including the Imperial and Coachella valleys, is characterized by wrench tectonics, crustal spreading, reactivated detachment faulting, seismicity,

Fig. 11. The distinct white band near the top of Travertine Rock marks a shoreline when this point was an island in Lake Cahuilla.

volcanism, and geothermal features related to hydrothermal activity, all in response to the relative movement northwestward of the Pacific Plate adjacent to the southeasterly-driven North American Plate. This divergent boundary occupies the largest area (over 2,000 square miles) of continental land below sea level in the Western Hemisphere, with the Salton Sea at its lowest part.

161.4 (4.9) North Marina Drive.

163.4 (2.0) TURN RIGHT on S22, the Borrego-Salton Seaway, in Salton City. This paved roadway was built in 1968 and follows the approximate trace of the old Truckhaven Trail. Much of the Borrego-Salton Seaway from here to Veronica Avenue is built on unconsolidated lacustral evaporites of the Plio-Pleistocene Borrego-Brawley facies (Tarbet, 1951; Wagoner, 1977), covered by Quaternary lakebed sediments of Lake Cahuilla. Crustal subsidence, dextral faulting, liquefaction, deformation and groundwater saturation and swelling of the underlying claystones have combined to cause the roadway to deform. As a result the hummocky pavement is a continual maintenance problem for repair crews.

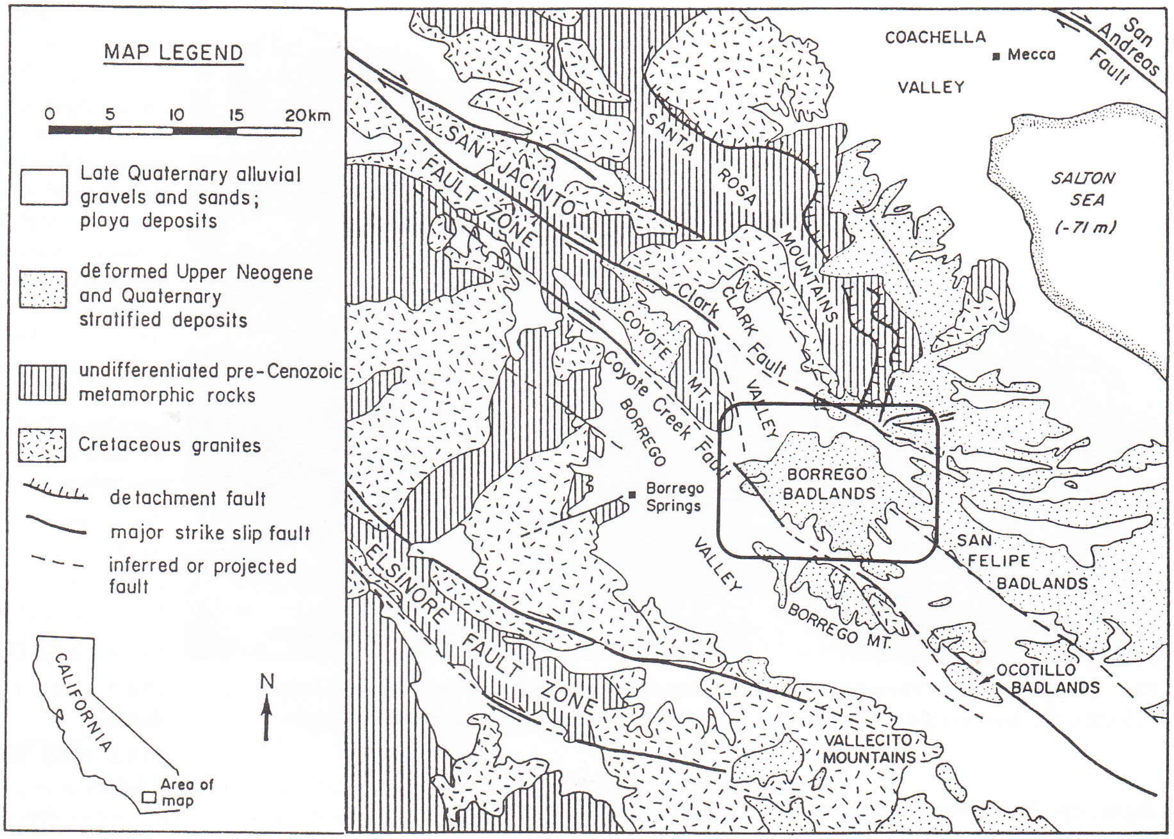

Map 1. Regional geology of the Borrego Badlands area, Anza-Borrego Desert State Park, California. Modified after Pettinga (unpubl. data, 1992).

163.8 (0.4) West Shorelines Clinic on the left.

165.0 (1.2) Lake View Court on the right.

166.5 (1.5) The broad low ridge represents a remnant strandline berm of Lake Cahuilla. Remeika (1991c) reports the occurrence of the Dudley Willow (*Salix gooddingii*) from lacustral evaporites of the pluvial lake. *Salix gooddingii* is a common species of willow, widespread throughout the southwest. During the Quaternary, it preferred the riparian distributary channels of the Colorado River and its presence confirms a climate of arid temperatures. Prior to its discovery, the oldest specimen preserved was collected in 1845 by John C. Fremont during his historic expedition to California. We are entering the BLM Desert Conservation Area.

The lacustrine Plio-Pleistocene Borrego formation, part of the Colorado River Group of Remeika (in White and others, 1991) makes up the dissected mud hills on the right. They have been

Fig. 12. Fault-related flexing in sediments at Clay Point.

mildly deformed and downfaulted to the east by northwest-trending faults in response to crustal subsidence. Faulting has juxtaposed fine-grained brown claystones down against cream-colored sandstones. We are at sea level and are proceeding westward towards the base of Clay Point.

166.9 (0.4) Note the presence of a yellowish-green lacustrine evaporite capping the mud hill. This claystone marker bed is remarkable laterally continuous throughout the Santa Rosa Badlands and Borrego Badlands, cropping out at Seventeen palms, Bank Wash, Rainbow Wash and Mammoth Cove. We will view this prominent marker bed again from Font's Point and directly below Vista del Malpais.

167.1 (0.2) Veronica Avenue on the left.

167.3 (0.2) STOP 9. Clay Point. Fault-related monoclinal flexing on the right involves redbeds of the Plio-Pleistocene Borrego formation (Fig. 12). Clay Point (elevation 92') consists of concretionary channel sandstone facies of the older Diablo formation mildly deformed and faulted downward on the east.

168.1 (0.8) Junction with dirt road on the left to Oh-My-God Hot Springs. The hot springs are actually an oil-test thermal well believed to have been drilled by the Department of the Interior's Water Reserve in the 1920s. Today it is a popular destination with desert visitors. It is surrounded by tamarisk trees.

168.3 (0.2) Mud hill exposures straight ahead and to the right are included in the Santa Rosa Badlands, part of the larger Borrego-San Felipe Basin (BSFB).

168.9 (0.6) Highway crosses Gettysburg Wash on the left and climbs mesa. On both sides are colorfully striped west-dipping nonmarine deltaic sediments of the Pliocene Colorado River Group overlain by gravelly Quaternary alluvium. A small, moderately-preserved, transported paleobotanical assemblage of silicified wood has been collected from similar redbeds. Remeika and others (1988) identified *Umbellularia salicifolia* (Lauraceae), *Juglans pseudomorpha* (Juglandaceae), *Populus* sp. and *Salix* sp. (Salicaceae). These ancestral hardwoods provide a preliminary picture of a more favorable temperate climate (with no rain shadow), which is consistent with the postulate that winters yielded more rainfall and summers were more equable than at present.

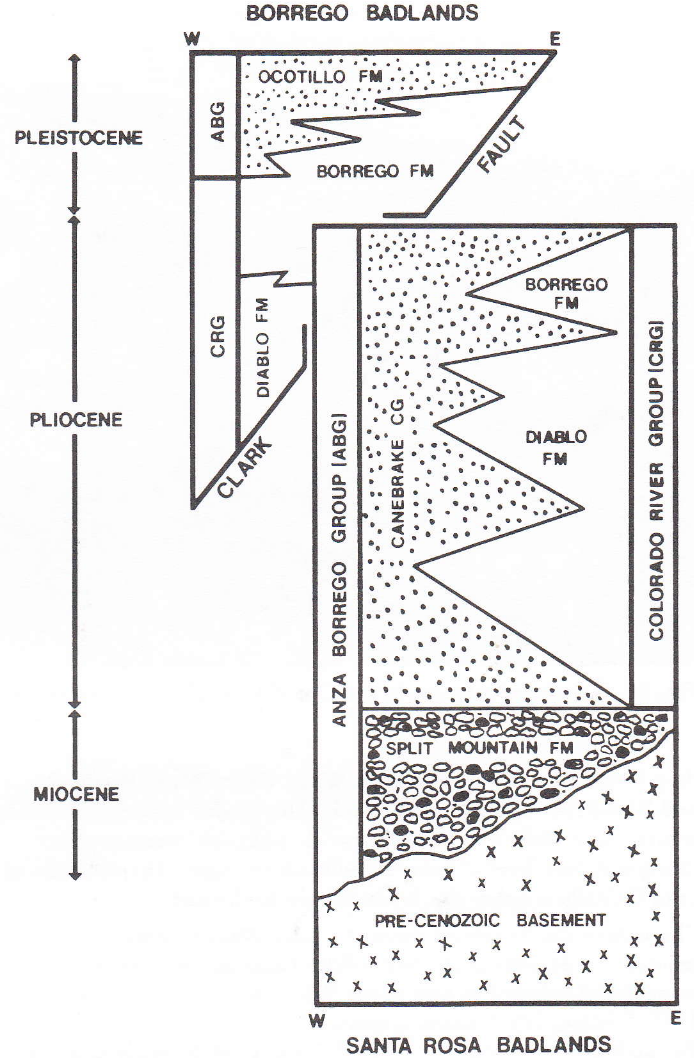

Table II. Summary of stratigraphic relationships of the Santa Rosa Badlands and associated rock units within the Borrego Badlands (modified after Pettinga, unpubl. data, 1992).

170.5(1.6+) Pedogenic carbonates are visible past the pullout on the right. Look at well-developed pavement overlying dissected Diablo formation. Note angular unconformity at top of Diablo Fm where terrace gravels contain pedogenic carbonates and prismatic structures.

171.8 (1.3-) TURN RIGHT onto really good dirt track; proceed north 1/4 mile and park.

172.1 (0.3) STOP 10. Santa Rosa Badlands Overlook. Two noticeable, flat-topped terraces characterize much of the immediate area. They are all that remain of a much more extensive pedimented tableland that existed here during the later Pleistocene (Figs. 13, 14, 15, 16). We are standing on the lower terrace. Finger remnants have been heavily dissected between modern entrenched desert washes, including the

Fig. 13. Four terraces are inset at different levels at the south end of the Santa Rosa Mountains.

Fig. 14. A series of terraces in the Ocotillo Conglomerate viewed from Stop 10.

deep barrancan tributaries of Palm Wash, Grave Wash, Big Wash, and Wonderstone Wash to the north. This eroded landscape is locally referred to as Blake's Ravines. Below us, additional terraces reflect changes in base level of Lake Cahuilla on the right. The shoreline of Lake Cahuilla is below the lowest terrace to the east.

Throughout the barrancan washes of Palm Wash (below), sedimentary deposits of the Santa Rosa Badlands were previously mapped and reported as part of the Palm Spring formation (Woodard, 1963; Dibblee, 1954) which is restricted in outcrop to the Vallecito Badlands of the Vallecito-Fish Creek Basin (VFCB) many miles to the south. As redefined by Remeika (1991b), they belong to the ancestral Colorado River delta-plain represented by the Diablo formation. Canebrake Conglomerate is to the northwest and shows light-tan on fresh surfaces (Table II).

Locally, recognition of basin-margin sediments versus Colorado River-derived sandstones and evaporites is useful in establishing correct nomenclature and stratigraphic control. Based on sedimentological, stratigraphic and paleontological differences, two distinct depositional suites form unrelated but, in part, coeval genetic-stratigraphic affinities that can be petrographically identified in the field. Locally-derived Anza Borregan sediments (herein referred to as the Anza Borrego Group) tend to be tan-gray, coarse to medium-grained, poorly-sorted, feldspar- and biotite-rich arkosic sandstones with gravelly conglomerates. The group includes the Split Mountain formation, the Canebrake Conglomerate and the Ocotillo formation. In marked contrast, Colorado River-derived lithologies (Borrego formation and Diablo formation of the SBFB) are pale orange, fine-grained, well-sorted, quartzose arenitic sandstone, with lesser red to brown claystones that, together, may form conspicuous strike ridges in folded terranes. The Diablo formation is the most extensively exposed Neogene sedimentary unit in the Anza Borrego area.

The DIABLO FORMATION is composed of a light-colored fine to very fine-grained, friable, massive quartzitic arenite, locally concretionary, with subordinate brown ripple-laminated overbank claystones that reflect delta-plain deposition. Petrographic investigations by Merriam and Bandy (1965) and Muffler and Doe (1968), and palynology research by Farley Fleming (written comm. to Remeika, 1991) concluded that Diablo sandstones debouched into Anza Borrego via the Colorado River, based on the presence of extralimital Late Cretaceous foraminifers with calcite-filled tests reworked from the Mancos Shale (Colorado Plateau) and the identification of the pollen *Proteacidites* which became extinct at the Cretaceous-Tertiary boundary. A review of the VFCB's paleontologic and paleomagnetic literature (Opdyke and others, 1977; Johnson and others, 1983) established the base of the Diablo at approximately 3.8 MYA with continued deposition spanning 1.2 MY. RETRACE ROUTE to S22.

172.4 (0.3) Pavement at S22. TURN RIGHT.

173.7 (1.3) View north at 3:00 reveals east-dipping Mio-Pliocene clastic sediments of the Santa Rosa Badlands, overshadowed on the west by Pyramid Peak (aka Traveler's Peak) at an elevation of 3,500' above sea level. The tall microwave tower is at the San Diego county

Fig. 15. View east from Stop 10 across terraces reflecting changes in base level of Lake Cahuilla. Salton Sea is distant.

line. We are leaving the BLM Desert Conservation Area and entering the 600,000+ acre Anza Borrego Desert State Park (ABDSP) on County Highway S-22. Anza Borrego is the largest state park in the contiguous United States, stretching 61 miles long by 30 miles wide. The state park is 85 miles east of San Diego and encompasses the easternmost 1/5 of San Diego County from the Mexican border to Riverside County.

Fig. 16. Late Pleistocene surface with well-developed desert pavement and pedogenic carbonates sits on top of Borrego formation at the Santa Rosa Badlands outlook.

In 1933, the state park was established specifically to protect and preserve in public trust a unique out-of-doors storehouse of geological and paleontological natural resources in small-scale tectonic paleobasins that have undergone a large amount of Cenozoic crustal extension and strike-slip faulting. Two post-detachment/faulting depositional basins include the Vallecito-Fish Creek Basin (VFCB) to the south, and the Borrego-San Felipe Basin (BSFB) to the north. Each contains nearly complete fossiliferous, synextension basinal deposits that accumulated rapidly and evolved in response to major strike-slip fault-induced environments of the Salton Trough-Gulf of California structural depression. Only the VFCB has a high resolution biostratigraphic magnetostratigraphic framework (Opdyke and others, 1977; Johnson and others, 1983). At present, the SBFB is undergoing stratigraphic revision and control.

Anza Borrego's rich and diverse paleontological resources, represented by five local faunas (Downs and White, 1968; Remeika, 1992a) list over 130 vertebrate taxa (Hemphillian – Rancholabrean LMA) including large grazing herbivores, carnivores, aquatic mammals, microtine rodents, amphibians, reptiles and fish, with a dozen holotypic specimens. Add nearly 200 species of marine invertebrates and the collected assemblage may represent the largest repository of Plio-Pleistocene mammalian/invertebrate faunas in North America (Remeika, 1992d).

PLEASE NOTE: It is a violation of federal and state regulations and Public Resource Codes to disturb, collect, or destroy geological/paleontologic resources on state lands under the jurisdiction of the California Park System.

174.4 (0.7) Truckhaven Trail/Calcite Mine area. On the right the Calcite Mine jeep route is a narrow, rough trail, extending 1.9 miles off the highway. Heyday of the district was during World War II. Optical-grade calcite crystals were used in bombsights and anti-aircraft weaponry because of its double-refraction properties. Calcite veining fills cross shears in the indurated sandstones along east-west trending dextral strike-slip faults. Proceed on S22.

174.6 (0.2) Milepost marker 38. The Salton View Scenic Overlook is on the right.

175.6 (1.0) Milepost marker 37. North of the highway, light-colored sandstones of the Diablo formation interfinger with locally-derived, tan-gray continental sandstones of the Pliocene Canebrake Conglomerate. Similar lithologies in the VFCB are represented by the Olla Member of the Canebrake Conglomerate (Winker, 1987). Within the upper reaches of Palm Wash, cameloid ichnofossils (footprints) have been discovered.

175.9 (0.3) Cannonball Wash overpass. Resistant Diablo redbeds form low-lying strike ridges littered with ferruginous sandstone concretions. They take on a myriad of bizarre shapes, including cylinders, ameboids and spheroids such as the well-known examples found at the Pumpkin Patch along Tule Wash. It is believed that concretions developed by diagenetic compaction of the deltaic sediments as a result of anomalies from localized concentrations of carbonate and/or hydrous calcium sulfate. Desert rose gypsum crystals (hydrated calcium sulfate) also occur in rosette-shaped aggregates throughout Diablo exposures.

176.2 (0.3) North Fork of Arroyo Salado overpass.

177.3 (1.1) TURN RIGHT onto paved turnout of unmarked scenic outlook and park. **STOP 11. Santa Rosa Anticline at Truckhaven** Rocks. The southernmost flank of the structurally-elevated Santa Rosa Mountains exposes a clastic succession of Mio-Pliocene nonmarine sedimentary fill (Pyramid Peak), consisting of syntectonic sedimentary facies reflecting a sensitive record of complex surface deformation along the BSFB margin. The highly distended landscape is creased by a labyrinth of vertical-walled gorges and slot canyons. The rock sequence, part of the locally-derived Anza Borrego Group, is openly folded into the southward-plunging Santa Rosa Anticline.

Pettinga (1991) presented a detailed review of the structural geology of the Truckhaven Rocks, and the following discussion draws heavily on his work. The east limb of the Santa Rosa Anticline is cut by east-west trending dextral strike-slip faults. As described by Pettinga (1991), these faults form an anastomosing system, with offsets up to 100 meters. Constraining and releasing bands and steps add considerable complexity to the deformation of strata. The southward dipping sequence is locally folded adjacent to the wrench faults, and strain is accommodated by considerable bending shear and stratal transposition within the stratigraphic pile. Fabric analysis indicates that thin bedding-controlled sheets have sheared and rotated relative to underlying and/or overlying strata.

At 11:00 the Truckhaven fault is exposed in the core of the anticline. It represents a sinistral wrench tear, antithetic to the nearby San Jacinto fault zone (SJFZ) (Clark fault), between the upthrown south-plunging east limb and the structurally lower west limb (Pettinga, 1991).

The genetic-stratigraphic cover section of the Truckhaven Rocks/Santa Rosa Badlands is ideally suited to discussion because of its unusual completeness, structural intactness and quality of exposures within the state park. Pyramid Peak consists of a Mio-Pliocene syntectonic interstratified nonmarine package (ANZA-BORREGO GROUP), including a basal, coarse clastic fanglomerate assigned to the Miocene Split Mountain formation below, and postextensional, torrentially-bedded proximal sandstones of the Plio-Pleistocene Canebrake Conglomerate above (undifferentiated), that accumulated marginal to the BSFB. Basinward, the sandstones are laterally equivalent with fine-grained sediments of the Colorado River Group. The Ocotillo formation, also within the Anza-Borrego Group, is divided into four members (Remeika and Jefferson, this volume).

The basal SPLIT MOUNTAIN FORMATION (Tarbet and Holman, 1944; Woodard, 1974; Winker, 1987) chronicles the initial deroofing of the ancestral highlands. It is approximately coeval with lower to middle Miocene detachment faulting (Pettinga, 1991), and volcanism (Alverson formation) recorded from the VFCB (Kerr, 1982, 1984; Kerr and Kidwell, 1991), ranging from 14.9 to 24.8 MYA (Gastil and others, 1979). The Split Mountain formation is composed of a thick arkosic series of red to reddish-brown monomictic matrix and framework-supported boulder conglomerate, breccias and debris flows resting with a high-angle buttress nonconformity against pre-Tertiary metasedimentary/crystalline basement terrane. The sequence terminates into coarse sheetflood pebble sandstones. Based upon lateral and vertical distribution, Pettinga (unpubl. data) informally subdivides the stratification into two lithofacies that may correlate with the informal Red Rock Canyon and Elephant Trees members of the Split Mountain formation (Winker, 1987) at Split Mountain Gorge. It is unconformably overlain by the Canebrake Conglomerate.

As defined by Dibblee (1984), the CANEBRAKE CONGLOMERATE is a locally-derived light-gray Plio-Pleistocene alluvial fan-floodplain sequence. Deposits consist of a thick 1000 m series of coarse unsorted arkosic conglomerate and lesser coarse sandstones containing a mixed-provenance granitic and gneissic clast suite from the Santa Rosa crystalline basement. Clasts range from subangular boulders to subrounded cobbles and pebbles. Pettinga (unpubl. data) recognizes several subfacies, ranging from proximal fanglomerates to distal gradation of indurated gravel and mixed-load pebbly sandstones, extending basinward to nonpebbly, finer-grained braided channel sandstones that interfinger with ancestral Colorado River sequences (Olla Member). RETURN TO S22.

177.4 (0.1-) TURN RIGHT onto S22.

178.7 (1.3) Milepost marker 35.

SOUTHERN SAN JACINTO FAULT ZONE

179.8 (0.1) Continue past Arroyo Salado Primitive Campground exit on the left. Arroyo Salado will serve as our dry campsite tonight. We are approaching the Clark fault (to the west), a southern branch of the San Jacinto fault zone. Coeval sedimentation and deformation fabrics within the west limb of the Santa Rosa Anticline are characterized by increased steeply-dipping, northwest-striking Canebrake Conglomerate (undifferentiated). It has been dextrally dragged from east to west along the southern end of the Santa Rosa Mountains.

178.9 (0.1) Pass Coachwhip Canyon/Ella Wash

179.2 (0.3) Pass an unmarked turnout on the left; we will stop here for an overlook on our way back to the Arroyo Salado campsite.

180.7 (1.5) Milepost marker 33. The flat-lying desert floor is characterized by a xerophytic community typical of the Lower Sonoran Life Zone. Common plants include the spindly-branched ocotillo, hardy creosote bush, cholla cacti and burroweed.

180.8 (0.1) Palo Verde Wash is on the left. Diagonally across the highway at 2:00 is an elongated shutter ridge squeezed up along the diffuse Clark fault. The unconsolidated sediments include clays and cobbled sandstones of the Pleistocene Ocotillo formation (Remeika and Pettinga, 1991). West of Smoketree Wash, stream channels, banks and bars of Pleistocene and Holocene alluvial fan surfaces have been laterally offset along the Clark fault. In 1988 a soil chronosequence study of the Clark fault where it traverses recently abandoned stream channels was undertaken by W.S. Bull's Geomorphology 650 field class from the University of Arizona (Tucson). Assuming that the displacement has not been constant since the Late Pleistocene, Jackson and Calderon (unpublished data) obtained a recent slip rate of about 4m/ka. At 3ka and 5 ka, slip rates were between 2.6 and 2.2 m/ka, respectively. At 55 ka, a lower rate of 1.2 m/ka was determined, and at 120 ka, a lower rate of 0.9 m/ka was obtained. The increase in slip rate suggests that the Clark fault has been very active in Late Holocene time.

181.7 (0.9) Milepost marker 32.

181.9 (0.2) Junction of Thimble Trail and Truckhaven Trail in saddle. To the north on the eastern edge of Sierra Ridge is Rattlesnake Canyon. There are two well-developed Pleistocene-Holocene alluvial fans adjacent to it on the right, developed along the southern base of the Santa Rosa Mountains. Both fans are laterally offset by multiple fault scarps along the Clark fault.

182.3 (0.4) The highway crosses lengthwise an elongated structural graben that runs northwest at 1:00 and is bounded on both sides by prominent northwest-trending fault scarps developed in unconsolidated blowsand sediments.

182.8 (0.5) Milepost marker 31

183.0 (0.2) Blowsand Turnout (unmarked) is on the right. To the right, located between the highway and the Santa Rosa Mountains, is a series of low-lying rolling hills known collectively as Lute Ridge. Although not obvious from our vantage point, the northeastern edge of Lute Ridge is a classic, textbook strike-slip normal fault scarp, extending two miles in length on the Clark fault. It represents the largest known fault scarp on the North American continent existing in unconsolidated sediments. Lute Ridge is a pressure ridge, continuing to be domed up, resulting in obvious and not-so-obvious unconformities throughout the area. The hummocky topography is deeply dissected. Six additional scarplets and visible on the south-facing slopes of Lute Ridge.

183.6 (0.6) Santa Rosa Mountains Overlook on the left. To the north is an excellent unobstructed panorama of the structurally-uplifted Santa Rosa Mountains. Its titanic ramparts guard northern Clark Valley on such a grandiose scale that they attain the greatest vertical rise of any mountain range in the state park. Local mountain heights include Villager Peak at 5756' and Rabbit Peak at 6666', with clear lines of sight following the ridgeline up to Toro Peak at 8716' above sea level.

Geologically the Santa Rosa Mountains mark the eastern boundary of the geomorphic Peninsular Range Province. The range is composed of cordilleran metasedimentary rocks (marble, biotite schist, quartzite, banded augen gneiss and amphibolite) and younger Mesozoic granitic (meta-quartz diorite, granodiorite and pegmatite) core complexes.

The Late Cretaceous to early Tertiary Eastern Peninsular Range Mylonite Zone (EPRMZ) affected the pre-Late Cretaceous crystalline/metasedimentary rocks of the Santa Rosa Mountains. This 100 km long deep-seated ductile shear zone is part of a much larger mylonite zone that extends southward from Palm Springs to the tip of Baja California (Sharp, 1967, 1979).

According to Simpson (1984), mylonization mostly affected mid-Cretaceous granodiorites, quartz diorites and quartz monzonites of the Peninsular Range Batholith, with minor involvement of older quartzites, marbles and mica-schists. K-Ar and fission-track studies have yielded an upper age limit of ca. 63 MYA for mylonite development (Dokka and Frost, 1978; Wallace and English, 1982). Sharp (1967, 1979) suggested that the EPRMZ represents post-mid Cretaceous unroofing of the batholith along a deep-seated shear zone. On the basis of east-plunging mineral elongation lineations, the EPRMZ originated from west-directed thrusting in response to the closure of a back-arc basin some 100 km inboard from a main east-dipping subduction zone along the ancestral California coast. Southwest tectonic transport of the structurally higher eastern Peninsular Range Batholith over the lower western batholith has also been postulated by Todd and Shaw (1979).

Post-Pliocene offset along the SJFZ has divided the NNW-SSE trending and east-dipping EPRMZ into three regionally significant fault block ranges: the Santa Rosa, Coyote and San Ysidro Mountains.

183.7(0.1+) Milepost marker 30.

184.4 (0.7-) TURN LEFT into Font's Wash, leaving paved S-22. **PARK** street vehicles and carpool for the off-road loop. Four-wheel-drive is strongly recommended to negotiate loose sand. Font's Wash drains much of the northwestern Borrego Badlands north of the Ocotillo Rim. Road conditions along this major watercourse are subject to change without notice. Seasonally, rampaging flash floods fill the arroyo from bank to bank, funneled northward into the topographically lower Clark Valley playa. Font's Wash displays many ephemeral components characteristic of desert arroyos, including choked tributaries, undercut banks, eroded hillslopes, incised channels and pediments with narrow interfluves.

184.6 (0.2) Red calichified sandstone on the right belongs to the Late Pleistocene Font's Point Sandstone.

185.2 (0.6) The first series of varicolored mud hills on the left include the Las Playas Member of the Ocotillo formation (Remeika and Jefferson, this volume). The mixed salmon-brown and greenish-colored micaceous claystones and siltstones with sandy interbeds represent a lacustrine fluvial-playa sequence. The exposures are capped by deeply-weathered consolidated reddish-brown sediments of the Font's Point Sandstone.

The vertebrate-bearing Ocotillo formation (Anza Borrego Group) represents a locally-deposited middle to early Late Pleistocene continental fluvial-floodplain succession of gravelly sandstones, silts and claystones exposed throughout the northernmost half of the western Borrego Badlands (informally referred to as Fault Block A) and Coyote Badlands (Remeika, 1992a). The stratotype is located west of Inspiration Wash in the Arroyo Otro-Mammoth Cove section, above and below the Ocotillo Rim northwest of the Inspiration Point fault. To establish stratigraphic control and age determinations, Remeika and Pettinga (1991) and Remeika (1992a) recognized three previously undefined lithofacies for the Ocotillo Conglomerate of Dibblee (1954). In ascending order they include a 74 m thick subaqueously-deposited distal alluvial fan sequence (Mammoth Cove Sandstone), an 87 m thick series of freshwater lacustrine claystones (Arroyo Otro Claystones), and a 216 m thick mixed composition fluvio-lacustrine interbeds (Inspiration Wash Member) that laterally grade into the Las Playas Member.

Bone-bearing sandstone interbeds of the Las Playas Member yield the last of the Pleistocene megafauna (Borrego Local Fauna) from the Anza Borrego Irvingtonian LMA. Over the past several years, paleontologists (under permit) have unearthed the fossil remains of now-extinct *Equus bautistensis*, *Mammuthus columbi*, *Odocoileus* sp., *Nothrotheriops* sp. cf. *N. shastensis*, and *Camelops huerfanensis*. Work initiated in the 1970s by Ted Downs and Harland Garbani (LACM), and continued by the late George Miller (IVCM) and Paul Remeika (ABDSP) have all led to cyclic prospecting and recovery of a rich vertebrate megafauna represented by 50 mammalian genera. This Borrego Local Fauna (LF) (Remeika, 1992a) consists of a fossil assemblage of at least 5,000 cataloged specimens, collected from more than 400 paleontologic localities of the Ocotillo formation. Most of the composite fauna is based upon fragmentary remains and only a few articulated specimens have been found.

185.7 (0.5) Roadway veers left and crosses the hidden trace of the Inspiration Point fault. Within the Mammoth Cove section of the Borrego Badlands, this prominent fault is a left-lateral cross-fault that is nearly orthogonal to the main right-lateral strike-slip Coyote Creek fault. It trends northeast across the entire breadth of the SJFZ. Hudnut and others (1989a) suggests that slip on related cross-faults locally decrease normal stress on the main faults. Hudnut and others (1989 a, b) hypothesize that surface rupture of the Inspiration Point fault may trigger rupture on either the Clark fault or Coyote Creek fault by a mechanism similar to that which occurred during the November 23 and 24, 1987 Superstition Hills Earthquake sequence.

185.8 (0.1) To the left, east-dipping Font's Point Sandstone conformably overlies uppermost gray-green claystones of the Las Playas Member, all capped by Late Quaternary alluvium. To the west, in Arroyo Otro, a pronounced angular unconformity near the top of the Inspiration Wash section is demonstrated by syndepositional erosion, uplift and close proximity to the active Coyote Creek fault before deposition of the overlying Font's Point Sandstone. The upper contact is defined by an erosion surface having a paleomagnetic signature of 0.37 MYA (Scheuing, written comm. to Remeika, 1991).

186.3 (0.5) Junction with Short Wash Trail on the left. Continue straight. The roadway soon veers right out of the main wash into a tributary arroyo. PROCEED SOUTHWEST, destination Font's Point.

186.7 (0.4) North-dipping unconsolidated brownish claystones and arkosic sandstones of the Inspiration Wash Member make up the low cohesion slopes of badland relief along the roadway.

187.0 (0.3) On the right, steeply-dipping strata are complexly folded approaching Cottontail fault. They form subtle topographic highs, indicating a northwest-plunging, fault-propagated anticlinal fold. Note a greenish claystone bed that defines the core of the fold. Ongoing deformation is suspected by a systematic decrease in the dip of bedding towards the north, away from the anticlinal axial surface.

187.2 (0.2) Cross trace of the high-angle, east-trending Cottontail fault. This secondary cross-fault is also transverse to the nearby major northwest-trending Coyote Creek fault. Its presence implies that crustal deformation is being accommodated by local folding, left-slip faulting and block rotation. Activity on this short fault has juxtaposed Font's Point Sandstone (south) down against the Inspiration Wash Member (north).

187.7 (0.5) Drive across calichified surface of Font's Point Sandstone.

188.4 (0.7) Y-intersection. Begin one-way loop drive. STAY LEFT. Sedimentary exposures are entirely of Font's Point Sandstone.

Fig. 17. The Ocotillo Rim, view east from Font's Point.

189.5 (1.1) STOP 12. Fonts' Point Overview. The approach to Font's Point has been through a rather flat, subdued landscape of ocotillo and creosote bush. Now, at the brink, is one of the most sublime spectacles in all of Anza Borrego (Fig. 17). Hike to the Ocotillo Rim at Font's Point, elevation 1294'. This is the climactic overlook of the Borrego Badlands. Unparalleled for scenic grandeur, the view is of one of the most seismically active regions in California: a transition region from the continental transform regime of the San Jacinto/San Andreas fault zones to the Gulf of California oceanic rifting regime (Hudnut and others, 1989).

On the southern horizon are the Fish Creek, Vallecito and Pinyon Mountains. The low mound of hills east of the Fish Creek Mountains is Superstition Mountain. On November 23 and 24, 1986, major twin earthquakes, measuring 6.2 and 6.6 respectively, hit along the Superstition Hills fault (part of the SJFZ). Weathered desiccation cracks atop Font's Point were noticeably enlarged. During the Borrego Mountain Earthquake of 1968, over six feet of rock at the tip of Font's Point tumbled down the cliffside. An additional five feet of cliffside collapsed along the southeastern tip during the Landers Earthquake of June, 1992.

To the south, the laterally-offset twin buttes of Borrego Mountain form a natural barrier along the San Felipe Wash drainage. San Felipe Wash follows the approximate trace of the Coyote Creek fault. Related Mio-Pliocene strata in the vicinity of Hawk Canyon and Borrego Mountain Wash have been thrust and folded, indicating northwesterly-directed shortening of the crust (Scheuing, written comm. to Remeika, 1988). Nearby, the tectonically subsiding Borrego Sink (sag pond) is the lowest structural feature in the area at 468 feet. As a result, the sink receives the greatest percentage of surface water streamflow and groundwater inflow entering the Borrego Valley aquifer.

To the east are the shimmering waters of the Salton Sea. To the north stand the impressive crystalline/metasedimentary basement terranes of the Santa Rosa Mountains and Coyote Mountain, separated by the enclosed graben of Clark Valley.

To the west is the great western mountain barrier protecting Borrego Valley. The San Ysidro Mountain Range rises abruptly nearly a vertical mile from the valley floor. San Ysidro Peak at 6,147' above sea level is the high point punctuating the skyline.

The Late Pleistocene Font's Point Sandstone forms the stratum capping sediments exposed in the receding cliffside of Font's Point. The unfossiliferous Font's Point Sandstone represents the thin blocky reddish-brown caprock and underlying braided stream sandstones of the promontory. Here it is crudely bedded and locally conglomeratic (pebbly). Distinctive mottled pedogenic zones of caliche indicate a semi-arid transitional environment of deposition during the Late Pleistocene.

The gray-buff basal stratum of the cliff is the fossiliferous Mammoth Cove Sandstone Member of the Ocotillo formation (Remeika, 1992a). It represents a locally-derived granule to bouldery conglomeratic distal alluvial fan facies. The coarseness and thickness of this sandstone unit generally increase proximally (southwest) while grain size and fan gradient decrease down fan (east), ultimately pinching out basinward east of Vista del Malpais. The Mammoth Cove Sandstone alluvial wedge is stratigraphically and petrologically similar to those of the Canebrake Conglomerate and are probably correlative. Lenticular bandings of sediment with parallel bedding, climbing ripple lamination, thin overbank splays of fine-grained biotite-rich silts and clays, and torrential bedding indicate rapid deposition. Basinward, the Mammoth Cove Sandstone mantles and interfingers with the uppermost fine-grained riverborne redbeds of the Borrego formation. The basal contact has yielded a paleomagnetic signature of 1.25 MYA (Schueing, written comm. to Remeika, 1989). Extinct vertebrates include *Mammuthus imperator, Equus (Dolichohippus) enormuus, Arctodus* sp. and *Camelops* sp. index the Irvingtonian LMA.

The Borrego formation of Tarbet (1951) represents a thick (900m-1900m) basinward lacustrine to brackish water shallow nearshore facies of the underlying Diablo formation. Basinal sediments exposed in Rainbow Wash and Hills of the Moon Wash directly below Font's Point are fine to very fine-grained light-gray to reddish-brown claystone and siltstone. Close examination of clay exposures reveals that many are thinly laminated while others appear structureless. All have been complexly deformed. Rare foraminifers, twig-sized fragments of petrified wood and a brackish-water microfauna (Taylor, 1981; Stearns, 1901) occur in the lower section. Microfaunal hydrobiids *Tryonia* sp., *Fontelicella* sp. and Planorbidae occur with the sphaeriid *Pisidium* sp. cf. *P. compressum* and unionid *Anodonta* sp. cf. *A. californiensis* restricted to the upper playa claystones of the Borrego formation. The Borrego formation bridges the Plio-Pleistocene boundary.

Return to vehicles and RETRACE the 4-mile route downwash (north) to the paved Borrego-Salton Seaway, S-22.

191.0 (1.5) Cross east-west Cottontail fault.

191.7 (0.7) Pass junction with Short Wash Trail

192.2 (0.5) Cross Inspiration Point fault which elevates the Las Playas Member sediments.

193.6 (1.4) Pavement at S22, Borrego Seaway. Cautiously TURN RIGHT toward Arroyo Salado Campground.

196.1 (2.5) Pass junction of Thimble Trail/Truckhaven Trail.

197.2 (1.1) Pass junction with Palo Verde Wash.

198.4 (1.2) Milepost marker 34. Prepare to turn right in 0.4 mile.

198.8 (0.4) TURN RIGHT into unmarked parking loop and park. **STOP 13. Borrego Badlands Overlook.** This scenic viewpoint overlooks Palo Verde Wash and the distant Vista del Malpais areas of the Borrego Badlands. The sedimentary fill of the Borrego Badlands includes a complex succession of marginal alluvial and more interior lacustrine lithostratigraphic facies (Ocotillo formation). Distal alluvial sheetflood deposits graphically intertongue with an impinging Colorado River lacustral environment (Borrego formation). Together, the sequence has been subsequently deformed, folded and cut by transcurrent cross-faults (i.e. Inspiration Point fault) that show left-lateral separation.

This location marks the epicenter of the 1954 Santa Rosa Mountains Earthquake which measured 6.2 on the Richter Scale. Leave vehicles and look at the fault scarp on the north side of S-22. Here, the Clark fault side-steps left from the Truckhaven Rocks, crossing the highway as three normal fault-scarp remnant features cutting the gravelly terrace of the alluvial fan surface in a northwest-southeast direction. Southward, the termination of the Clark fault in surface trace is caused by a complex basement-cover decollement. The over-riding cover of Quaternary sediments is being progressively deformed into a series of complex asymmetric *en echelon* folds. Aftershock data indicates that a 15-17 km section of the buried fault strand ruptured to the south (Pettinga, unpubl. data). The northwest-trending Clark fault represents the easternmost branch of the San Jacinto fault zone.

Beginning on the north side of the San Gabriel Mountains, the SJFZ (Given, 1981; Hill and others, 1975; Sharp, 1967) represents a well-defined master break in the earth's crust, part of the San Andreas fault system which has long been recognized as the major transform lithospheric plate boundary between the North American and Pacific plates. The SJFZ has a well-documented recent history of seismicity (Allen and others, 1972; Thatcher and others, 1975). It has a measured length of approximately 180 miles. In Anza Borrego this through-going fault zone consists of many smaller strands and *en echelon* lineaments that network between major zones of displacement. Some of the most spectacular examples of fault-related landforms along the Santa Rosa Mountains include numerous graben, pull-apart, pop-up and pressure ridges. Primary topographic expressions are sharp and clear, accompanied by crushed zones of crystalline basement rock, aligned canyons and arroyos, beheaded, deflected and offset drainages, linear fault-line escarpments that can be traced for miles, Holocene quake swarms, slumping and landslides, alignment of hot springs and sag ponds, and numerous recorded earthquakes.

As a rule, large-scale movements have been right-lateral, strike-slip. Cumulative right separation is about 24 km (Sharp, 1967). There is also a vertical component. Large earthquakes, registering M6 or greater on the Richter Scale (Sanders and others, 1986; Rasmussen, 1982) occur along the SJFZ on an average every 8 years. The last recorded event was the major twin earthquakes, measuring 6.2 and 6.6 respectively on November 23 and 24, 1987, along the Superstition Hills fault (Kahle and others, 1988). Return to vehicles.

198.9 (0.1) TURN RIGHT onto S-22; prepare to turn right into Arroyo Salado Campground.

199.3 (0.4) TURN RIGHT into Arroyo Salado Primitive Campground. It is 1/4 mile down this dirt road to the dry camp. This route is also the old Truckhaven Trail. Arroyo Salado Primitive Campground is just that: primitive. There is no water, no trash cans, and no toilet facilities. Campfires are allowed only in metal containers.

END OF DAY ONE

START DAY TWO

Meet at the bulletin board at Arroyo Salado Primitive Campground. Proceed north on Borrego-Salton Seaway S-22. Stop at pavement. Between here and Borrego Springs, we will be looking at sediments, some of which have been deformed, that lie between the Clark fault and the Coyote Creek fault, east and west branches, respectively, of the San Jacinto fault zone.

SOUTHERN SAN JACINTO FAULT ZONE

0.0 (0.0) Junction of S-22 and Arroyo Salado Primitive Campground road. Watch for cross traffic. Cautiously turn left onto S-22. Within 1/10 mile immediately TURN LEFT into sandy Ella Wash, marked with a "restricted area" sign.

0.1 (0.1) This short sandy arroyo is named after Ella Calvert, the wife of ABDSP's first park supervisor. Proceed southwest down Ella Wash. This arroyo has been incised into a relic alluvial geomorphic surface washed basinward from the fan-frayed Santa Rosa Mountains. The alluvial fan ranges in age from approximately 7-13 ky (Onken and Rathburn, written comm. 1988).

0.7 (0.6) **STOP 1. Shutter Ridge.** Park and walk west to east end of ridge. faulting associated with the nearby Clark fault has raised, rotated and deformed older alluvial sediments, dipping 36 degrees to the southwest. Exposed here, ca. 800 feet above sea level, Pettinga (p.c. to Remeika, 1990) discovered two strata of calcareous tufa-covered boulder deposits similar to those seen at the base of the section at Manix Lake. Although these may record evidence of a pluvial lake that possibly existed prior to Lake Cahuilla within the Salton Trough, the cover of coarse sands and gravels suggests fluvial deposition. The two distinctly layered cobble beds occur, *in situ*, with thin imbricating laminae of microcrystalline calcium carbonate encrusting alluvial clasts. The presence of calcareous tufa strandlines is an interesting feature and may not only document the existence and desiccation of a vanished lake(?) but shows a combination of tectonism, Quaternary glacial-interglacial climatically-induced warming and increased aridity were fundamental variables in the desertification of Anza Borrego prior to the terminal Pleistocene (Remeika 1991a). Return to vehicles. CONTINUE SOUTHWEST, down wash.

1.4 (0.7) Steeply-dipping beds of the Inspiration Wash Member of the Ocotillo formation.

1.6 (0.2) T-intersection with Palo Verde Wash. TURN RIGHT (northwest) and follow the main wash.

1.8 (0.2) Junction with Palo Verde Wash on right, at post. Stay in the main wash (Short Wash) as it veers left, and proceed up Short Wash. Tentatively assigned strata of the Short Wash Member of Pettinga (in press) make up cliff exposures. These beds, representing Fault Block B, are a time-equivalent to the Inspiration Wash Member (Fault Block A) but come from a different source area.

2.0 (0.2) Hidden Canyon Wash on right. Along Short Wash, the Short Wash Member overlies the distal sandstone tongue of the Mammoth Cove Sandstone. Good exposures occur between Inspiration Wash and Font's Wash, striking eastward through Short Wash and lower Palo Verde Wash. Here, sediments consist of a mixed composition sequence of alternating light gray to salmon-brown sandstones and siltstones, well indurated buff-colored sandstones with pebbly gravels, and an occasional greenish lacustrine claystone interbed. Within the claystones, ripple drift cross lamination and mudcracks are common. The majority of sandstones are fine to medium-grained, well to moderately well sorted, with occasional coarse-grained interbeds. Granule, pebble, and torrentially-bedded conglomeratic sandstones are common, reflecting a locally-derived alluvial source area.

2.4 **(0.4)** Cross intra-terrane transcurrent fault. This oblique slip structure connects two anticlinal folds on opposite sides of Short Wash: Fault Wash Anticline on the south and Hidden Canyon Anticline on the north.

2.5 **(0.1)** Junction with Fault Wash on the left.

3.4 **(0.9)** Junction of Short Wash Trail on the right. At the signpost, continue straight toward the tamarisk tree, destination Vista del Malpais.

3.6 **(0.2)** Park at the tamarisk tree. **STOP 2: Vista del Malpais.** Hike 1/2 mile southwest along tributary arroyo (an established roadway) to Vista del Malpais overview. Atop the Ocotillo Rim, Vista del Malpais affords an excellent view of the state park and the eastern Borrego Badlands sedimentary section. To the south are the Vallecito-Pinyon, Fish Creek and Superstition Mountains. In the middle distance are the laterally offset buttes of Borrego Mountain.

Northwest, the overall physiographic feature is anticlinal with the fold hinge plunging northeastward in the vicinity of Valle Escondido. The SW-NE steeply-dipping Valle Escondido cross-fault, perpendicular to the strike of the main bounding Coyote Creek fault, has thrust and dramatically folded Plio-Pleistocene strata along the east-dipping limb of the anticline. The southwest edge of this anticline coincides with the surface break termination of the major 1968 Borrego Mountain seismogenic rupture. At present, the kinematic relationship of the cross-fault remains unresolved.

Directly below, the vista takes in much of the Borrego formation of Taret and Holman (1944) and Dibblee (1954, 1984). The mudhill exposures consist of a thick reddish-brown lacustral/brackish water basinal sequence of interbedded light-gray to red claystones with typically light yellow-gray to pale orange siltstones and sandstones. Also note the presence of the green playa claystone marker bed that overlies a Mammoth Cove Sandstone interbed. The Borrego beds locally grade downward into the proximal delta-plain facies of the Diablo formation. For the most part, the lacustral terrigenous sediments are compositionally distinctive (Merriam and Bandy, 1965; Muffler and Dow, 1968; Van De Kamp, 1973; Winker, 1987; Remeika, 1991b) and are easily recognized in the nonmarine stratigraphic package of the Borrego Badlands.

The quartz-rich siltstones and sandstones are moderately well to very well sorted, ranging from fine to very fine-grained. Mica is scarce or absent. Winker (1987) reported that the reddish coloration of the sediments represents the original ferric-oxide content of suspended load material of the ancestral Colorado River and appear very similar to Diablo overbank deposits. The depositional environment of the Borrego formation may, in fact, represent a distal, lower energy lacustrine facies to the Diablo formation. Basinward, in the vicinity of the San Felipe Hills and Ocotillo Badlands, the Borrego formation is succeeded by the younger Brawley formation.

The mixed lacustrine, brackish-water microfauna is represented by *Pisidium* cf. *P. compressum*, *Tryonia* sp., *Planorbella tenuis*, *Physa virsata*, *Fontelicella* sp., *Gyraulus* sp. cf. *G. parvus*, *Anodonta* sp. cf. *A. californiensis*, *Elphidium gunteri*, *Nonion saltonensis*, *Streblus sobrinus*, *S. tepidus*, *Chara oogonia*, reworked foraminifera and twig-sized fragments of petrified wood (Wagoner, 1977; Dibblee, 1954, 1984; Winker, 1987). Due to its stratigraphic position, it is believed to be upper Pliocene to middle Pleistocene in age.

Above the Borrego redbeds, the Mammoth Cove Sandstone Member of the Ocotillo formation figures quite prominently within the Neogene lithostratigraphic record of the Borrego Badlands. Sandstones are compositionally distinct from the finer-grained terrigenous detritus of the ancestral Colorado River and are regarded as a localized basin-margin clastic unit. Clasts reflect a locally-derived source area, attributed to plutonic granodiorites, quartz diorites and quartz monzonites of the Peninsular Range Batholith (Todd and Shaw, 1979) and, to a lesser extent, quartz-rich carbonate metasediments from the Santa Rosa, Coyote and San Ysidro mountain ranges (Simpson, 1984).

The Mammoth Cove Sandstone is clearly differentiated into sheetflood deposits, represented by lenticular bands of granule-to-pebbly conglomerates and sandstones with thin overbank sequences of finer-grained, biotite-rich sands and silts. Sedimentary structures such as crossbedding, parallel bedding, climbing ripple lamination and poorly-imbricated gravel are compatible with other distal alluvial fan-fluvial systems. Scheuing (unpublished data) estimates an average sedimentation rate of .55 km/MY. Winker (1987) reports that framework-grain compositions consist of subequal amounts of quartz and feldspar. Plagioclase constitutes 62%-85% of the total feldspar content. Biotite ranges from 11% to 32% of the framework grain size. At cliffside, fresh exposures tend to be gray, olive-gray or tan in coloration. Weathered surfaces may range from brown to yellowish-tan.

Basinward (east), the Mammoth Cove Sandstone laterally pinches out, overlain by younger Short Wash Member. Regionally, coeval sediments have been reported from the Coyote Badlands (Sharp and others, 1972) and Mecca Hills (Babcock, 1974). Return to vehicles and retrace to junction with Short Wash Trail.

3.8 (0.2) Turn left (north) onto Short Wash Trail.

4.1 (0.3) For the next 0.4 mi, wash exposures consist of red-brown Font's Point Sandstone. It is fluvial in aspect, subaerially-deposited, braided stream strata of distal alluvial fans. Note overbank deposits, carbonates, soil horizons with disseminated carbonate nodules, and erosion surfaces suggesting a variety of depositional environments.

4.9 (0.8) Climb dirt roadway to top of mesa.

5.1 (0.2) TURN RIGHT (north) at junction with Thimble Trail, destination S-22. Short Wash Trail would proceed west to Font's Wash. We are driving on the surface of Font's Point Sandstone deflated to the depth of the pedogenic carbonate. Thimble Trail traverses fault-controlled topography produced by Quaternary activity along the master Clark fault.

5.3 (0.2) Cross a scarp and shutter ridge of Font's Point Sandstone. View southeast reveals complexly-folded Hidden Canyon strata of undifferentiated Ocotillo formation with Borrego formation exposed in the middle of the anticlinal fold, detached at a very shallow depth. Surface faulting/folding throughout the Borrego Badlands may account for the majority of displacement along the Clark fault beneath the Palo Verde-Arroyo Salado area.

6.1 (0.8) Saddle between shutter ridges.

6.5 (0.4) Road crosses a relatively uneroded closed graben. Ahead, the northwest-trending steep-walled ridgeline is one of a population of *en echelon* shutter ridges developed adjacent to the Clark fault. Multi-stranded fault scarps indicate that this portion of the badlands is presently undergoing fault-parallel shortening accommodated by folding and faulting in response to strike-slip and irrotational-slip movements on the master fault. These strands terminate to the northwest against the Inspiration Point cross-fault.

6.9 **(0.4)** Roadway descends to the desert floor. Across the highway, at 10:00, Lute Ridge is riveted with right-lateral, sinistral shear and oblique normal faults. At 12:00 note the significant number of large-scale late Quaternary offset landform features directly east of Lute Ridge, along southern fan-frayed base of the Santa Rosa Mountains. Multiple fault scarps, laterally offset stream channels and fans, banks and bars, and deflected drainage lines apparent at the surface show geologic recency of movement. Horst and graben structures appear between fault scarps.

7.2+ **(0.3)** STOP at the pavement of Borrego-Salton Seaway, S-22. Carefully TURN LEFT. Immediately to the north is the old Truckhaven Trail. Built in 1929 by A. A. "Doc" Beaty, this historic route connected Borrego Springs with the Coachella Valley. Construction was accomplished by volunteer labor, hand tools, horses, and mule-drawn scrapers.

8.1 **(0.9)** Milepost marker 31. On the right, hidden from view on the southwest flank of Lute Ridge, is an underground seismograph recording station. Located throughout the SJFZ a battery of instruments--accelerometers, creepmeters, strainmeters, tiltmeters, leveling lines, geochemical sensors, magnetometers, and a dense network of seismometers--measure and record fault movements (Remeika and Lindsay, 1992).

9.0 **(0.9)** Santa Rosa Mountains roadside pullout on the left.

9.1 **(0.1)** Milepost marker 30.

9.3 **(0.2)** To the right the closed triangular tectonic basin of Clark Valley (elevation 400' above sea level), sandwiched between Coyote Mountain on the west and the Santa Rosa Mountains on the north and east (Fig. 18), represents a dynamic pull-apart structural basin controlled by master strike-slip faults (Clark, Coyote Creek and Coyote Mountain Frontal) within the SJFZ. The margin between Clark Valley and the Santa Rosa Mountains is discretely marked by the Clark fault which lies beneath Holocene alluvium of the Clark's Dry Lake depocenter. The basin presumably formed during the clockwise rotation of the Borrego Badlands away from the irrotational Coyote Mountain block (Scheuing, written comm. 1987). In 1986, geodetic measurements in Clark Valley included a resurvey of benchmarks installed prior to 1969. Hudnut and Seeber (1987) report astroazimuth investigations produced evidence for clockwise rotation of the basin (5±3 microradians per year) and for right-lateral deformation on the Clark fault.

Reflecting the recency of crustal movements, the desert here is actively splitting open, being extended as it undergoes rapid subsidence, rotation and tilting, part of a widening oblique transform motion within the fault zone (Nicholson and Seeber, 1989). There are no foothills. Fault scarps are everywhere. Seismic activity, always persistent, continues to occur. Note the abandoned building in the middle of Clark's Dry Lake. This structure once served as the Clark Lake Radio Observatory. It marks the epicenter of the 1969 M5.9 Coyote Mountain Earthquake. Aftershocks of this event were restricted to depths of between 10-14 km (Thatcher and Hamilton, 1973). Focal mechanisms define an elongated high-angle left-slip cross-fault whose major axis was oriented northeasterly (Peterson and others, 1987).

9.8 **(0.5)** Cross Font's Wash.

10.1 **(0.3)** Milepost marker 29.

10.3 **(0.2)** At 1:00 Coyote Mountain (elevation 3192' above sea level) represents a fractured, elongated block of metasediments and minor granitics that has been dramatically uplifted along the active Coyote Creek fault on its western side. The eastern face is likewise bounded by the Coyote Mountain Frontal fault. Note triangular facets developed in bedrock. These tectono-geomorphic features are reliable criterion of active range-front faulting. Also note steep profiles of immature alluvial fans. Their steepness strongly reflects basin dropping relative to mountain uplift. Older fans are covered with a modest coating of desert varnish.

Fig. 18. Clark Valley, viewed across Inspiration Point (center); Coyote Mountain is left, and Santa Rosa Mountains distant.

10.7 **(0.4)** Cross Inspiration Wash.

11.2 **(0.4)** Milepost marker 28. We are temporarily leaving ABDSP.

12.2 **(1.0)** Milepost marker 27.

12.3 **(0.1)** Approach unmarked Beckman Wash, a difficult turn to see. A microwave dish mounted on a tower is at 1:00 on the right. Wooden telephone pole line on right side of road. Pull to the right and stop between the first and second pole. Watch for cross traffic.

12.4 **(0.1)** Turn left across the pavement onto dirt track leading southeast. Proceed south along unmarked Beckman Wash loop drive.

12.5 **(0.1)** We are driving on Font's Point Sandstone surface that gently dips north to northwest.

13.9 **(1.4)** Re-enter ABDSP.

14.5 **(0.6)** To the left (east) bluff exposures preserve angular unconformity near top of the Inspiration Wash Member. The resistant caprock of Font's Point

Sandstone is younger than 0.37 MYA. Font's Point sandstones can be differentiated from underlying beds on the basis of stratigraphic position, presence of caliche-mottled horizons, and absence of fossils. Additional evidence for syndepositional deformation includes clastic dikes, intraformational unconformities, discordance in bedding dip across bedding planes, thrust faulting in fold hinges (Mammoth Cove) and chaotic folding suggesting liquefaction.

14.6 (0.1) Possible Bishop Tuff bed in saddle to the left. Road bears left. White beds to the left may be reworked tuff.

15.0 (0.4) Saddle. Proceed over south lip of saddle. Fossiliferous overbank sediments include finer-grained siltstones and claystones of the Inspiration Wash Member.

The Inspiration Wash Member in the westernmost Borrego Badlands (Fault Block A) overlies the distal tongue of the Mammoth Cove Sandstone Member and a thin unnamed lacustrine unit. Between Arroyo Otro (to the east) and Beckman Wash, it consists of about 200 m of fluvially-deposited terrestrial floodplain facies of interbedded sheetflood gravelly sandstones and fine-grained overbank siltstones/claystones. Striking eastward, the section laterally grades into purplish-gray playa claystones of the Las Playas Member. Within the claystones, ripplemarks and mudcracks are common. Also, various-sized cameloid footprints comparable to the coeval ichnogenus *Pecorpieda (Ovipeda)* sp. cf. *Camelops* sp. have been discovered in the Arroyo Otro Claystone (Remeika, 1992a).

Diagnostic fossil vertebrates include *Smilodon gracilis*, *Gigantocamelus* sp., *Panthera atrox* and *Equus bautistensis* of the Borrego LF. A late Irvingtonian LMA is indicated. The occurrence of *Microtus californicus*, *Lepus* sp. cf. *L. californicus*, and ?*Ovibos moschatus* appear only in the youngest levels (possible early Rancholabrean LMA) above a recently discovered tephra which may correlate to the Bishop Tuff at .74 MY (Izette, 1981) marking the Matuyama-Bruhnes geomagnetic boundary. Depending on the time scale used, the base of the ABDSP Irvingtonian is between 1.6-1.9 MYA with the transition between Irvingtonian-Rancholabrean at .35-.45 MYA.

At present, interdisciplinary studies continue on the Borrego LF and its host sediments. Stratigraphic revision and correlation between Fault Blocks A and B, vertebrate biostratigraphy, magnetostratigraphy and tephrochronology of the local Borrego Badlands section will greatly enhance its importance in the Pleistocene history of western North America.

15.1 (0.1) South side of road is a resistant cemented arkosic sandstone marker bed that holds up the Ocotillo Rim above Mammoth Cove. Drive over dipping resistant sandstone and PARK near canyons running south to Mammoth Cove Overview.

STOP 3. Leave vehicles and walk south for view of the Mammoth Cove sedimentary sequence (Fault Block A) and deformation fabric beneath the Ocotillo Rim. Landscape of the small drainage basin of Mammoth Cove is characteristic of arid regions undergoing seismogenic crustal tectonics and extreme denudationary processes. Highly-eroded tan-gray crossbedded and massive sandstones are Mammoth Cove Sandstone Member of the Ocotillo formation. Closely coupled to the strike-slip Coyote Creek fault, several high-angle cross-faults indicate contractional Quaternary tectonism in the deformation process of strain rotation. Folding is gentle to isoclinal. Fault-parallel shortening, discretely shown by northeast-trending tightly-folded lacustrine evaporites of the Borrego formation may demonstrate the presence of a detachment surface at shallow depth, suggesting a conjugate relationship that allows fault blocks to decouple and rotate on cross-faults. Previous published paleomagnetic investigations confirm that a clockwise rotation has occurred in the Borrego Badlands (Bogen and Seeber, 1986; Schueing and others, 1988). Scheuing (unpublished data) has documented block rotation of 23±13 degrees and 37-40 degrees for Mammoth Cove, depending on the relative age of the sediments; older Borrego sediments show twice the rotation observed than for the Ocotillo formation. Return to vehicles and proceed west.

15.3 (0.2) ABDSP boundary sign.

15.4 (0.1) Turn right (east) up unnamed tributary wash.

15.7 (0.3) STOP 4. Bishop Tuff. Park at end of wash. Inspiration Wash Member exposures to the north contain 6-inch thick bed of white ash which may represent the middle Pleistocene Bishop Tuff (Geochron labs, in progress 1993) derived from the Long Valley-Glass Mountain Center in eastern California. Within the Salton Trough, the Bishop Tuff is reported from the Mecca Hills (Babcock, 1974; Rymer, 1991) and Coyote Badlands. Contemporaneous Bishop Tuff exposures (Fryant Ash Member) in the Coyote Badlands are defined by five closely-spaced ashfall beds fingerprinted in Ash Wash (Miller, pers. comm. to Remeika, 1985). Identification of the ash was based on its chemical composition (Sarna-Wojcicki, pers. comm. to Remeika, 1984). The Coyote Badlands are inferred to be right-laterally displaced from the western Borrego Badlands along the strike-slip Coyote Creek fault. Beckman Wash samples are in the process of being geochemically examined (Reynolds, pers. comm. 1993). Return to Beckman Wash.

16.0 (0.3) TURN RIGHT at Beckman Wash.

16.8 (0.8) Last outcrop of Font's Point Sandstone. We are approaching approximate trace of the Coyote Creek fault projecting south from the west side of Coyote Mountain. Proceed down wash.

17.2 (0.4) Continue straight, avoiding ORV roads on right and left.

17.6 (0.4) Turn right out of wash and pass left of last two tamarisk trees. Then veer left (northwest).

17.7 (0.1) At tamarisk tree, turn left (west) toward cement standpipe and ruined metal water tank. Cross intersection of dirt roads. Proceed west on road 50 feet north of the water tank, destination S-22.

18.3 (0.6) Stop, turn left (south) onto S-22, Pegleg Road.

at S-22. We are on the approximate trace of the active Coyote Creek fault which runs northwest up Coyote Canyon along the western side of Coyote Mountain. The co-seismic right-lateral, strike-slip Coyote Creek fault is the major western branch of the SJFZ. On April 9, 1968, the M6.5 Borrego Mountain Earthquake hit Anza Borrego. It was a classic example of seismic triggering of a main shock, with an epicenter in the Borrego Badlands near Third Wash, and epicentral distribution of aftershocks covering a broad area around the Ocotillo Badlands-Borrego Mountain. Ground rupture occurred along 31 miles of the fault near Ocotillo Wells, terminating southwest of Vista del Malpais.

West of the Borrego Badlands, the hidden trace of the fault has been determined by magnetometer survey (Trelkeld, unpubl. data, 1984). *In situ* stress measurements along the seismogenic fault zone across the central rupture break have been made by Keller and others (1978). Using theodolite alignment arrays, they found a slip rate of about 10 mm/yr, calculating a recurrence interval of about 200 years for major events on the fault. Sharp (1981) has estimated minimum horizontal displacements along the fault zone of between 5.7 and 8.6 km during the late Pleistocene.

18.9 (0.6) View to the left, beyond white storage tank, is of highly-eroded Mammoth Cove dominated by the profile of the Font's Point promontory.

19.8 (0.9) S-22 makes a sharp right turn. We are now heading west on Palm Canyon Drive.

21.4 (1.6) Borrego Springs Airport.

22.8 (1.4) Stop sign at Borrego Valley Road.

24.3 (0.5) Christmas Circle rotary. Continue west through town of Borrego Springs on Palm Canyon Drive.

24.4 (0.1) BEAR RIGHT on Palm Canyon Drive.

25.9 (1.5) Junction with S-22 (Montezuma Valley Road) on the left. We will continue straight on Palm Canyon Drive to the ABDSP Visitor Center.

26.1 (0.2) Borrego Palm Canyon Campground entrance on road to the right.

26.2 (0.1) ABDSP Headquarters on the left.

26.4 (0.2) STOP 5. Anza-Borrego Desert State Park Visitor Center. Constructed in 1979 this underground interpretive center is designed to blend into the desert. It has exhibits on the park's natural history and cultural history. Information, literature, publications and rest room facilities are available here. Future plans include addition of the Colorado Desert Research Center, for the advancement of scientific/educational research endeavors, adjacent to the visitor center.

To the west the awesome sierran-like eastern escarpment of the San Ysidro Mountains rise behind the visitor center. These mountains are among the most impressive of Anza Borrego due to their steepness along the western edge of Borrego Valley. Indianhead (elevation 3960') is the pronounced pinnacle on the northwest skyline. Towering above Borrego Palm Canyon, it consists of a faulted and sheared metasedimentary sequence of Paleozoic marble, gneiss and quartzite resembling the suite from the Santa Rosa Mountains. Retrace route to S-22.

27.0 (0.6) TURN RIGHT (south) onto Montezuma Valley Road, S-22.

27.1 (0.1) At the upcoming bend in the road, the left-lateral strike-slip Hellhole Canyon fault has thrust the Church Spur ridge at 9:00 into Borrego Valley.

27.8 (0.3) We have reentered ABDSP at elevation 800'. At 3:00, Hellhole Canyon is a major eastward-flowing drainage cut deep into the San Ysidro Mountain escarpment.

28.2 (0.4) Exposed in the first series of double road-cuts are tightly infolded reddish-brown, angular-weathered cataclastic metasedimentary quartzite, gneiss, phyllite, marble and schist of Ordovician(?) age. These rocks have been drag-folded, thrust-faulted and deformed by a late Cretaceous west-vergent overthrust system (Simpson, 1984; Schultejann, 1984; Hamilton, 1978).

Montezuma Grade was built in 1963. This 11-mile roadway represents a classic "palms to pines" highway. From Borrego Springs to Ranchita, this byway ascends through three plant life zones. The Lower Sonoran Life Zone of the desert floor is characterized by mesquite, cat claw, smoke tree, indigo, California fan palms and creosote bush.

28.8 (0.6) Milepost marker 16.

29.4 (0.6) Entering the Borrego Springs Mylonite Zone (BSMZ) of the Eastern Peninsular Ranges Mylonite Zone (EPRMZ) of Sharp (1979). Vertical cliffs of highly-fractured plutonic rocks are deformed into a penetrative tectonic fabric of protomylonite, S/C mylonite and ultramylonite (Simpson, written com. to Remeika, 1992) exposed in double road cuts.

29.5 (0.1) Milepost marker 15.

30.0 (0.9) Milepost marker 14.5

30.4 (0.4) Milepost marker 14

30.8 (0.4) Dry Canyon on the left (south). The Upper Sonoran Life Zone is represented here on the rocky desert slopes by an ocotillo, agave, barrel cactus and cholla xerophytic assemblage. Keep an eye out for the elusive desert bighorn sheep *(Ovis canadensis cremnobates)* that inhabit the rough eastern slopes of the San Ysidro Mountains.

31.9 (1.1) In double road cuts, foliated and lineated plutonic rocks have undergone mylonization at greenschist facies (Simpson, 1985). At present, the precise age of extension-related ultramylonite and cataclasite deformation in the BSMZ remains uncertain.

32.2 (0.3) Crawford Overlook (elevation 2300') to the left (east) is the most easily accessible viewpoint in ABDSP. To the north stand two NW-SE trending mountain ranges: the Santa Rosa Mountains reach elevations above 8000', and closer at hand, the lesser ridgeline of Coyote Mountain. Both ranges are bounded by active fault strands that delineate the major SJFZ. Eastward sprawl the Borrego Badlands. Beyond, on a clear day, the low-lying Salton Sea and Chocolate Mountains can be seen, 28 and 53 miles away, respectively.

32.6 (0.4) Milepost marker 12

33.2 (0.6) Leaving the BSMZ boundary. The geology along the highway ahead consists of spheriodally-weathered bouldery exposures of medium to coarse-grained late Cretaceous plutonic rocks (Ranchita Pluton) of the Peninsular Ranges Batholith. Crystallization of the tonalitic pluton occurred at 94-93 MYA (Silver and others, 1979).

33.6 (0.4) Milepost marker 11.

34.6+ (1.0) Milepost marker 10.

35.4+ (0.8) Culp Valley Primitive Campground on the right (north). 35.8(0.4)Double road cuts ahead consist of freshly-exposed undecomposed tonalitic core rock. Note lighter-colored pegmatite dikes coursing throughout the countryside.

36.7 (0.9) Milepost marker 8.

36.8 (0.1) Chaparral plant community. Chaparral is a densely-spaced, wood-scrub botanical community with over 150 species of plants. Examples here include yucca, toyon, manzanita, mountain lilac, ceanothus, scrub oak, laurel sumac, buckwheat, chamise and red shank. They all grow together as a stunted elfin forest about 3-8 feet above the ground.

37.8 (1.0) Milepost marker 7.

38.3 (0.5) Leaving the ABDSP boundary at the mountain crest (4275' above sea level). To the north is the pine-clad, saw-tooth ceiling of the San Ysidro Mountains, part of the Los Coyotes Indian Reservation.

38.8 (0.5) The highway crosses the mature tableland and oak-grown canopy of the Montezuma Valley. This old erosional surface has been mentioned in Ellis and Lee (1919), Sauer (1929), Miller (1935), Larsen (1948), Gastil (1961) and Minch (1970). It forms an extensive intermontane plateau over much of Montezuma Valley developed on mid to late Cretaceous granodiorite. According to Minch, (1970, 1979), this erosional surface formed as a result of unroofing of the Peninsular Ranges Batholith (late Cretaceous) and before the Miocene opening of the Gulf of California.

39.6 **(0.8)** Ranchita city limits.

ELSINORE FAULT ZONE

42.3 **(2.7)** Cross the trace of the San Felipe fault (part of the Agua Caliente fault Zone). We are entering a zone of anastomosing faults which include the Agua Caliente fault (on the east) and the Elsinore fault zone (on the west). The San Felipe fault extends southward from Warner Springs along the western margin of Montezuma Valley following Grapevine Canyon down across the southern edge of Pinyon Ridge to The Narrows of ABDSP.

43.0 **(0.7)** Milepost marker 2.

43.9 **(0.9)** Cross Pacific Crest Trail.

44.5 **(0.6)** Quartz monzonite and dikes are exposed in road cut.

45.0 **(0.5)** T-intersection with County Highway S-2 (end of S-22). TURN RIGHT (north) on S-2. For the next 5 miles, this highway segment closely follows the historic route of the Butterfield Overland Mail (1858-1861).

46.0 **(1.0)** Palomar Observatory is visible ahead, on ridgeline.

46.8 **(0.8)** Note arkosic sediments in road cut.

47.5 **(0.7)** Ruins of the post-Butterfield Kimble-Wilson Store, built in 1866, are at 2:00.

49.0 **(1.5)** To the right is the historic Warner Ranch House which served as a Butterfield stage way-station during 1858-1861 (Hill, 1927).

49.9 **(0.9)** Stop at T-intersection with State Highway 79 (end of S-2). **TURN RIGHT**, destination Warner Springs and Temecula. We are crossing terraces of old Pleistocene alluvium. We are in the Elsinore fault zone; the steep escarpment of Angel Mountain in the Santa Ysabel range (southwest) marks the trace of the Elsinore fault. Lake Henshaw (directly ahead, but not visible from this vantage point) is drained by the San Luis Rey River which runs north around Pine Mountain, then southwest to reach the Pacific Ocean at Oceanside. The Peninsular Range batholith to the southwest (Walawender and others, 1991) contains Pre-Cretaceous metasedimentary roof pendants. Note cross-bedded sands and gravels in upcoming road cuts.

51.7 **(1.8)** View north across valley showing dissected arkosic sediments between the Agua Tibia fault on the left (west) and the Agua Caliente fault on the right (northeast). The Agua Tibia fault runs northwest through Barker Canyon, separating granitic basement rocks of Aguanga Mountain (east) and Palomar Mountain (west).

53.4 **(1.7)** Bear northwest (left) at Warner Springs. The Agua Caliente fault zone is on the right (northeast).

53.7 **(0.3)** Pass Stage Road.

55.2 **(1.5)** Arkosic sediments overlain by gravels in road cut.

57.2 **(2.0)** The terraced sediments between the Agua Caliente fault zone (northeast) and the Agua Tibia fault zone (southwest) have been dissected in response to lowering of base level, perhaps in response to fault activity. Note paleosols within arkosic sediments. Fracture planes in road cuts strike west-northwest and dip 70 degrees east.

62.1 **(4.9)** Sunshine Summit, elevation 3277'. To the southwest is the scarp of the Agua Caliente fault zone. Drainage is northwesterly into Temecula Creek and the Santa Margarita River near the junction of Highway 79 and I-15. We are passing from one drainage basin, the Lake Henshaw basin of the San Luis Rey system, into the drainage of the Elsinore trough.

64.4 **(2.3)** Chihuahua Valley Road. Pegmatites to the right have yielded herderite (see Ordway, this volume).

67.5 **(2.9)** Oak Grove. Historic stage station.

68.0 **(0.5)** Historic marker for Camp Wright, 1861 to 1866. Established on Warner's Ranch to guard the communication between California and Arizona, it was named for Brigadier General George Wright, commander of the Pacific Department and California District at the time. It was actually commanded by Major Edward Rigg of the First California Volunteers.

69.4 **(1.4)** We are driving on an erosional surface of deeply weathered granitic rocks.

71.9 **(2.5)** Road cut exposes Plio-Pleistocene? green arkosic sands on top of the deeply eroded granitics.

73.0 **(1.1)** Cross north of the Aguanga fault at switchbacks on the east side of the valley which forms a boundary between Temecula Arkose and crystalline rocks (see Reynolds and Reynolds, this volume). The first outcrops of Temecula Arkose we will see are past the next stop sign.

74.1 **(1.1)** Junction of Highway 371 at Aguanga (Hill, 1947). Continue west on Highway 79.

74.2 **(0.1)** Stop sign at Highway 371. Continue on Highway 79.

77.4 **(3.2)** Road cut exposes paleosols in the Temecula Arkose (Fig. 19).

Fig. 19. Paleosol near Radec indicates slow soil deposition; it is overlain by the fast-deposited Temecula Arkose.

Fig. 20. Temecula Arkose overlaps an erosional surface at the entrance to Shamrock quarry.

78.0 (0.6) Radec Junction. Proceed on Hwy 79.

79.1 (1.1) STOP 6. Shamrock Rock Quarry. EXIT RIGHT to Shamrock Rock Quarry. Park near the sand and gravel quarry entrance. Here we see the Temecula Arkose onlapping over an erosional surface developed on the Aguanga tonalite (Fig. 20) (Mann, 1955). Reynolds and Reynolds (this volume) discuss the early Blancan age of the Temecula Arkose and its vertebrate fauna. The Oak Mountain landslide complex (Fig. 21) (Hart, 1991) is to the west-northwest and Oak Mountain can be seen through the gate to the rock quarry. The landslide rests on the Temecula Arkose and thus is younger. It is along the Lancaster fault on the north side of Aguanga Basin. Notice also the scarp of the Aguanga fault to the south. RETURN to pavement.

79.2 (0.1) TURN RIGHT (west) onto Highway 79.

79.3 (0.1) Temecula Creek.

80.2 (0.9) Look to the northwest (right) toward Vail Lake for a view of the Oak Mountain landslide (Hart, 1991). Volcanic rocks are rare in the Peninsular Range. Vail Mountain is west of Vail Lake and southwest of Oak Mountain. The basalts of Vail Mountain have been dated at 8.3 Ma and 7.7 Ma (Kennedy, 1977) and thus should predate the Temecula Arkose. The Santa Rosa basalts to the west are discussed at milepost 95.0.

81.5 (1.3) Dripping Springs campground. Mann (1955) maps the coarse-grained Dripping Springs formation (to the south) as overlying the Temecula Arkose and the Pauba formation.

81.9 (0.4) Red soils and lag gravels for the next 0.2 miles are developed on the Dripping Springs formation.

84.0 (2.1) Pedogenic carbonates developed in soil horizons within the Temecula Arkose.

84.7 (0.7) Pauba Road junction. Proceed through junction with Pauba Road.

85.0 (0.3) View north of terraced Pauba formation, deposited and subsequently dissected by Pauba Creek.

86.6 (1.6) Cross the Temecula River. Highway 79 bears westerly through Pauba Valley.

89.5 (2.9) Pauba Mesa localities are due north of highway, where development exposed vertebrate fossils in the Pauba formation. Inset pond sediments contained wood dated at 33,000 ybp. McDonald (this volume) discusses sloth remains found here.

91.1 (1.6) Stop sign and view of Santa Rosa Plateau. From northwest to southeast, drainages of the Elsinore trough include Murrieta Creek, Warm Springs Creek, Tucalola Creek, Santa Gertrudis Creek, Temecula Creek, and Pechanga Creek. These join to form the Santa Margarita River which cuts the antecedent Temecula Gorge through the granitics comprising the Santa Rosa Plateau, straight ahead to the west. The Santa Margarita River empties into the Pacific at Oceanside. Proceed on Highway 79.

91.8 (0.7) ENTER I-15 FREEWAY, heading north.

95.0 (3.2) Move to left lanes of freeway. We are driving parallel to the Wildomar fault on the east side of the Elsinore fault zone. The

Fig. 21. Landslide debris are shed southward from Oak Mountain (peak at right) over Temecula Arkose.

scarp on the west side of the Elsinore fault zone is the Willard fault, at the base of the Santa Rosa Plateau. Basalts at Vail Mountain (milepost 80.2) range in age from 8.3 to 7.7 Ma (Kennedy, 1977). The Santa Rosa Basalts, on top of the Santa Rosa Plateau (Mesa de Burro) to the west and within the Elsinore fault zone, date from approximately 9.9 Ma to 11.0 Ma. Kennedy (1977) notes that these basalts have dropped vertically 300 m, and as deep as 1000 m, within the Elsinore trough on the east side of the Willard fault. However, there seems to be only 100 m difference in overall elevation of basalts that date to around 11 Ma (Kennedy, 1977) across the Elsinore trough between the Santa Rosa Basalts on the west (elevation 600 m) and basalts at the Hogbacks (elevation 500 m) to the east of I-215.

We are now passing through Plio-Pleistocene sediments (the unnamed sandstone and overlying Pauba formation) that have been truncated by a terrace at approximate elevation 1200' (400 m).

96.6 (1.6) TAKE I-15 northwesterly at the junction of I-215/I-15.

97.5 (0.9) Murrieta Hot Springs Road. Springs occur northeast along the trace of the Murrieta Hot Springs fault, an east-west fault which joins the Wildomar fault east of California Oaks Road.

98.5 (1.1) Proceed past California Oaks Road.

99.2 (1.5) Chaney Hill, to the left (southwest) contains the Bishop Ash (740,000 ybp) (Kennedy, 1977). Datable ashes and faunas allow determination of the timing of deposition of sediments in basins between faults in inland southern California.

100.7 (1.5) EXIT FREEWAY at Clinton-Keith Road.

101.0 (0.3) STOP, turn right onto Clinton-Keith Road and proceed to Nutmeg.

103.0 (2.0) As you merge left, prepare to turn right.

103.2 (0.2) TURN RIGHT on Nutmeg and proceed south to Jackson. Dark diorite and gabbro of the Southern California Batholith are to the left.

103.7 (0.5) Leave granodiorite and enter the unnamed sandstone formation.

104.3 (0.6) Stop sign. TURN LEFT on Jackson. The Nutmeg Fauna is discussed by Reynolds and Reynolds (Reynolds and Reynolds, 1991, revised in this volume).

104.8 (0.5) Cross over east-trending fault that separates mid Pliocene Blancan from late Pliocene Blancan LMA sediments. CONTINUE east to California Oaks Road.

105.5 (0.7) Stop sign at California Oaks Road. TURN LEFT.

105.7 (0.2) TURN RIGHT at Lincoln and stop in the school parking lot. **STOP 7. California Oaks Road**. The California Oaks area contains numerous faunas with multiple mammalian age indicators that suggest sediments were deposited in mid Blancan, late Blancan, and late Irvingtonian times. We are in an area bounded by the northwest-trending Wildomar fault, parallel to the west side of I-15, and the east-trending Murrieta Hot Springs fault, to our southeast. The relationship of the fossil localities suggest that the Blancan faunas are separated by faults which have a down-to-the-south aspect. After faulting and erosion, the Pauba formation was deposited unconformably on the unnamed sandstone (Kennedy, 1977). The school site where we are parked is in the Pleistocene sediments of the Pauba formation. RETRACE via Lincoln to California Oaks Road.

105.9 (0.2) Stop light at California Oaks Road. TURN RIGHT.

106.4 (0.5) Stop sign at Hancock.

107.0 (0.6) Cross unnamed sandstone and enter diorite of the Southern California Batholith, which here contains dark lenses of gabbro. We are leaving rocks affected by the Elsinore fault zone.

107.4 (0.4) Clinton-Keith Road. Stop, TURN RIGHT.

108.7 (1.3) ENTER 215 FREEWAY and go north toward Perris.

110.6 (1.9) View north and northeast of Perris Plain, where exposures of gabbro and tonalite have intruded and metamorphosed the Bedford Canyon formation and the Santiago Peak volcanics (Morton and Gray, 1971).

116.5 (5.9) McCall Blvd. in Sun City.

120.2 (3.7) The view to the north-northeast shows the San Timoteo Badlands below Mt. San Bernardino (left) and Mt. San Gorgonio (right).

122.0 (1.8) Continue on I-215, passing Highway 74 to Perris/Lake Elsinore. The Lake Mathews formation is 12 miles to the northwest; it contains the only Clarendonian LMA Miocene river channel deposits on the Perris Block, indicating that the erosional surface developed on granitic rocks is older than 12 million years (Morton and Gray, 1971; Proctor and Downs, 1963; Woodford and others, 1971).

126.6 (4.6) EXIT at the Ramona Expressway, heading east.

126.9 (0.3) TURN RIGHT at stop light.

128.2 (1.3) Traffic light at Perris Boulevard. At 10:00 you can see the Lake Perris dam.

129.5 (1.3) Traffic light at Center Street, with a good view of the dam.

131.0 (1.5) Pass through quartz diorite with dark xenoliths of the Bernasconi Hills (Morton and Gray, 1971).

132.0 (1.0) At 12:00, to the right of the conical butte, you can see Lakeview Hot Springs. Trees mark the site of the Deep Trench (Reynolds and Reynolds, 1991). C^{14} dates indicate that extinct Pleistocene taxa occur within 15' of the surface.

133.2 (1.2) Pass the entrance to Lakeview Hot Springs.

134.9 (1.7) Lakeview Avenue.

NORTHERN SAN JACINTO FAULT ZONE

135.8 (0.9) The Nutrilite Plant and the Southern Pacific Silica Quarry are on the right. The quarry has yielded monazite, garnet, and tourmaline. You can see badlands exposures to our east, running from due north, on the other side of the San Jacinto fault. Between Aguanga and our return to I-214, we examined the Temecula Arkose, which is early Blancan or younger (Reynolds and Reynolds, this volume). At Murrieta we saw sediments of the unnamed sandstone, of mid Blancan, late Blancan, and late Irvingtonian age, deposited within the trough of the Elsinore fault zone and on the east side of the fault zone lapping onto the weathered granitic rocks. We crossed the eroded granitic terrain of the Perris Plain and are now entering the San Jacinto fault zone. On the east side of the fault we will enter a basin between the San Jacinto fault zone and the San Andreas fault where deposition started with the late Hemphillian Mt. Eden formation (5.4-5 Ma, May and Repenning, 1982). After an erosional unconformity, the early deposition of the San Timoteo formation started in Blancan times (4.2 Ma, May and Repenning, 1982). The later (upper) San Timoteo formation continued to be deposited through the early Irvingtonian LMA, 1.901.3 Ma (Reynolds and Reeder, 1991). Although possibly separated by a granitic highland, there may have been concurrent deposition with similar faunas in both the Elsinore trough and the San Timoteo basin during the Blancan LMA.

138.1 (2.3) Bridge Street. Ordinarily, Bridge Street crosses the San Jacinto River and leads us directly to stops along Jack Rabbit Trail in the San Timoteo Badlands. At this writing, however, the river crosses Bridge Street (Fig. 22), so proceed straight ahead. (When Bridge Street is repaired, turn left and skip to milepost 151.1). The river marks the approximate trace of the Casa Loma fault.

Fig. 22. Bridge Street, crossed by the San Jacinto River, view south in April 1993.

140.4 (2.3) Stop light at Warren; continue straight ahead. The hill at 10:00 is Casa Loma, on the northeast side of the Casa Loma fault which we are crossing. We are entering a rapidly-subsiding, poorly-drained graben in the San Jacinto Valley developed on the south side of the San Jacinto fault (Morton and Sadler, 1989). In early 1993, the graben was filled with water to a depth that left only the Ramona Expressway and Gilman Springs Road passable. Rasmussen (1981) suggests that the basin is subsiding at a rate of 0.3-0.6 cm/year since the late Pleistocene, and more rapidly in the last 20 years. The San Jacinto fault zone is the most active strand of the San Andreas system (Given, 1981; Morton and Matti, 1993).

142.0 (1.6) Stop light at Sanderson; continue straight. Look southeast (12:00) to the Bautista Badlands, which are the same age as the San Timoteo Badlands. The face of Claremont Mountain (11:00) has perched terraced landslides (Morton and Sadler, 1989) developed during its history of uplift.

144.3 (2.3) TURN LEFT at traffic signal on State Highway 79.

145.7 (1.4) Cross the San Jacinto River and TURN LEFT onto Gilman Springs Road. We are traveling northwestward on the trace of the San Jacinto fault. Alluvial fans are not developed along the San Jacinto fault due to San Jacinto River sedimentation keeping pace with basin subsidence (Morton and Sadler, 1989).

148.2 (2.5) Stop sign at Sanderson. Proceed straight on Gilman Springs Road; do not follow Lamb Canyon to the right. Red beds of the lowest Mt. Eden formation can be seen along Lamb Canyon to the northeast.

Fig. 23. The graben on the south side of the San Jacinto fault is recognizable as Mystic Lake in April 1993.

151.1 (2.9) Continue past Bridge Street (left). View northwest is the graben (Mystic Lake, filled with water in early 1993) between the Casa Loma fault and the San Jacinto fault (Fig. 23).

153.1 (2.0) TURN RIGHT onto Jack Rabbit Trail.

153.9 (0.8) STOP 8. Pull out at turn to see fault contact between Mt. Eden Beds (Frick 1921) (= Mt. Eden Fm of Ferguson, 1922) and younger San Timoteo formation (Potrero Creek Deposits, Frick 1921). Clasts in the San Timoteo formation are from highlands in the Peninsular Range basement such as Mt. Eden (see Albright and Woodburne, this volume).

154.1 (0.2) STOP 9, past bend in road. The first occurrence of clasts from the Transverse Ranges occur in the San Timoteo formation at this point.

155.7 (1.6) STOP 10. Pull out at wide turnouts on east or west side of

Fig. 24. View northwest into San Timoteo Canyon drainage of the Santa Ana River. Mt. San Bernardino is distant, right.

165.9 (1.0) We cross the trace of the San Jacinto fault at Highland and reenter the San Timoteo Badlands. The Mt. Eden formation and San Timoteo formation span late Hemphillian through Irvingtonian time and record depositional and structural events between the San Jacinto fault and the San Andreas fault (Reynolds and Reeder, 1986, 1991; Morton and Matti, 1993). Note the folded sediments between the faults which form a broad, east-plunging anticline (Morton, 1978a, 1978b; Matti and Morton, unpubl. mapping).

166.8 (0.9) Cross the northwest-trending axis of the anticline.

168.5 (1.7) San Timoteo Canyon Road. Stop, TURN LEFT.

169.5 (1.0) Terraces as discussed by Kendrick (this volume) are visible as we reach Live Oak Canyon Road.

170.2 (1.2) Alessandro Blvd. Proceed on San Timoteo Canyon Road.

the hill. We are near the transition between San Timoteo formation units 3 and 4 (Matti and Morton, 1975). This is the beginning of massive northeast-dipping conglomerates alternating with well-developed soil horizons (Dibblee, 1967).

156.1 (0.4) Red paleosols become abundant.

157.0 (0.9) Cross into San Timoteo Canyon drainage. We are at a point midway between the San Jacinto fault zone on the southwest and the San Andreas fault zone to the northeast (Fig. 24). Note Pleistocene erosional surface developed prior to dissection of badland topography (see Kendrick, this volume). Five miles to the north-northwest, near two white water tanks, are Interstate 10 and County Line Road. Sediments of the San Timoteo formation in this area contain the youngest faunas (1-3 Ma) from a stratigraphically high position within the formation (Reynolds and Reeder, 1991).

157.4 (0.4) Stop, TURN LEFT onto Highway 60.

160.8 (3.4) Notice that beds exposed along the highway dip northeast.

161.4 (0.6) Beds, including well-developed paleosols, now dip southwest. We have crossed the northwest-trending axis of the anticline that is the major structural feature of the northern San Timoteo formation.

163.2 (1.8) Gilman Springs Road.

164.7 (1.5) EXIT HIGHWAY 60 to Redlands Boulevard.

164.9 (0.2) Stop, TURN RIGHT (north) onto Redlands Boulevard.

170.7 (1.5) TURN LEFT onto Refuse Road; notice terraces at 12:00.

171.3 (0.6) Pass through gate to landfill (closed at 5 P.M.)

171.5 (0.2) Cross under power lines.

171.6 (0.1) Park at County landfill weighing area. **STOP 11.** We are on surface Q1, the youngest surface studied by Kendrick (this volume). The age estimate for this surface is 27.5 ka. The landfill has completely altered the surface upslope and to the south of this site, and an age estimate based on the degree of soil development can not be determined. The slightly higher surface to the east-southeast is Q2

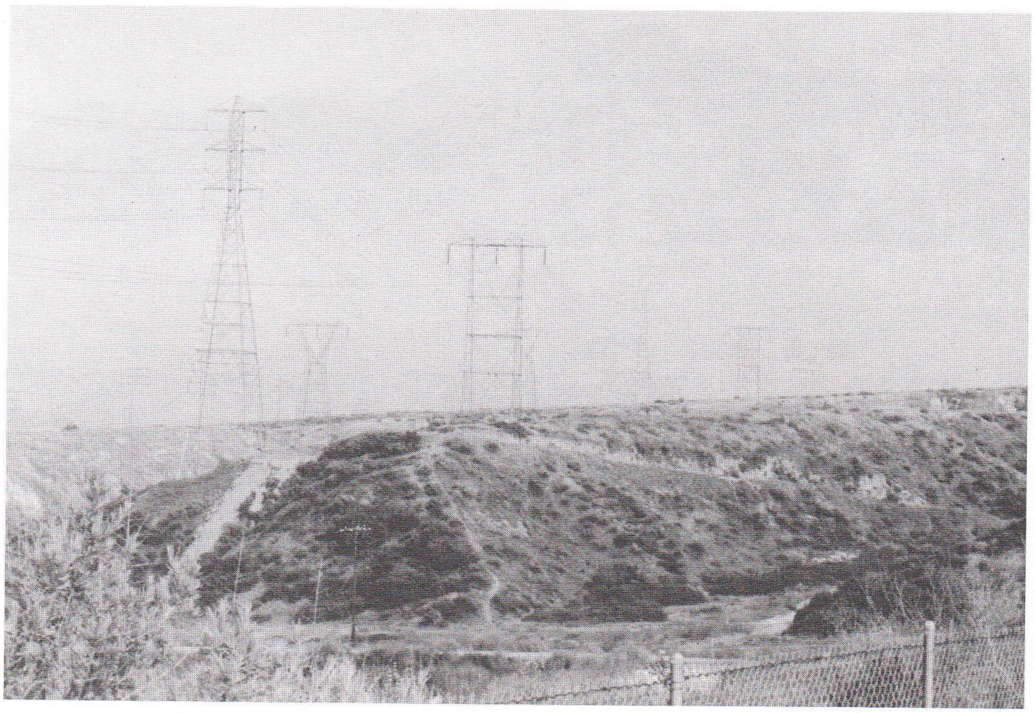

Fig. 25. Surface Q2 developed near the landfill in San Timoteo Canyon.

(Fig. 25). Both buried and surface soils are present in association with this surface. Across San Timoteo Canyon to the north, underneath the houses, is the oldest surface described by Kendrick (this volume), Q3/4. There is a good view of the buried soil from this vantage point. The surface has an overall antiform morphology, and Q4 is defined as part of the surface where the buried soil has merged with the surface soil, and represents a longer duration of pedogenesis.

RETRACE to San Timoteo Canyon Road

172.7 (1.1) Stop, TURN LEFT onto San Timoteo Canyon Road.

173.2 (0.5) Cross railroad tracks and San Timoteo Creek. San Timoteo Canyon winds its way toward Barton Road.

174.6 (1.4) Barton Road. Stop, TURN LEFT.

175.1 (0.5) California Street. TURN RIGHT.

176.1 (1.0) Redlands Boulevard. Proceed on California.

176.4 (0.3) Interstate 10 and the San Bernardino County Museum.

-- END DAY 2 --

SUMMARY

Our route has taken us through sediment-filled basins along three of the major northwest-trending fault zones in southern California: the San Andreas fault zone, the San Jacinto fault zone and, parallel and to the west, the Elsinore fault zone. Outcrops of the Bishop Ash are exposed in the Mecca Hills of the San Andreas fault zone (Rymer, 1991), in the unnamed sandstone of the Elsinore trough (Kennedy, 1977) and possibly in the Ocotillo formation (Remeika and Jefferson, this volume). The Bishop Ash has not been found in the San Timoteo formation: it may have been removed by erosion, or may never have been deposited there (Albright and Woodburne, this volume).

Ten Ma sediments of the Coachella Fanglomerate (Peterson, 1975), in the San Andreas fault zone near Whitewater, represent the earliest deposition in Banning Pass. The marine Imperial formation was then deposited along the San Andreas and the southern and possibly the northern San Jacinto fault zones (Reynolds and Reeder, 1991). Contemporaneously, the Puente formation was being deposited and appears today in the northern Elsinore fault zone.

Fluvial deposition continued in all fault zones. The Borrego formation, a marine incursion, is present in the southern San Andreas fault zone and in the southern San Jacinto fault zone in the Anza-Borrego area. Fluvial deposition continued to fill all the basins until latest Pleistocene times. However, there is apparently a pronounced erosional hiatus between the San Andreas fault and the northern San Jacinto fault in the last two-thirds of the Pleistocene after deposition of the San Timoteo fm and prior to deposition of old alluvium.

Radiometric dating of sediments in these basins depends on the presence of the Bishop Ash and of basalt flows, as well as numerous local fossil faunas which are indicators of specific land mammal ages.

ACKNOWLEDGMENTS

We thank all the authors whose papers appear in this volume for their contributions which offer supporting data for this field trip. We also thank Michael B. Moore, Richard R. Gundry, and Jed and Jennifer Reynolds for their assistance in planning the route and logging mileage intervals.

LITERATURE CITED

Allen, C.R., 1957. The San Andreas fault zone in San Gorgonio Pass, southern California. Geological Society of America Bulletin, 68:313-349.

Allen, C.R. and J.M. Nordquist, 1972. Foreshock, main shock and larger aftershocks of the Borrego Mountain earthquake. U.S. Geological Survey Profession Paper, 787:16-23.

Allen, C.R., M. Wyss, J.N. Brune, A. Grantz, and R.E. Wallace, 1972. Displacements on the Imperial, Superstition Hills, and San Andreas faults triggered by the Borrego Mountain earthquake, *in* The Borrego Mountain Earthquake of April 9, 1968. U.S. Geological Survey Profession Paper, 787:87-104.

Babcock, E.A., 1974. Geology of the northeast margin of the Salton Trough, Salton Sea, California. Geological Society of America Bulletin, 85:321-332.

Baldwin, Joel, 1986. Martinez Mountain rock avalanche, *in* Geology of the Imperial Valley, California, P.D. Guptil, E.M. Gath and R.W. Ruff (eds). South Coast Geological Society, Annual Field Trip Guidebook, 14:37-48.

Biehler, S. and R.W. Rex, 1971. Field trip no. 2, Structural geology and tectonics of the Salton Trough, southern California, *in* Geological excursions in southern California, W.A. Elders (ed). University of California, Riverside Campus Museum Contributions, 1:30-42.

Bohannon, R.G., 1975. Mid-Tertiary conglomerates and their bearing on Transverse Range tectonics, Southern California, *in* San Andreas fault in southern California, J.C. Crowell (ed). California Division of Mines and Geology Special Report, 118:75-82.

Bogen, N.L. and L. Seeber, 1986. Neotectonics of rotating blocks within the San Jacinto fault zone, southern California. Abstract, Eos Trans. AGU, 67(44):1200.

Bortugno, E. J. and T.E. Spittler, 1986. Geologic map of California, San Bernardino sheet, scale 1:250,000. California Division of Mines state geologic map.

Clark, M.M., A. Grantz, and R. Meyer, 1978. Holocene activity of the Coyote Creek fault as recorded in the sediments of Lake Cahuilla, *in* U.S. Geological Survey Misc. Investigation, 741:46.

Crowell, J.C., 1962. Displacement along the San Andreas Fault, California. Geological Society of America Special paper, 71: 61 p.

___, 1975a. Geologic sketch of the Orocopia Mountains, southeastern California, *in* San Andreas fault in southern California, J.C. Crowell (ed). California Division of Mines and Geology Special Report, 118:99-110.

___, 1975b. The San Andreas fault in southern California, *in* San Andreas fault in southern California, J.C. Crowell (ed). California Division of Mines and Geology Special Report, 118:7-27.

Dibblee, T.W. Jr., 1954. Geology of the Imperial Valley region, California. California Division of Mines Bulletin, 170(2):21-28.

___, 1964. Geologic map of the San Gorgonio Mountain quadrangle, San Bernardino County, California. U.S. Geological Survey Misc. Geological Investigations Map I-431, 1:62,500.

___, 1968. Geologic map of the Banning (15') quadrangle, California (A.R. Brown, ed). South Coast Geological Society.

___, 1977. Sedimentology and diastrophism during Oligocene time relative to the San Andreas fault system, *in* Late Mesozoic and Cenozoic sedimentation and tectonics in California, T.H. Nilsen (ed). San Joaquin Geological Society Short Course:99-108.

___, 1981. Geology of the San Jacinto Mountains and adjacent areas, *in* Geology of the San Jacinto Mountains, A.R. Brown and R.W. Ruff (eds). South Coast Geological Society Annual Field Trip Guidebook, 9:1-47.

___, 1982. Geologic map of the Banning (15') quadrangle, California. South Coast Geological Society, Geologic Map SCGS-2, scale 1:62,500.

___, 1984. Stratigraphy and tectonics of the San Felipe Hills, Borrego Badlands, Superstition Hills and vicinity, *in* The Imperial basin--tectonics, sedimentation, and thermal aspects, C.A. Rigsby (ed). Sacramento, SEPM Pacific Section:31-44.

Dokka, R.K. and E.G. Frost, 1978. Fission-track ages from the Santa Rosa Mylonite and its protolith and their relation to the cooling history of the Southern California Batholith. Geological Society of America, Abstracts with Program, 10:103.

Downs, T., and J.A. White, 1968. A vertebrate faunal succession in superposed sediments from late Pliocene to middle Pleistocene in California, *in* Tertiary/Quaternary boundary. Prague, International Geol. Congress 23, 10:41-47.

Durham, D.L. and R.F. Yerkes, 1964. Geology and oil resources of the eastern Puente Hills area, southern California. U.S. Geological Survey Professional Paper, 420-B: 62 p.

Dutcher, L.C. and W.L. Burnham, 1970. Geology and ground water hydrology of the Redlands-Beaumont area, California, with special reference to ground water outflow. U.S. Geological Survey open-file report, 1:24,000.

Elders, W.A., 1979. Historical preface: man and the nature on the Colorado Delta, *in* Geology and geothermics of the Salton Trough, W.A. Elders (ed). Geological Society of American 92nd Annual Meeting Guidebook, Field Trip 7, University of California Riverside Campus Museum Contributions, 5:v-vii.

___, 1985a. Historical preface, man and the nature of the Colorado delta, *in* Geology and geothermal energy of the Salton Trough, L. Herber (ed). Field guide, National Association of Geology Teachers, Far Western section:20-23.

___, 1985b. The Salton Trough as a delta, *in* Geology and geothermal energy of the Salton Trough, L. Herber (ed). Field guide, National Association of Geology Teachers, Far Western section:24-26.

Elders, W.A., R.W. Rex, T. Meidav and P.T. Robinson, 1970. Crustal spreading in southern California. University of California, Riverside, Institute of Geophysics and Planetary Physics Technical Report, 3: 12 p.

Ellis, A.J. and C.H. Lee, 1919. Geology and groundwaters of the western part of San Diego County, California. U.S. Geological Survey Water-supply paper, 446:15-75.

Fritsche, A.E., 1977a. Miocene paleogeography of California, *in* Late Mesozoic and Cenozoic sedimentation and tectonics in California, T.H. Nilsen (ed). San Joaquin Geological Society Short Course:

___, 1977b. Miocene sedimentation and tectonics in California, *in* Late Mesozoic and Cenozoic sedimentation and tectonics in California, T.H. Nilsen (ed). San Joaquin Geological Society Short Course:

Gastil, R.G., 1961. The elevated erosion surfaces, *in* Guidebook for field trips, B.E. Thomas, ed. San Diego, 57th Annual Meeting, Cordilleran Section, Geological Society of America:1-4.

Gastil, G., J. Kimbrogh, Y. Tainosho, M. Shimizu, and S. Gunn, 1991. Plutons of the eastern Peninsular Ranges, southern California, USA and Baja California, Mexico, *in* Geological excursions in southern California and Mexico, M.J. Walawender and B.B. Hanan (eds). Geological Society of America Guidebook, 1991 Annual Meeting, San Diego State University:319-331.

Gastil, R.G., D. Krummenacher, and J. Minch, 1979. The record of Cenozoic volcanism around the Gulf of California. Geological Society of America Bulletin Part 1, 90:839-857.

Gath, E. and others, 1986. Geology of the Salton Trough field trip road log, *in* Geology of the Imperial Valley, California, P.D. Guptil and others (eds). South Coast Geological Society Annual Field Trip Guidebook 14:181-225.

Given, D.D., 1981. Seismicity of the San Jacinto fault zone, *in* Geology of the San Jacinto Mountains, A.R. Brown and R.W. Ruff (eds). South Coast Geological Society Annual Field Trip Guidebook 9:55-60.

Grannell, R.B., 1985. Land deformation in the Salton-Mexicali trough, *in* Geology and geothermal energy of the Salton Trough, L. Herber (ed). Field guide, National Association of Geology Teachers, Far Western section:136-139.

Hamilton, W., 1978. Mesozoic tectonics of the western United States, *in* Mesozoic paleogeography of the western United States, D.G. Howell and K.A. McDougall (eds). Los Angeles, Pacific Coast Paleogeography Symposium 2, SEPM Pacific Section:33-70.

Harden, J.W. and J.C. Matti, 1992. Holocene and Late Pleistocene slip rates on the San Andreas fault in Yucaipa, California, using displaced alluvial-fan deposits and soil chronology, *in* Earthquake geology, San Andreas fault system, Palm Springs to Palmdale. Association of Engineering Geologists, Southern California section, 35th annual meeting guidebook and reprint volume:99-110.

Hart, M.W., 1991. Landslides in the Peninsular Ranges, southern California, *in* Geological excursions in southern California and Mexico, M.J. Walawender and B.B. Hanan (eds). Geological Society of America Guidebook, 1991 Annual Meeting, San Diego State University:349-371.

Herzig, C.T. and D.C. Jacobs, 1991. Late Cenozoic basaltic magmatism in the Salton Trough, *in* The diversity of mineral and energy resources of southern California, M.A. McKibben (ed). Society of Economic Geologists, Guidebook Series, 12:77-86.

Hill, D.P., P. Mowinckel and L.G. Peake, 1975. Earthquakes, active faults and geothermal areas in the Imperial Valley, California. Science, 188:1306-1308.

Hill, J.J., 1927. The history of Warner's Ranch and its environs. Los Angeles:94-111.

Hill, R.I., 1981. Field, petrological and isotopic studies of the intrusive complex of San Jacinto Mountain, *in* Geology of the San Jacinto Mountains, A.R. Brown and R.W. Ruff (eds). South Coast Geological Society Annual Field Trip Guidebook, 9:76-89.

Hillemeyer, F.L., M.D. Johnson and R.R. Kern, 1991. Introduction to the Salton Trough rift, *in* The diversity of mineral and energy resources of southern California, M.A. McKibben (ed). Society of Economic Geologists, Guidebook Series, 12:139-155.

___, 1992. Geology, alteration and mineralization of the Modoc Hot Springs gold prospect, Imperial County, California, *in* SEM-AIME fall field trip, Salton trough gold deposits:139-155.

Howell, D.C., 1975. Early and Middle Eocene shoreline offset by the San Andreas fault, southern California, *in* San Andreas fault in southern California, J.C. Crowell (ed). California Division of Mines and Geology Special Report, 118:69-74.

Hudnut, K.W. and L. Seeber, 1986. Astroazimuth geodetic measurements of block rotation in the southern San Jacinto fault zone, California. Abstract, Eos Trans. AGU, 68:287.

Hudnut, K.W., L. Seeber, T. Rockwell, J. Goodmacher, R. Klinger, S. Lindvall and R. McElwain, 1989a. Surface ruptures on cross-faults in the 24 November 1987 Superstition Hills, California, earthquake sequence. Bulletin of the Seismological Soc. Am., 79(2):282-296.

Hudnut, K.W., L. Seeber and J. Pachico, 1989b. Cross-fault triggering in the November 1987 Superstition Hills earthquake sequence, southern California. Geophysical Research Letters, 16(2):199-202.

Izett, G.A., 1981. Volcanic ash beds: recorders of Upper Cenozoic silicic pyroclastic volcanism in the western United States. Journal of Geophysical Research, 86(B11):10200-10222.

Jefferson. G.T., 1986. Fossil vertebrates from late Pleistocene sedimentary deposits in the San Bernardino and Little San Bernardino Mountains region, *in* Geology around the margins of the eastern San Bernardino Mountains, M.A. Kooser and R.E. Reynolds (eds). Redlands, Publications of the Inland Geological Society:77-80.

Johnson, N.M., C.B. Officer, N.D. Opdyke, G.D. Woodard, P.K. Zeitler, E.H. Lindsay, 1983. Rates of late Cenozoic tectonism in the Vallecito-Fish Creek basin, western Imperial Valley, California. Geology, 11:664-667.

Jorgensen, M., 1991. Paleontology resource management plan [draft]. Borrego Springs, California Department of Parks and Recreation, Colorado Desert District, ABDSP: 21 p.

Kahle, J.E., C.J. Wills, E.W. Hart, J.A. Treiman, R.B. Greenwood, R.S. Kaumeyer, 1988. Surface rupture--Superstition Hills earthquake of November 23 and 24, 1987, Imperial County,California. California Geology, 41(4):75-84.

Keller, R.P., C.R. Allen, R. Gilman, N.R. Goulty, and J.A. Hileman, 1978. Monitoring slip along major faults in southern California. Bull. Seis. Soc. Am, 63(4):1187-1190.

Kennedy, M.P., 1977. Recency and character of faulting along the Elsinore fault zone in southern Riverside County, California. California Division of Mines and Geology Special Report, 113:1-12.

Kerr, D.R., 1982. Early Neogene continental sedimentation, western Salton Trough, California. M.S. thesis, San Diego State University: 138 p.

___, 1984. Early Neogene continental sedimentation in the Vallecito and Fish Creek Mountains, western Salton Trough, California. Sedimentary Geology, 38:217-246.

Kerr, D.R. and S.M. Kidwell, 1991. Late Cenozoic sedimentation and tectonics, western Salton Trough, California, *in* Geological excursions in southern California and Mexico, M.H. Walawender and B.B. Hanna (eds). San Diego, Geological Society of American Annual Meeting guidebook:397-416.

Larsen, E.S. Jr., 1948. Batholith and associated rocks of Corona, Elsinore, and San Luis Rey quadrangles, southern California. Geological Society of America Memoir, 29: 182 p.

Maloney, N.J., 1986. Coastal landforms of Holocene Lake Cahuilla, northeastern Salton Basin, California, *in* Geology of the Imperial Valley, California, P.D. Guptil, E.M. Gath and R.W. Ruff (eds). South Coast Geological Society, Annual Field Trip Guidebook, 14:151-158.

Mann, J.F., 1955. Geology of a portion of the Elsinore fault zone, California. California Division of Mines and Geology Special Report, 43:1-22.
Matti, J.C., B.F. Cox and S.R. Iverson, 1983. Mineral resource potential map of the Raywood Flat Roadless Area, San Bernardino and Riverside counties, California. U.S. Geological Survey open-file report, 85-365:27 p, scale 1:24,000.
Matti, J.C. and D.M. Morton, 1975. Geologic history of the San Timoteo Badlands, southern California. Geological Society of America Abstracts with Programs, 7(3):344.
Matti, J.C., D.M. Morton and B.F. Cox, 1985. Distribution and geologic relations of the fault systems in the vicinity of the central Transverse Ranges, southern California. U.S. Geological Survey open-file report, 85-365: 23 p.
___, 1992. The San Andreas fault system in the vicinity of the central Transverse Ranges province, southern California, *in* Earthquake geology, San Andreas fault system, Palm Springs to Palmdale. Association of Engineering Geologists, Southern California section, 35th annual meeting guidebook and reprint volume:13-62.
May, S.R. and C.A. Repenning, 1982. New evidence for the age of the Mount Eden fauna, southern California. Journal of Vertebrate Paleontology, 2(1):109-113.
McKibben, M.A., 1991. Introduction to the Salton Trough rift, *in* The diversity of mineral and energy resources of southern California, M.A. McKibben (ed). Society of Economic Geologists, Guidebook Series, 12:77-86.
Meidav, T. and R.W. Rex, 1970. Geophysical investigations for geothermal energy sources, Imperial Valley, California. University of California, Riverside, Institute of Geophysics and Planetary Physics Technical Report, 3: 54 p.
Merriam, R. and O.L. Bandy, 1965. Source of upper Cenozoic sediments in Colorado delta region. Journal of Sedimentary Petrology, 35:911-916.
Miller, W.J., 1935. Geomorphology of the southern Peninsular Range of California. Geological Society of America Bulletin, 46:1535-1562.
Minch, J.A., 1970. Early Tertiary paleogeography of a portion of the northern Peninsular Range, *in* Pacific slope geology of northern Baja California and adjacent Alta California. Pacific sections AAPG, SEPM and SEG:83-86.
___, 1979. The late Mesozoic-early Tertiary framework of continental sedimentation, northern Peninsular Ranges, Baja California, Mexico, *in* Eocene depositional systems, San Diego, California, P.L. Abbott (ed). Los Angeles, SEPM, Pacific section:43-67.
Morton, D.M., 1978a. Geologic map of the Redlands 7.5 minute quadrangle, San Bernardino and Riverside counties, California. U.S. Geological Survey open-file report.
___, 1978b. Geologic map of the San Bernardino South 7.5 minute quadrangle, San Bernardino and Riverside counties, California. U.S. Geological Survey open-file report.
Morton, D.M., B.F. Cox and J.C. Matti, 1980. Geologic map of the San Gorgonio Wilderness, San Bernardino County, California. U.S. Geological Survey Misc. Investigation Field Studies Map MF-1161-A.
Morton, D.M. and C.H. Gray, 1971. Field trip no. 4, Geology of the northern Peninsular Ranges, southern California, *in* Geological excursions in southern California, W.A. Elders (ed). University of California, Riverside Campus Museum Contributions, 1:60-93.
Morton, D.M. and J.C. Matti, 1993. Tectonic synopsis of the San Gorgonio Pass and San Timoteo Badlands areas, southern California. Redlands, San Bernardino County Museum Association Quarterly, 40(2):3-14.
Morton, D.M., J.C. Matti and J.C. Tinsley, 1992. Banning fault, Cottonwood Canyon, San Gorgonio Pass, southern California, *in* Earthquake geology, San Andreas fault system, Palm Springs to Palmdale. Association of Engineering Geologists, Southern California section, 35th annual meeting guidebook and reprint volume:67-98.
Morton, D.M. and P. Sadler, 1989. Landslides flanking the northeastern Peninsular Ranges and in the San Gorgonio Pass area of southern California, *in* Landslides in a semi-arid environment. Redlands, Publications of the Inland Geological Society.
Morton, P.K., 1977. Geology and mineral resources of Imperial County, California. California Division of Mines and Geology County Report, 7.
Muffler, L.F.P. and B.R. Doe, 1968. Composition and mean age of detritus of the Colorado River delta in the Salton Trough, southeastern California. Journal of Sedimentary Petrology, 38:384-399.
Murphy, M.A., 1986. The Imperial formation at Painted Hill, near Whitewater, California, *in* Geology around the margins of the eastern San Bernardino Mountains, M.A. Kooser and R.E. Reynolds (eds). Redlands, Publications of the Inland Geological Society, 1:63-70.
Nicholson, C. and L. Seeber, 1989. Evidence for contemporary block rotation in strike-slip environments: examples from the San Andreas fault system, southern California, *in* Paleomagnetic rotations and continental deformation. C. Kissel and C. Laj (eds). Kluwer Academic Publishers:247-280.
Opdyke, N.D., E.H. Lindsay, N.M. Johnson, and T. Downs, 1977. The paleomagnetism and magnetic polarity stratigraphy of the mammal-bearing section of ABDSP, California. Quaternary Research, 7:316-329.
Pajak, A.F., R.E. Reynolds and R.L. Reynolds, 1991. A marine and terrestrial assemblage from the Puente formation that relates the Hemphillian Land Mammal Age to the Mohnian foraminiferal stage, Prado Dam quadrangle, San Bernardino County, California. Journal of Vertebrate Paleontology, 11(3A):49A.
Petersen, M.D., L. Seeber, and K.W. Hudnut, 1987. Importance of transverse features along the southern San Jacinto fault zone, California. Abstract, Eos Trans. AGU, 68:1507.
Peterson, M.S., 1975. Geology of the Coachella fanglomerate, *in* San Andreas fault in southern California, J.C. Crowell (ed). California Division of Mines and Geology Special Report, 118:
Pettinga, J.R., 1991. Structural styles and basin margin evolution adjacent to the San Jacinto fault zone, southern California. San Diego, Geological Society of America Abstracts with Program:A257.
Powell, R.E., 1982. Crystalline basement terranes in the southern eastern Transverse Ranges, California, *in* Geologic excursions in the Transverse Ranges, J.D. Cooper (compiler). Guidebook for field trip numbers 5, 6, 11, 78th annual meeting Cordilleran section, Geological Society of America, Anaheim:109-136.
Proctor, R.J., 1968. Geology of the Desert Hot Springs - Upper Coachella Valley area, California. California Division of Mines and Geology Special Report, 94: 50 p.
Proctor, R.J. and T. Downs, 1963. Stratigraphy of a new formation containing Early Pliocene vertebrates at Lake Mathews, near Riverside, California. Geological Society of America Special Paper, 73:1-59.
Rasmussen, G.S., 1981. Nature of surface rupture and recurrence interval, Casa Loma fault, *in* Geology of the San Jacinto Mountains, A.R. Brown and R.W. Ruff (eds). South Coast Geological Society Annual Field Trip Guidebook, 9:48-54.
___, 1982. Historic earthquakes along the San Jacinto fault zone, San Jacinto, California, *in* Neotectonics in southern California, J.D. Cooper (ed). Anaheim, Geological Society of America, Cordilleran Section, 78th Annual Meeting:115-121.
Remeika, P., 1991a. A preliminary report of calcareous tufa deposits from the Palo Verde Wash area: evidence for the existence of a pre-Lake Cahuilla strandline in the Borrego Badlands, ABDSP, California [abstract]. Borrego Springs, Anza Borrego Foundation, Symposium on the Scientific Value of the Desert: 12.
___, 1991b. Formational status for the Diablo Redbeds: differentiating between Colorado River affinities and the Palm Spring formation [abstract]. Borrego Springs, Anza Borrego Foundation, Symposium on the Scientific Value of the Desert: 12.
___, 1991c. Additional contributions to the Neogene paleobotany of the Vallecito-Fish Creek basin and vicinity, ABDSP, California [abstract]. Borrego Springs, Anza Borrego Foundation, Symposium on the Scientific Value of the Desert: 13.
___, 1992a. Preliminary report on the stratigraphy and vertebrate fauna of the Middle Pleistocene Ocotillo formation, Borrego Badlands, ABDSP, California. Redlands, San Bernardino County Museum Quarterly, 39(2):25-26.
___, 1992b. Paleontology collection management policy [draft]. Borrego Springs, California Department of Parks and Recreation, Colorado Desert District, ABDSP: 46 p.
___, 1992c. Paleontological program development at Anza Borrego Desert State Park, California. Kemmerer, Abstracts with Program, Third Conference on Fossil Resources in the National Park Service, 14-17 September, Fossil Butte National Monument: 25.
___, 1992d. Landscapes of time. Outcroppings, paleontology, and geologic history of Anza Borrego Desert State Park [unpubl. ms]. Borrego Springs, Anza Borrego Desert Natural History Association: 336 p.

Remeika, P., I.W. Fischbein, and S.A. Fischbein, 1988. Lower Pliocene petrified wood from the Palm Spring formation, Anza Borrego Desert State Park, California. Review of palaeobotany and palynology, 56:183-198.
Remeika, P. and L. Lindsay, 1992. Geology of Anza Borrego: Edge of Creation. Dubuque, Kendall/Hunt Publishing Company: 208 p.
Remeika, P. and J.R. Pettinga, 1991. Stratigraphic revision and depositional environments of the middle to late Pleistocene Ocotillo Conglomerate, Borrego Badlands, ABDSP, California [abstract]. Borrego Springs, Anza Borrego Foundation, Symposium on the Scientific Value of the Desert: 13.
Reynolds, R.E. and M.A. Kooser, 1986. Field trip road log, *in* Geology around the margins of the eastern San Bernardino Mountains, M.A. Kooser and R.E. Reynolds (eds). Redlands, Publications of the INland Geological Society, 1:7-50.
Reynolds, R.E. and W.A. Reeder, 1986. Age and fossil assemblages of the San Timoteo formation, Riverside County, California, *in* Geology around the margins of the eastern San Bernardino Mountains, M.A. Kooser and R.E. Reynolds (eds). Publications of the Inland Geological Society, 1:51-56.
___, 1991. The San Timoteo formation, Riverside County, California, *in* Inland southern California: the last 70 million years, M.O. Woodburne, R.E. Reynolds and D.P. Whistler (eds). Redlands, San Bernardino County Museum Association Quarterly, 38(3,4):44-48.
Reynolds, R.E. and R.L. Reynolds, 1991. The Pleistocene beneath our feet: near-surface Pleistocene fossils in inland southern California basins, *in* Inland southern California: the last 70 million years, M.O. Woodburne, R.E. Reynolds and D.P{. Whistler (eds). Redlands, San Bernardino County Museum Association Quarterly, 38(3,4):41-43.
Reynolds, R.E., R.L. Reynolds and A.F. Pajak III, 1991. Blancan, Irvingtonian and Rancholabrean(?) Land Mammal Age faunas from western Riverside County, California, *in* Inland southern California: the last 70 million years, M.O. Woodburne, R.E. Reynolds and D.P. Whistler (eds). Redlands, San Bernardino County Museum Association Quarterly, 38(3,4):37-40.
Reynolds, R.E. and Turner, W.G., 1971. Petroglyph dating, *in* Three essays on petroglyphology. San Bernardino County Museum Association Quarterly, 19(1):28-34.
Rymer, M.J., 1991. The Bishop Ash bed in the Mecca Hills, *in* Geological excursions in southern California and Mexico, M.J. Walawender and B.B. Hanna (eds). San Diego, Geological Society of America Annual Meeting Guidebook:388-396.
Sanders, C., H. Magistrale, and H. Kanamori, 1986. Rupture patterns and preshocks of large earthquakes in the southern San Jacinto fault zone. Bulletin of Seis Soc. Am, 76(5):1187-1206.
Sauer, C.O., 1929. Landforms of the Peninsular Range of California as developed about Warner's Hot Springs and Mesa Grande. Univ. Pub. in Geography, 3:199-290.
Savage, D.E. and D.E. Russell, 1983. Mammalian paleofaunas of the world. Reading Mass, Addison-Wesley: 432 p.
Scheuing, D.F., L. Seeber, K.W. Hudnut, and N.L. Bogen, 1988. Block rotation in the San Jacinto fault zone, southern California. AGU abstract, 1988 fall meeting.
Schultejann, P.A., 1984. The Yaqui Ridge antiform and detachment fault: mid-Cenozoic extensional terrane west of the San Andreas fault. Tectonics, 3:677-691.
Sharp, R.V., 1967. San Jacinto fault zone in the Peninsular Ranges of southern California. Geological Society of America Bulletin, 78:705-730.
___, 1979. Some characteristics of the eastern Peninsular Ranges mylonite zone, *in* Proceedings, Conference VIII--Analysis of actual faults in bedrock. U.S. Geological Survey:258-267.
___, 1981. Variable rates of late Quaternary strike slip on the San Jacinto fault zone, southern California. Journal of Geophysical Research, 86(B3):1754-1762.
Sharp, R.V. and others, 1972. The Borrego Mountain earthquake of April 9, 1968. U.S. Geological Survey Professional Paper, 787: 207 p.
Sheehan, J.R., 1986. A tectonic model of the Salton trough, *in* Geology of the Imperial Valley, California, P.D. Guptil, E.M. Gath and R.W. Ruff (eds). South Coast Geological Society, Annual Field Trip Guidebook, 14:165-172.
Shifflett, H., P. Nicolay, E. Wiebe and R. Crisman, 1986. Holocene offsets, San Andreas fault, Mecca Hills, California, *in* Geology of the Imperial Valley, California, P.D. Guptil, E.M. Gath and R.W. Ruff (eds). South Coast Geological Society, Annual Field Trip Guidebook, 14:159-164.
Sieh, K.E. and J.C. Matti, 1992. The San Andreas fault system between Palm Springs and Palmdale, southern California: field-trip guidebook, *in* Earthquake geology, San Andreas fault system, Palm Springs to Palmdale. Association of Engineering Geologists, Southern California section, 35th annual meeting guidebook and reprint volume:1-12.
Sieh, K.E. and P.L. Williams, 1992. Behavior of the southernmost San Andreas fault during the past 300 years, *in* Earthquake geology, San Andreas fault system, Palm Springs to Palmdale. Association of Engineering Geologists, Southern California section, 35th annual meeting guidebook and reprint volume:63-80.
Silver, L.J., H.P. Taylor Jr., and B. Chapell, 1979. Some petrological, geochemical and geochronological observations of the Peninsular Ranges batholith near the international border of the U.S.A. and Mexico, *in* Mesozoic Crystalline Rocks, Peninsular Ranges batholith and pegmatites, Point Sal Ophiolite, P.L. Abbott and V.R. Rodd (eds). Dept. Geol. Sciences, San Diego State University:83-110.
Simpson, C., 1984. Borrego Springs-Santa Rosa mylonite zone: a late Cretaceous west-directed thrust in southern California. Geology, 12:8-11.
___, 1985. Deformation of granitic rocks across the brittle-ductile transition. Journal of Structural Geology, 7:503-511.
Slade, R.C., 1981. Hydrogeologic conditions in the Mission Creek subbasin, upper Coachella Valley, California, *in* Geology of the San Jacinto Mountains, A.R. Brown and R.W. Ruff (eds). South Coast Geological Society Annual Field Trip Guidebook, 9:151-163.
Stearns, R.E.C., 1901. The fossil freshwater shells of the Colorado Desert: their distribution, environment and variation. Proceedings of the U.S. National Museum, 24(1256):271-299.
Sylvester, A.G., 1991. Geologic structure, transpression, and neotectonics of the San Andreas fault in the Salton Trough, California, part 1, Palm Tree structure in the central Mecca Hills, *in* Geological excursions in southern California and Mexico, M.J. Walawender and B.B. Hanan (eds). Geological Society of America Guidebook, 1991 Annual Meeting, San Diego State University:378-387.
Sylvester, A.G. and R.R. Smith, 1975. Structure section across the San Andreas fault zone, Mecca Hills, *in* San Andreas fault in southern California, J.C. Crowell (ed). California Division of Mines and Geology Special Report, 118:111-118.
___, 1991. Structure section in Painted Canyon, Mecca Hills, southern California, *in* Geological excursions in southern California and Mexico, M.J. Walawender and B.B. Hanan (eds). Geological Society of America Guidebook, 1991 Annual Meeting, San Diego State University:372-377.
Tarbet, L.A., 1951. Imperial Valley. American Association of Petroleum Geologists Bulletin, 35:260-263.
Tarbet, L.A. and W.H. Holman, 1944. Stratigraphy and micropaleontology of the west side of Imperial Valley, California. American Association of Petroleum Geologists Bulletin, 28:1781.
Taylor, D.W., 1981. Freshwater mollusks of California: a distributional checklist. California Fish and Game, 67(3):149-163.
Thatcher, W. and R.M. Hamilton, 1973. Aftershocks and source characteristics of the 1969 Coyote Mountain earthquake, San Jacinto fault zone, California. Bulletin Seismological Society America, 63:647-661.
Thatcher, W., J.A. Hileman, and T.C. Hanks, 1975. Seismic slip distribution along the San Jacinto fault zone, southern California, and its implications. Geol. Soc. Amer. Bulletin, 86:1140-1146.
Todd, V.R. and S.E. Shaw, 1979. Structural, metamorphic and intrusive framework of the Peninsular Ranges batholith in southern San Diego County, California, *in* Mesozoic crystalline rocks. Peninsular Ranges batholith and pegmatites, Point Sal Ophiolite, P.L. Abbot and V.R. Todd (eds). Dept. Geological Sciences, San Diego State University:177-231.
Turner, W.G. and R.E. Reynolds, 1977. Dating the Salton Sea petroglyphs. Science News, 111 (February).
Van de Kamp, P.C., 1973. Holocene continental sedimentation in the Salton Basin, California, a reconnaissance. Geological Society of America Bulletin, 84:847-848.
Wagoner, J.L., 1977. Stratigraphy and sedimentation of the Pleistocene Brawley and Borrego formations in the San Felipe Hills area, Imperial Valley, California [M.S. thesis]. University of California, Riverside: 128 p.
Walawender, M.J., G.H. Girty, M.R. Lombardi, D. Kimbrough, M.S. Girty and C. Anderson, 1991. A synthesis of recent work in the Peninsular Ranges batholith, *in* Geological excursions in southern California and Mexico, M.J.

Walawender and B.B. Hanan (eds). Geological Society of America Guidebook, 1991 Annual Meeting, San Diego State University:297-318.

Wallace, R.D. and D.J. English, 1982. Evaluation of possible detachment faulting west of the San Andreas, southern Santa Rosa Mountains, California, *in* Mesozoic-Cenozoic tectonic evolution of the Colorado River region, California, Arizona and Nevada, E.G. Frost and D.L. Martin (eds). San Diego, California Publishers:503-509.

Wesnousky, S.G, C.S. Prentice, and K.E. Sieh, 1992. An offset Holocene stream channel and the rate of slip along the northern reach of the San Jacinto fault zone, San Bernardino Valley, California, *in* Earthquake geology, San Andreas fault system, Palm Springs to Palmdale. Association of Engineering Geologists, Southern California section, 35th annual meeting guidebook and reprint volume:111-120.

White, J.A., E.H. Lindsay, P. Remeika, B.W. Stout, T. Downs, and M. Cassiliano, 1991. Society of Vertebrate Paleontology field trip guide to the Anza Borrego Desert, San Diego, Society of Vertebrate Paleontology 51st Annual Meting, 23 p.

Wilke, P.J., 1978. Late prehistoric human ecology at Lake Cahuilla, Coachella Valley, California. Contributions of the University of California Archaeological Research Facility, 38: 168 p.

___, 1979. Prehistoric weir fishing on recessional shorelines of Lake Cahuilla, Salton Basin, southeastern California. Proc. Desert Fishes Council, Vol. XI:101-102.

Willingham, C.R., , 1981. Gravity anomaly patterns and fault interpretations in the San Bernardino Valley and western San Gorgonio Pass area, southern California, *in* Geology of the San Jacinto Mountains, A.R. Brown and R.W. Ruff (eds). South Coast Geological Society Annual Field Trip Guidebook, 9:164-174.

Winker, C.D., 1987. Neogene stratigraphy of the Fish Creek-Vallecito section, southern California: implications for early history of the northern Gulf of California and Colorado delta [Ph.D. dissertation]. University of Arizona, Tucson: 494 p.

Woodard, G.D., 1968. The Cenozoic succession of the west Colorado Desert, San Diego and Imperial counties, southern California [Ph.D. dissertation]. University of California, Berkeley: 173 p.

___, 1974. Redefinition of Cenozoic stratigraphic column in Split Mountain Gorge, Imperial Valley, California. American Association of Petroleum Geologists Bulletin, 58:521-539.

Woodburne, M.O., 1975. Cenozoic stratigraphy of the Transverse Ranges and adjacent areas, southern California. Geological Society of America Special Paper, 162: 91 p.

Woodburne, M.O. and D.P. Whistler, 1973. An early Miocene oreodont (Merychyinae, Mammalia) from the Orocopia Mountains, southern California. Journal of Paleontology, 47(5):908-912.

Woodford, A.O., J.S. Shelton, D.O. Doehring and R.K. Morton, 1971. Pliocene-Pleistocene history of the Perris block, southern California. Geological Society of America Bulletin, 83:3421-3448.

Discoveries of Fossil Whales in the Imperial Formation, Riverside County, California, and the Northern Extent of the Proto-Gulf of California

HOWELL W. THOMAS and LAWRENCE G. BARNES, *Section of Vertebrate Paleontology, Natural History Museum of Los Angeles County, 900 Exposition Boulevard, Los Angeles, California 90007*

ABSTRACT

Fossil whales have been found in outcrops of the marine Imperial formation in the Painted Hill-Super Creek area, near White Water, below San Gorgonio Pass, Riverside County, California. The Imperial formation at this site has previously yielded significant Late Miocene marine mollusks that are some distance stratigraphically below circa 6 Ma volcanic sediments. Field parties from the Vertebrate Paleontology Section at the Natural History Museum of Los Angeles County (LACM) have now made three trips to the site to excavate the whale specimens. Previous prospecting had not yielded any vertebrate fossils at this locality, and the whale bones are reported here as newly documented occurrences.

SETTING

Marine vertebrate fossils had been previously found in the Imperial formation, but they were found much farther south than White Water, in the Ocotillo Wells area, Imperial County. These included the aberrant walrus-like pinniped, *Valenictus imperialensis* Mitchell, 1961, a camel, and sharks.

Fossil mollusks from the northern exposures of the Imperial formation at Super Creek and Painted Hill have been described by Bramkamp (1935), Schremp (1981), and Powell (1985, 1988). The gastropods are related to both Caribbean and Gulf of California fossil and living taxa. The fossil bivalves reported by Powell (1985) from the Super Creek area were collected from the same and nearby sites as the presently reported cetacean fossils.

The Imperial formation in the Super Creek area is represented by the stratigraphically lower Latrania Sand Member (named by Hanna, 1926; see Powell, 1985), and the overlying Burrobend Member. A field party, including volunteers from the Natural History Museum of Los Angeles County (LACM) under the supervision of one of us (HWT), had been asked to inspect these outcrops of the Imperial formation by Edward C. Wilson, Section Head of Invertebrate Paleontology at the Museum. Vertebrae of whales had been found by Wilson on a previous trip, exposed in the lower Latrania Sand Member of the Imperial formation on the side of a steep cliff. It was during subsequent trips that further cetacean remains, including the distal part of a rostrum from a mysticete skull, were also found in the upper Burrobend Member of the Imperial formation. The site is located a short distance north of the Banning fault, one of several parallel faults that are part of the San Andreas fault zone in San Gorgonio Pass. The fossil locality is in an area that is very disrupted by right lateral movement of a series of parallel faults in the San Andreas fault zone. In fact a minor fault extends right through the whale skull that we found, further attesting to the tectonic activity in this area.

PALEONTOLOGY

The present report constitutes a new geographic province for discovery of fossil whale bones. The other nearest cetacean fossils that have been documented in the Gulf of California realm are from the geologically younger Tirabuzon formation near Santa Rosalia, Baja California Sur, México (Flores and Barnes, 1991). These fossils are of Pliocene age, considerably younger than the Late Miocene whales at White Water. The cetaceans from Santa Rosalia are mostly small odontocetes and represent oceanic types like delphinids and phocoenids; these are the type of cetaceans now found in the present lower Gulf of California.

Fossil whales of Late Miocene age are not known from elsewhere in the Gulf of California realm (Barnes, 1976). Geologically younger cetaceans of Pliocene age, are known from Santa Rosalia, Baja California (Flores and Barnes, 1991). Late Miocene cetaceans, approximately correlative with those from the Imperial formation, are known from Isla de Cedros, off the Pacific coast of Baja California (Barnes, 1973, 1984, 1991, 1992a, b), and from Oceanside along the Pacific coast in southern California (Barnes, et al., 1981). It is possible that the whales we have discovered in the Imperial formation might represent animals not found in the previously studied assemblages from coastal deposits of Late Miocene age in California and Mexico. Coral fossils in the Super Creek exposures of the Imperial formation (*fide* E.C. Wilson) indicate that in Late Miocene time the northern Gulf of California was relatively open or had open current circulation. Powell (1985) concluded that the Latrania Sand Member of the Imperial formation was deposited in shallow subtidal depths of 10 to 40 meters. The presence of large baleen whales in the deposit is compatible with this suggestion. If upon further study the new whale material is determined to belong to pelagic types, then this would further corroborate the idea of open circulation in the upper Gulf.

EXTENT OF PROTO-GULF

The locality near Super Creek where the fossil whales were found is on the southwest (Pacific) side of the San Andreas fault. Accounting for estimates of prior lateral (northward) displacement along the San Andreas fault of the terrane on the Pacific side of the fault (see Hill and Dibblee, 1953; and Crowell, 1975), we estimate that in late Miocene time the original location of deposition of the Super Creek outcrops of the Imperial formation was approximately 150 miles farther south than it is now. This offset would place the original site of deposition much further south within the realm of the Proto-gulf of California, and these deposits may be regarded as a more open-water continuum of the brackish water, near-shore sediments of the Bouse formation farther to the east. The Bouse formation represents the northernmost undisturbed Proto-Gulf sediments, still flat-lying in the areas where they were deposited.

The presence of these whale fossils, and other marine fossils in the San Gorgonio Pass region are relevant to discussions about the size, antiquity, and nature of the formation of the Proto-Gulf of California (eg. Powell, 1987a, b). For example, Moore and Curray (1982) suggested a date as recent as 5.5 Ma (Early Pliocene) for the opening of the southern Gulf of California, and the more northern deposits in California were thought to be another embayment. This would appear to be contradicted, however, by the discovery of 11 to 12 Ma late Miocene deposits on Isla Tiburon in the Gulf (Smith, 1991). Smith (1991:Table 1) stated that "The San Gorgonio Pass area has some of the same fossils as in the upper Middle Miocene section on Isla Tiburón in the northern Gulf of California." Furthermore, the mollusks that were reported from the Super Creek area have affinities with the Caribbean and Gulf of California, not with the California Pacific coast, and many species are, in fact, found only in the Imperial formation and in the Caribbean realm (Powell, 1988). These lines of evidence indicate that the Imperial formation in Riverside County was deposited as part of the Gulf of California, and not part of some other basin. Smith (1991:Table 1) also reported K-Ar dates of 6.04 ± 0.18 and 5.94 ± 0.18 Ma on a basalt flow in the Painted Hill formation directly overlying the Imperial formation, and a 10 Ma date for the underlying Coachella Fanglomerate (Peterson, 1975; cited by Powell, 1988). Applegate (1992) has summarized evidence that the Proto-Gulf of California was fully formed and open to the south before Pliocene time.

The occurrences of the Imperial formation this far northward also support contentions that the Gulf of California has a relatively long history (eg. Applegate, 1992) and was extensive (Buising, 1989, 1990). Zullo and Buising (1989) have reported brackish water barnacles in the Bouse formation as far north as Parker, Arizona, further evidence for an extensive upper gulf. This material is late Pliocene in age (approximately 4 Ma), and therefore considerably younger than the fossil whale material that we have found near White Water.

Preliminary identification of the Super Creek whale bones is tenuous, but it is clear that the skull fragment represents a baleen whale (suborder Mysticeti) that had a wide, flat rostrum, probably a member of the family Balaernopteridae or Cetotheriidae, and would have probably measured at least six meters in total body length. What they will reveal about paleobiogeography and paleoecology of the upper Gulf must await preparation and study of these and other specimens.

ACKNOWLEDGMENTS

We are grateful to Dr. Edward C. Wilson for first bringing to our attention the existence of fossil whale bones in this part of the Imperial formation. Stephen K. Jarvis, a volunteer of the Vertebrate Paleontology Section (LACM), discovered the whale skull on a subsequent trip, and was helpful in other ways. Other volunteers, Alan Brookman and Debora Lee, also assisted in the field, and we thank them for their help. We thank Tony Crotsenburg and Zond Systems, Inc., for allowing us access to the fossil sites near Super Creek. We also thank Edward C. Wilson, John M. Harris, and Robert E. Reynolds for advice and review of the manuscript.

LITERATURE CITED

Applegate, S.P. 1992. The Protogulf revisited, p. 64-73, *In* A. Carillo-Chávez and A. Alvarez-Arellano, eds., Primera Réunion Internacional sobre Geología de la Península de Baja California, Memorias, Universidad Autónoma de Baja California Sur, La Paz, Baja California Sur, México, 166 p.

Barnes, L.G. 1973. *Praekogia cedrosensis*, a new genus and species of fossil pygmy sperm whale from Isla Cedros, Baja California, Mexico. Contributions in Science, Natural History Museum of Los Angeles County, 247:1-20.

___, 1976. Outline of eastern North Pacific fossil cetacean assemblages. Systematic Zoology, 25(4):321-343.

___, 1984. Fossil odontocetes (Mammalia: Cetacea) from the Almejas formation, Isla Cedros, Mexico. PaleoBios, Museum of Paleontology, University of California, 42:1-46.

___, 1991. The fossil marine vertebrate fauna of the latest Miocene Almejas formation on Isla Cedros, Baja California, Mexico. Resúmenes, Primera Réunion Internacional sobre Geología de la Península de Baja California (First International meeting on Geology of the Baja California Peninsula.), La Paz, Baja California Sur, México, April, 1991, p. 10-11.

___, 1992a. The fossil marine vertebrate fauna of the latest Miocene Almejas formation, Isla Cedros, Baja California, México, p. 147-166, *In* A. Carillo-Chávez and A. Alvarez-Arellano, eds., Primera Réunion Internacional sobre Geología de la Península de Baja California, Memorias, Universidad Autónoma de Baja California Sur, La Paz, Baja California Sur, México, 166 p.

___, 1992b. Latest Miocene marine vertebrates from the Almejas formation, Isla de Cedros, Baja California, México. Journal of Vertebrate Paleontology 12 (supplement to no. 3, abstracts):18A.

Barnes, L.G., Hildegarde Howard, J. Howard Hutchison, and Bruce J. Welton. 1981. The vertebrate fossils of the marine Cenozoic San Mateo formation at Oceanside, California, p. 53-70. *In* P.L. Abbot and S. O'Dunn, eds., Geologic Investigations of the San Diego Coastal Plain, San Diego Association of Geologists, San Diego, California.

Bramkamp, R. 1935. Stratigraphy and molluscan fauna of the Imperial formation of San Gorgonio Pass, California. Unpublished Ph.D. dissertation, University of California, 371 pp.

Buising, A.V. 1989. The influence of high-relief basin topography on deltaic sedimentation: deltaic and alluvial facies of the Bouse formation, lower Colorado River area, southeastern California - western Arizona, p. 53-72, *In* Colburn, I.P., P.L. Abbott, and J. Minch, eds., Conglomerates in Basin Analysis, A symposium dedicated to A.O. Woodford, Pacific Section, Society of Economic Paleontologists and Mineralogists, vol. 62.

___, 1990. The Bouse formation and bracketing units, southeastern California and western Arizona: implications for the evolution of the Proto-Gulf of California and the lower Colorado River. Journal of Geophysical Research, 95(B12):20111-20132.

Crowell, J.C. 1975. The San Andreas fault in southern California, p. 7-27, *In* J.C. Crowell, editor, San Andreas fault in southern California. A guide to the San Andreas fault from Mexico to Carrizo Plain. California Division of Mines and Geology, Special Report, 118.

Flores, V.J., and L.G. Barnes. 1991. Colección de cetáceos del Plioceno de la Formación Tirabuzón, Santa Rosalia, Baja California Sur, Mexico. (The Pliocene cetacean assemblage from the Tirabuzon formation at Santa Rosalia, Baja California Sur, Mexico.) Programa y Resúmenes, Abstracts, XVI Réunion Internacional para el Estudio de los Mamíferos Marinos, Nuevo Vallarta, Nayarit, México, April, 1991:6.

Hanna, G D. 1926. Paleontology of Coyote Mountains, Imperial County, California. Proceedings of the California Academy of Sciences, Series 4, 14(18):427-503.

Hill, M.L., and T.W. Dibblee, Jr. 1953. San Andreas, Garlock, and Big Pine faults. A study of the character, history, and significance of their displacement. Geological Society of America Bulletin, 64(4):443-458.

Mitchell, E.D. 1961. A new walrus from the Imperial Pliocene of southern California: with notes on odobenid and otariid humeri. Contributions in Science, Natural History Museum of Los Angeles County, 44:1-28.

Moore, D.G., and J.R. Curray. 1982. Geologic and tectonic history of the Gulf of California, p. 1279-1294 *In* Initial reports of Deep Sea Drilling Project, J. Blakeslee, L.W. Pratt, and L.N. Stout, eds., vol. 64, part 2,

National Science Foundation.
Peterson, M.S. 1975. Geology of the Coachella Fanglomerate, p. 119-126, *In* J. C. Crowell, editor, San Andres fault in southern California. A guide to San Andreas fault from Mexico to Carrizo Plain. California Division of Mines and Geology, Special Report, 118.
Powell, C.L., II. 1985. Bivalve molluscan paleoecology of northern exposures of the marine Neogene Imperial formation in Riverside County, California. Western Society of Malacologists Annual Report, 1984, 17:29-32 (August 1985).
___, 1986. Stratigraphy and bivalve molluscan paleontology of the Neogene Imperial formation in Riverside County, California. M.S. Thesis, San Jose State University, 325 pp.
___, 1987a. Paleogeography of the Imperial formation and timing of the opening of the Gulf of California. Abstract, 4th International Congress on Pacific Neogene Stratigraphy, Berkeley, California.
___, 1987b. Correlation between sea level events and deposition of marine sediments in the proto-Gulf of California during the Neogene. Abstracts, Geological Society of America Annual Meeting, Phoenix, Arizona, Abstracts with programs, 19(7):809.
___, 1988. The Miocene and Pliocene Imperial formation of southern California and its molluscan fauna: an overview. Western Society of Malacologists Annual Report, 1987, 20:11-18 (March 1988).
Schremp, L.A. 1981. Archeogastropoda from the Pliocene Imperial formation of California. Journal of Paleontology, 55(5):1123-1136.
Smith, J.T. 1991. Cenozoic marine mollusks and paleogeography of the Gulf of California, p. 637 - 666, In J. P. Duaphin and B.R. T. Simoneit, editors, The Gulf and Peninsular Province of the Californias, American Association of Petroleum Geologists Memoir, 47.
Zullo, V.A., and A.V. Buising. 1989. An unusual species of the *Balanus amphitrite* Darwin complex (Cirripedia, Balanidae) from the ancestral Colorado River delta in western Arizona and southeastern California. Proceedings of the Biological Society of Washington 102(4):924-932.

Factors Determining the Occurrence of the Desert Fan Palm, *Washingtonia filifera*

JAMES W. CORNETT, *Natural Science Department, Palm Springs Desert Museum, Palm Springs CA 92262*

ABSTRACT

The desert fan palm, *Washingtonia filifera*, ranges throughout the Colorado Desert of southeastern California where springs, seeps or streams supply a permanent supply of water. The occurrence of this species is a result of three factors: a permanent moisture supply, suitable climate and dispersal opportunity.

INTRODUCTION

The desert fan palm, *Washingtonia filifera*, is generally the largest plant occurring at permanent seeps, springs and streams in California's Colorado Desert. This fact, together with a rich green crown of fronds, make the desert fan palm a striking addition to the flora of the approximately 150 desert oases where it occurs (Cornett, 1991). Its visual dominance is so great that any oasis is popularly identified as a "palm oasis" when the desert fan palm is present (Henderson, 1961; Kirk, 1973).

Such visual distinctiveness is made all the more striking when contrasted with the surrounding terrain. The vast majority of palm oases occur in the Colorado Desert, the lowest, hottest and driest subdivision of the North American Desert (Jaeger, 1957). In this region vegetation is scant and what plants do exist are typically small and generally dormant. Desert fan palms stand in dramatic contrast to such surroundings. It is small wonder that they have been the subject of public curiosity and popular writing for decades.

SOURCES OF MOISTURE

The desert fan palm requires a permanent or near permanent source of moisture in order for seeds to germinate and seedlings to grow to maturity (Cornett, 1989). Without a permanent supply of moisture a tree will decline, as revealed by a reduction in leaf size and lack of fruit production. The decline may take place over a period of several years, and a palm can be revitalized should a permanent moisture source be reestablished.

Over 90 percent of wild desert fan palms are found either along the eastern base of the Peninsular Range in California and Baja California Norte, or the San Andreas fault in Riverside County, California (Cornett and others, 1986). Numerous locations in both of these regions provide a permanent source of moisture.

The Peninsular Range runs in the northwest direction beginning at the tip of the Baja Peninsula and extending northward approximately 900 miles to the San Gorgonio Pass in Riverside County, California (Oakeshott, 1971). The range reaches its greatest elevation, 10,805 feet above sea level, at its northern terminus.

The Peninsular Range intercepts eastward-traveling storms, resulting in appreciable amounts of precipitation falling on the mountain slopes. Year-round runoff in the form of streams or seeps occurs in many of the canyons draining the slopes. The reliability and quantity of this source of moisture support over 75 percent of the wild fan palm population. All of these trees occur in canyons draining the eastern or leeward side of the Peninsular Range, and the majority occur in the northeastern portion of the range where elevations are higher and watersheds greater. In addition, the northerly portions of the range receive more precipitation in winter since the region lies closer to Southern California's winter storm track (Bailey, 1966).

THE SAN ANDREAS FAULT

Approximately 15 percent of all wild deert fan palms occur along the San Andreas fault in the Colorado Desert of southeastern California (Figure 1). At no less than 15 locations along the fault, groundwater reaches the surface and is available to desert fan palsm.

The finely ground soil along the fault prevents groundwater from passing through it as the moisture flows downslope from north to south (Iacopi, 1964). With the continual flow of water, the water table rises at the fault, eventually reaching the surface. Water does not seep upward over the entire length of the fault; it only reaches the surface at a dozen or so locations where underground conditions promote the rise of groundwater. Although it is generally believed that earth movements can rapidly affect the amount and location of seepage, this has not yet been documented along the Colorado Desert portion of the San Andreas fault.

DESERT SPRINGS

There are about a dozen additional palm oases that do not occur at the base of the Peninsular Range or the San Andreas Fault. These ocases occur at isolated desert springs where faults allow water to rise to the surface, a condition similar to those along the San Andreas fault.

THE INFLUENCE OF CLIMATE ON THE OCCURRENCE OF WILD DESERT FAN PALMS

It appears there is no locality in North America where high, summertime temperatures directly prohibit the occurrence of the desert fan palm. The species occurs throughout the Colorado Desert, the hottest subdivision of the North American Desert, and Death Valley, where summer temperatures average the hottest in the world (Jaeger, 1957).

Low temperatures, however, do seem to prohibit the occurrence of the desert fan palm. Desert fan palms have never been found at elevations over 4,000 feet, although there are Colorado Desert locations at such altitudes where a permanent supply of moisture is available. Nor have they been found north of latitude 38°N (Cornett, 1988). Again, it is assumed that this reflects an intolerance to cold conditions. It should be noted that at high latitudes and elevations growth of desert fan palms is considerably slower than in warmer climates.

It is less obvious why desert fan palms do not occur in the coastal climates of southern California. Winter temperatures are relatively mild and locations where pemanent moisture can be obtained are numerous. It is the author's belief that relatively cool summer temperatures and/or frequent fires are responsible for the absence of the palms. Cool sumer temperatures may slow the growth of desert fan palms so that they cannot compete effectively with other

Figure 1. Willis Palms on the San Andreas fault; Mt. San Jacinto distant.

arborescent species around springs. A more frequent fire regime might either eliminate young palms or reduce the competitiveness of palms. Although the desert fan palm is quite resistent to fire, it may not be able to maintain the viability of its populations when subjected to the kind of fire regime experienced by coastal plant communities of southern California.

LACK OF DISPERSAL OPPORTUNITY AS AN INFLUENCE IN PALM DISTRIBUTION

The present distribution of desert fan palm represents the locations where the desert fan palm has occurred since its appearance as a distinct species, or the locations to which the seeds have been effectively transported by birds, humans or other mammals. It is likely that the desert fan palm occurs at certain locations because of successful dispersal by animals other than humans.

There are numerous locations where the conditions seem suitable for the occurrence of the desert fan palm, but none are present. Their absence could be attributed to a lack of dispersal opportunity. There are numerous springs in western Arizona, southern Nevada and the Mojave Desert where the climate seems suitable, but the palms are absent. The most reasonable explanation for their absence is that there has been no bird or mammal that has yet transported the seeds to the sites. At some point in the future seed transport may occur, and the desert fan palm may become established.

ACKNOWLEDGMENTS

The author would like to thank the Richard King Mellon Foundation of Pettsburgh, Pennsylvania, for the financial support that made research on the ecology of desert fan palms oases possible. Appreciation is also extended to Barbara McAlpine who reviewed and edited the manuscript.

REFERENCES CITED

Bailey, H.P., 1966. Weather of southern California. University of California, Berkeley.

Cornett, J.W., 1988. Naturalized populations of the desert fan palm, *Washingtonia filifera*, in Death Valley National Monument, *in* Plant biology of eastern California, C.A. Hall Jr. and V. Doyle-Jones, eds. Los Angeles, University of California Press.

___, 1989. Desert palm oasis. Palm Springs, Palm Springs Desert Museum.

___, 1991. Population dynamics of the palm, *Washingtonia filifera*, and global warming. Redlands, San Bernardino County Museum Association Quarterly, 38(2):46-47.

Henderson, R., 1961. On desert trails. Los Angeles, Westernlore Press.

Iacopi, R., 1974. Earthquake country. Menlo Park, Lane Books.

Jaeger, E.C., 1957. The North American deserts. Stanford University Press.

Kirk, R., 1973. Desert the American Southwest. Boston, Houghton-Mifflin Company.

Oakeshott, G.B., 1971. California's changing landscapes. New York, McGraw-Hill Book Company.

Geomorphic and Soil Stratigraphic Evaluation of a Faulted Alluvial Sequence, Eastern Coachella Valley, California

STEPHEN G. WELLS and SEAN CONNELL, *Dept. of Earth Sciences, University of California, Riveride CA 92521*
JAY J. MARTIN *CHJ Inc., 1355 E. Cooley Drive, Colton CA 92324*

INTRODUCTION

A major problem facing geologists working in tectonically active settings is the ability to determine the history of fault activity in areas where conventional dating techniques, such as radiocarbon dating, are unabailable. The careful use of soil chronosequences can provide age constraints for fault activity provided the rupture history can be bracketed by geomorphic surfaces with distinctive soil characteristics. Soil stratigraphic studies conducted in the Indio Hills (Keller and others, 1982) and the Eastern Mojave-Silver Lake area (Wells and others, 1987) can provide age constraints on the basis of soil development.

This paper presents results from a study conducted by Gary S. Rasmussen and Associates (1992) for a proposed low-level sanitary landfill extension in the Coachella Valley, Riverside County, California. The proposed landfill site, termed here as the Coachella Landfill Extension (CLE), is north of the town of Indio and is underlain by a faulted alluvial fan and pediment complex of the Little San Bernardino Mountains piedmont. The primary goal of this paper is to present the soil stratigraphic, geomorphic, and neotectonic setting of this part of the Little San Bernardino Mountains piedmont.

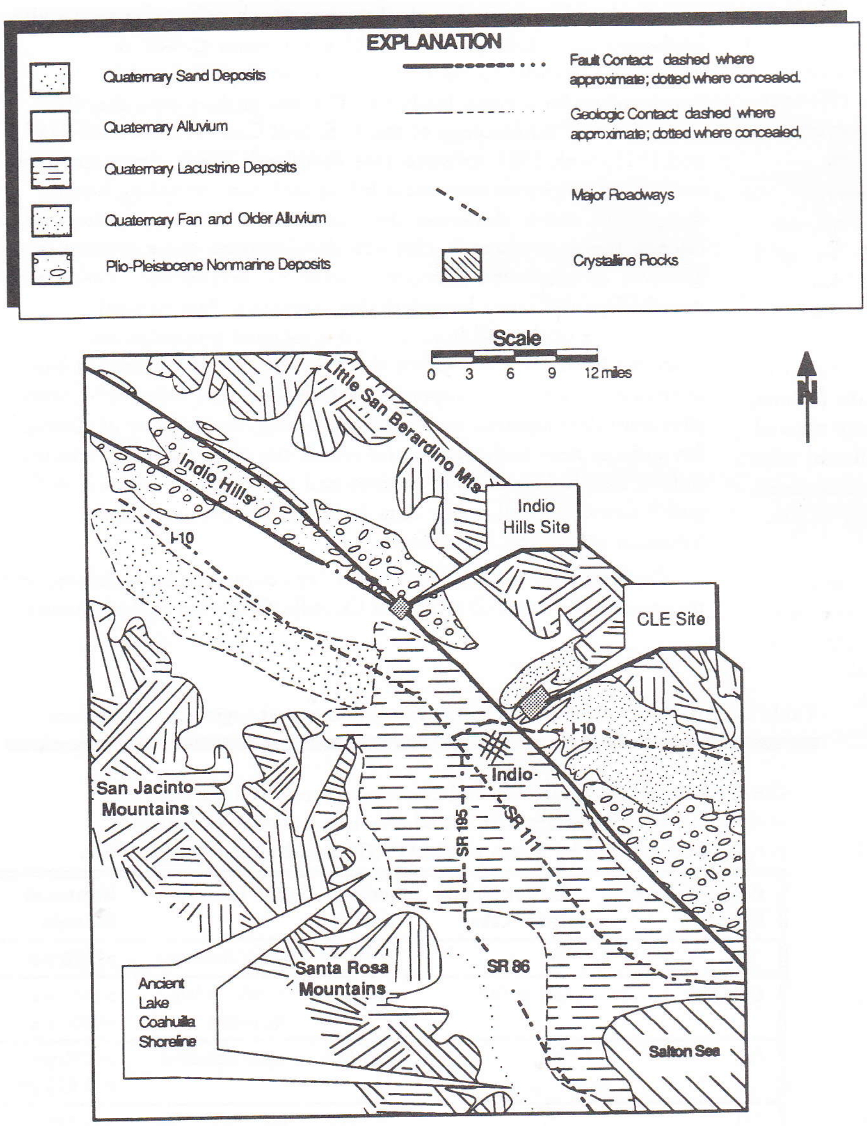

Figure 1. Generalized geologic location map of the Coachella Valley area, southern California, depicting locations of the Coachella Landfill Extension (CLE; see Fig.2) and the Indio Hills site (Fig.3).

The CLE site (Figs. 1 & 2) is south of the Indio Hills and north of the Mecca Hills. The Indio Hills are composed of a series of northwest-trending hills deformed by the Mission Creek and Banning fault segments of the San Andreas fault zone. The southern Indio Hills and the CLE study area are underlain by the Ocotillo and Palm Spring(?) formations, which consist of deformed sandstone and fanglomerate (Dibblee, 1954; Popenoe, 1959).

The climate is very arid with hot summers and moderate to cool winters, a mean annual temperature of approximately 21°C (72°F) and a mean annual precipitation of approximately 10 cm (Knecht, 1980).

GEOLOGY AND GEOMORPHOLOGY

The study area is on the northeastern piedmont of the Coachella Valley between the Little San Bernardino Mountains, to the east, and the San Jacinto and Santa Rosa Mountains, to the west. The Coachella Valley is structurally dominated by the San Andreas fault which is located less than 520 m (1700 ft) southwest of the site (Dibblee, 1954; Crowell, 1975; Sylvester and Smith, 1976; Rymer, 1991). The CLE site is between the Indio and Mecca hills, where the strike of the San Andreas fault is approximately N43°W and parallel to the prevailing plate motion vector (Sylvester, 1991). The Indio Hills lie to the north of the study area and consist of uplifted Plio-Pleistocene sedimentary rocks of the Palm Spring and Ocotillo formations as well as younger Quaternary alluvium (Fig. 3). The Indio and Mecca Hills represent structural culminations, or uplifted segments, that developed in response to compression along restraining bends in the San Andreas fault, where the

Table 1. Soil profile descriptions for Coachella landfill extension site. Soil descriptions from field measurements. Colors based on Munsell notation. Profile terminology follows that of Soil Survey Staff (1951 and 1975) with revisions in Birkeland (1984).

Alluvial Unit	Pedon Number	Profile Horizon Designation	Carbonate Morphology
Qf5	2	Avk-Bk1-Bk2-2Bk-3Bk-4Bwkb	disseminated to weak Stage I
Qf3a	4	A-AvBwk-Bwk1-Bwk2-Bk1-Bk2-Cox-2Btkb	disseminated to weak Stage I
Qf2	3	Ak-AvBwk-Bwk1-Bwk2-Bwk3-Bwk4-Bk-C-2Ck-3Bwkb1-3Bwkb2-4Kb-4Bkb-4Btkb	Stage I
Qf1	1	Ak-AvBwk-Btkl-Btk2-Avkb-Btkb-2Avkb-2Btkb	Stage I+ to II

fault strike is typically about N48°W (Sylvester, 1991). The piedmont along the western flank of the Little San Bernardino Mountains is disrupted by the Indio Hills, which deflect most drainages. However, major drainages, such as Pushwalla and Thousand Palms canyons, have been able to transect the Indio Hills.

The CLE site is underlain by an areally extensive pediment-alluvial fan complex, mapped as Qf1 (Fig. 2). This pediment is cut into sandstone and conglomerate of the Ocotillo and Palm Spring(?) formations and is part of an alluvial fan associated with several drainages heading in the Little San Bernardino Mountains. An poorly-exposed ash along the southern portion of the study area may be the 0.74 Ma Bishop ash which has been found to occur within the upper part of the Palm Spring Formation in the Mecca Hills (Rymer, 1991). At least six distinct late Holocene to late Pleistocene alluvial fan deposits have been differentiated on the site. These alluvial units represent geomorphic surfaces that have developed due to base level lowering in response to stresses along the San Andreas fault (Clark, 1984).

Mapping of geomorphic surfaces was performed on the basis of geomorphic position and surface alteration. Surface alternation was evaluated on the basis of stone pavement development, degradation of exposed clasts, presence of rock varnish and depositional topography (e.g., presence of depositional bars and swales). Several trenches were excavated in order to evaluate the subsurface character of faulting and to establish geomorphic and stratigraphic control of late Quaternary fault activity. The primary focus of this paper is on soil stratigraphic relationships. The nature and style of faulting at the site will only be briefly discussed.

An extensive trenching program for the Coachella Landfill Extension (Figs. 2, 4, & 5) has resulted in the delineation of several northwest- to northeast-trending faults that cut a pediment surface and alluvial fan deposits. Ages of alluvial an deposits were made on the basis of correlations between soil chronosequences established at Silver Lake (Wells and others, 1987), approximately 195 km (120 miles) north of the site, and ages determined on an offset pediment-alluvial fan complex (Keller and others, 1982) in the Indio Hills (Fig. 3).

Determination of geomorphic surface ages was made following analyses of terrace stratigraphy, geomorphology and detailed geomorphic-surface mapping by Gary S. Rasmussen and Associates. Descriptions of soil morphology, characterization of a soil chronosequence and correlation with other soil sequences were then made.

SOIL MORPHOLOGY DESCRIPTION

Studies of soil morphology and soil-profile development were used to aid in the subdivision and correlation of unconsolidated surficial sediments and to aid in providing age estimates for these sediments. Four pedons (profile descriptions) were established and described in four trenches, designated at pedons 1, 2, 3 and 4 (Fig. 2, Tables 4, 5, 6, & 7) which expose late Quaternary alluvial fan deposits and continental sedimentary rocks of the Quaternary Ocotillo formation. At each pedon location, field descriptions of soil morphology and landscape conditions were used to establish detailed soil stratigraphic relations. Soil stratigraphic relations were, in turn, used to interpret and assign age estimates for geomorphic surfaces and soil stratigraphic units.

Soil profiles were described at sites which reflect the most stable landscapes (i.e., surfaces which display minimum erosion or deposition) in order to assess the maximum degree of soil development for a given landform. The soil profiles were described using the field terminology of the U.S. Soil Conservation Staff (1951 and 1975) with 1981 revisions (see Birkeland, 1984). Approximately twelve soil properties were recorded at each site, including horizon designation, depth, thickness, dry and moist color, texture, structure, dry and moist consistency, clay film development, stone content, root and pore development, pedogenic carbonate development, carbonate morphology and lower boundary characteristics. The vertical arrangement of the soil horizons and associated properties are described from the land surface down to the parent material or base of trench. In addition, properties such depositional topography, stone pavement development and clast weathering observations of alluvial fan surfaces near each trench and profile site were recorded; selected surface morphology data are summarized in Table 3. Tables 1, 4, 5, 6 and 7 summarize soil profile data from the trenches at selected locations on alluvial fan surfaces.

The similarity in parent materials (eg., coarse-grained plutonic and metamorphic clasts and reworked Ocotillo formation and sediments

Table II. Age estimates based on soils morphology and regional correlations

Comparison of the Coachella soil chronosequence and surface morphological parameters with dated chronosequences and surface properties described by Wells et al.(*1987) and Keller et al.(+1982).

Coachella Landfill Extension	Eastern Mojave Silver Lake	Indio Hills	Age Estimate	Numerical Estimate
Qf5	Qf5	unit Qal	latest Holocene	>1000 yrs
Qf3a	Qf3 or Qf4	unit Qf1	middle to late Holocene	>1000 yrs, <8000 yrs
Qf2	Qf2	unit Qf1	early Holocene	>8000 yrs, <11,000 yrs
Qf1	Qf1	unit Qf2	late Pleistocene	>22,000 yrs, <50,000 yrs

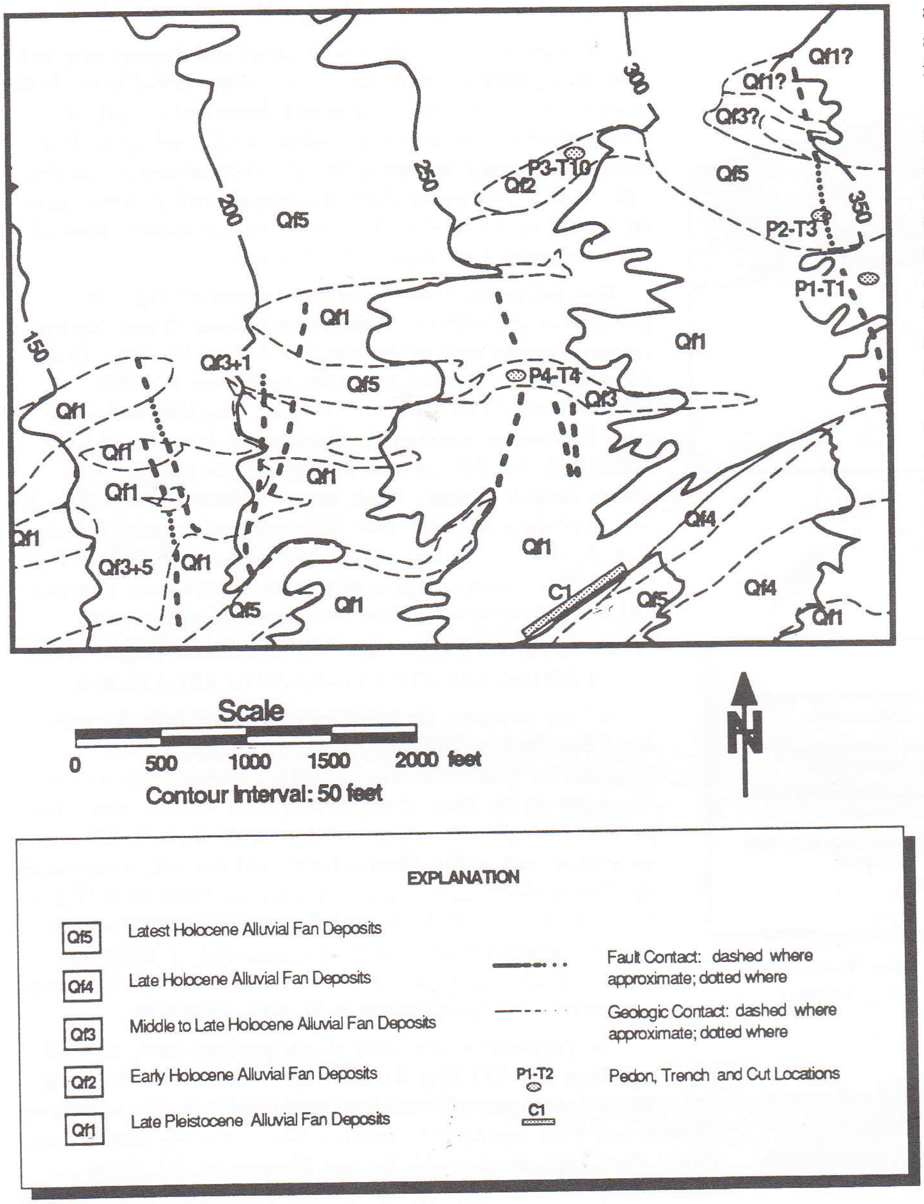

Figure 2. Generalized geologic map of the Coachella Landfill Extension site (CLE) illustrating major mapped units and faults. Redrawn and simplified from original (1:2400) map by Rasmussen (1992).

derived from the Little San Bernardino Mountains) has allowed for comparisons of soil development on landforms of different fans without encountering problems normally associated with different rates of soil development in different parent materials.

SURFACE AND SOIL MORPHOLOGY OF LATE QUATERNARY STRATIGRAPHIC SEQUENCE

Unit Qf5

Surfaces of alluvial fan unit Qf5 are characterized by well-developed, depositional bar and swale topography with greater than 30 cm (1 ft) of relief (Table 3). Clasts on this surface exhibit minor rock varnish and very slight rubefication (reddening) on clast undersides, which indicate fan surface stability. Most of the coarse-grained plutonic and metamorphic clasts show minor disintegration and slight splitting. The lack of weathering and alteration of surface clasts suggest a very young age for this unit.

The soil profile of unit Qf5 is characterized by a thin Avk horizon overlying several thin Bk horizons (Tables 1 & 4). The Avk horizon is greater than 2.5 cm in thickness and is composed of a vesicular sandy loam with 2.5Y hues, platy structure, and disseminated, as well as reworked, pedogenic calcium carbonate. The Avk horizon is underlain by four Bk horizons with a total thickness of approximately 76 cm (30 in). The morphology of these horizons is dominated by translocated (pedogenic) calcium carbonate which resulted in the Bk horizon designation, as opposed to the commonly but erroneously used Ck horizon. The morphology of the sand-textured Bk horizons are typified by single grain structure (loose, non-sticky, and non-plastic consistency) and disseminated to weak stage I calcium carbonate. This profile rests above a buried soil developed in older Quaternary deposits. This buried profile was not described. The thin nature (81 cm; 32 in.) of unit Qf5 demonstrates the "strath-like" character of this young fan deposit.

Unit Qf3a

The surface of alluvial fan unit QF3a is characterized by well-developed bar and swale depositional topography with weakly developed stone pavements in swale areas (Table 3). The depositional relief is typically less than 20 cm. Coarse-grained plutonic surface clasts exhibit moderate pitting and disintegration, whereas the metamorphic clasts only exhibit minor amounts of splitting and disintegration. Thin coatings of rock varnish typically cover 50% of the tops and sides of clasts on the surface of Q5a (Table 5). The undersides of the varnished clasts display rubefication with hues ranging from 7.5YR to 5YR. Weak 7.5TY hues are typical of the pavement clasts on unit Qf3a (Table 3).

The profile of alluvial unit Qf3a is characterized by relatively thin horizons (Table 1 & 5). The AvBwk horizon has 2.5Y hues on ped faces, reflecting the downward migration of 2.5Y-hued loamy sand along ped faces from the overlying Ak horizon. More weathered vesicle-rich ped interiors are exhibited by 10YR hues and sandy clay loam textures of the AvBwk horizon. Secondary (pedogenic) calcium carbonate has accumulated in the interior and base of these peds as demonstrated by violent effervescence. Six 15-cm thick Bwk horizons exhibit 10YR hues, loamy sand to sand textures, colloidal staining and bridges, and weak stage I calcium carbonate. These horizons overlie two thin Bk horizons with 2.5Y hues and exhibit very weak stage I calcium carbonate. These horizons overlie two thin Bk horizons with 2.5Y hues and exhibit very weak stage I to disseminated calcium carbonate morphology. A thin (7.5 cm; 3 in) Cox horizon exhibiting 10YR hues is overlain by the Bk horizons. This profile rests on a buried soil that was not described.

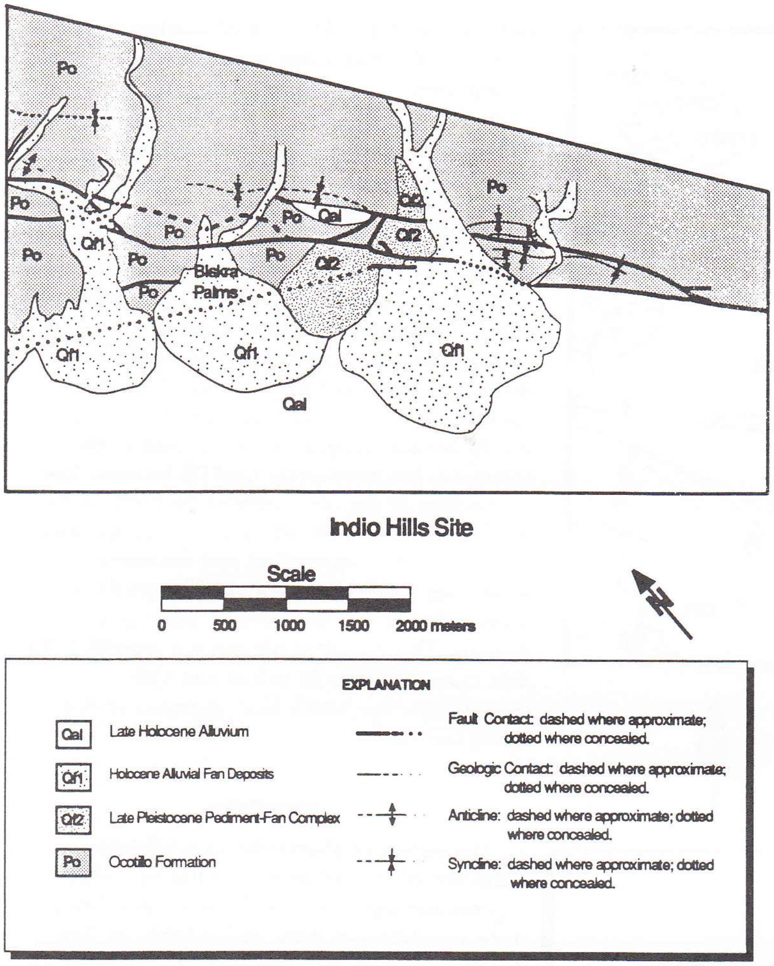

Figure 3. Generalized geologic map of the Indio Hills site illustrating major mapped units and faults. Modified from Keller et al. (1982).

Unit Qf2

The surface of alluvial fan unit Qf2 has been modified sufficiently such that only faint bar and swale topography exists (Table 3). Moderately developed stone pavement with interlocking clasts occurs on swales and bars. Relief on the surface is produced by individual clasts and not by clast aggregates. Clasts of coarse-grained plutonic rocks exposed at the surface are significantly more fractured than the clasts of units Qf5 and Qf3a and also show significant amounts of disintegration whereby clasts are eroded down to the level of the stone pavements. Rock varnish coatings are thin due to the increased weathering of surface clasts. Rubefication on surface clast undersides varies from weak to strong with hues ranging from 2.5Y to 7.5YR.

The soil horizons of this unit are moderately thick (Table 6). The AvBwk shows advanced development of morphological properties in unit Qf2 compared to unit Qf3a, such as a more platy structure and the presence of clay films on ped faces. The Bwk horizons have a total thickness of approximately 56 cm (22 in) with 8.5YR hues on ped faces and sandy loam textures. Colloidal stains and bridges dominate over clay film development in the Bwk. Carbonate stage morphology has a weak stage I development. The hues shift to 10YR and 2.5Y in the underlying Bk and C horizons. Unit Qf2 overlies a buried soil consisting of Bwkb horizons and a K horizon (stage III+ calcium carbonate morphology), indicating that the buried soil is very well developed and truncated.

Unit Qf1

The surface of unit Qf1 is widespread and displays very well developed pavements with no traces of depositional relief. Rock varnish coatings on clasts is less well developed on Qf1 as compared to varnish coatings present on Qf2 and Qf3a. This reflects an increase in clast splitting and disintegration on this older surface. Numerous clasts of coarse-grained plutonic rocks are eroded to the level of the ground surface. Rubeficiation of clast undersides have hues to 2.5YR (Table 7).

This soil profile exhibits the most advanced stages of pedogenesis as compared to the other surfaces. It also displays cumulic features such as the burial of AvBwk horizons. Thin Ak and AvBwk horizons are underlain by two thin Btk horizons with 7.5YR hues, thin to thick clay films and weak stage I carbonate morphology. Below these horizons lie two buried Avk and Btk horizons with properties similar to the surface AvBwk horizon. Weak stage I carbonate morphology is typical of these horizons. Five 2Bkb horizons decrease in hue with depth (over 46 cm) with a carbonate morphology of I+ and II. These morphological parameters demonstrate that unit Qf1 is significantly older than the other fan surface units.

AGE ESTIMATES, REGIONAL CORRELATIONS AND LANDSCAPE-STRATIGRAPHIC RELATIONS

Soil age estimates are based on correlation with the well-dated Eastern Mojave-Silver Lake soil chronosequence described by Wells and others (1987). The oldest fan unit is correlated on the basis of soil development with an offset fan-pediment complex described by Keller and others (1982) near the intersection of the Mission Creek and Banning segments of the San Andreas fault zone in the southern Indio Hills (Fig. 3). Comparison of the CLE site soil chronosequence and surface morphological parameters with soils described by Keller and others (1982) and Wells and others (1987) allow the tentative correlations and age estimates to be made (Table 2).

The piedmont in the study area is predominantly mantled late Quaternary unit Qf1 (Fig. 2). Unit Qf1 is variable in thickness and apparently rests unconformably to conformably on the underlying Ocotillo and Palm Spring(?) formations. We tentatively correlate unit Qf1 of the Coachella area with the late Pleistocene Qf1 of the Eastern Mojave-Silver Lake area which has a minimum age constraint of approximately 22 Ka derived from radiocarbon dates and lacustrine sedimentation rates and an upper age limit of approximately 40 to 50 Ka based on experimental surface-exposure ages. Such age estimates are compatible with those of Keller and others (1982) for a similar alluvial unit in the Indio Hills (Table 2). Inset below the Qf1 surfaces are units Qf2 through Qf5 which are inferred to range in age from early to late Holocene based upon the degree of soil development.

CONCLUSIONS

Tectonic deformation within the Coachella landfill extension (CLE) site is dominated by dip-slip faults that strike between N20°W and N20°E. This site is between the Indio and Mecca hills, immediately east of the main trace of the San Andreas fault zone. Faults mapped at the CLE site do not exhibit significant lateral offset. In contrast, the offset pediment-fan complex (Keller and others, 1982) in the Indio Hills exhibits significant right-lateral oblique slip and folding that has occurred since the late Pleistocene.

The Indio Hills and Coachella landfill extension site exhibit significant differences in along-strike tectonic style over relatively short distances. The style of faulting along the San Andreas fault in

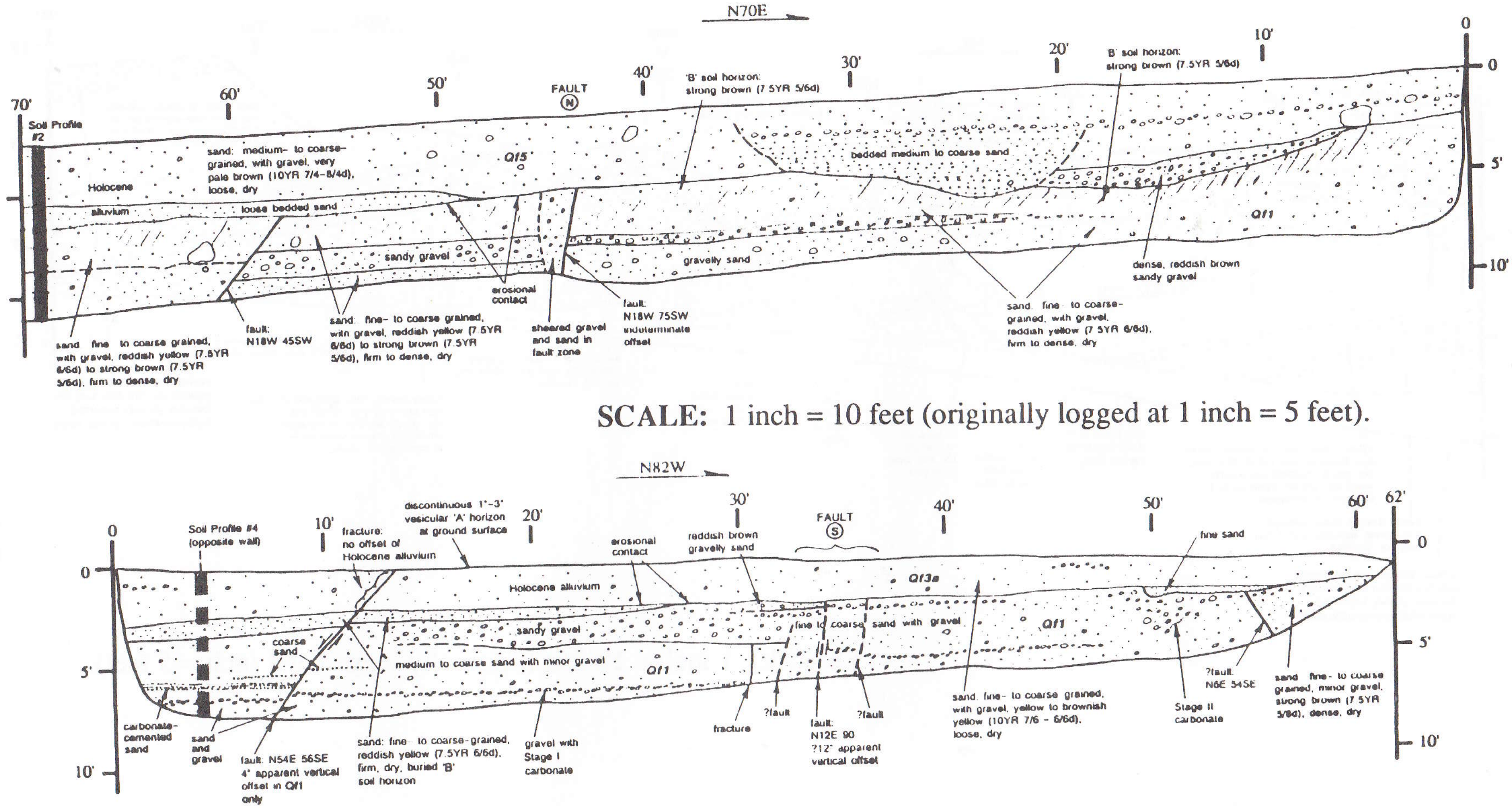

Figure 4. Geologic Logs of backhoe excavations in the Coachella Landfill Extension Site. Trench 3, pedon 2 (top) exhibits undeformed latest Holocene (Qf5) fan deposits. Trench 4, pedon 4 (bottom) exhibits undeformed early to middle Holocene alluvial fan deposits (Qf3) (From Rassmussen, 1991).

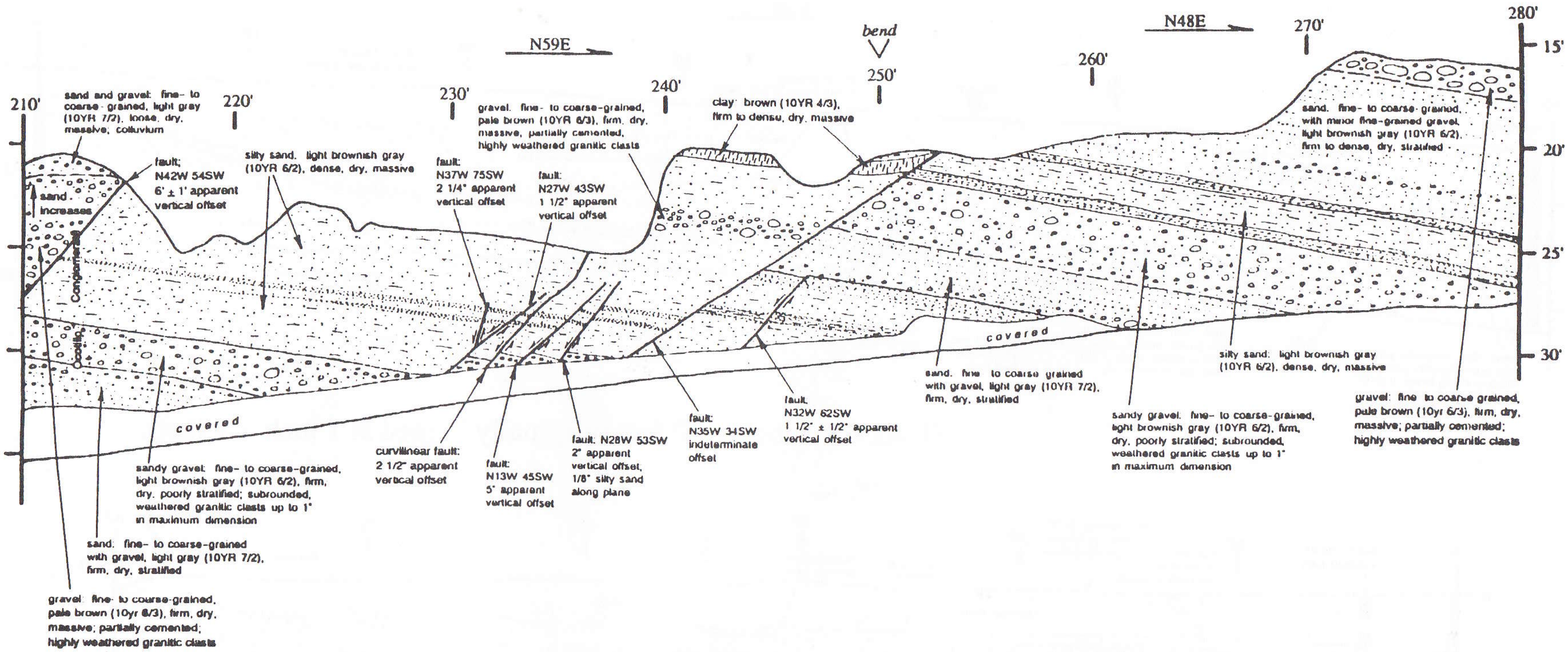

SCALE: 1 inch = 10 feet (originally logged at 1 inch = 5 feet).

Figure 5. Geologic Log of bulldozer excavation in the Coachella Landfill Extension Site. This cut (Cut 1) exhibits deformed Ocotillo Formation (From Rassmussen, 1991).

Table III. Surface morphology and stone pavements of alluvial fan deposits, CLE.

Alluvial Unit	Depositional Bar Relief	Reddening on Clast Undersides* Cover (a)	Max. Color (b)	Clast Varnish+ Color (c)	Cover/Thickness (d)
Qf5	> 1 ft strong bar & swale	n.m.	n.m.	[very weak to no varnish]	
Qf3a	< 3/4 ft strong bar & swale	weak	5YR 5/8	5YR 2.5/1	75-100%/T
		weak	7.5YR 5/6	5YR 3/2	50%/T
		n.o.	n.m.	5YR 3/2	50%/T
		weak	7.5YR 6/8	10YR 2/2	<25%/T
		weak	7.5YR 5/8	5YR 2.5/1	75-100%/T
		moderate	7.5YR 5/8	5YR 2.5/1	50%/T
		weak	7.5YR 6/8	5YR 3/1	75%/T
		weak	5YR 4/6	7.5YR 2/0	75-100%/T
		weak	7.5YR 5/6	5YR 2.5/1	50%/T
Qf2	single clast faint bar & swale	weak	2.5YR 5/8	5YR 2.5/1	75%/T
		weak	5YR 5/8	5YR 3/2	50-75%/T
		weak	7.5YR 6/8	5YR 2.5/2	75-100%/T
		moderalte	5YR 5/8	5YR 3/1	25-50%/T
		weak	5YR 5/8	10YR 2/2	25%/T
		weak	5YR 5/8	10YR 2.5/1	25%/T
		strong	5YR 5/8	5YR 3/2	50-75%/T
		moderate	5YR 5/6	7.5YR 3/2	25-50%/T
		n.o.	n.m.	5YR 2/5/1	50%/T
		weak	7.5YR 5/6	7.5YR 3/2	50-75%/T
Qf1	single clast no bar & swale	moderate	5YR 6/8	5YR 3/2	50-75%/T
		strong	2.5YR 4/6-8	5YR 3/2	50-75%/T
		weak	5YR 3/2	2.5YR 2.5/0	25-50%/T
		weak	7.5YR 5/8	10YR 4/1	25-50%/T
		moderate	5YR 5/8	5YR 3/2	25-75%/T
		moderate	5YR 5/8	5YR 2.5/2	75%/M
		moderate	5YR 5/4	5YR 2.5/1	<25%/T
		weak	5YR 6/8	5YR 3/2	<25%/T
		moderate	2.5YR 5/8	5YR 3/2	25-50%/T
		weak	7.5YR 2.5/1	5YR 2.5/1	25-50%/T

Surface descriptions are from field measurements. Colors are measured dry and are based on Munsell notation.

***Reddening on Clast Undersides**

(a) Maximum color observed is given

(b) Cover and thickness estimates:

weak = clast lithology clearly visible and <30% of underside reddened

moderate = clast lithology faintly visible and 30-60% of underside reddened

strong = clast lithology obscured and >60% of underside reddened

+Clast Varnish

(c) Darkest color observed

(d) Cover and thickness estimated:

classes = 0%, 0-25%, 25%, 25-50%, 50%, 50-75%, 75%, 75-100%, 100%

T = thin, mineralogy observable; M = moderate, mineralogy partially obscured; Th = thick, mineralogy completely obscured

the eastern Coachella Valley is geomorphically manifested by the development of linear hills where compression along restraining bends result in local uplift with subsequent dissection and exposure of subsurface structure. This tectonic style is contrasted by the adjoining southern fault-zone segment in the CLE area, which has an orientation parallel to the prevailing plate motion vector of approximately N43°W (Sylvester, 1991). The style of faulting along this segment is manifested by smaller magnitude dip-slip faulting and basinward lowering of base-level. This results in partial burial of Quaternary deposits towards the valley floor, rather than compression, uplift and the formation of hills to the north and south of the CLE.

Stresses generated along the restraining bend in the San Andreas fault zone, north of the CLE site, are taken up by folding and uplift, which results in the formation of structural culminations, such as the Indio Hills. Smaller magnitude slip and deformation at the CLE site results in a geomorphic expression of an uplifted pediment and fan complex. The differences in geomorphology between these two areas are probably the result of changes in the stress field near the

Table IV. Soil profile description of Pedon Number 2, Alluvial Fan Unit Qf5, CLE, Riverside Co.

Pedon description conducted by S.G. Wells & S. Connell on 8/27/92. Soil descriptions from field measurements. Colors based on Munsell notation for dry (d) or moist (m) colors. Profile terminology follows that of Soil Survey Staff (1951 and 1976) with revisions in Birkeland (1984).

SURFICIAL SETTING

Landform: alluvial fan and terrace with well-developed bar & swale topography

Parent Material: alluvium reworked from Ocotillo fm and sediment from Little San Bernardino Mts

Vegetation: creosote bush *(Larrea tridentata)*, mormon tea *(Ephedra)*, pencil cholla *(Opuntia ramosissima)*, paloverde *(Parkinsonia* spp), four-wing saltbush *(Atriplex canescens)(?)* **Aspect/slope**: southwest/<4 degrees **Elevation**: ~345 ft

PROFILE DESCRIPTION

Horizon	Depth (in)	Description
Avk	0 - 1.5	2.5Y 6/3 light yellowish brown on ped face (d), 2.5Y 4/2 grayish-brown (m), 2.5Y 6/3 light yellowish brown (crushed); sandy loam; moderate coarse platy; slightly hard (d), slightly sticky non-plastic (md); few thin colloidal stains on larger grains; 50% gravel; few very fine roots; fine common vesicles coated with siltans; strongly effervescent, disseminated pedogenic $CaCO_3$; clasts appear to have reworked stage I $CaCO_3$ larger clasts; abrupt smooth
Bk1 [Ck1]*	1.5 - 7.5	2.5Y 7/3 pale yellow (d), 2.5Y 5/2 grayish brown (m); sand; single grain; loose (d), non-sticky, non-plastic (md); very few thin colloidal stains; 40-50% gravel; common very fine to fine roots; many medium pores; strongly effervescent, disseminated to very weak stage I $CaCO_3$; large wide void spaces under large clasts which have sand caps; clear smooth
Bk2 [Ck2]*	7.5 - 13.5	2.5Y 6/3 light yellowish brown (d), 2.5Y 5/2 grayish brown; sand; single grain; loose (d), non-sticky, non-plastic; 25% gravel; common very fine to fine roots; common medium pores; strongly effervescent, very weak stage I $CaCO_3$; clear wavy
2Bk [2Ck]*	13.5 - 24	2.5Y pale yellow (d); 2.5Y 5/2 grayish brown (m); sand; single grain; loose (d), non-sticky, non-plastic (m); very few thin colloidal stains on larger clasts; 5% gravel; few very fine roots; strongly effervescent, disseminated $CaCO_3$; clear wavy
3Bk [3Ck]*	24 - 32	2.5Y 6/3 light yellowish brown (d); 2.5Y 5/2-3 grayish brown to light olive brown (m); sand; single grain; loose (d), non-sticky, non-plastic (m); very few thin colloidal stains on larger grains and clasts; 50% gravel; very slightly effervescent, disseminated to weak stage I $CaCO_3$; sand caps on clast tops; abrupt smooth
4Bwkb	32 +	buried soil (not described)

*Horizon designation of Ck is not considered proper by the Soil Staff Manual if pedogenic calcium carbonate has been translocated in profile; however, the Ck horizon designation is commonly used rather than the proper horizon designation of Bk. Both horizon designations are given for clarification.

intersection of the Mission Creek and Banning faults.

ACKNOWLEDGMENTS

This project was performed at the request of G.S. Rasmussen and Associates for the County of Riverside. The authors would like to especially thank Mr. Gary Rasmussen and Mr. Frank Jordan for their assistance with this project.

REFERENCES CITED

Birkeland, P.W., 1984. Soils and geomorphology. Oxford University Press: 372 p.

Clark, M.M., 1984. Map showing recently active breaks along the San Andreas fault and associated faults between Salton Sea and Whitewater-Mission Creek, California. U.S. Geological Survey Misc. Inv. Map I-1483, scale 1:24,000.

Crowell, J.C., 1975. Geological sketch of the Orocopia Nountains, southeastern California, *in* San Andreas fault in southern California, J.C. Crowell, ed. California Division of Mines and Geology Special Report, 118.

Dibblee, T.W. Jr., 1954. Geology of the Imperial Valley region, California. California Division of Mines and Geology Bulletin, 170:21-28.

Keller, E.A., M.S. Bonkowski, R.J. Korsch, and R.J. Schlemon, 1982. Tectonic geomorphology of the San Andreas fault zone in the southern Indio Hills, Coachella Valley, California. Geological Society of America Bulletin, 93:46-56.

Knecht, A.A., 1980. Soil survey of Riverside County, California, Coachella Valley area. U.S. Department of Agriculture, Soil Conservation Service: 89 p, 21 pl.

Popenoe, F.W., 1959. Geology of the southeastern portion of the Indio Hills, Riverside County, California [MA thesis]. Los Angeles, University of California: 153 p.

Soil Survey Staff, 1975. Soil taxonomy. U.S. Department of Agriculture, Soil Conservation Service Handbook, 436: 754 p.

___, 1951. Soil Survey manual. U.S. Department of Agriculture, Soil Conservation Service Handbook, 18: 503 p.

Rasmussem, G.S. and Associates, 1992. Geologic evaluation of faulting, Coachella sanitary landfill expansion, southern portion of section 22, T.5S, R.8E, east of Indio, California. San Bernardino, Gary S. Rasmussen and Associates, Project 3118, Oct. 12, 1992: 27 p.

Rymer, M.J., 1991. Geologic structure, transpression and neotectonics of the San Andreas fault zone in the Salton trough, California: Part 2, the Bishop Ash bed in the Mecca Hills, *in* Geologic excursions in southern California and Mexico, M.J. Walawender and B.B. Hanon, eds. Geological Society of America Annual Meeting Guidebook, San Diego:388-396.

Sylvester, A.G., 1991. Geologic structure, transpression and neotectonics of the San Andreas fault zone in the Salton trough, California: Part 1, palm tree structure in central Mecca Hills, *in* Geologic excursions in southern California and Mexico, M.J. Walawender and B.B. Hanon, eds. Geological Society of America Annual Meeting Guidebook, San Diego:378-387.

Sylvester, A.G. and R.R. Smith, 1976. Tectonic transpression and basement controlled deformation in the San Andreas fault zone, Salton trough, California. American Association of Petroleum Geologists Bulletin, 60(12):1208-2102.

Wells, S.G., L.D. McFadden, and J.D. Dohrenwend, 1987. Influence of late Quaternary climate changes on geomorphic processes on a desert piedmont, eastern Mojave Desert, California. Quaternary Research, 27:130-146.

Table V. Soil profile description of Pedon Number 4, Alluvial Fan Unit Qf3a, CLE.

Pedon description conducted by S.G. Wells & S. Connell on 8/28/92. Soil descriptions from field measurements. Colors based on Munsell notation for dry (d) or moist (m) colors. Profile terminology follows that of Soil Survey Staff (1951 and 1976) with revisions in Birkeland (1984).

SURFICIAL SETTING

Landform: thin alluvial fan with well-developed bar & swale topography which overlies Ocotillo fm (?)
Parent Material: alluvium reworked from Ocotillo fm and sediment from Little San Bernardino Mts
Vegetation: creosote bush *(Larrea tridentata)* **Aspect/slope**: southwest/4 degrees **Elevation**: ~284 ft

PROFILE DESCRIPTION

Horizon	Depth (in)	Description
A	0 - 0.25	2.5Y 6/3 light yellowish brown (d), 2.5Y 6/2 light brownish-gray (m); loamy sand; single grain; loose (d), non-sticky, non-plastic (m); 0% gravel; strongly effervescent, disseminated $CaCO_3$; very abrupt smooth
AvBwk	0.25 - 1.25	2.5Y 6/2 light brownish gray on ped face, 10YR 7/3 very pale brown on ped interiors, crushed (d); 10YR 4/3 brown (m); sandy clay loam; moderate medium to coarse subangular blocky; slightly hard (d), sticky, very slightly plastic; few thin discontinuous colloid stains and bridges; 30% gravel; few very fine roots; many fine vesicles and tubular pores; violently effervescent, disseminated to stage I $CaCO_3$; very abrupt smooth
Bwk1	1.25 - 5.25	10YR 7/2-3 light gray to very pale brown (d), 10YR t/3 brown (m); loamy sand; weak fine to medium subangular blocky; weakly coherent (d); very slightly sticky, non-plastic (m); few thin colloid stains and bridges on large grains and clasts; 5-10% gravel; common very fine roots; few fine pores in krotovina; strongly effervescent, disseminated to very weak stage I $CaCO_3$; clear wavy
Bwk2	5.25 - 5.25	10YR 7/3 very pale brown (d), 10YR 6/3-4 pale brown to light yellowish brown (m); sand; single grains to weak medium granular; loose (d); non-sticky, non-plastic (m); few very thin colloid stains and bridges on larger grains and clasts, bridges on larger grains; 15-20% gravel; few very fine roots, few fine pores; strongly effervescent, weak stage I $CaCO_3$; abrupt smooth
Bk1	5.25 - 11.25	2.5Y 7/3 pale yellow (d), 2.5Y 6-5/3 light yellowish brown to light olive brown (m); sand; single grain to weak medium subangular blocky; loose to slightly hard (d), non-sticky, non-plastic (m); few thin colloid stains on large grains; 15% gravel; few very fine roots; few fine pores; strongly effervescent, disseminated to very weak atage I $CaCO_3$; abrupt smooth
Bk2	11.25 - 17.25	2.5Y 7/4 to 10YR 7/4 pale yellow to very pale brown (d), 2.5Y 6-5/3 light yellowish brown to light olive brown (m); sand; single grain to weak medium to coarse granular; loose to weakly coherent (d), non-sticky, non-plastic (m); few thin colloid stains; 10-15% gravel; common very fine roots; few fine pores; strongly effervescent, disseminated $CaCO_3$; abrupt wavy
Cox	17.25 - 20.25	10YR 6/4-6 light yellowish brown to brownish yellow (d), 10YR 6/4-6 light yellowish brown to brownish yellow (m); sand; single grain; loose (d), non-sticky, non-plastic (m); few thin colloid stains, bridges on large grains; 5% gravel; no effervescence; abrupt smooth
2Btkb	20.25 - 72.5	buried soil (not described)

Table 6. Soil profile description of Pedon Number 3, Alluvial Fan Unit Qf2, CLE.

Pedon description conducted by S.G. Wells & S. Connell on 8/28/92. Soil descriptions from field measurements. Colors based on Munsell notation for dry (d) or moist (m) colors. Profile terminology follows that of Soil Survey Staff (1951 and 1976) with revisions in Birkeland (1984).

SURFICIAL SETTING

Landform: alluvial fan with faint bar & swale topography

Parent Material: alluvium reworked from Ocotillo fm and sediment from Little San Bernardino Mts

Vegetation: creosote bush *(Larrea tridentata)* **Aspect/slope**: southwest/4 degrees **Elevation**: ~292 ft

PROFILE DESCRIPTION

Horizon	Depth (in)	Description
Ak	0 - 0.25	2.5Y 6/3 light yellowish brown (d), 2.5Y 4/2 dark grayish brown (m); sandy loam; single grain; loose (d), very slightly sticky, non-plastic (m); very slightly effervescent, disseminated $CaCO_3$; very abrupt
AvBwk	0.25 - 2.25	2.5Y 6/3 light yellowish brown on ped top, 10YR 6/4 light yellowish brown on ped underside, 10YR 7/4 very pale brown crushed (d), 10YR 4/3 dark brown (m); clay loam; moderate coarse platy and subangular blocky to very coarse subangular blocky; slightly hard (d), sticky moderately plastic (m); few thin colloid stains and bridges with few thin to merately thick films on larger grains; 5% gravel; few very fine roots; many common vesicles; strongly effervescent on ped undersides to slightly effervescent on ped sides, disseminated $CaCO_3$; abrupt smooth
Bwk1	2.25 - 3.75	10YR 6/4 light yellowish brown (d), 10YR 5/6 yellowish brown (m); sandy loam; weak fine subangular blocky; loose to slightly hard (d); sticky to moderately plastic (m); few thin colloid stains and bridges with few thin clay films on larger grains; 5-10% gravel; few very fine roots; few very fine pores; violently effervescent, disseminated to weak stage I $CaCO_3$; abrupt smooth
Bwk2	3.75 - 10.25	8.5YR 6/4 light yellowish brown to light brown on ped, 10YR 6/4 light yellowish brown (crushed) (d), 10YR t/r yellowish brown (m); sandy loan; weak fine subangular blocky; loose to slightly hard (d), slightly sticky, non-plastic (m); common bridges with few thin colloid stains on large clasts, few thin films on clasts with few locally thick films on larger clasts; 15% clasts; common fine and medium roots; few fine pores; slightly effervescent, disseminated to very weak stage I $CaCO_3$; clear smooth
Bwk3	10.25 - 14.25	10YR 6/4-6 light yellowish brown to yellowish brown (d), 10YR 5/8 yellowish brown (m); sandy loam; single grain to weak fine granular; loose to slightly hard (d), slightly sticky non-plastic (m); few thin colloid stains & bridges; 30-40% gravel; few very fine roots; few fine pores; strongly effervescent, disseminated to weak stage I $CaCO_3$; clear smooth
Bwk4	14.25 - 24.25	8.5Y 6/6 reddish yellow to brownish yellow (d), 8.5YR 5/6 yellowish brown to strong brown (m); sandy loam; single grain to weak very fine granular; loose to slightly hard (d), slightly sticky non-plastic (m); few thin colloid stains on grains & few thin colloid, bridges, & films larger grains & clasts; 60% gravel; slightly effervescent, disseminated $CaCO_3$ near horizon top & weak stage I $CaCO_3$ on clasts; clear smooth
Bk	24.25 - 30.25	10YR 6/4 light yellowish brown (d), 10YR 6/3 pale brown (m); sand; single grain; loose (d), non-sticky non-plastic (m); very few thin colloid stains on large grains; 60% gravel; matrix non-effervescent, very weak stage I $CaCO_3$ on clasts; clear smooth
C	30.25 - 36.75	2.5Y 7/4-6 pale yellow to yellow (d), 2.5Y 6/3 light yellowish brown (m); sand; single grain; loose (d), non-sticky non-plastic (m); very few thin colloid stains on large grains and clasts; 40% gravel; matrix non-effervescent with slightly disarticulated $CaCO_3$ rinds & reworked carbonate coatings; clear wavy
2Ck	36.75 - 44.75	2.5Y 6/3 light yellowish brown (d), 2.5YR 5/3 light olive brown (m); sand; weak fine to medium granular to subangular blocky; loose to slightly hard (d), non-sticky non-plastic; few thin colloid stains; <5% gravel; matrix non-effervescent, strongly effervescent on clast undersides; clear wavy
3Bwkb1	44.75 - 50.75	10YR 5/6 yellowish brown (d), 10YR 4/3 brown (m); sandy loam; weak medium to coarse subangular blocky; loose to weakly coherent (d), slightly sticky non-plastic (m); few thin colloid stains on clasts; 5% gravel; few fine pores; matrix non-effervescent, slightly effervescent on clast undersides, few discontinuous coatings on large grains; abrupt wavy
3Bwkb2	50.75 - 54.25	10YR 5/8 yellowish brown (d); 10YR 5/3 brown (m); sandy loam; weak medium to coarse subangular blocky; loose to slightly hard (d), slightly sticky, very slightly plastic (m); few thin colloid stains and bridges on large grains & clasts; <5% gravel; slight effervescent, disseminated to weak stage I; few siltans; abrupt wavy
4kb	54.25 - 61.25	10YR 8/1 white on ped faces, 10YR 8/2 very pale brown crushed (d), 10YR 7/3 very pale brown (m); sandy clay loam; moderate coarse angular blocky; very hard; slightly sticky slightly plastic; very few thin colloid stains on clasts; <3% gravel; violently effervescent, stage III $CaCO_3$, incipient discoutinuous laminar layers; gradual wavy
4Bkb	61.25 - 68.25	10YR 6/3 pale brown (d), 10YR 7/2 light gray (m); loamy sand; weak fine to medium granular; weakly coherent (d), non-sticky non-plastic (m); very few thin colloid stains on clasts; 5-10% gravel; violently effervescent, stage I to stage II+ $CaCO_3$; abrupt irregular
4Btkb	68.25 - 74.5	10YR 6/4 light yellowish brown (d), 10YR 5/3 brown (m); loamy sand; weak medium subangular blocky to granular; slightly hard; slightly sticky, non-plastic; few thin bridges on grains & granules, moderately thick clay films on clasts; 10-15% gravel; common fine pores; strongly effervescent, stage I+ w/local pockets of stage II+ $CaCO_3$

Table 7. Soil profile description of Pedon Number 1, Alluvial Fan Unit Qf1, CLE.

Pedon description conducted by S.G. Wells & S. Connell on 8/27/92. Soil descriptions from field measurements. Colors based on Munsell notation for dry (d) or moist (m) colors. Profile terminology follows that of Soil Survey Staff (1951 and 1976) with revisions in Birkeland (1984).

SURFICIAL SETTING

Landform: alluvial fan with stone pavement and no bay & swale topography

Parent Material: alluvium reworked from Ocotillo fm and sediment from Little San Bernardino Mts

Vegetation: creosote bush *(Larrea tridentata)* & pencil cholla *(Opuntia ramosissima)* **Aspect/slope**: west/5 degrees **Elevation**: ~360 ft

PROFILE DESCRIPTION

Horizon	Depth (in)	Description
Ak	0 - 0.50	10YR 6/4 light yellowish brown (d), 10YR 4/3 dark brown (m); loamy sand; single grain; loose (d), non-sticky, non-plastic (m); very slightly effervescent, disseminated $CaCO_3$; very abrupt smooth
AvBwk	0.50 - 1.50	10YR 7/3 very pale brown on ped tops & sides, 8.5YR 6/6 reddish yellow to brownish yellow on ped undersides, 10YR 6/4 light yellowish brown crushed (d), 10YR 4/4 dark yellowish brown (m); sandy clay loam; strong fine to coarse subangular blocky, slightly hard (d), sticky plastic (m); very few to few thin bridges & colloid stains on clasts; 5-10% gravel; few very fine roots; common fine vesicles; very slightly effervescent on ped tops & violently effervescent on ped undersides, disseminated $CaCO_3$, very abrupt wavy
Btk1	1.50 - 3.50	10YR 6/6 reddish yellow crushed (d), 7.5YR 4/6 strong brown (m); sandy loam; single grain to weak very fine granular; loose (d), slightly sticky, non-plastic (m); few thin colloid stains & few moderately thick bridges; 10% gravel; few very fine roots; very slightly effervescent, disseminated $CaCO_3$; abrupt smooth
Btk2	3.50 - 5.50	7.5YR 6/4 light brown crushed (d), 10YR 4/4 brown (m); sandy loam; single grain; loose (d), slightly sticky, non-plastic (m); few thin colloidal stains & bridges, few thin to moderately thick clay films & bridges on large clasts; 10% gravel; few fine roots; very slightly effervescent, very weak stage I to disseminated $CaCO_3$; abrupt smooth
Avkb	5.50 - 7.0	7.5YR 7/2 pinkish gray on ped faces, 7.5YR 6/4 light brown crushed (d), 7.5YR 4/6 strong brown (m); sandy loam; moderate fine to coarse subangular blocky; hard (d), slightly sticky, non-plastic (m); few thin bridges and colloid stains with few to common thin films on ped face; 5% gravel; few fine roots; common fine vesicles; violently effervescent, weak stage I $CaCO_3$; horion discontinuous, varying from 0-1.5" thickness; very abrupt wavy
Btkb	7.0-8.50	7.5Y 7/6 reddish yellow (d), 7.5YR 4/6 reddish yellow (m); sandy loam; single grain; loose (d), slightly sticky non-plastic (m); few to common thin bridges & colloid stains & few to common thin films on clasts; 5-10% gravel; gravels disintegrate under slight pressure; few fine roots; strongly effervescent, disseminated to very weak stage I $CaCO_3$; very abrupt wavy
2Avkb	8.50 - 10.0	7.5YR 6/3 light brown on ped face, 7.5YR 6/3 light brown crushed, 7.5YR 5/4 brown (m); sandy loam; moderate very coarse subangular blocky; hard (d), slightly sticky, non-plastic (m); common thin bridges & colloid stains, few thin films on clasts & grains; 15% gravel, edges of clasts disintegrate under moderate pressure; few fine roots; common fine vesicles; violently effervescent, stage I to disseminated $CaCO_3$; abrupt wavy
2Btkb	10.0 - 14.0	7.5YR 6/6 reddish yellow (d), 7.5YR 5/6 strong brown (m); loamy sand; single grain to weak fine subangular blocky; loose to slightly hard (d), very slightly sticky, non-plastic (m); few thin colloid stains with few thin films on clasts & grains; 15-20% gravel; few very fine roots; violently effervescent, disseminated with pockets of very weak stage I $CaCO_3$; clear wavy
2Bkb1	14.0 - 18.0	10YR 6/4-6 light yellowish brown to brownish yellow (d), 10YR 5/6 yellowish brown (m); sand; weak fine sub-angular blocky; loose to slightly hard (d), non-sticky, non-plastic; few thin colloid stains & bridges w/ few thin clay films on large clasts; 35% gravel; few very fine roots; very slightly effervescent, stage I $CaCO_3$; clear wavy
2Bkb2	18.0 - 25.50	10YR 6/4-6 light yellowish brown to brownish yellow (d), 10YR 6/4 light yellowish brown (m); sand; single grain; loose, non-sticky, non-plastic; few thin colloid stains, bridges & clay films; 50% gravel; few very fine roots; violently effervescent, stage I $CaCO_3$; siltans 1-1.5 mm thick around larger clasts; clear wavy
2Bkb3	25.50 - 31.50	2.5Y 7/3 pale yellow (d); 2.5Y light yellowish brown (m); sand; weak fine to medium subangular blocky; loose to hard (d), non-sticky, non-plastic (m); very few thin colloid stains on clasts & large grains; >50% stones; common medium pores; slightly to violently effervescent, stage I+ $CaCO_3$; abrupt wavy
2Bkb4	31.50 - 50.0	2.5Y 7/3 pale yellow (d), 2.5Y 6/4 light yellow brown (m); sand; single grain to weak fine to coarse subangular blocky; loose to hard; non-sticky, non-plastic; very few thin colloid stains on clasts and large grains; >50% gravel; common medium pores; slightly to violently effervescent, varies disseminated to stage II $CaCO_3$ near and bottom of horizon; gradual irregular
2Bkb5	50.0 - 71+	2.5 Y 7/3 pale yellow (d), 2.5Y 6/3 light yellowish brown (m); sand; single grain to weak medium to fine subangular blocky; loose to hard (d), non-sticky, non-plastic (m); very few thin colloids on clasts & grains; >50% gravel; violently effervescent, disseminated to stage I $CaCO_3$ base of trench.

Archaeology at Joshua Tree National Monument: Preliminary Results of a Stratified Random Sample Inventory

JOAN S. SCHNEIDER *University of California, Riverside CA 92521*
CLAUDE N. WARREN *University of Nevada, Las Vegas NV 89154*

INTRODUCTION

Joshua Tree National Monument encompasses both high desert (Mojave) and low desert (Colorado) environments and the transition zone between them. This makes the area ideal for testing hypotheses concerned with the past movements of populations, including human populations, between these environmental zones.

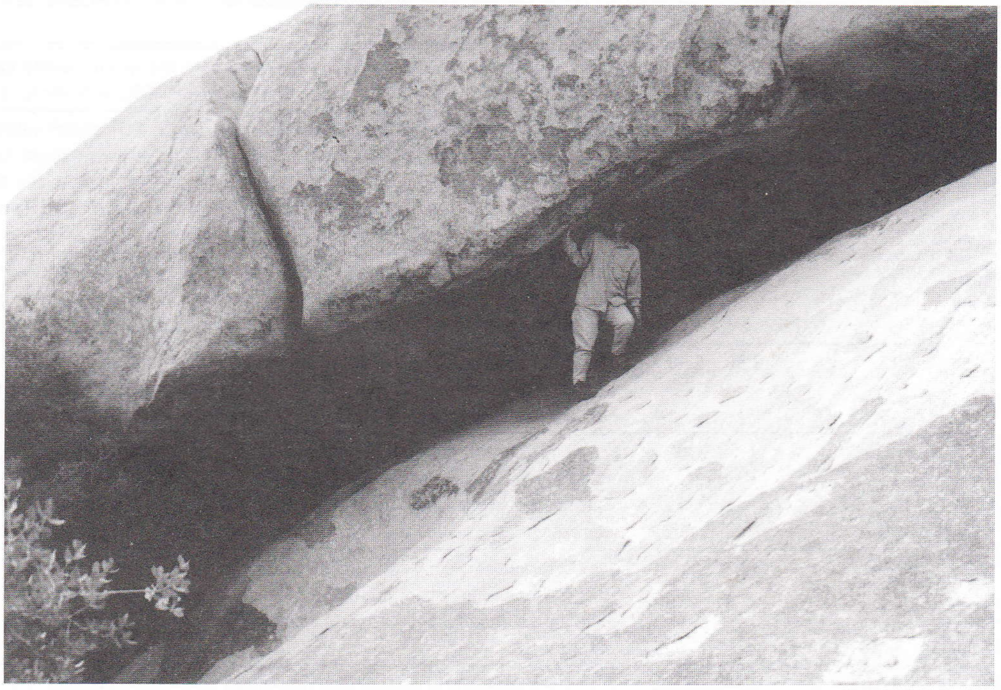

Figure 1. Rock overhang with red pigment pictographs in the "C" vegetational stratum.

PHASE I

Vegetational Strata

Phase I of the first systematic archaeological inventory of Joshua Tree National Monument has recently been completed. A stratified random sample of the area of the Monument was generated by first dividing the Monument into five regions: Queen/Lost Horse, Covington, Cottonwood, East Pinto Basin, and West Pinto Basin. Within each of the five regions, vegetational strata were identified.

The vegetational strata were derived from previous mapping by Leary (1977), but were modified, both for practicality and as areas were "ground-truthed" during the project. Zones included

A(a) Granitic Outcrop Plant Community
A(b) Southern Bench Plant Community
B Creosote Bush Plant Community
C Oak, Pinyon Pine, Juniper Community
E Blackbrush, Burroweed Plant Community
F Joshua Tree Plant Community
G Mojave Yucca Plant Community
H Playa Margin Plant Community.

Zone D, intermittent juniper, was eliminated from the inventory due to inaccessibility and extreme topography.

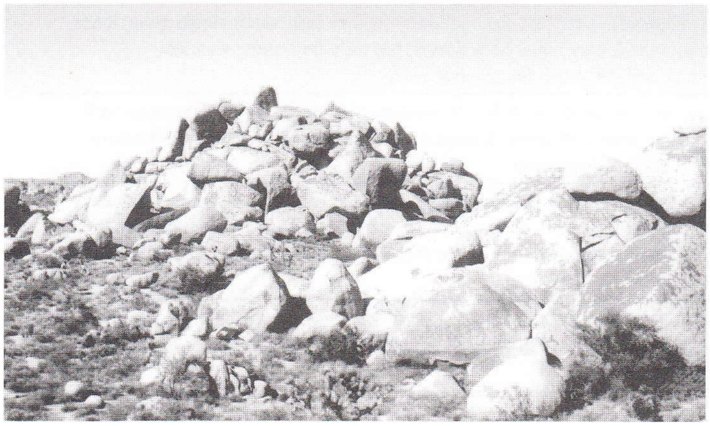

Fig. 2. Within these weathered granitic boulder "inselbergs" is an extensive complex of rockshelters used during late prehistoric times. This area is in the "G" vegetational stratum and is close to a semi-permanent water source.

Transects

A number of 0.1 square kilometer transects were randomly selected within each vegetational stratum present within each region. The number of transects was proportional to the area of each vegetational stratum.

In all, 105 randomly selected transects were intensively surveyed on foot during Phase I of the project, a total of 10.5 square kilometers. Ninety-three archaeological sites were identified, recorded, mapped, and surface collected, approximately 8.8 sites per square kilometer. These included both historical and prehistoric sites representing a wide range of human activity, varying from single episodes (e.g., lithic reduction) to habitation areas used on a regular basis (e.g., large complexes that included rockshelters, structural remains, milling features and rock art) (Table 1, Figs. 1-3).

Table 1
Cumulative Number, Type and Distribution
of Archaeological Sites and Isolated Artifacts
in 105 Randomly Selected 0.1 Square Kilometer Transects
UNLV-JOTR Archaeological Project

	VEGETATIONAL STRATA							
SITE TYPE	A	B	C	D	E	F	G	H
Ceramic Scatter	3	4	0	0	2	0	4	1
Historic Trash	1	2	0	0	1	1	2	0
Historic Feature/Structure	0	1	3	0	0	2	0	0
Single Feature	5	0	1	0	2	1	3	0
Rockshelter w/ Midden	6	1	6	0	0	1	4	0
Open Site w/ Variety	5	4	1	0	2	2	6	0
Pictograph/Petroglyph	0	0	3	0	0	1	0	0
Lithic Scatter	3	0	3	0	1	1	2	0
Quarry	1	0	0	0	0	0	0	0
TOTAL 92	24	12	17	0	8	9	21	1
ISOLATE TYPE								
Flake	7	23	14	0	3	17	25	0
Metate	2	2	0	0	0	1	0	2
Shert	9	37	6	0	0	5	‘3	0
Historic	1	8	0	0	1	1	2	0
Biface	1	2	0	0	2	2	8	0
Core/Flake Tool	3	9	3	0	1	4	6	0
Other	0	3	0	0	0	0	1	0
TOTAL 224	23	84	23	0	7	30	55	2

Two hundred and twenty-three isolated artifacts were also recorded during the project, or approximately 21 isolates per square kilometer. Sherds of ceramic vessels and percussion flakes of a variety of lithic materials (both local and exotic) were most common (Table 1).

Distribution

As expected, aboriginal and historic land use varied with vegetation zone, availability of water, and region. The highest densities of sites were in the "A" and "C" vegetational strata, while the lowest density was in the "B" vegetational stratum (Table 2). The distribution of isolated artifacts was only partially concordant with the distribution of sites (Table 2). Data derived from Phase I of the sample inventory indicate that several historical and prehistorical land-use patterns can be recognized within the Monument.

PHASE II

Phase II of the project, now underway, involves analyses of the geographical and elevational distribution of archaeological sites and isolated artifacts and analyses of faunal, shell, ceramics, and lithics collections. The data generated by the analyses will be used to address a number of research questions posed at the outset of the project (Warren and Schneider, 1991) and especially to test hypotheses derived from the Deep Desert Model (Warren, 1991). This model proposed changes in prehistoric land-use over time and population movements in response to climatic changes starting at the end of the

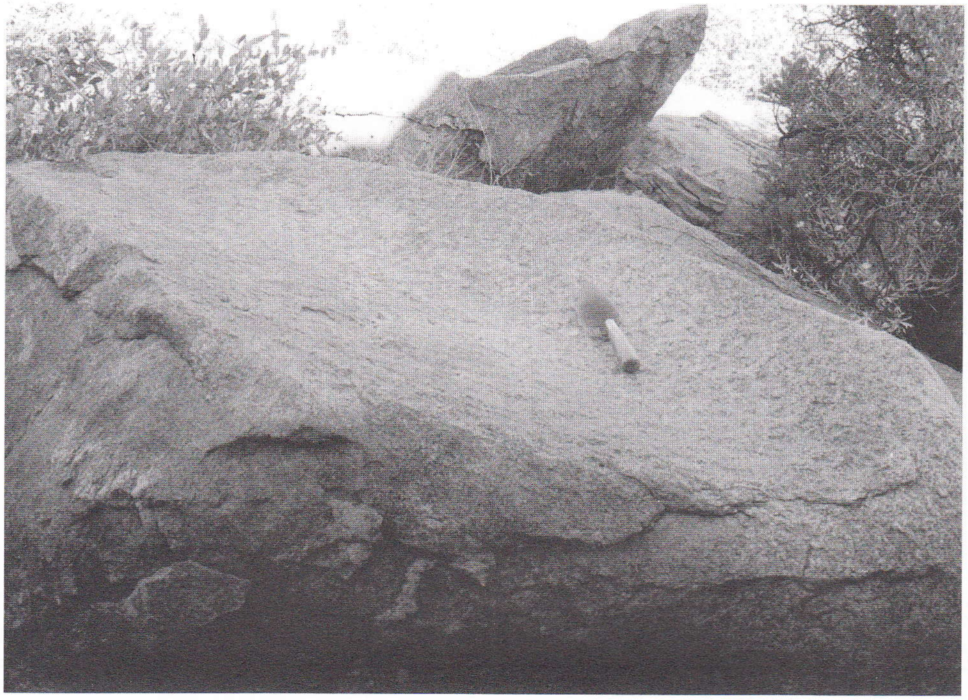

Fig. 3. This large bedrock milling feature is part of a large open site complex in and around a boulder grouping in the "G" vegetational stratum.

Pleistocene. Other research questions to be addressed include those involving (1) changes in human subsistence patterns over time, (2) identification of late prehistoric cultural boundaries in the eastern Mojave Desert, (3) identification of ceramic types and production in the area, and (4) exchange patterns during prehistory (Warren and Schneider, 1992).

REFERENCES CITED

Leary, P.J., 1977. Investigation of the vegetational communities of Joshua Tree National Monument, California. M.S. thesis, University of Nevada, Las Vegas.

Warren, C.N. and J.S. Schneider, 1991. Proposal for phase I of an archaeological inventory of Joshua Tree National Monument. ms on file at National Park Service, Western Region, San Francisco.

___, 1992. Proposal for phase II of an archaeological inventory of Joshua Tree National Monument. ms on file at National Park Service, Western Region, San Francisco.

Warren, Claude N., 1991. Early Holocene people of the Mojave Desert: a case of cultural adaptation? Paper presented at the 56th Annual Meeting of the Society for American Archaeology, New Orleans.

Table 2
Projected Number of Sites & Isolated Artifacts *per Square Kilometer*, by Vegetation Zone
UNLV-JOTR Archaeological Project

VEGETATION ZONE	# Sites	# Isolates
A	22	21
B	3	19
C	21	29
D	--	--
E	9	8
F	10	33
G	9	24
H	10	20
ALL ZONES	8.8	21.3

Vegetation Zones in Joshua Tree National Monument
Zone A Granitic Outcrop, Southern Bench Plant Communities
Zone B Creosote Bush Plant Community
Zone C Oak, Pinyon Pine, Juniper Plant Community
Zone D Juniper Woodlands
Zone E Blackbrush, Burroweed Plant Community
Zone F Joshua Tree Plant Community
Zone G Mojave Yucca Plant Community
Zone H Playa Margin Plant Community

adapted from Leary, 1977

The Significance of the Orocopia Mountains Region in the Displacement History of the San Andreas Fault System

JOHN C. CROWELL *Institute for Crustal Studies and Department of Geological Sciences, University of California, Santa Barbara CA 93106-1100*

INTRODUCTION

Rocks older than mid-Miocene within the Orocopia Mountains region consist of pre-Tertiary granitic and gneissic complexes, Eocene marine strata, Tertiary volcanics, and Oligo-Miocene nonmarine beds. Facies of these units, which are near Interstate 10 and Highway 195, are displaced about 300 km by Late Cenozoic offsets on faults of the San Andreas and related systems since about 12 m.y. ago (Fig. 1). Studies of the Orocopia region in concert with the central Transverse Ranges have therefore played a significant role in working out the tectonic history of southern California. Tectonic blocks consisting of these rocks have also been rotated clockwise during Miocene and later times, both before and during San Andreas displacements. In addition, Mesozoic thrust faults and Tertiary low-angle detachment faults are significant in the structure of the region.

Little was known about the bedrock regions east of the San Andreas zone before World War II. Published information on the regional geology begins with Mendenhall (1909) followed by details around mining districts (e.g. Harder, 1912; see also Haxel and others, 1988). The first reconnaissance geologic map was prepared by Brown (1923) and comments concerning the geology are included in the guidebook of sites along railroad routes by Darton (1933). The names Chuckwalla Complex and Orocopia Schist were established by Miller (1944) who made a geologic sketch map of a strip between Indio and Blythe.

In early 1949, while on a holiday stroll with my wife in Painted Canyon in the Mecca Hills, I recognized anorthosite and related gabbros which appeared similar to rocks exposed along Soledad Canyon in the northern San Gabriel Mountains. Study of a few thin sections confirmed the similarity, so, with student groups I made several trips to the Painted Canyon region and on eastward through the Orocopia Mountains and into adjacent areas. Two years before, in 1947, I had completed doctoral studies in the Tejon Pass region, near Gorman, where I had mapped units of the basement complex and so was familiar with their field appearance. On reconnaissance trips I had briefly examined exposures in the San Gabriel Mountains and Soledad Pass region. These trips, including those to the Orocopias, disclosed that a complex suite of rocks, all revealing similar emplacement or depositional sequences, were present in three regions: Orocopia, Soledad Pass, and Tejon Pass. At first it seemed reasonable that they constituted only preserved patches within the widespread

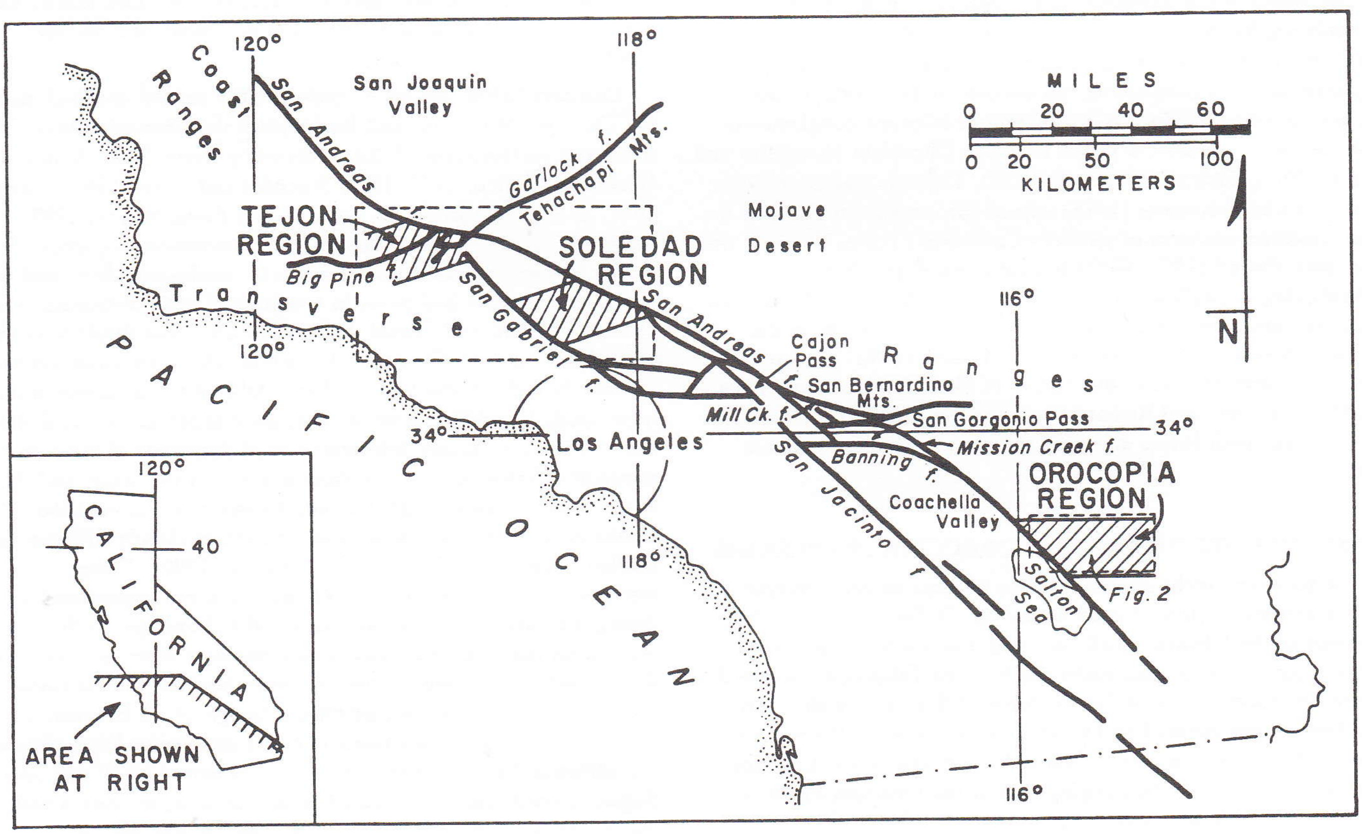

Fig. 1. Tejon, Soledad, and Orocopia terranes in southern California, displaced by San Andreas fault system. [figure reproduced from Crowell (1962, Fig. 5)]

basement complex of southern California or that they constituted a belt of these rocks trending southeasterly across southern California and diagonally across southern California. In the early 1950s, however, on several student trips we learned that the bodies of distinctive rocks met the San Andreas fault at a high angle and appeared to be truncated by it. Moreover, by the early 1950s I had learned enough concerning the San Gabriel fault in the central Transverse Ranges to suggest that it had right-lateral displacement of at least 40 km (Crowell, 1952). My students and I were therefore conditioned to the concept of major strike slip and began speculating on the possibility that the Orocopia region was displaced by the San Andreas 200 km or so from the Soledad Pass region in addition to the displacement on the San Gabriel fault. We delved into papers by Noble (1926) and Vickery (1925) and were especially stimulated by the work of Mason Hill and Tom Dibblee (1953) – cherished colleagues throughout my career. Papers were also appearing on the likelihood of major strike slip on faults in other parts of the world such as in Scotland (Kennedy, 1945).

On a student trip in 1955 we discovered marine Eocene beds in the north-central Orocopia Mountains, now named the Maniobra Formation (Crowell and Susuki, 1959). Three students (Gillies, 1958; Kirkpatrick, 1958; Williams, 1956) undertook Masters Thesis investigations in critical areas and I obtained intermittent leave from classes during the spring of 1957 to map in the Orocopia Mountains. Three papers resulted from this research presenting evidence for displacement on the combined San Andreas – San Gabriel faults of more than 260 km (Crowell, 1960, 1962; Crowell and Walker, 1962). Since then many geologists have contributed to understanding the long displacement history of the fault system in southern California (see reviews by Crowell, 1975a, 1981, 1992a; Hill, 1981; Dibblee, 1989; Ehlert, 1989; Stewart and Crowell, 1992).

The dating of the basement rocks, especially those of the Precambrian, has been undertaken by Silver (1968, 1971) and the volcanics by Crowe, Crowell, and Krummenacher (1979). Ehlig, frequently my field companion, has documented the long-distant displacement by the San Andreas system of Miocene conglomeratic debris washed from sources in the northern Chocolate Mountains and vicinity (Ehlig, Ehlert, and Crowe, 1975). Through studies of Oligo-Miocene rocks Bohannon (1975) refined the correlation between the three displaced segments of southern California (Tejon, Soledad, and Orocopia). Powell (1981, 1982) has contributed greatly to understanding crystalline terranes adjoining the Orocopia Mountains to the east and north, and to their displaced counterparts in the central Transverse Ranges. Powell and Weldon (1992) present a kinematic interpretation of the history of block displacements since mid-Miocene time, and Richard (in press) has included rotations of crustal blocks both before and after the birth of the San Andreas fault.

TECTONIC SECTORS OF THE OROCOPIA MOUNTAINS

The basement rocks of the Orocopia Mountains occur in four distinct tectonic sectors or complexes (Fig. 2). Sectors 1 and 2 lie northeast of the Clemens Well fault and 3 and 4 to the southwest. Sector 1 consists of granitic rocks north of the Diligencia basin and Sector 2 of augen gneiss to the southeast of this basin with a contact of unknown type covered by Diligencia rocks between the two very different basement complexes. Sector 3, southwest of the Clemens Well fault, constitutes the hanging wall of the Orocopia thrust, a complex of anorthosite, syenite, granitics, and other rocks. Sector 4 lies beneath the Orocopia thrust and consists of Orocopia Schist.

The oldest rocks so far recognized within the Orocopia Mountains are augen gneisses and associated migmatites (Sector 2) dated isotopically at 1670±15 m.y. (Silver, 1971). The Orocopia thrust sheet (Sector 3) includes patches of gray gneisses, distinctly different from the augen gneisses, and are about 1425 m.y. old. These were intruded by an anorthosite-syenite complex at about 1220 m.y. (Silver, 1968, 1971). The anorthosite group is composed of gabbro, diorite, transition rock between gabbro and diorite, and mafic bodies and basic dikes (Crowell and Walker, 1962). Judging from cross-cutting relations, rocks of the anorthosite group are slightly older than those of the syenite group. This group consists of syenite, quartz-bearing syenite, alkali granite, granophyre, and pegmatite. Similar rocks to those of the Orocopia thrust plate occur in deep canyons of the Hidden Springs area and to the west in the Painted Canyon region. These are interpreted as also lying above the Orocopia thrust at depth. Porphyritic granodiorite crops out in a few small areas within the Chocolate Mountains to the south of the Salton Wash fault, probably confined here also to the Orocopia thrust plate (Sector 3). The rock is correlated with the Lowe Granodiorite of the San Gabriel Mountains on the basis of petrographic similarity and an isotopic age of 220±10 m.y. (Triassic) (Silver, 1968, 1971; Ehlig, 1981).

Granitic rocks of several types are widespread in the region. Leucoquartz monzonite invades the gneiss-anorthosite-syenite complex of the Orocopia thrust plate. In the northern and eastern Orocopia Mountains gray and buff granite containing inclusions of gneiss has been correlated with the White Tank quartz monzonite (Miller, 1944; Rogers, 1954), and has been dated by K-Ar methods at 74.8±1.5 m.y. (Armstrong and Suppe, 1973). The granitic bodies throughout the region, however, have not yet been separated and it is likely that there were several crystallization episodes within the Cretaceous, and some may be Triassic and Jurassic in age, as is the case farther east (Tosdal, Haxel, and Wright, 1989; Barth, Tosdal, and Wooden, 1990).

Orocopia Schist (Sector 4) underlies the central and high part of the Orocopia Mountains and lies beneath the Orocopia thrust. The schist was metamorphosed during thrusting about 80 or 90 m.y. age (Haxel and Dillon, 1973, 1978; Burchfiel and Davis, 1981; Crowell, 1981; Ehlig, 1981; Jacobson, Dawson, and Postlethwaite, 1988; Jacobsen, 1990). The unit consists of a monotonous sequence of greenschist reconstituted from graywacke, mudstone, chert, and basic volcanics, probably laid down in late Jurassic and Cretaceous times (Mukasa, Dillon, and Tosdal, 1984). The Orocopia thrust is viewed as part of the Vincent, Chocolate Mountain, Orocopia thrust system, present throughout much of southern California, and contains slices of mylonite formed by movements at great depth as well as shallow reactivation cataclasites. Interpretation of directions of tectonic transport inferred from minor structures within the schist and the thrust zone is controversial: tectonic transport was toward the northeast, or toward the southwest, or both at slightly different times (Dillon, Haxel, and Tosdal, 1990; Simpson, 1990). These interpretations have led to two different tectonic reconstructions during deposition of the sedimentary and volcanic protolith. One view holds that the schist was formed primarily from sediments taken down a subduction zone dipping eastward beneath the continent, and the other, from sediments that filled a trough or rift between the continent and a separated block of continental crust lying offshore in the Mesozoic Pacific. As this offshore continental block was later displaced northeastward in Late Cretaceous time, sediments within the trough were severely deformed and metamorphosed as it closed. Later, Cenozoic reactivation has taken place along the thrust resulting in clay gouge and low-angle normal slip indicators (Crowell, 1974, 1975b; Robinson and Frost, 1989; Dillon, Haxel, and Tosdal,

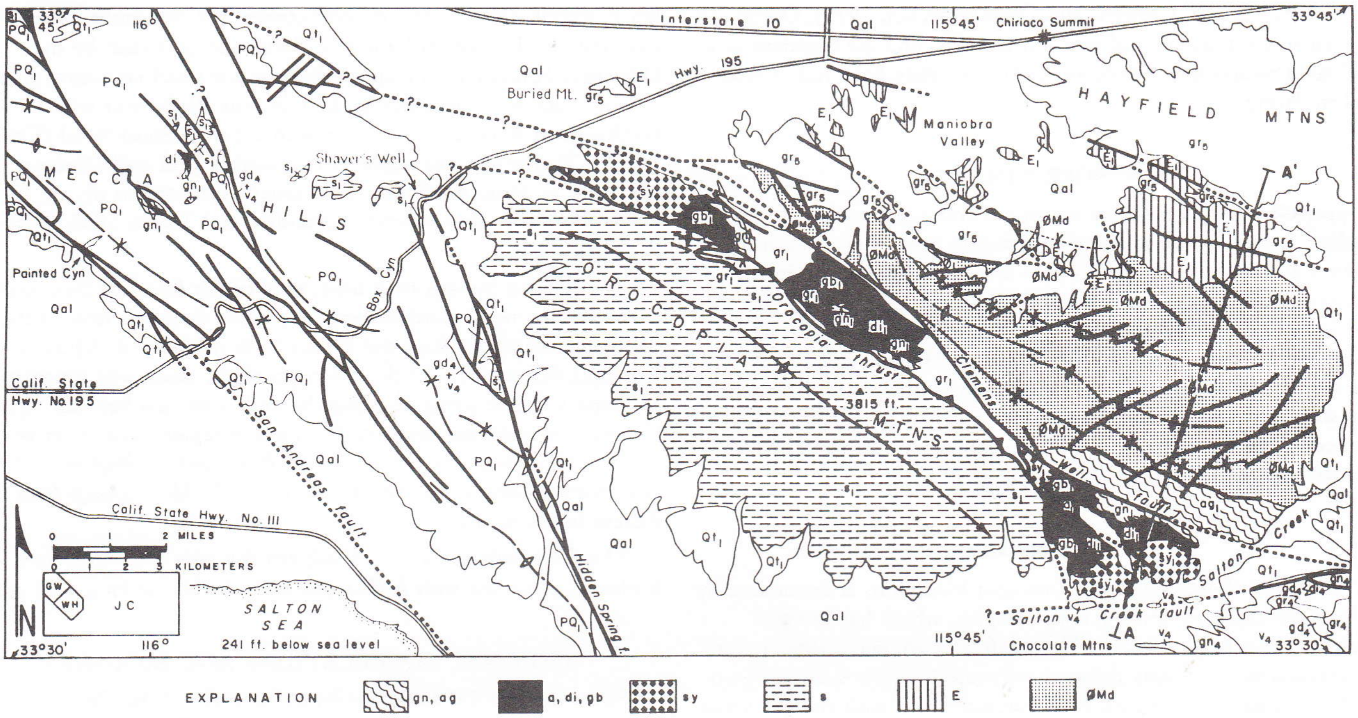

Fig. 2. Geologic sketch map of the Orocopia Mountains, southeastern California. Subscript numbers differentiate different rock units of similar types (refer to Crowell 1972, 1975b, and this volume). With reference to insert rectangle at lower left, the data are modified and simplified from unpublished mapping by Hays (WH) (1957), Ware (GW) (1958), and Crowell (JC). A-A' = Line of cross section, published in Crowell (1975b, Fig. 2) but not in this paper. Precambrian rocks: gn = blue-quartz gneiss, ag = augen gneiss and migmatite, a = anorthosite, di = diorite, gb = gabbro, sy = syentie. Other pre-Tertiary basement rocks: gr = granitic rocks of several types, s = Orocopia Schist. Cenozoic rocks: v = volcanics of several types, E - Eocene Maniobra Formation, OMd = Oligocene-Lower Miocene Diligencia Formation, PQ = Plio-Pleistocene formations, but may include Upper Miocene nonmarine strata, Qt = Quaternary terrace and fanglomerate deposits, Qal = Quaternary alluvium and lake deposits. [Fig. reproduced from Crowell, 1975b, Fig. 1].

1990), during uplift, unroofing, and regional extension. The Orocopia antiform constitutes a core complex, arched up during mid-Tertiary time, and displaced later from correlated antiforms in the central Transverse Ranges by San Andreas displacements.

EOCENE STRATA

Maniobra Formation

The sedimentary section begins with about 1460 m of shale, sandstone, conglomerate, and sedimentary breccia lying unconformably upon granitic basement to the northeast of the Clemens Well fault and assigned to the Maniobra Formation (Crowell and Susuki, 1959). In the eastern Orocopia Mountains a rugged Eocene shoreline is preserved, along which there were sea stacks and huge blocks that skidded into shallow water from steep cliffs. The formation consists primarily of indurated brown sandstone and intercalated shale lying above lenses of basal conglomerate and sedimentary breccia. Fossils include pelecypods, gastropods, orbitoids, and smaller foraminifera, which place the age of the deposits in the Middle Eocene. Regional reconstructions, involving displacements on the San Andreas system, suggest that the deposits correlate with those of the Tejon Region (Kirkpatric, 1958; Howell, 1975). They probably preserve the displaced and rotated eastern margin of an Eocene forearc basin. Outcrops of the basal units are easily reached at the eastern end of Buried Mountain north of Highway 195, but thicker and more fossiliferous sections occur in hills around Maniobra Valley.

OLIGOCENE/LOWER MIOCENE STRATA

Diligencia Formation

The nonmarine Diligencia Formation, consisting of as much as 2000 m of conglomerate, sandstone, shale, and volcanic rocks, unconformably overlies the Eocene maniobra Formation on the north and augen gneiss on the south (Bohannon, 1975; Crowell, 1975b, in press; Spittler and Arthur, 1982). The formation was deposited within an intermontane basin with coarse facies around the margin and fine-grained deposits, including some evaporitic lake beds in central parts. Basalt and andesite occur as flows, dikes, sills, and irregular intrusions within strata of the formation, including tuff beds. The best exposures are found in the southeastern Orocopia Mountains in the vicinity of Canyon Springs.

Tertiary volcanic dikes of several compositions occur here and there in the region (Crowell, 1975b). These include distinctive rapakivi-textured quartz latite porphyry of pre-San Andreas age that has been significant in documenting slip on the fault (Ehlig, Ehlert, and Crowe, 1975). The porphyry crops out primarily in the northern Chocolate Mountains and within the upper reaches of Painted Canyon. Distinctive debris washed from this southeastern source, east of the San Andreas, is present in the Mint Canyon and Caliente formations of Soledad basin and western Tejon Pass area, to the west of the fault.

The age assigned to the Diligencia Formation, which ranges from Late Oligocene into the Early Miocene, depends on both potassium-argon dating (between 25.9 and 21.0 m.y.) and a jawbone of a horse (Crowell, 1975b; Woodburne and Whistler, 1973; Spittler and

Arthur, 1982; Crowe, Crowell, and Drummenacher, 1979). Other fossils include ostracodes and rare fish remains, and the fragment of a camel jaw (Squires and Advocate, 1982), but they have not proved useful in dating.

YOUNGER STRATA

Upper Ceonzoic nonmarine sandstone and conglomerate, including some siltstone and shale, aggregate more than 1500 m in thickness and crop out in the western Orocopia Mountains, including the Mecca Hills. These beds are assigned to the Palm Spring and other formations (Dibblee, 1954; Sylvester and Smith, 1976). They are strongly deformed near the San Andreas, Hidden Spring, and other fault zones and were mainly deposited as deformation continued along with sedimentation. The youngest units in the region, of Late Pleistocene and Recent age, include fanglomerates, terrace deposits, alluvium, and beds laid down by Lake Cahuilla.

TECTONICS

The structural geology of the Orocopia Mountains is dominated by the huge Orocopia antiform, a core complex, which has brought Orocopia Schist to the surface. The uplift and accompanying erosion has breached the Orocopia thrust, a regional Mesozoic structure with mylonites along it. The uplift, however, associated with the unroofing of the originally deeply buried schists, has reactivated the thrust zone at places with low-angle normal-slip, primarily during mid-Miocene and later displacements. These shallow level unroofing structures, characterized by gouge, demonstrate reactivation with normal-slip and detachment indicators.

Both the thrust and the antiform are truncated by the Clemens Well fault which trends southeasterly across the region. So far as now known, the Clemens Well fault does not meet the San Andreas although it projects northwestward beneath an area of deformed fanglomerate that is also on trend with the Hidden Springs fault zone. On the southeast, the Clemens Well fault is probably truncated by the Salton Creek fault but the inferred intersection is covered by alluvium. Strands of the Clemens Well fault are exposed in arroyos bordering the foothills of the Orocopia Mountains south of Highway 195 in the Buried Mountain region. Here the fault zone consists of crushed rock and gouge up to 10 m wide with slices of volcanic rock suggesting a minimum right slip of several km from similar rock within the Diligencia Formation. Its total right slip is unknown, however, and its possible correlation with faults in the Transverse Ranges, such as the San Francisquito and/or St. Francis, is still under study (Smith, 1977; Powell and Weldon, 1992). In the central and eastern parts of the Orocopia Mountains the Clemens Wells fault is enmeshed with strands of the Orocopia thrust system and displays reactivated movement, downdip to the northeast. Here the fault zone is interpreted as displaying normal oblique-slip associated with regional extension (Goodmacher and others, 1989) superposed upon previous right slip. The fault zone is overlapped by Holocene fanglomerate and is therefore not considered active.

Two major fault zones with east-west trend demarcate the Orocopia Mountains from adjoining ranges and lie beneath thick undisturbed alluvium: the Chiriaco fault on the north (beneath and parallel to Interstate 10, but not shown on Fig. 2) and the Salton Creek fault on the south (between the Orocopia and Chocolate Mountains). The Chiriaco fault has about 11 km of left offset as shown by displaced dikes and contacts (Powell, 1975, 1981). Rocks on either side of the Salton Creek fault are largely dissimilar, but if a suspected antiform in the Chocolate Mountains is the same as the Orocopia antiform, the left offset of the antiformal crest is about 10 km (Crowell, 1992b). The region between the two faults, and especially in the eastern Orocopia Mountains underlain by the Diligencia Formation, is characterized by a marked conjugate system of faults: one set subparallel to the Clemens Wells fault with a northwestern trend and the other with a northeastern trend (Crowell, 1975b). This is also the region where marked post-mid-Miocene clockwise tectonic rotations are documented by means of paleomagnetic studies (Carter, Luyendyk, and Terres, 1987; Richard, in press).

The Hidden Springs fault zone, an offshoot from the San Andreas fault trending north-northwesterly, separates the main mass of the Orocopia Mountains from the Mecca Hills to the west. Slices of Orocopia Schist, rocks of the Orocopia thrust plate, and a variety of Miocene volcanic rocks lie along the fault zone and beneath Upper Cenozoic non-marine strata in this western region. The latter belong to the same formations exposed along Box Canyon (Highway 195) and Painted Canyon. Active strands of the Hidden Springs fault cut Recent fanglomerates.

The San Andreas fault itself adjoins the area dealt with here and is clearly associated with folded and faulted strata of Holocene age.

REGIONAL CORRELATIONS AND SUMMARY

Since the late 1950s the pre-Miocene rocks of the Orocopia Mountains region have been recognized as holding a key position in understanding the displacement history of the San Andreas fault system. Geologists recognized that the Orocopia terranes were indeed similar to those in the Soledad basin region of the central Transverse Ranges, and with those in the Frazier Mountain region near Tejon Pass. Some geologists emphasized the differences, whereas others, such as I, considered the differences only what would be expected from place to place in any continguous complex terrane. In the late 1940s and early 1950s it was not yet established that linear geologic belts in all three of the separated terranes (Tejon, Soledad, and Orocopia) trended into the San Andreas, and were truncated and offset by it. Moreover, it was not yet known that the sequence of events recorded within rocks was also similar, and that similar appearing rocks were of the same age. Many geologists have contributed to studies in all three regions, especially P. L. Ehlig, L. T. Silver, R. E. Powell, T. W. Dibblee, Jr., D. G. Howell and R. G. Bohannon, and many others to important investigations within the separated blocks. Studies of basement rocks in recent years strengthen the correlation between the Tejon and Orocopia regions (Powell, 1981, 1982; Frizzell and Powell, 1982; Frizzell and Vedder, 1986). Whereas anorthosite and related rocks were not recognized in the Tejon region in the early 1960s, this distinctive rock with the same petrologic characteristics has since been discovered (Ehlig and Crowell, 1982). In the central Transverse Ranges work remains to determine the partitioning of right-slip during the Late Cenozoic on several strands of the San Andreas and other fault systems, such as the Clearwater, Liebre, San Francisquito, Punchbowl and others faults (e.g. Crowell, 1982; Frizzell, Mattison, and Matti, 1986; Powell and Weldon, 1992). The principle strand of the San Andreas from Tejon Pass to the Salton Sea region acquired displacement beginning about 5 m.y. ago, and there may not have been an older strike-slip fault of the system along this part of its course before then (Crowell, 1982). The now-abandoned San Gabriel fault connected the regions before that, back in time to about 12 m.y. ago. This date of 12 Ma marks the birth of the San Gabriel fault as shown by the dating of the Violin Breccia (Crowell, 1982). The San Gabriel was the main strand of the onshore San Andreas system at that time, and somehow extended southeastward into the Salton Trough.

Strike slip of about 300 km in southeastern California received credence through the work of Hill and Dibblee (1953) along the San Andreas northwest of the Transverse Ranges. Work of those such as Addicott (1968), Huffman (1972) and Matthews (1973, 1976) documented major strike slip along this northwestern reach of the fault more fully. With the development of plate tectonic concepts in the late 1960s, the manner that the San Andreas system fitted into a global tectonic scheme began to come clear, especially through the work of Atwater (1970, see also 1989).

At present, much work needs to be done in southern California in order to understand more fully the Miocene and younger tectonic events along the San Andreas system. The recognition of block rotations and the prevalence of flat faults—many with normal slip and detachment affinities—show that complex tectonic overprintings have taken place along the San Andreas belt since its inception. In addition, strike slip along the belt has moved from strand to strand. A truly acceptable historical sequence of tectonic events for southern California is not yet at hand.

REFERENCES CITED

Addicott, W.O., 1968. Mid-Tertiary zoogeographic and paleogeographic discontinuities across the San Andreas fault, California, *in* Proceedings of Conference on geologic problems of San Andreas fault system, W.R. Dickinson and A. Grantz, eds. Standford University Publications, Geological Sciences 11:144-156.

Atwater, Tanya, 1970. Implications of plate tectonics for the Cenozoic tectonic evolution of western North America. Geological Society of America Bulletin 81:3513-3536.

___, 1989. Plate tectonic history of the northeast Pacific and western North America, *in* The Geology of North America, The eastern Pacific Ocean and Hawaii, E.L. Winterer, D.M. Hussong and R.W. Decker, eds. Geological Society of America, N21-72.

Armstrong, R.L. and J. Suppe, 1973. Potassium-argon geochronometry of Mesozoic igneous rocks in Nevada, Utah, and southern California. Geological Society of America Bulletin, 84:1375-1392.

Barth, A.P., R.M. Tosdal and J.L. Wooden, 1990. A petrologic comparison of Triassic plutonism in the San Gabriel and Mule Mountains, southern California. Journal of Geophysical Research, 95:20,075-20,096.

Bohannon, R.G., 1975. Mid-Tertiary conglomerates and their bearing on Transverse Range tectonics, southern California, *in* San Andreas fault in southern California, J.C. Crowell, ed. California Division of Mines and Geology Special Report, 118:75-82.

Brown, J.S., 1923. The Salton Sea region, California. U.S. Geological Survey Water-supply Paper, 497:292 p.

Burchfiel, B.C. and G.A. Davis, 1981. Mojave Desert and environs, *in* The geotectonic development of California, W.G. Ernst, ed. Englewood Cliffs NJ, Prentice-Hall Inc, Rubey Volume 1:217-252.

Carter, J.N., B.P. Luyendyk, and R.R. Terres, 1987. Neogene clockwise tectonic rotation of the eastern Transverse Ranges, California, suggested by paleomagnetic vectors. Geological Society of America Bulletin, 93:199-206.

Crowell, B.M., J.C. Crowell and D. Krummenacher, 1979. Regional stratigraphy, K/Ar ages, and tectonic implications of Cenozoic rocks, southeastern California. American Journal of Science, 279:186-216.

Crowell, J.C., 1952. Probable large lateral displacement on San Gabriel fault, southern California. American Association of Petroleum Geologists Bulletin, 36:2026-2035.

___. 1960. The San Andreas Fault in southern California. Copenhagen, International Geological Congress Report, 21(18):45-52.

___. 1962. Displacement along the San Andreas Fault, California. Geological Society of America Special paper, 71: 61 p.

___. 1974. The Orocopia thrust, southeastern California (abs). Geological Society of America, Abstracts with Programs, 6:159.

___. 1975a. The San Andreas fault in southern California, *in* San Andreas fault in southern California, J.C. Crowell, ed. California Division of Mines and Geology Special Report, 118:7-27.

___. 1975b. Geologic sketch of the Orocopia Mountains, southeastern California, *in* San Andreas fault in southern California, J.C. Crowell, ed. California Division of Mines and Geology Special Report, 118:99-110.

___. 1981. An outline of the geologic history of southeastern California, *in* The geotectonic development of California, W.G. Ernst, ed. Englewood Cliffs NJ, Prentice-Hall Inc: Rubey Volume 1:583-600.

___. 1982. The tectonics of Ridge basin, southern California, *in* Geologic History of Ridge Basin, southern California, J.C. Crowell and M.H. Link, eds. Pacific section, Society of Economic Paleontologists and Mineralogists:25-42.

___. 1992a. Cenozoic faulting in the Little San Bernardino - Orocopia Mountains region, southern California, *in* Deformation associated with the Neogene Eastern California Shear Zone, southeastern California and southwestern Arizona, S. M. Richard, ed. Redlands, San Bernardino County Museums Special Publication 92-1:16-19.

___. 1992b. Tectonic mobility of the San Andreas fault belt bordering the Mojave and Colorado deserts southern California, *in* Deformation associated with the Neogene Eastern California Shear Zone, southeastern California and southwestern Arizona, S. M. Richard, ed. Redlands, San Bernardino County Museums Special Publication 92-1:20-23.

___. in press. The Diligencia Formation, Orocopia Mountains, southeastern California, *in* Tertiary stratigraphy of the highly extended terranes, California, Arizona, and Nevada, D.R. Sherrod and J.E. Nielson, eds. U.S. Geological Society Bulletin.

Crowell, J.C. and T. Susuki, 1959. Eocene stratigraphy and paleontology, Orocopia Mountains, southeastern California. Geological Society of America Bulletin, 70:581-592.

Crowell, J.C. and J.W.R. Walker, 1962. Anorthosite and related rocks along the San Andreas fault, southern California. University of California Publications in Geological Sciences, 40(4):219-288.

Darton, N.H., 1933. Guidebook of the western United States, Pt. F, Southern Pacific lines. U.S. Geological Survey Bulletin, 845: 304 p.

Dibblee, T.W. Jr., 1954. Geology of the Imperial Valley region, California. California Division of Mines Bulletin, 170(2):21-28.

___. 1989. The San Andreas fault and major rock terranes of California displaced by it and its tectonics, *in* San Andreas fault: Cajon Pass to Wallace Creek, E.J. Baldwin, J.H. Foster, W.L. Lewis, and J.K. Hardy, eds. Santa Ana, South Coast Geological Society, v. 1, Guidebook 17:223-276.

Dillon, J.T., G.B. Haxel and R.M. Tosdal, 1990. Structural evidence for northeastward movement on the Chocolate Mountain thrust, southeasternmost California. Journal of Geophysical Research, 95:19,953-19,972.

Ehlert, K.W., 1989. Historical overview of displacement studies along the San Andreas fault in southern California, *in* San Andreas fault: Cajon Pass to Wallace Creek, E.J. Baldwin, J.H. Foster, W.L. Lewis, and J.K. Hardy, eds. Santa Ana, South Coast Geological Society, v. 1, Guidebook 17:21-46.

Ehlig, P.L., 1981. Origin and tectonic history of the basement terrane of the San Gabriel Mountains, central Transverse Ranges, *in* The geotectonic development of California (Rubey Volume 1), W.G. Ernst, ed. Englewood Cliffs NJ, Prentice-Hall Inc:253-283.

Ehlig, P.L., K.W. Ehlert and B.M. Crowe, 1975. Offset of the Upper Miocene Caliente and Mint Canyon formations along the San Gabriel and San Andreas faults, *in* San Andreas fault in southern California, J.C. Crowell, ed. California Division of Mines and Geology Special Report, 118:83-92.

Frizzell, V.A. Jr. and R.E. Powell, 1982. Crystalline rocks near Frazier and Alamo Mountains, Western Transverse Ranges, California (abs). Geological Society of America, Abstracts with Programs, 144:164.

Frizzell, V.A. Jr., J.M. Mattinson, and J.C. Matti, 1986. Distinctive Triassic megaporphyritic monzogranite: evidence for only 160 km offset along the San Andreas fault, southern California. Journal of Geophysical Research, 92:14,080-14,088.

Frizzell, V.A. Jr. and J.G. Vedder, 1986. Geologic map of roadless areas and the Santa Lucia Wilderness in the Los Padres National Forest, southwestern California. U.S. Geological Survey Miscellaneous Field Studies Map MF-1655A.

Gillies, Warren, 1958. Geology of portion of Cottonwood Springs quadrangle, Riverside County, California (unpubl. MA thesis). University of California, Los Angeles: 70 p.

Goodmacher, J., L. Barnett, G. Buckner, L. Ouachrif, A. Vidigal and E. Frost, 1989. The Clemens Well fault in the Orocopia Mountains of southern

California: a strike-slip or normal-fault structure? (abs). Geological Society of America, Abstracts with Programs, 21:85.

Harder, E.C., 1912. Iron ore deposits of the Eagle Mountains, California. U.S. Geological Survey Bulletin, 503: 81 p.

Haxel, G.B. and J.T. Dillon, 1973. The San Andreas fault system in southeasternmost California, *in* Proceedings of conference on tectonic problems of the San Andreas fault system, R.L. Kovach and A. Nur, eds. Stanford University Publications, Geological Sciences, 35:322-333.

___. 1978. The Pelona-Orocopia Schist and Vincent-Chocolate Mountains thrust system, southern California, *in* Mesozoic paleogeography of the western United States, D.G. Howell and K.A. McDougall, eds. Pacific section, Society of Economic Paleontologists and Mineralogists, Pacific Coast Paleogeography Symposium 2:453-469.

Haxel, G.B., C.B. Smith, C.L. Whittington, A. Griscom, D.V. Diveley-White, R.E. Powell, and T.J. Kreidler, 1988. Mineral resources of the Orocopia Mountains Wilderness Study Area, Riverside County, California. U.S. Geological Survey Bulletin, 1710-E: 22p.

Hays, W.H., 1957. Geology of part of the Cottonwood Springs quadrangle, Riverside County, California (unpubl. Ph.D. diss). Yale University: 324 p.

Hill, M.L., 1981. San Andreas fault: history of concepts. Geological Society of America Bulletin, 92(1):112-131.

Hill, M.L. and T.W. Dibblee, Jr., 1953. San Andreas, Garlock, and Big Pine faults, California. Geological Society of America Bulletin, 64:443-458.

Howell, D.G., 1975. Early and Middle Eocene shoreline offset by the San Andreas faults, southern California, *in* San Andreas fault in southern California, J.C. Crowell, ed. California Division of Mines and Geology Special Report, 118:69-74.

Huffman, O.F., 1972. Lateral displacement of Upper Miocene rocks and the Neogene history of offset along the San Andreas fault in central California. Geological Society of America Bulletin, 83:2913-2946.

Jacobson, C.E., 1990. The 40Ar/39Ar geochronology of the Pelona Schist and related rocks, southern California. Journal of Geophysical Research, 95:509-528.

Jacobson, C.E., M.R. Dawson, and C.E. Postlethwaite, 1988. Structure, metamorphism, and tectonic significance of the Pelona, Orocopia, and Rand schists, southern California, *in* Metamorphism and crustal evolution in the western United States (Rubey Volume 7), W.G. Ernst, ed. Prentice-Hall: 1153 p.

Kennedy, W.Q., 1945. The Great Glen fault. Quarterly Journal, Geological Society of London, 102:41-76.

Kirkpatrick, J.C., 1958. A study of some marine middle Eocene formations in southern California (unpubl. MA thesis) University of California, Los Angeles: 75 p.

Matthews, V, III, 1973. Pinnacles-Neenach correlations: a restriction for models of the origin of the Transverse Ranges and the Big Bend in the San Andreas fault. Geological Society of America Bulletin, 84:683-688.

___. 1976. Correlation of Pinnacles and Neenach volcanic formations and their bearing on San Andreas fault problem. American Association of Petroleum Geologists Bulletin, 60:2128-2141.

Mendenhall, W.C., 1909. Groundwater of the Indio region, California, with a sketch of the Colorado Desert. U.S. Geological Survey Water-supply paper, 244: 81 p.

Miller, W.J., 1944. Geology of Palm Springs–Blythe Strip, Riverside County, California. California Journal of Mines and Geology, 40:11-72.

Mukasa, S.B., J.T. Dillon, and R.M. Tosdal, 1984. A Late Jurassic minimum age for the Pelona-Orocopia schist protolith, southern California (abs). Geological Society of America, Abstracts with Programs, 16:323.

Noble, L.F., 1926. The San Andreas rift and some other active faults in the desert region of southeastern California. Carnegie Institution of Washington Year Book, 25:315-428.

Powell, R.E., 1981. Geology of the crystalline basement complex, eastern Transverse Ranges, southern California (unpubl. Ph.D. diss). Pasadena, California Institute of Technology: 441 p.

___. 1982. Crystalline basement terrances in the southern eastern Transverse Ranges, California, *in* Geological excursions in the Transverse Ranges, California, J.D. Cooper, ed. Cordilleran section, Geological Society of America Volume and Guidebook:109-151.

Powell, R.E. and R.J. Weldon, 1992. The evolution of the San Andreas fault, *in* Annual Review of Earth and Planetary Sciences, 20, G.W. Wetherill, A.L. Albee, and K.C. Burke (eds):431-468.

Richard, S.M., in press. Palinspastic reconstruction of southeastern California and southwestern Arizona for the Middle Miocene. Tectonics.

Robinson, K. and E. Frost, 1989. Orocopia Mountains detachment system: progressive ductile to brittle development of a tilted crustal slab during regional extension (abs). Geological Society of America, Abstracts with Programs, 21:135.

Rogers, J.J. W., 1954. Geology of portion of Joshua Tree National Monument, Riverside County. California Division of Mines Bulletin, 170: Map Sheet 24.

Silver, L.T., 1968. Pre-Cretaceous basement rocks and their bearing on large-scale displacements in the San Andreas fault system (abs), *in* Proceedings of conference on geologic problems of San Andreas fault system, W.R. Dickinson and A. Grantz, eds. Stanford University Publications, Geological Sciences, 11:279-280.

___. 1971. Problems of crystalline rocks of the Transverse Ranges (abs). Geological Society of America, Abstracts with Programs, 3:193-194.

Simpson, C., 1990. Microstructural evidence for northeastward movement on the Chocolate Mountains fault zone. Journal of Geophysical Research, 95:529-538.

Smith, D.P., 1977. San Juan–St. Francis fault—hypothesized major middle Tertiary right-lateral fault in central and southern California. California Division of Mines and Geology Special Report, 129:41-50.

Spittler, T.E. and M.A. Arthur, 1982. The Lower Miocene Diligencia Formation of the Orocopia Mountains, southern California, *in* Cenozoic nonmarine deposits of California and Arizona, R.V. Ingersoll and M.O. Woodburne, eds. Pacific section, Society of Economic Paleontologists and Mineralogists:83-100.

Squires, R.L. and D.M. Advocate, 1982. Sedimentary facies of the nonmarine Lower Miocene Diligencia Formation, Canyon Spring area, Orocopia Mountains, southern California, *in* Cenozoic nonmarine deposits of California and Arizona, R.V. Ingersoll and M.O. Woodburne, eds. Pacific section, Society of Economic Paleontologists and Mineralogists:101-107.

Stewart, J.H. and J.C. Crowell, 1992. Strike-slip tectonics in the Cordilleran region, western United States, *in* The Cordilleran orogen: conterminous U.S., The Geology of North America, B.C. Burchfiel, P.W. Lipman and M.L. Zoback, eds. Geological Society of America, G-3:609-628.

Sylvester, A.G. and R.R. Smith, 1976. Tectonic transpression and basement-controlled deformation in San Andreas fault zone, Salton Trough, California. American Association of Petroleum Geologists Bulletin, 60:2981-2102.

Tosdal, R.M., G.B. Haxel, and J.E. Wright, 1989. Jurassic geology of the Sonoran Desert region, southern Arizona, southeast California, and northernmost Sonora: construction of a continental-margin magmatic arc, *in* Jenney, J.F. and Reynolds, S.J., Arizona Geological Society Digest, 17:397-434.

Vickery, F.P., 1925. The structual dynamics of the Livermore region. Journal of Geology, 33:608-628.

Ware, G.C., 1958. The geology of a portion of the Mecca Hills, Riverside County, California (unpubl. M.A. thesis). University of California, Los Angeles: 60 p.

Williams, J.J., 1956. Geology of part of the Orocopia Mountains, Riverside County, California (unpubl. M.A. thesis) University of California, Los Angeles: 44 p.

Woodburne, M.O. and D.P. Whistler, 1973. An early Miocene oreodont (Merychyinae, Mammalia) from the Orocopia Mountains, southern California. Journal of Paleontology, 47:908-912.

INSTITUTE FOR CRUSTAL STUDIES CONTRIBUTION NO. 0140-34TC

The Upper Quaternary Strata of Shavers Valley, California

DAVID P. BRIDGES and NORMAN MEEK, *Department of Geography, California State University, San Bernardino CA 92407*

ABSTRACT

Shavers Valley is a dissected Quaternary basin located just north of the Mecca Hills in the southwestern Mojave Desert. The uppermost sediments in the basin center are playa and shallow lacustrine clayey sands. A detailed examination and mapping of these strata provided no microfossil or other age-diagnostic indicators. This suggests that water in the basin did not stand long enough for ostracodes to develop. These strata provide evidence of ponding before the Shavers Valley basin was breached. Like the Manix basin, this dissected basin provides another example of an arid river network growing in a downstream direction.

INTRODUCTION

The purposes of this paper are to provide a detailed description of the upper Quaternary strata of Shavers Valley, CA (see Fig. 1), and to discuss the implications of these strata on the regional drainage evolution. Shavers Valley is located in the southwestern Mojave Desert, and may be named for Shavers Well, located where the basin drains into Box Canyon. It is bounded on the north by U.S. Interstate 10 and the Mecca Hills on the south. California Highway 195 transects the basin and continues southward through Box Canyon. The basin's center can be found at approximately latitude 33°37'00" N and longitude 115°53'30" W.

DESCRIPTION

The lacustrine/playa clayey sand deposits in the Shavers Valley basin rest upon an alluvial fan that existed before significant local ponding occurred (see Fig. 2). The clayey sand deposits are capped by a protective fanglomerate layer. Figures 3 and 4 show the measured stratigraphic section of the upper basin fill. The thickest exposure available was measured. The clayey sand deposits at this site have been exposed by lateral erosion of an active alluvial fan. The measured outcrop is positioned on the steep east face of the tallest hill in the basin's center. The measured section is approximately 4.88 meters in height. The section is located at UTM coordinates 601880 mE and 3729339 mN (zone 11).

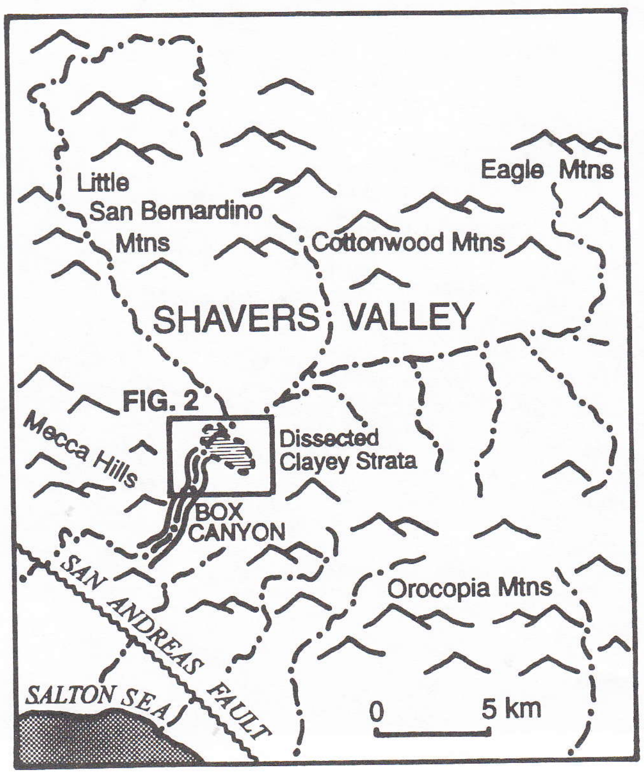

Figure 1. Map of the Shavers Valley region showing the study area with the dissected upper Quaternary ponded strata.

To determine the section elevation, a levelling survey was made from a USGS point elevation near Shavers Well to the top of the measured section. The accuracy of the survey was limited by our ability to locate and remeasure the ambiguous USGS Shavers Well point elevation, and the survey error of ± 2 cm.

In much of the Mojave Desert, green clays are normally indicative of lacustrine conditions. Therefore, the greenest-appearing clays in the measured section were sampled at three levels for evidence of microfossils (see Fig. 3). These samples were examined for ostracodes and other microfossils by Jim Steinmetz, who has done similar work in the Manix basin (Steinmetz, 1988). No evidence of ostracode fossils was found (written comm, 12/92).

A reconnaissance of Shavers Valley led to the discovery of clayey sand deposits approximately 1.2 km NW of the measured section at roughly the same altitude (see Fig. 2). Based on a topographic reconstruction of the basin, these deposits suggest that the lacustrine/playa deposits of Shavers Valley once covered between 4 and 5 square kilometers. Throughout the reconnaissance, no geomorphic or stratigraphic evidence of shorelines could be found.

Strike and dip measurements of the fanglomerate underlying the clayey sand deposits were made throughout the basin (see Fig. 2). The dips of the fanglomerate bedding gradually increase in a south-southwesterly direction. The dip angle eventually reaches a 9 degree maximum where the fanglomerate contacts the Mecca Hills bedrock at the southern edge of Shavers Valley. The imbrication of the fanglomerate clasts, even in the northward-dipping sections, indicates a northeast-to-southwest paleocurrent direction during deposition of the alluvial fan.

Figure 2 displays the distributions of the exposed clay deposits, the exhumed fanglomerate surfaces, and the more recent alluvial fans. No attempt was made to map any of the bedrock/fanglomerate contacts near the southern margin of the basin.

DISCUSSION AND IMPLICATIONS

The imbrication of the clasts in the exhumed fanglomerate immediately underlying the lacustrine/playa clayey sand deposits indicates that the regional drainage probably flowed southward across the Mecca Hills before ponding occurred in Shavers Valley. Tectonic activity associated with the San Andreas fault is most

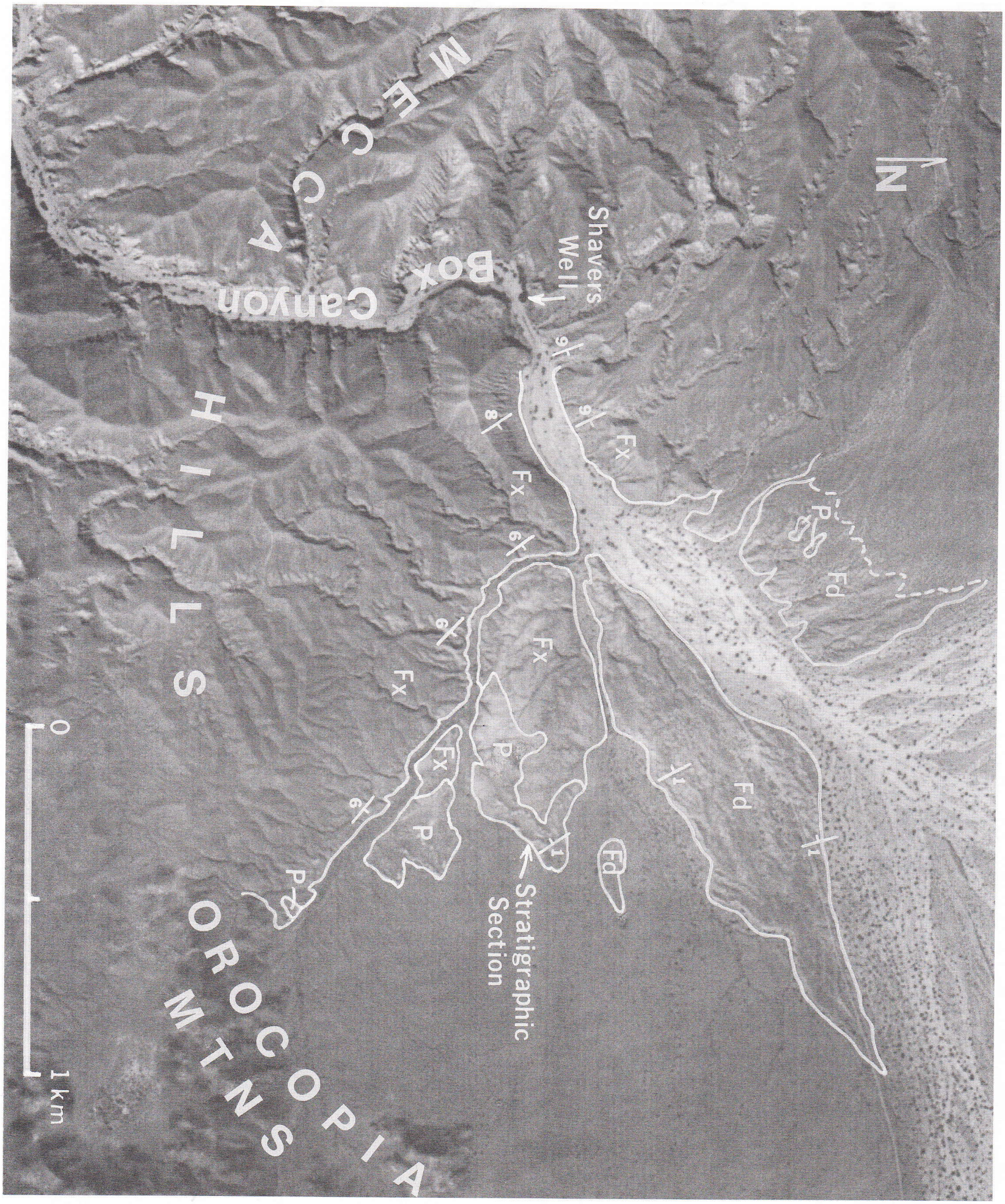

Figure 2. Geologic map of a portion of Shavers Valley. Fd = dissected alluvial fans; Fx = exhumed fanglomerate; P = remnant lacustrine/playa deposits.

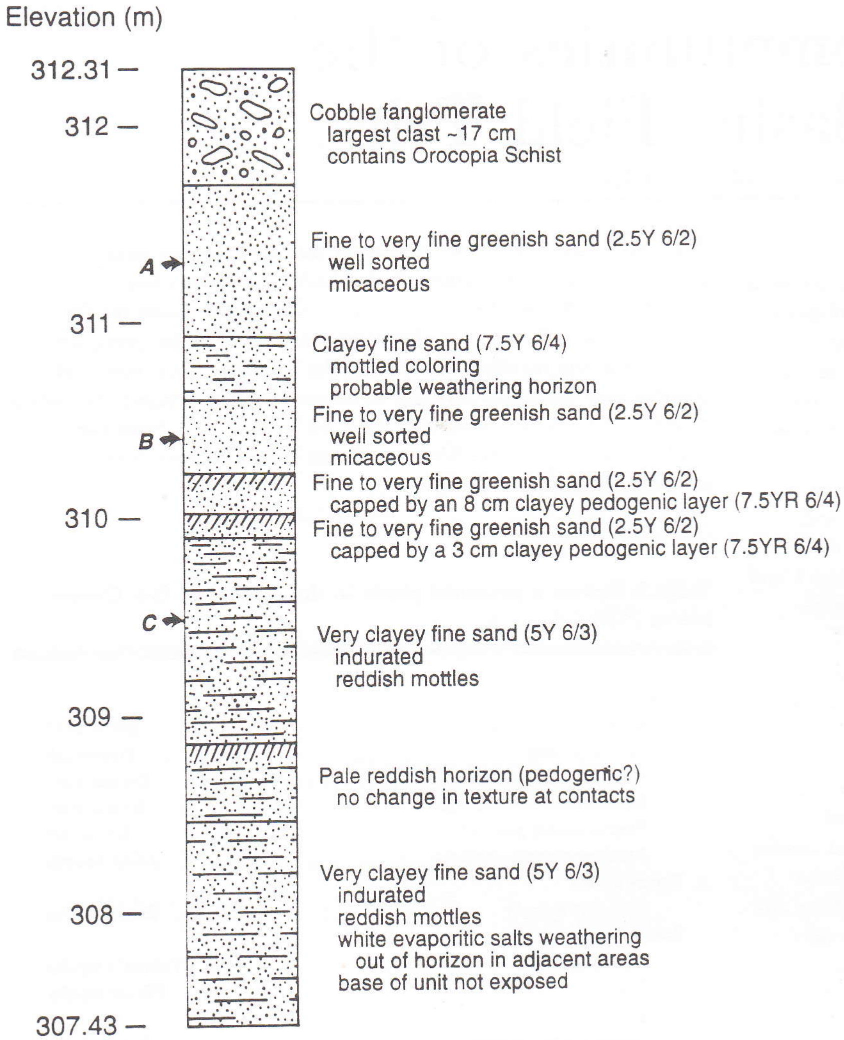

Figure 3. Stratigraphic section of the upper Quaternary strata in Shavers Valley. The letters A, B and C indicate the ostracode sampling locations.

Figure 4. Photograph of the stratigraphic section (12/92).

likely responsible for the upward warping of the older alluvial fan and the formation of the basin. Strike and dip measurements show the fanglomerate warping up to 9 degrees as it nears the Mecca Hills. Given the thin post-fanglomerate clayey strata in the basin, this upward warping is probably no older than the late Pleistocene.

As a result of this upward warping, the regional drainage was ponded in Shavers Valley. Using average deposition rates of 30 to 70 cm/100 years for clay deposits in other Mojave Desert basins (Smith, 1991:342) the >4.28 m of clayey sand deposits in Shavers Valley indicates that the basin was probably intact for at least 6,100 to >14,300 years. The small clast size of the alluvial fans entering the basin near the time of ponding represent the distal margins of such fans, and further indicate that the basin did not have through-flowing drainage for a lengthy period. However, the absence of ostracodes and other microfossil evidence leads us to believe that, although the basin was intact for at least 6,100 years, water did not stand continuously enough for their development. Along with the complete absence of shorelines, this indicates that the lake was probably not perennial. Rather, the clayey sand deposits reflect periodic shallow ponding and playa conditions.

It is probable that the basin was breached during an abnormally wet year when floodwaters overflowed the basin rim. Thus, overflow from a shallow lake cresting at an elevation of greater than 312 m was most likely responsible for initially incising Box Canyon at Shavers Well.

The incision of Shavers Valley must postdate the accumulation of the clayey sand deposits. The ponded deposits indicate that the breaching of the Shavers Valley basin was probably not the result of headward growth by the Box Canyon drainage, but rather, it occurred because of the overspilling of a shallow lake. Thus, the Shavers Valley basin, along with the Manix basin along the Mojave River (Meek, 1989), provides further evidence of arid stream networks growing in a downstream direction following the tectonic activity that created the basins.

REFERENCES CITED

Meek, N., 1989. Geomorphic and hydrologic implications of rapid incision of Afton Canyon, Mojave Desert, California. Geology, 17:7-10.

Smith, G.I., 1991. Stratigraphy and chronology of Quaternary-age lacustrine deposits, *in* The geology of North America, vol. K-2, Quaternary nonglacial geology: conterminous U.S. The Geological Society of America:339-346.

Steinmetz, J.J., 1988. Biostratigraphy and paleoecology of limnic ostracodes from the late Pleistocene Manix formation. M.S. thesis, Pomona, California State Polytechnic University: 64 p.

Sylvester, A.G. and R.R. Smith, 1976. Tectonic transpression and basement-controlled deformation in San Andreas fault zone, Salton Trough, California. AAPG Bulletin, 60(12):2081-2102.

Plants and Plant Communities of the Ashes, Faults and Basins Field Trip

JACK H. BURK, *Professor of Biology, California State University, Fullerton CA 92634*

INTRODUCTION

The botanical resources of southern California are among the most diverse of any terrestrial habitat outside the tropics. The combination of dramatic topographic relief, mild climate, coastal proximity, and latitude combine to establish an astounding diversity of habitats. In addition, the rich paleoflora found where the Neotropical-Tertiary, and Arcto-Tertiary, and the Madro-Tertiary Geofloras contacted and migrated back and forth during millennia of continental movement and climate change, provides a wide variety of genetic resources to populate diverse microhabitats. While pursing Ashes, Faults, and Basins of southern California you will pass through many of the vegetation types that now occupy this diverse landscape. Tables I and II list plants that you may encounter at Box Canyon and Arroyo Salado Canyon.

The environmental factors that are responsible for the major patterns of vegetation are reducible to three regional climate zones. Cismontane Mediterranean climate areas are dominated by shrub, woodland, and grassland communities tolerant of hot dry summers and cool moist winters. Fire frequently modifies the landscape mosaic in these communities. Montane habitats of the Peninsular and Transverse mountain ranges are inhabited by conifer or mixed conifer and hardwood forests where elevations are high enough to receive some summer precipitation from thunderstorms or monsoons from the south and winter snow. To the lee side of the mountains the rain shadow and a global position of 32-35°N combine to form the western Sonoran Desert at elevations below about 600 m (2000 ft).

INLAND VALLEYS

Prior to urbanization, cismontane inland valleys of eastern Los Angeles, western San Bernardino, and western Riverside counties were broad expanses of coastal sage scrub vegetation dominated by aromatic, summer deciduous subshrubs. The characteristic species were coastal sagebrush (*Artemesia californica*), black, white, and purple sage (*Salvia mellifera, S. apiana* and *S. leucophylla*) and California buckwheat (*Eriogonum fasciculatum*). Scattered here and there in these low shrubs were larger, evergreen shrubs such as holly leaved red berry (*Rhamnus ilicifolia*), lemonade berry (*Rhus intergrifolia*), sugar bush (*Rhus ovata*) and holly leaved cherry (*Prunus ilicifolia*). A modified coastal sage scrub community known as alluvial scrub supports an interesting array of both desert and coastal species along the often flood-disturbed margins of major waterways such as the Santa Ana River flood plain located just north of the San Bernardino County Museum. California juniper (*Juniperus californica*) and the Mojave yucca (*Yucca schidigera*) find cismontane homes only in the alluvial scrub. Forests of phreatophytic trees such as Fremont cottonwood (*Populus fremontii*) and a variety of willows (*Salix* spp.) dominated the palustrine landscape adjacent to the water courses. These coastal sage scrub communities are rapidly disappearing under the ever expanding urban sprawl.

Rolling foothills surrounding the inland valleys were a mosaic of valley grassland, coastal sage scrub, and chaparral communities. The grasslands were, prior to domestic livestock grazing and the introduction of a wide variety of often competitively superior alien annual plants, dominated by perennial bunch grasses such as *Stipa*, *Poa*, and *Aristida*. Most of the species that now occupy valley grasslands of southern California are herbs and grasses from Europe (e.g. *Avena, Bromus, Festuca, Erodium*). Chaparral occurs on the cooler slopes and at higher elevations where orographic precipitation increases as the maritime air reaches the foothills. This mosaic of communities continues at lower eleations to San Gorgonio Pass where coastal winds are funneled into the Coachella Valley. Here rain shadow prevails and the Sonoran Desert begins its stretch over southern Arizona and Sonora.

Table I. Common perennial plants in the vicinity of Box Canyon, Mecca Hills CA

Asteracea	
Ambrosia dumosa	Burro bush
Bebbia juncea	Sweetbush
Hymnenoclea salsola	Cheese bush
Machaeranthera cognata	Mecca aster
Pleurocoronis pluriseta	Arrow leaf
Psathyrotes ramosissima	Velvet rosette
Bignoniaceae	
Chilopsis linearis	Desert willow
Boraginaceae	
Tiquilia palmeri	Palmer's tiquilia
T, plicata	Plicate tiquilia
Cactaceae	
Opuntia ramosissima	Pencil cholla
Chenopodiaceae	
Atriplex canescens	Four-winged saltbush
A. hymenelytra	Desert holly
A. polycarpa	Atriplex polycarpa
Fabaceae	
Acacia greggii	Catclaw acacia
Cercidium floridum	Paloverde
Hoffmannseggia microphylla	Small-leaf hoffmannsegia
Olneya tesota	Desert ironwood
Psorothamnus spinosa	Smoke tree
Fouquieriaceae	
Fouquieria splendens	Ocotilla
Lamiaceae	
Hyptis emoryi	Desert lavender
Loasaceae	
Petalonyx thurberi	Sandpaper plant
Polygonaceae	
Chamaesyce spp.	Spurge
Solanaceae	
Nicotiana trigonophylla	Desert tobacco
Physalis crassifolia	Chinese lanterns
Tamaricaceae	
Tamarix aphylla	Aphyl
T. ramosissima	Salt cedar
Viscaceae	
Phoradendron californicum	Mistletoe
Zygophyllaceae	
Larrea tridentata	Creosote bush

Table II. Common perennial plants near Arroyo Salado Primitive Camp, Anza Borrego State Park, CA

Asteraceae	
Ambrosia dumosa	Burro bush
Bebbia juncea	Sweetbush
Encelia farinosa	Incienso
Ilymenoclea salsola	Cheese bush
Stephanomeria pauciflora	Desert straw
Cactaceae	
Opuntia echinocarpa	Silver cholla
O. ramosissima	Pencil cholla
Chenopodiaceae	
Atriplex canescens	Four-winged salt bush
A. hymemelytra	Desert holly
A. polycarpa	Lenscale
Fabaceae	
Acacia ghreggii	Catclaw acacia
Psorothamnus emoryi	Emory psorothamnus
P. schottii	Indigo bush
P. spinosus	Smoke tree
Fouquieriaceae	
Fouquieria spendens	Ocotilla
Krameriaceae	
Krameria grayi	White ratany
Nytaginaceae	
Mirabilis begelovii	Wishbone bush
Poaceae	
Ililaria rigida	Galleta grass
Polygonaceae	
Eriogonum inflatum	Desert trumpet
Solonaceae	
Nicotinana trigonophylla	Desert tobacco
Physalis crassifolia	Chinese lanterns
Zygophyllaceae	
Larrea tridentata	Creosote bush

COLORADO DESERT

The Colorado Desert portion of the Sonoran is, like the rest, covered by creosote bush scrub. The dominant plants on all of the gently sloping bajadas are creosote bush (*Larrea tridentata*) and burro bush (*Ambrosia dumosa*). This "low" desert is distinguished from the Mojave by having a greater variety of cacti, and the arroyos support a wash woodland community dominated by trees in the pea family such as palo verde (*Cercedium floridum*), desert ironwood (*Olneya tesota*), and smoke tree (*Psorothamnus spinosus*). Where water is forced to the surface, such as along the San Andreas fault, desert fan palm oases are found. *Washingtonia filifera* is a relict of a once widespread, less arid-adapted community that dominated these areas prior to the formation of deserts during the past 10,000– 20,000 years. Where ground water is near the surface such as near the Salton Sea, and along major drainages in open areas, communities of phreatophytes including mesquite (*Prosopis juliflora* var. *torreyana*), screw bean mesquite (*Prosopis pubescens*), cottonwood (*Populus fremontii*) and willows (*Salix* spp.) predominate. Many of these wet areas are eclipsed by salt cedar *Tamarix* spp.), natives of Asia and the Middle East that have naturalized over much of the Southwest.

PENINSULAR RANGE

The western edge of the Sonoran Desert east of Borrego Springs rises abruptly to the Peninsular Range. Intermediate elevation transition zones support a very diverse plant community—up to 150 vascular plant species/2.5 km^2 (1 mi^2)—characterized by one of the highest concentrations of endemism in California. At the upper desert margins succulent plants become more common along with species commonly associated with the Mojave Desert (e.g. *Yucca shidigera*). In some areas the desert plants are replaced at higher elevations by piñon-juniper woodland (*Pinus monophylla* and *Juniperus californica*). In other areas it is replaced by a diverse community called desert chaparral that supports a potpourri of species from a variety of communities. Representative species are: from coastal chaparral, chamise (*Adenostoma fasciculatum*), big berry manzanita (*Arctostaphylos glauca*) and mountain mahogany (*Cercocarpus betuloides*); from piñon-juniper woodland, California juniper (*Juniperus californica*), antelope bush (*Purshia glandulosa*) and scrub oak (*Quercus turbinella*); and from desert chaparral, desert almond (*Prunus fasciculata*) and desert apricot (*Prunus fremontii*). Red shanks chaparral occurs in isolated pockets in southern California. Red shanks (*Adenostoma sparcifolium*) is a close relative of chamise. The plant is very attractive with bright green foliage and shedding red bark, the source of another common name: ribbon wood.

With increasing coastal and decreasing desert influence, first along canyon bottoms and on north slopes, coastal chaparral and southern oak woodland communities appear. Most of the southern oak woodland is composed principally of coast live oak (*Quercus agrifolia*) and toyon (*Heteromeles arbutifolia*) whereas in some isolated areas the rare Engelmann oak (*Quercus engelmannii*) is dominant. In the inland valleys the oak woodlands remain in the protected areas, coastal sage scrub occupies the drier sites, chaparral the higher elevation protected slopes, and valley grassland is situated on the heavy soils of the rolling hills.

REFERENCES

Barbour, Michael G. and J. Major (eds), 1988. Terrestrial vegetation of California. California Native Plant Society Special Publication, 9.

Barbour, Michael G. and W. Dwight Billings (eds), 1988. North American terrestrial vegetation. Cambridge University Press.

Brown, David E., 1982. Biotic communities of the American Southwest - United States and Mexico. Special Issue - Desert Plants, 4:1-342.

Munz, Philip A., 1974. A flora of southern California. Berkeley, University of California Press.

Ornduff, Robert, 1974. Introduction to California plant life. Berkeley, University of California Press.

Coachella Valley Prehistory: A Brief Chronology

DREW PALLETTE *Brian F. Mooney Associates, 9903 Businesspark Avenue, San Diego CA 92131-1120*

INTRODUCTION

Over twelve thousand years of human occupation may be postulated for the Coachella Valley and the Colorado Desert area. The sequence of archaeologically and ethnohistorically identified cultures in the region is generally recognized by the anthropological community, although specific interpretation of chronology and cultural patterns differ among researchers. A range of approaches to the cultural history may be found in the writings of Rogers (1966), Johnson (1979), Crabtree (1981), von Werlhof (1984), Pendleton (1984), Shackley (1984), Warren (1984), and Schaefer (1982, 1986). The reader is directed to these sources for a detailed discussion of cultural sequence and of some specific questions concerning cultural definitions and changes through time. Although differing in terminology and time ranges, all basically follow the sequence of cultural patterns outlined below.

Six successive cultural patterns, extending in time over a period of at least twelve thousand years, have been defined for the Colorado Desert, including 1) Malpais (Early Man), 2) San Dieguito, 3) Desert Archaic, 4) Patayan, 5) Ethnohistoric, and 6) Historic. Of these the Malpais and the San Dieguito are not represented in the upper (northern) Coachella Valley. One of the only documented stratigraphic sites with an Archaic component is the Indian Hill Rockshelter (McDonald 1992) located in present-day Anza-Borrego Park. A pre-ceramic rockshelter site, probably dating from the same period, was found in Tahquitz Canyon, Palm Springs (Bean and Schaefer, on-going research). As Wilke states, "The known prehistory of human occupation in the Coachella Valley does not extend back very far into the past. Nearly all the available evidence is assignable to the last stand of Lake Cahuilla (ca A.D. 1300-1500)" (Sutton and Wilke 1988:4). For these reasons, this brief introduction will concentrate on providing the chronological framework for the study area starting with the Patayan Period.

PATAYAN PERIOD

The Patayan cultural pattern is marked by the introduction of pottery on the lower Colorado River approximately 1,200 years ago (Warren 1984). A pre-ceramic phase can also be discerned by the introduction of Desert Side-notched and Cottonwood type projectile points into the region. Techniques of flood plain agriculture were introduced into the area at the same time as pottery. Burial practices also changed from extended inhumanations to cremations. All these new traits are typical of the Hohokam Culture and it is quite probable that they reached the Colorado River from southern Arizona via inhabitants of the Gila River. From the Colorado River the cultural complex spread west and north. Agriculture may not have been adopted beyond the eastern Peninsular Range until very late Prehistoric times or after European contact. The appearance of ceramics and new projectile point types occurs locally in the Salton Basin after 900 A.D.

The Patayan Culture is typified by small mobile groups living in seasonal settlements along the Colorado River and Lake Cahuilla. They erected rock-outlined jacal structures, simple ramadas, or brush huts, depending on the season and function of the settlement. Long distance travel to special resource collecting zones, trading expeditions, and possibly some warfare are reflected by the numerous trail systems throughout the Colorado Desert and adjoining mountains that have associated ceramic pot drops, trail-side shrines, and other evidence of transitory activities. Many of the pictographs, petroglyphs, and bedrock grinding surfaces in the Colorado Desert have also been associated with the Patayan pattern, although direct dating and cultural affiliation of such features is difficult to determine.

The Patayan sequence is divided into three periods that are distinguished by different pottery types and regional site distributions. Patayan village and temporary camp sites are characterized by pottery and lithic scatters, groundstone implements, Cottonwood Triangle and Desert Side-notched projectile points, cremation burials, fire hearths, house pits, and midden deposits containing shell, bone, charcoal and other organic remains. Patayan site types can range from trail systems and lithic quarry loci to extensive occupational complexes.

Patayan I

Patayan I period sites are found on the Colorado River and further east into Arizona. Dating between A.D. 500 and 1050, this period is marked by riverine-oriented hunters and gatherers. Increasing evidence is being found for a "Yuman Phase" with similar Patayan-type assemblages developing from the Desert Culture of the Great Basin. The relationship of coastal and Colorado River peoples in the Patayan I period is not well understood nor is the nature of occupation between the two regions. The introduction of Cottonwood and Desert Side-notched projectile points occured during this period. Tizon Brown Ware is the dominant ceramic type.

Patayan II

The Patayan II period is characterized by the spread of the assemblage from the Colorado River into the California and Mojave Deserts between A.D. 950 and 1500. This is a period of three major Lake Cahuilla lacustral episodes and the periodic occupation of both the east and west shorelines. Earlier lacustral intervals are also documented as far back as 500 B.C. (Waters 1983:383). Extensive midden deposits, including preserved human coprolites retrieved from excavations at Myoma Dunes near Indio, provide the most detailed picture of subsistence and diet of people living on the shoreline (Wilke 1976). Shellfish, fish, waterfowl, cattails, and mesquite beans were consumed as well as a variety of other resources. A late spring-early summer occupation of the shoreline is suggested by the presence of cattail pollen in the midden deposits, fish bone from species with known seasonal runs in accessible shallows, and mesquite pollen from Dunaway Road (Schaefer 1986), Myoma Dunes (Wilke 1978), and La Quinta (Sutton and Wilke 1988). While Wilke proposed that the shoreline sites were intensively-used "villages" with large populations spending a major portion of the year at one locality, Weide (1976) contends that the shoreline occupation was limited to small groups staying only a short time. At least along the southwest maximum infilling shoreline an ephemeral occupation is indicated by the low density artifact scatter (Schaefer 1981, 1986; Gallegos 1984a, 1984b; Shackley 1984). A similar situation is documented on the east shoreline: small sites described as temporary camps associated with beaches, marsh edges and mesquite dunes (Davis 1980; Gallegos

1986).

Proximity to other viable ecozones differs between the east and west shorelines. There are many more inland sites on the west side, associated with the large washes and springs at the base of the nearby Peninsular Range. On the east side, however, there are only two viable occupation zones—the shoreline and the Colorado River. Between the two were few areas that could sustain anything more than short-term temporary camps and limited activity areas. Therefore, sites on the eastern relic shoreline tend to be concentrated on the beach with no substantial "inland" occupation.

Wilke (1978:103-107) inferred a large sedentary population on the northwestern shores of Lake Cahuilla. Permanent, year round base camps (i.e., "villages") were established, according to Wilke, that could exploit plant and animal resources that came into season throughout the year. Supplemental resources such as agave, pinyon nuts, mule deer and desert big horn sheep would be acquired by seasonal expeditions to the Peninsular Range (specifically the Santa Rosa Mountains) where temporary camps were established. Wilke recognized that not all parts of the shoreline supported a wide array of reliable resources. While Myoma Dunes consists of ten miles of extensive midden deposits, other areas contain few sites because of less favorable habitat associations. Wilke therefore cautions against applying his intensive village model to other parts of the Coachella Valley, not to mention the central and southern Lake Cahuilla shoreline. An alternative model to that of Wilke's intensive year round base camp exploitation of Lake Cahuilla has been sugested by Weide (1976) who instead proposes a flexible seasonal transhumance model of hunters and gatherers who opportunistically moved between the mountains and lake shore. Evidence of periodic fluctuations in the shoreline levels suggested that a sustained focus on the lacustrine habitat was not viable and that the distribution of artifacts and sites did not justify an inferred "village" settlement model.

Subsequent surveys, tests and data recovery projects on West and East Mesa tend to support Weide's model for the southern half of Lake Cahuilla (Gallegos 1986; Schaefer 1986). Most recently this conclusion was reached for the several northwest Lake Cahuilla shoreline sites in the La Quinta region (Sutton and Wilke 1988:162). Sites are characteristically low to high density artifact scatters containing only shallow midden deposits. Sites are indeed non-randomly distributed and tend to focus on marshy embayments protected by sand bars or where major washes empty into the lake. The same types of resources present at Myoma Dunes are indicated, although preservation is not nearly as good, but in the case of one well preserved recessional shoreline site, a springtime seasonal focus is indicated (Schaefer 1986). The depth of deposit and distribution of sites, however, clearly indicate seasonal temporary camps rather than permanent villages. One explanation for the difference at Myoma dunes is suggested by Gallegos (1986:6-3). A steeper grade to the basin on the north end of Lake Cahuilla than at the south end would result in less extreme changes in the shoreline habitat. Deeper shoreline water levels in the north would cause less abrupt recessions than in the shallow waters of the south. It is therefore possible that the lacustrine habitat was more stable and reliable for the people of Myoma Dunes than for East or West Mesa and could support a more permanent population. Myoma Dunes may be the exception rather than the rule, however.

Studies up to the present all propose a model, whether of base camps or temporary camps, of people occupying the area immediately adjacent to the shoreline and focusing on lacustrine littoral habitats and surrounding desert, particularly mesquite dunes or woodland wash habitats. The Lake Cahuilla shoreline is viewed as the magnet attracting these hunter and gatherers from their base camps in the foothills and eastern end of the Peninsular Range.

A different settlement strategy has been documented on West Mesa west of the Superstition Mountains (Schaefer 1988). Here, an unusually large array of temporary camps have been documented that are not focused on the Lake Cahuilla shoreline, although they are only 1.5 miles away and prove to be contemporary. With the infilling instead, they indicate a focus on ephemeral pans that supported an alkali sink habitat. This pattern of alkali pan exploitation may extend back more than 1000 years B.P. to even before the first recession and indicates another aspect of the opportunistic and flexible nature of hunter-gatherer adaptations in the Colorado Desert.

Current research thus supports the Weide model. If the Lake Cahuilla shores were occupied by short-term seasonal encampments, then many of the Patayan II base camps may be hypothesized to be at the eastern foot of the Peninsular Range near perennial streams and springs and in ecotones between the Upper and Lower Sonoran life zones. Such strategic locations would provide access to a wider variety of resources.

Patayan III

After at least four, probably five, recession and infilling sequences, Lake Cahuilla receded for a final time after A.D. 1580. This marks the beginning of the Patayan III period which lasted until the disruption of traditional cultural patterns by Euro-American incursions. Dates for the first four lacustrine phases are tentatively assigned, based on radiocarbon dated archaeological deposits and lacustrine geomorphic structures (Waters 1983). Evidence now exists for a fifth partial infilling to sea level that dates somewhere between A.D. 1158 and 1710 (Schaefer 1986). During the Patayan III period the population made final use of the transitory receding shoreline habitats. But as the water became too saline to maintain lacustrine life, probably somewhere below the 100-foot below mean sea level (BMSL) contour, the population had to abandon the area for any extended seasonal resource exploitation. Within the Imperial Valley, populations focused on mesquite dunes, springs, wells, and arable lands along the New and Alamo Rivers, extending south to the Gulf of California. Most of the population reoriented their activities to previously important ecozones, west to the Peninsular Range and east to the Colorado River.

The intensity of occupation at Myoma Dunes, combined with the observed increased density of late period sites in the Peninsular Range foothills, lead Wilke (1978:113-118) to infer major population shifts following the last maximum stand of Lake Cahuilla at about A.D. 1540. Weide (1976) suggests that when the final recession began, the native population needed only to shift their emphasis to the Peninsular Range, Colorado River, or to springs, wells, or seeps on the dissociated lake bottom. No major ecological or demographic adjustments had to be made in the characteristically flexible hunter-gatherer settlement and subsistence strategy.

Whether the final desiccation of Lake Cahuilla around A.D. 1600 caused an abandonment of the desert floor areas remains unknown. Shackley (1984) has documented a change in emphasis on certain plant species such as agave in the Post-Lake Cahuilla period. Whether this change also included an increase in the use of desert plants such as mesquite remains to be demonstrated. However, certainly by the late Patayan III and early ethnohistoric periods, permanent villages had been established on the desert floor in areas such as Toro, Indian Wells, and San Felipe Creek and at the mouths of major canyons such as Andreas and at Palm Springs. The seasonal scheduling and mobility continued to be practiced, with people moving from the desert floor to the higher elevations to gather resources as they became available.

ETHNOHISTORIC PERIOD

By the time of first European contact, the Desert Cahuilla of Coachella Valley were well established, occupiing about 14 villages and numbering perhaps 3,000 persons. Most villages were located on the valley floor in areas of a high water table where large mesquite groves grew and walk-in wells could be dug, or at reliable springs (e.g.,Thousand Palms, Andreas). Agriculture was being practiced when Romero came through the valley in 1825.

Only limited archaeological investigations have been conducted on Post-Lake Cahuilla sites. Most of what is known is detailed in oral traditions of the Cahuilla Indians of Coachella Valley. Early 20th century ethnographers recorded many these traditions (Wilke and Lawton 1975; Wilke 1978). Oral traditions tell of life around Lake Cahuilla, fishing and hunting there, and of the final desiccation. Ethnographic evidence provided by Cahuilla living in the Toro area claim that they originally were located in the higher elevations of the Santa Rosas (Rockhouse and Coyote Canyons) to the west of the present day village (Wilke and Sutton 1988; Bean 1990). Wilke has argued that this oral tradition provides evidence of abandonment of the shoreline after the final recession, movement to higher elevation, and the subsequent repopulation of the valley floor after the establishment of substantial mesquite groves (Wilke and Sutton 1988:9). Of course, the same stories lend credence to a post-lake model where the population moves from already existing residential villages in the mountains or foothills to the desert floor following the drying up of the lake. In any event, until more Post-Lake Cahuilla sites and villages are studied we are left with differing theories that are primarily based on ethnographic and historic studies.

REFERENCES CITED

Crabtree, Don E., 1981. Archaeology, *in* A Cultural Resources Overview of the Colorado Desert Planning Units edited by Elizabeth von Till Warren, et al., pp. 25-54. Bureau of Land Management, California Desert District, Riverside.

Davis, Emma Lou, 1980. Stage 3 Inventory-Archaeological Notes and View of East and West Mesas, *in* Class II Cultural Resource Inventory East Mesa and West Mesa Regions, Imperial Valley, California. Volume 1 pp. 151-176. Report prepared by Westec Services, Inc. for the U.S. Department of Interior, Bureau of Land Management, Riverside, California.

Gallegos, Dennis, 1980. Class II Cultural Resource Inventory of the East Mesa and West Mesa Regions, Imperial Valley, California (Vol. I). Report prepared by WESTEC Services, Inc. for the U.S. Department of Interior. Bureau of Land Management, Riverside, California.

___, 1984a. Cultural Resource Data Recovery Program for SDG&E's Imperial Valley to La Rosita 230KV Transmission Line. Report prepared by WESTEC Services, Inc. for San Diego Gas and Electric Company.

___, 1984b. West Mesa Cultural Resource Survey and Site Evaluation, Imperial Valley, California. Report prepared by WESTEC Services, Inc. for the U.S. Department of Interior, Bureau of Land Management.

___, 1986. Patayan II and Patayan III Occupation of IMP-4434 and IMP-5167, East Mesa, Imperial County, California. Report prepared by WESTEC Services, Inc. for Ryerson Concrete Company.

Johnson, Francis, 1977. The Bradshaw Trail. Historical Commission Press, Riverside, California.

McDonald, Alison M., 1992. Indian Hill Rockshelter and Aboriginal Cultural Adaptation in Anza-Borrego Desert State Park, Southeaster California. Unpublished Ph.D. dissertation, Department of Anthropology, University of California, Riverside.

Pendleton, Lorann, 1984. Archaeological Investigations in the Picacho Basin. Report prepared for San Diego Gas and Electric by Wirth Environmental, San Diego.

Rogers, Malcolm, 1936. Yuman Pottery Making. San Diego Museum of Man Paper No. 2.

___, 1945. An Outline of Yuman Prehistory. Southwestern Journal of Anthropology 1(2):167-198.

___, 1966. Ancient Hunters of the Far West. Union-Tribune Publisher, San Diego.

Shackley, M. Steven, 1984. Archaeological Investigations in the Western Colorado Desert: A Socio-ecological Approach. Report prepared by Wirth Environmental Services for San Diego Gas and Electric.

Schaefer, Jerry, 1981. Phase II Archaeological Survey of the La Rosita 230 KV Interconnection Project. report prepared for Cultural Systems Research, Inc. for San Diego Gas and Electric.

___, 1986. Late Prehistoric Adaptations During the Final Recessions of Lake Cahuilla: Fish Camps and Quarries on West Mesa, Imperial County, California. Report prepared by Mooney-LeVine and Associates for the USDI, Bureau of Land Management, El Centro Resource Area.

___, 1988. Lowland Patayan Adaptations to Ephemeral Alkali Pans at Superstition Mountain, West Mesa, Imperial County, California. Report prepared by Brian F. Mooney Associates for the USDI, Bureau of Land Management, El Centro, California.

Sutton, Mark Q. and Philip J. Wilke (editors), 1988. Archaeological Investigations at CA-RIV-1179, CA-RIV-2823, and CA-RIV-2827, La Quinta, Riverside, California. Archives of California Prehistory, Number 20. Coyote Press, Salinas, California.

von Werlhof, Jay, 1984. Archaeological Investigations of the Gold Fields Mesquite District. Report prepared by the Imperial Valley College Museum, El Centro, California for the Gold Fields Mining Company, Inc.

Warren, Claude, 1984. The Desert Region. In California Archaeology, edited by Michael J. Moratto pp.339-430, Academic Press, Orlando.

Waters, Michael R., 1980. Lake Cahuilla: Late Quaternary Lacustrine History of the Salton Trough, California. Master's thesis, University of Arizona.

___, 1982. The Lowland Patayan Ceramic Typology, *in* Hohokam and Patayan, edited by Randall H. McGuire and Michael B. Schiffer, pp. 537-570. Academic Press, New York.

___, 1983. Late Holocene Lacustrine Chronology and Archaeology of Ancient Lake Cahuilla, California. Quaternary Research 19:373-387.

Weide, Margaret L., 1976. A Cultural Sequence for the Yuha Desert. In Background to Prehistoric of the Yuha Desert Region, edited by Philip J. Wilke, pp. 81-94. Ballena Press Anthropological Papers No. 5; Ramona, California.

Wilke, Philip J., 1976. Ethnography, *in* Deep Canyon, A Desert Wilderness for Science, edited by Irwin P. Ting and Bill Jennings, pp. 97-105. University of California Philip L. Boyd Deep Canyon Desert Research Center, Riverside.

___, 1978. Late Prehistoric Human Ecology at Lake Cahuilla, Coachella Valley, California. Contributions of the University of California Archaeological Research Facility Number 38. University of California, Berkeley.

Wilke, Philip J. and H.W. Lawton, 1975. Early Observations on the Cultural Geography of Coachella Valley. Ballena Press Anthropological Papers No. 3 (1):9-43.

Rise and Fall of the Desert Pupfish, *Cyprinodon macularius*, at the Salton Sea

ALLAN A. SCHOENHERR *Fullerton College, 321 E. Chapman Ave. Fullerton, CA 92634*

INTRODUCTION

The Desert Pupfish, *Cyprinodon macularius*, and its allies were formerly common in sloughs and backwaters of the Gila River in Arizona, and the lower Colorado River in the United States and Mexico. They also were common in shoreline pools and irrigation drains of the Salton Sea in California. Despite their remarkable tolerance for environmental extremes and high reproductive potential, the species has undergone a serious decline in numbers. Since the late 1800s fish have disappeared in association with activities of humans such as dam building, diversions of water, ground-water pumping, and pesticides. They have been further threatened by encroachment of non-native vegetation such as Tamarisk, *Tamarix* spp. The most rapid decline has occurred in recent years in association with introduced fishes. Through predation, aggression, and various behavioral activities that interfere with reproduction, introduced species have driven Desert Pupfish to the brink of extinction (Schoenherr, 1988).

HISTORY OF THE DESERT PUPFISH

The Bouse Embayment was a Mio-Pliocene body of water that covered an area that includes today the lower Colorado River and Salton Trough (Miller, 1981; Smith 1981). It appears that the Desert Pupfish descended from fish that occupied that estuary. Furthermore, it appears that all the other pupfishes that occur in the Death Valley area probably descended from *Cyprinodon macularius* or a *C. macularius*-like ancestor. It is interesting to note that the Owens Pupfish, *Cyprinodon radiosus*, native to the upper Owens river drainage, near Bishop, is the nearest relative of the Desert Pupfish (Soltz and Hirshfield, 1981). Through the 1800s Desert Pupfish occupied mostly quiet water habitats, particularly sloughs and backwaters along major drainages such as the Gila and lower Colorado Rivers (Miller, 1961; Minckley and Deacon, 1968).

Natural populations of Desert Pupfish occur today at Quitobaquito Spring in Organ Pipe Cactus National Monument in Arizona (a distinct subspecies) and in the Santa Clara Slough, near the mouth of the Colorado River in Sonora, Mexico. Natural populations of insecure status, subject to wide fluctuations in density, occur south of Quitobaquito in Rio Sonoyta, Sonora, Mexico, and in California in Salt Creek (Riverside County), San Felipe Creek (Imperial County), and in shoreline pools of the Salton Sea. Populations in irrigation drains that lead to the Salton Sea come and go with vagaries of conditions such as weather, introduced species, weed eradication, channelization, road building, etc.

The origin of Rio Sonoyta fish clearly was the Colorado River Delta (Miller and Fuiman, 1987). Sometime within the past 100,000 years, eruptions of the Pinacate Volcanic Fields blocked the original westward course of the river and isolated the fish. The present population at Quitobaquito Spring, now described as a distinct subspecies, *C. m. eremus* (Miller and Fuiman, 1987) has been isolated probably since Pleistocene times. There is no evidence of a historical connection to Rio Sonoyta although fossil springs west of Quitobaquito probably overflowed to Rio Sonoyta during times of high water flow, presumably at some time in Holocene or Pleistocene (Miller and Fuiman, 1987).

Drying of Lake Cahuilla about A.D. 1500 eliminated from the Salton Basin what was essentially a Colorado River Fauna. Old fish traps and middens bear witness that Cahuilla Indians used these fishes, including the Desert Pupfish, as food (Wilke, 1979). Natural rerouting of the Colorado River about 600 years ago diverted water away from Lake Cahuilla and into the Gulf of California. Estimates of shoreline retreat, based on distances between rows of fish traps, imply that it took about 55 to 60 years for the lake to dry completely (Wilke, 1979), probably leaving the Desert Pupfish isolated in certain springs of the Salton Basin.

In the early 1900s a period of arroyo cutting associated with cattle grazing and compaction began (Hastings, 1959; Hastings and Turner, 1965; Miller, 1961). Drying of wetlands and diversion of water for agriculture led to a decline of pupfish habitat. Nevertheless, pupfish flourished locally in Arizona, adjacent Sonora, Mexico, and the Salton Sea in California until about the 1930s (Deacon and Minckley, 1974). At about that time, native fishes began to be replaced by introduced species. Through various interactions such as aggression and predation, these introduced species began to cause native fish populations to become reduced to locally isolated entities (Schoenherr, 1981b).

The 1905 flooding that refilled the Salton Sea fortuitously reintroduced the Desert Pupfish. In the early 1960s, shoreline pools contained thousands of them (Barlow, 1961). History of their disappearance is directly correlated with the introduction of non-native species (Schoenherr, 1979; 1981b). Shoreline pool habitats are now mostly occupied by Sailfin Mollies, *Poecilia latipinna*. Irrigation drains appeared to be a refuge until the "weed-eating" Zill's Cichlid, *Tilapia zilli* was introduced (Schoenherr, 1981a).

CURRENT STATUS

The population of the Quitobaquito Pupfish in Organpipe Cactus National Monument remains healthy, although introduced Golden Shiners, *Notemigonus crysoleucus*, of inexplicable origin had to be removed in 1969 (Schoenherr, 1988). In California, as recently as 1991 it was believed that Desert Pupfish had been eliminated from all habitats except Salt Creek, near Dos Palmas in Riverside County, and San Felipe Creek near Highway 86 in Imperial County. In 1991 and 1992 they "reappeared" in certain irrigation drains and shoreline pools. A long period of cold weather during the winter of 1991 may have eliminated Zill's Cichlid from those habitats allowing reinvasion of the Desert Pupfish from unknown low density refugia. Buffers against extinction include a number of small populations maintained as refugia in artificial impoundments that require constant supervision to prevent encroachment by aquatic vegetation or introduced non-native fishes of mysterious origin.

LITERATURE CITED

Barlow, G. W., 1961. Social behavior of the desert pupfish, *Cyprinodon macularius*, in the field and in the aquarium. Amer. Midl. Nat., 65:339-358.

Deacon, J. E., and W. L. Minckley, 1974. Desert fishes. Pp. 385-488 in Desert Biology, Vol II (G. W. Brown, Jr. ed), Academic Press, New York.

Hastings, J. R., 1959. Vegetation change and arroyo cutting in southeastern Arizona. Jour. Ariz. Acad. Sci., 1:60-67.

Hastings, J.R. and R. M. Turner, 1965. The changing mile. Univ. Ariz Press, Tucson, Arizona.

Miller, R. R., 1961. Man and the changing fish fauna of the American Southwest. Pap. Michigan Acad. Sci. Arts, Lett., 46:365-404.

___, 1981. Coevolution of deserts and pupfishes (genus *Cyprinodon*) in the American Southwest. Pp. 39-94 *in* Fishes in North American deserts (R. J. Naiman and D. L. Soltz, eds.), John Wiley and Sons, New York.

Miller, R.R. and L. A. Fuiman, 1987. Description and conservation status of *Cyprinodon macularius eremus*, a new subspecies of pupfish from Organ Pipe Cactus National Monument, Arizona. Copeia, 593-609.

Minckley, W. L. and J. E. Deacon, 1968. Southwestern fishes and the enigma of "Endangered Species." Science, 159:1424-1432.

Schoenherr, A. A., 1979. Niche separation within a population of freshwater fishes in an irrigation drain near the Salton Sea. Bull. Southern Calif. Acad. Sci., 78:46-55.

___, 1981a. Replacement of *Cyprinodon macularius* by *Tilapia zilli* in an irrigation drain near the Salton Sea. Proc. Desert Fishes Council, Vol. XIII:65-66.

___, 1981b. The role of competition in the replacement of native fishes by introduced species. Pp. 173-203 *in* Fishes in North American deserts (R. J. Naiman and D. L. Soltz, eds.), John Wiley and Sons, New York.

___, 1988. A review of the life history and status of the Desert Pupfish, *Cyprinodon macularius*. Bull. Southern Calif. Acad. Sci., 87:104-134.

Smith, M. L. 1981. Late Cenozoic fishes in the warm deserts of North America: a reinterpretation of desert adaptations. Pp. 11-38 *in* Fishes in North American deserts (R. J. Naiman and D. L. Soltz, eds.), John Wiley and Sons, New York.

Soltz, D. L., and M. F. Hirshfield, 1981. Genetic differentiation of pupfishes (genus *Cyprinodon*) in the American southwest. Pp. 291-333 *in* Fishes in North American deserts. (R. J. Naiman and D. L. Soltz, eds.), John Wiley and Sons, New York.

Wilke, P. J., 1979. Prehistoric weir fishing on recessional shorelines of Lake Cahuilla, Salton Basin, southeastern California. Proc. Desert Fishes Council, Vol. XI:101-102.

The San Andreas Fault of the Salton Trough Region, California, as Expressed on Remote Sensing Data

FRANCESCO V. CORONA *Energy Resources Technology Division, P. O. Box 76 , Brea, California 92621*
FLOYD F. SABINS, JR. *Remote Sensing Enterprises, 1724 Celeste Lane, Fullerton, California 92633*

ABSTRACT

The San Andreas fault and related structures in the Salton trough region are readily expressed on Landsat images and high-altitude aerial photographs, having diagnostic surface characterisitics that are typical of a wrench-fault assemblage. These characteristics include a principal strike-slip displacement zone that is relatively straight and long, inconsistent structural relief along major wrench faults, the occurrence of *en echelon* structures adjacent to the major strike-slip faults, and lateral offset of structural, natural, and man-made features. Wrench-fault transpression and transtension occur in places along the San Andreas fault system, recognized respectively by the dominance of contractional or extensional structures. All of these surface manifestations are clearly discriminated on the remote sensing data and define criteria that distinguish wrench-fault assemblages from other structural styles.

INTRODUCTION

The southern extent of the San Andreas right-lateral, strike-slip fault lies along the northeastern margin of the Salton trough in southern California (Figure 1). This fault is tectonically active, well exposed, and well documented in this region (many authors; e.g., Crowell, 1962; Dibblee, 1977; Crowell and Sylvester, 1979; Sylvester, 1988; Hutton and others, 1991), thus offering an ideal locality to study the San Andreas fault and the structural assemblage that is commonly associated with wrench-fault tectonics (Figure 2; Wilcox and others, 1973; Harding, 1974; Reading, 1980; Christie-Blick and Biddle, 1985; Harding, 1990). Wrench-fault assemblages have unique structural characteristics that differentiate them from other styles of deformation (Harding and Lowell, 1979; Lowell, 1990). Likewise, wrench-fault assemblages have distinguishing surface manifestations that can be detected and analyzed using remote sensing data (Corona, 1993).

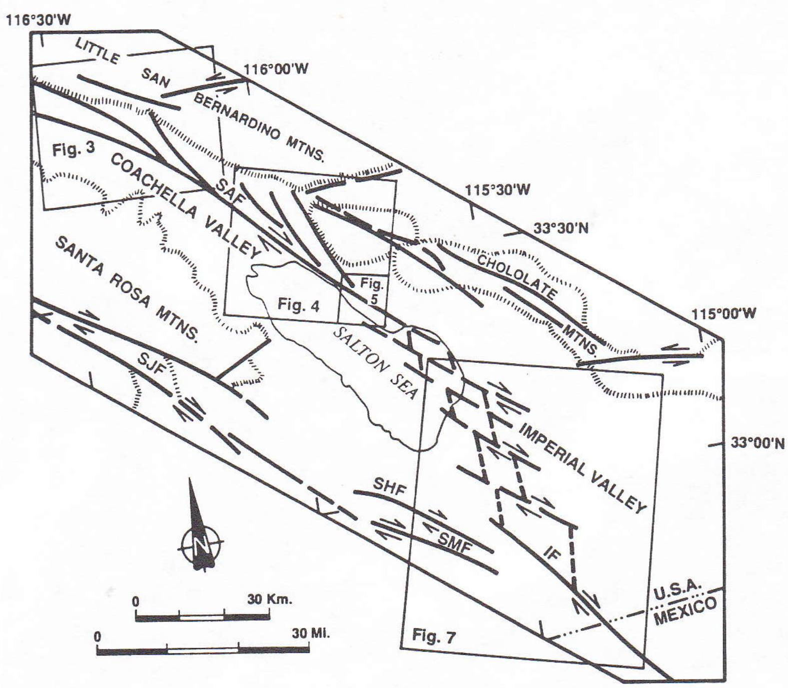

Figure 1. Location map of the Salton trough region of southern California showing the major strike-slip (wrench) fault systems and areas of investigation (Figures 3, 4, 5, and 7). These areas are, from northwest to southeast, the Indio Hills, the Mecca Hills, the Durmid Hills, and the Imperial Valley. **IF**, Imperial fault; **SAF**, San Andreas fault; **SHF**, Superstition Hills fault; **SJF**, San Jacinto fault; **SMF**, Superstition Mountain fault.

The San Andreas wrench-fault system in the Salton trough region is profoundly displayed on remote sensing data (Corona and others, 1993). Examination of this fault system using these data yields diagnostic surface characteristics that define criteria to distinguish a wrench-fault structural assemblage from other structural styles. The following discussion describes the identification criteria of wrench-fault assemblages from remote sensing data utilizing Landsat Thematic Mapper images and high-altitude aerial photographs along this Salton trough segment of the San Andreas fault system.

AREAS OF INVESTIGATION

Four areas along the San Andreas fault system in the Salton trough are selected to show the diagnostic surface characteristics of wrench-fault assemblages as expressed on remote sensing data (see Figure 1). These areas are the Indio, Mecca, and Durmid hills, and the Imperial Valley. The Indio Hills display classic neotectonic wrench-fault morphology, whereas the Mecca Hills reveal a suite of wrench-related structural elements. Wrench-fault transpression dominates the Durmid Hills, and transtension is prevalent in the Imperial Valley. These areas conjointly constitute most of the structural characteristics that typify a wrench-fault structural style. In turn, these structural characteristics provide the criteria for the identification of wrench-fault assemblages from remote sensing or any geologic-map data. The compilation of these criteria are summarized at the end of this discussion.

Indio Hills

The Indio Hills form a low northwest-trending ridge along the northeastern margins of the Coachella Valley and Salton trough (Figure 3). The uplift is 20 miles long, up to four miles wide, and rises to maximum elevations of 1600 to 1700 feet.

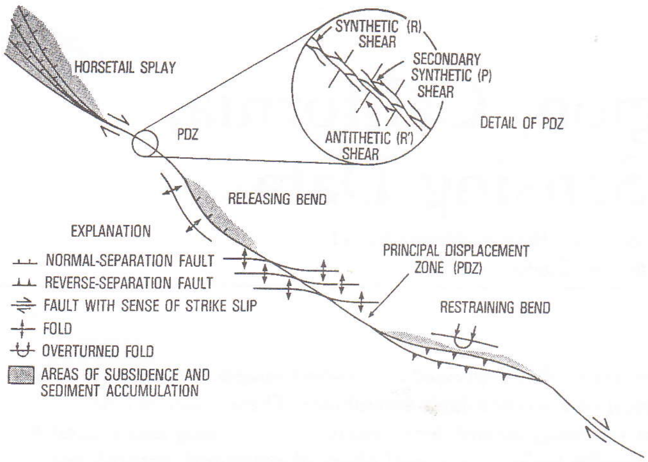

Figure 2. An idealized right-slip wrench fault in map view showing structural elements that are commonly associated with such a wrench-fault system (from Christie-Blick and Biddle, 1985).

An alluvial valley up to two miles wide separates the Indio Hills from the Little San Bernardino Mountains to the northeast, which consist of crystalline bedrock. The Indio Hills are bordered on the southwest by the Coachella Valley that is being developed into housing tracts, resorts, golf courses, and agriculture. The Landsat Thematic Mapper data shown in Figure 3 depict irrigated vegetation and palm trees as a dark signature, exposed rocks as gray tones, and windblown sand with sparse native vegetation (creosote bush, mesquite, tamarisk) as light gray to white.

The generalized stratigraphic section of the Indio Hills consists of Plio-Pleistocene nonmarine clastic strata that were deposited upon a basement of granitic rocks (Cretaceous) and associated crystalline rocks. These rocks are exposed in the Little San Bernardino Mountains and are the source of the granitic and metamorphic detritus in the Neogene strata. The ridge-and-slope topography of the Indio Hills is composed of moderately indurated conglomeratic sandstone and micaceous siltstone of the Pliocene Palm Spring formation (Sabins, 1967). This contrasts with the uniform slopes formed by the equivalent Canebrake Conglomerate and younger Ocotillo Conglomerate (Pleistocene). The Pliocene-age Imperial and Mecca formations that underlie the Palm Spring formation occur in a few small outcrops in the northern and southern portions of the Indio Hills, but are not recognizable on the satellite data.

The northwestern two-thirds of the Indio Hills are cut by the sub-parallel Mission Creek and Banning right-slip faults. These faults merge southeastward as the continuation of the San Andreas fault and form the southwestern boundary of the Indio Hills. To the northwest, one or both of the Banning and Mission Creek faults merge with the San Andreas fault, but the relationship is not clear. The Banning and Mission Creek faults are both active faults with numerous historic earthquakes.

The Mission Creek fault passes through the town of Desert Hot Springs and strikes southeastward through the valley for six miles to the northwestern end of the Indio Hills. For three miles southeast of Desert Hot Springs the northeastern side of the fault is marked by a row of low hills of older alluvium that are truncated on their southwestern flanks by linear fault scarps. These fault-controlled hills are obvious on the Landsat image (see Figure 3). Southeast from the

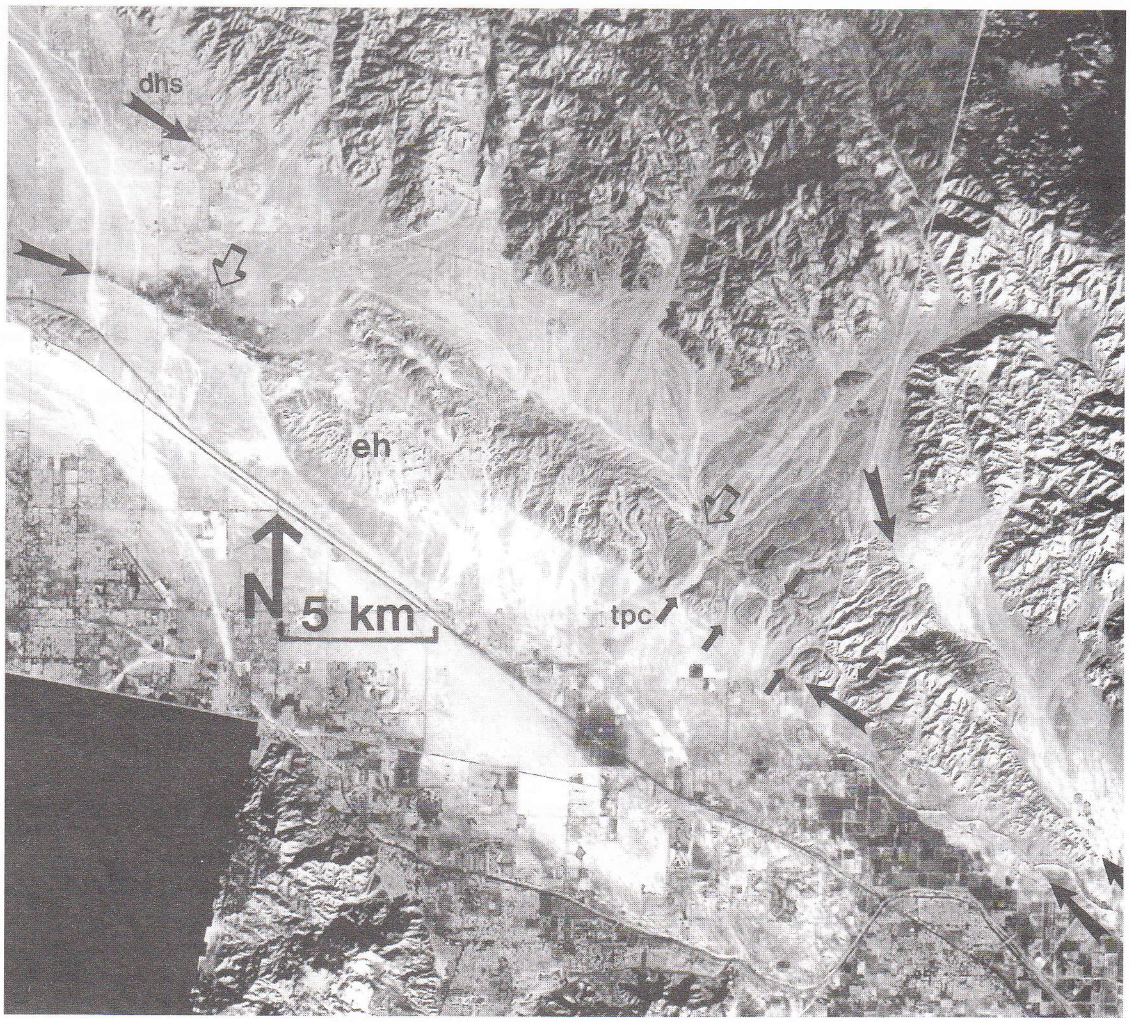

Figure 3. Landsat Thematic Mapper mosaic of the Indio Hills region, California. Large black arrows mark the three major right-slip faults that cut the uplift: from southwest to northeast, Banning, Mission Creek, and Indio faults. Small black arrows depict right-slip offset of canyons along the strike-slip faults, and open arrows point to where the strike-slip faults act as barriers to groundwater flow. **eh**, Edom Hill; **dhs**, Desert Hot Springs; **tpc**, Thousand Palms Canyon. Images were processed at Chevron Oil Field Research Company, La Habra, California.

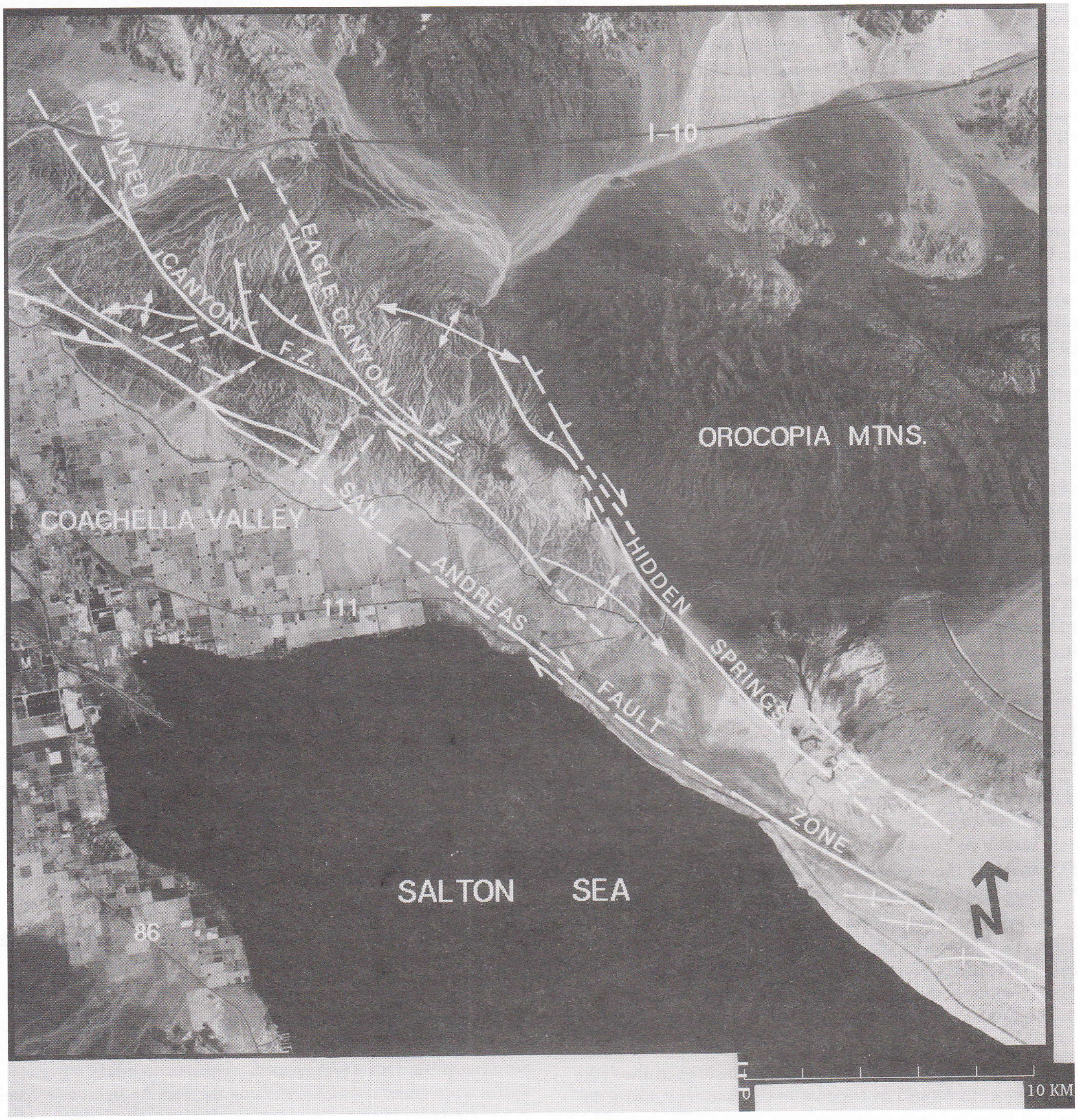

Figure 4. Landsat Thematic Mapper image of the Mecca Hills area, California, showing the major structures associated with the San Andreas fault system. The Mecca Hills lie between the Coachella Valley and Orocopia Mountains. Image was processed at Unocal Remote Sensing Laboratory, Brea, California.

hills, the Mission Creek fault forms the northeastern margin of the Indio Hills. Note that the topographic and corresponding structural relief have shifted along the right-slip fault. Further southeast, the Mission Creek fault crosses Thousand Palms Canyon where it forms a barrier to groundwater that results in springs and the Thousand Palms Oasis on the northeastern side of the fault. The oasis supports a dense grove of native palm trees. Southeast from Thousand Palms Canyon, the Mission Creek fault cuts diagonally through the Indio Hills and offsets the southwest-flowing canyons in a right-lateral sense.

The Banning fault strikes eastward along the northern margin of San Gorgonio Pass and curves southeastward across the northern end of Coachella Valley. The Banning fault separates Edom Hill on the south from the northern portion of the Indio Hills. Southeast from Edom Hill, the fault is the southern margin of the Indio Hills. Again, the structural and associated topographic highs have shifted along the strike-slip fault (see Figure 3). Five miles southeast of Thousand Palms Canyon, the Banning and Mission Creek faults merge and strike southeastward along the Indio Hills as the San Andreas fault.

The trace of the Banning fault is marked by a conspicuous linear tonal anomaly on the Landsat image (see Figure 3). The northeastern side of the fault has an anomalous dark signature with scattered patches of irrigated vegetation and some housing developments. To the southwest, the tone changes abruptly to the light-colored signature that is characteristic of the windblown sand that covers much of the northern Coachella Valley. Housing developments and irrigated vegetation are lacking in this barren region. The remarkably sharp linear contact between these contrasting Landsat signatures extends northwest along the Banning fault for four miles where it is concealed beneath windblown sand. The following explanation for this Landsat anomaly is based on field observations here and at similar anomalies along other faults in the region. In the northern Coachella Valley, the Banning fault is a barrier to the southward flow of groundwater. Along the northeastern side of the fault the water table is shallow which supports phreatophytes such as tamarisk, mesquite, and creosote bushes. This vegetation blocks the eastward migration of windblown sand; therefore, the terrain on the northeast side of the fault is a combination of bare soil and phreatophytes with scattered houses and patches of irrigated vegetation. The spectral properties of this soil regime produce the dark signature that contrasts with the regional light-colored signature of the barren, sand-mantled Coachella Valley.

Along the southeastern margin of the Indio Hills where the Banning fault merges with the Mission Creek fault to form the San Andreas fault, the merged faults cause several groundwater seeps that support small groves of native palms. These palm groves are readily detected on Landsat images at 1:100,000 scale. At the smaller scale of Figure 3, however, these groves are not detectable.

Figure 5. High-altitude aerial photograph of the Durmid Hills structural culmination along the San Andreas right-slip fault (dotted line), California. Deformation associated with this Neogene wrench fault consists of a system of east-trending folds arranged in an *en echelon* pattern and oblique to the San Andreas fault. Figure 6 is a photographic enlargement depicting some of these folds. Note the youthful drainage pattern associated with this uplift and indicative of regional dip. Also note the right-lateral offset of Salt Creek along the San Andreas fault.

The northeastern margin of the southeastern Indio Hills is a northeast-facing, linear scarp framed by the Indio Hills fault. This fault is projected northward into the foothills of the Little San Bernardino Mountains. The Indio Hills fault has a distinctive linear topographic appearance on the Landsat image (see Figure 3).

There are a number a small anticlines and synclines in the Indio Hills that apparently formed in response to displacements along the Banning and Mission Creek right-slip faults. Most of the folds are only a few miles long with steeply dipping limbs that locally are overturned. The folds are most obvious in the well-bedded sandstone and siltstone of the Palm Spring formation. The folds are not recognizable on the images because of their small size and complex erosion patterns.

One recognizable fold is Edom Hill at the northwestern end of the Indio Hills (see Figure 3). The broad, doubly plunging anticline is four miles long and trends northwest, parallel with the Banning fault that cuts the flank of the fold. Edom Hill rises over a thousand feet above the desert floor, with its geomorphology controlled by the anticline. Radial drainage channels are beginning to erode the slopes of the hill which is underlain by poorly stratified Ocotillo Conglomerate. The domal shape, radial drainage, and local flatirons are keys in recognizing the anticline on the Landsat image. Many years ago, Texaco drilled an unsuccessful oil test on the crest of Edom Hill.

Mecca Hills

The Mecca Hills lie between Interstate 10 and Highway 111 in the southeastern part of the Coachella Valley just north of the Salton Sea (Figure 4). This wedge-shaped, northwest-trending topographic welt is a structural culmination along the San Andreas fault system, as are the Indio Hills to the northwest and the Durmid Hills to the southeast (Sylvester, 1988). The Mecca Hills offer one of best localities for viewing the complex folding and faulting that commonly occur along the San Andreas and other wrench-fault systems.

The stratigraphy of the Mecca Hills is similar to that of the Indio Hills with the addition of deeper exposures into the basement complex. Much of the gravel-covered frontal slopes of the Mecca Hills is underlain by poorly lithified, Pleistocene-age Ocotillo Conglomerate which contains schists detritus derived from the Orocopia Mountains to the east. On the southwestern margin of the hills, the conglomerate has been offset about 15 miles northwestward along the San Andreas fault since its deposition (Crowell and Sylvester, 1979). The higher, rugged parts of the Mecca Hills are composed of Plio-Pleistocene Palm Spring formation consisting of light-colored, well-indurated, arkosic sandstone and conglomerate.

These terrestrial sedimentary rocks grade southwestward and basinward into siltstone, and northeastward into alluvial-fan facies of the Canebrake Conglomerate.

In the core of the Mecca Hills, the lower part of the Palm Spring formation is interbedded and underlain by the Late Miocene(?)-Pliocene Mecca formation, a reddish to dark reddish-brown unit of thick-bedded sandstone, claystone, conglomerate, and breccia (Sylvester and Smith, 1976). The detrital material of these rocks is composed chiefly of Mesozoic and Precambrian basement debris. The Mecca formation, in turn, lies nonconformably on a heterogeneous basement complex of Precambrian gneiss, Mesozoic granitic rocks, and mid-Tertiary hypabyssal felsic dikes which, in the subsurface, is in thrust-fault contact over the late Mesozoic(?)-age Orocopia Schist. The young Cenozoic sedimentary section in the Mecca Hills is interrupted by numerous diastems and abrupt facies changes that reflect Pliocene-Pleistocene episodes of folding and faulting along the northeastern rim of the Salton trough.

The Mecca Hills uplift is bounded by the San Andreas fault on the southwest and the Hidden Springs fault on the northeast, and is cut longitudinally by the Painted Canyon and Eagle Canyon faults (see Figure 4). These faults form prominent canyons or valleys in the Mecca Hills or control right-slip offsets along major drainage courses. The more northerly Painted Canyon, Eagle Canyon, and Hidden Springs faults are normal-oblique, right-slip, horsetail-splay structures off the northwest-trending San Andreas fault. This fault-splay system is well expressed on the Landsat image as linear topographic features, and is characterisitic of a wrench-fault zone. The Plio-Pleistocene strata that make up much of the Mecca Hills exhibit complex faulting and folding associated with Neogene wrench-fault deformation. Strike-slip faults, normal oblique-slip and reverse oblique-slip faults, flower structures, inward-verging transpressive structures, and *en echelon* folds and faults are common structural elements within the Mecca Hills uplift. The details of these features are too small to be recognized on the Landsat image; however, major right-slip faults, large anticlinal culminations, and significant subsidiary faults are readily expressed on the remote sensing data.

Durmid Hills

The tectonic regime in the Durmid Hills is dominated by right-slip, wrench-fault transpression associated with the San Andreas fault (Figure 5). In these low hills, a sequence of layered, soft, lacustrine sedimentary rocks are deformed pervasively into a system of east-trending folds that are arranged in a right-stepping, *en echelon* pattern and oblique to the San Andreas fault (Figure 6). These folds are associated with wrench-fault deformation along the San Andreas fault, suggestive to the wrench-fault clay models as presented by Wilcox and others (1973).

The folds in the Durmid Hills are generally noncylindrical with thinned limbs and thickened hinges (i.e., *similar* style of folding; Burgmann, 1991). Their surface expression on the high-altitude aerial photographs consists of pronounced elliptical to elongate-elliptical outcrop patterns (see Figure 6). Wavelengths and amplitudes of the folds range from centimeters to hundreds of meters. As noted above, the folds at the Durmid Hills are arranged in an *en echelon* pattern, oblique to the San Andreas fault (see Figure 6). The mean trend of fold-axial traces is about N74°W, about 27° to the N47°W strike of the adjacent San Andreas fault (Burgmann, 1991). The angle between the fold-axial trace and the strike of the San Andreas fault commonly decreases toward the fault. That is, the folds trend toward parallelism with the San Andreas fault immediate to the fault (see Figure 6).

The present-day uplift of the Durmid Hills is shown by the youthful drainage pattern in the area, peaked by the San Andreas fault (see Figures 5 and 6). The Durmid Hills themselves, rising to a height of about 60 meters (200 feet), are geomorphic evidence for tectonic uplift. A leveling array over the uplift indicates that the Durmid Hills rose relative to the Salton Sea at a rate of about 1 mm/yr from 1985 to 1987 (Sylvester, 1988). The antecedent Salt Creek (see Figure 5) cuts about 40 meters (130 feet) into the uplifted Durmid Hills in the last 25,400 ± 2200 years, giving an uplift rate of about 1 to 2 mm/yr (Burgmann, 1991). Based on the exposed stratigraphy of the Pleistocene Borrego formation in the Durmid Hills, a total uplift of 200 to 1300 meters in 740,000 years (age of Bishop Ash) was estimated (Burgmann, 1991). This corresponds to uplift rates of 0.27 to 1.76 mm/yr over the last 740,000 years.

Right-lateral separation along the San Andreas fault is evident at Salt Creek where it has been offset by about 600 to 800 meters (see Figure 5). Vertical stratigraphic separation across the San Andreas fault has been measured at about 500 to 1120 meters with the northeast side relatively higher than the southwest side of the fault (Babcock, 1974). This vertical separation along the San Andreas fault in the Durmid Hills is associated with transpressive movement of the right-slip, wrench-fault zone.

The San Andreas right-slip fault appears to die at the southern end of the Durmid Hills. At this point, the fault system is believed to jog southwestward across the Imperial Valley to the right-lateral, normal-oblique slip Imperial fault (see Figure 1). The following discussion focuses on this right-stepping fault jog of the San Andreas fault system in the Imperial Valley.

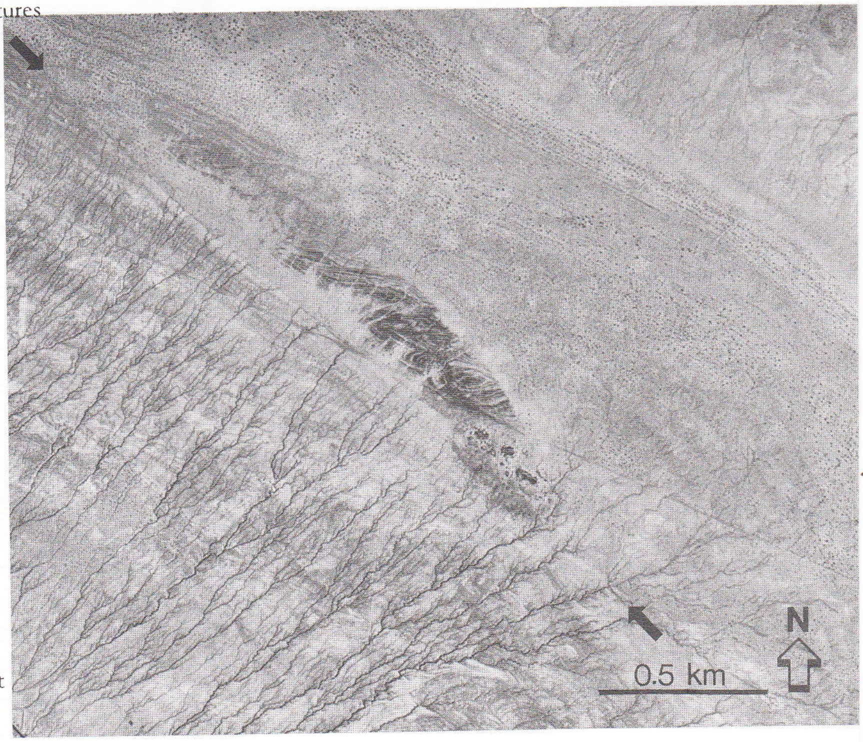

Figure 6. High-altitude aerial photograph of east-trending, right-stepping, *en echelon* folds on the northeast side of the San Andreas fault (arrows) in the Durmid Hills, California (see Figure 5 for location). Note the youthful drainage pattern that defines the recently uplifted, southwestern margin of the San Andreas fault.

Imperial Valley

The Imperial Valley of southern California represents the transition from the San Andreas transform-fault system on the northwest, to the Gulf of California right-transform system on the southeast. Neotectonics in the valley are indicative of right-slip transtension presumably associated with the San Andreas right-lateral, transform, wrench-fault system. The main strand of the San Andreas fault in this region is last exposed in the Durmid Hills along the southeastern margin of the Salton Sea (see Figure 1). From there, the fault system is believed to jog southeastward across the Imperial Valley through a system of northwest-trending, right-slip faults interconnected by transtensional basins (e.g., Hill, 1977; Elders, 1979; Sharp, 1982; Lachenbruch and others, 1985; Sibson, 1987; Lonsdale, 1989; Corona and others, 1991). The presence of active geothermal systems in the Imperial Valley and Salton trough results from the transtensional opening of the valley.

Structures in the Imperial Valley associated with the neotectonic activity along the San Andreas-Imperial fault system are obscured by the major agricultural development in the valley (Figure 7). However, the synoptic character of the Landsat Thematic Mapper data does reveal hints of the underlying structural geology. Linear features defined by straight stream segments and low-relief topographic scarps appear to correspond, in many cases, to known, subtly exposed, surface faults (e.g., Imperial fault), to buried extensions of well-defined surface faults (e.g., Superstition Hills and Superstition Mountain faults), or to postulated subsurface faults.

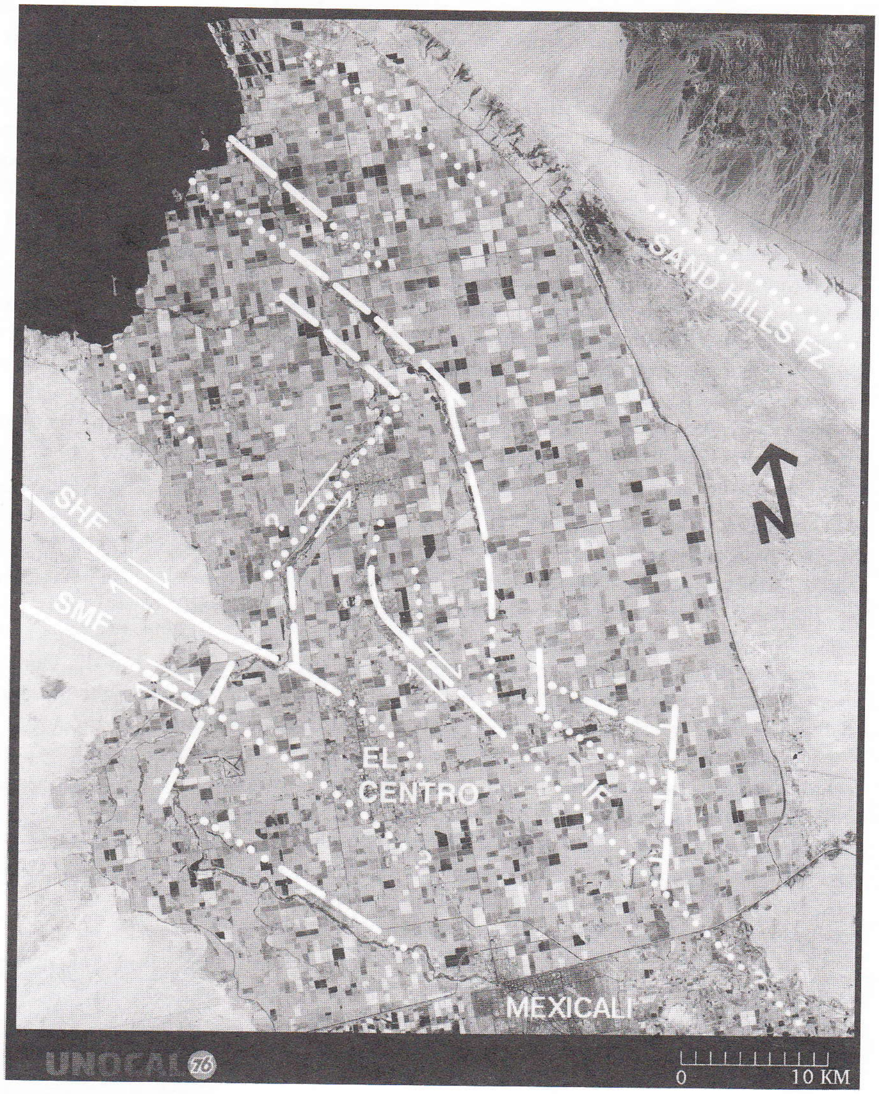

Figure 7. Landsat Thematic Mapper image of the Imperial Valley area, California, with structures and linear features identifiable on the satellite data. Line weight (i.e., solid, dashed, and dotted) correspond to the level of expression of the mapped feature. Note that northwest-trending features are probably right-slip faults, north-striking elements may be extensional in nature, and northeast-trending structures are likely to be left-slip faults. **IF**, Imperial fault; **SHF**, Superstition Hills fault; **SMF**, Superstition Mountain fault.

Three principal trends can be delineated on the satellite image in the Imperial Valley: northwest, north-south, and northeast (see Figure 7). Northwest-trending features are probably related to primary or secondary right-lateral, strike-slip faults; north-striking elements may be extensional or oblique-normal slip in nature; and northeast-trending structures are likely to be subsidiary, conjugate, left-slip faults. Actual slip sense of these features are difficult to determine from the Landsat data; however, field observations and published literature support the implied displacements.

Analysis and interpretation of potential field data in the Imperial Valley concur with a right-stepping, right-slip, fault-jog system (Corona and others, 1991). From these data, the tectonic framework of the Imperial Valley was interpreted to be dominated by northwest-trending, right-stepping, right-lateral strike-slip faults that are connected by a series of basins or basinal blocks and cut in places by northeast-trending left-slip structures. The basins appear to be bounded and segmented by north-trending structures that are oblique to the northwest-trending right-slip faults. These structures may be basin-forming faults or dike-injected fracture zones that are interpreted to be extensional in nature. This structural configuration is compatible with wrench-fault transtension.

SUMMARY AND CONCLUSIONS

In summary, wrench faults and their structural-style assemblage can be identified on remote sensing or surface geologic data with the following criteria:

- The principal fault or displacement zone is long and relatively straight to slightly curved.
- Major strike-slip fault zones commonly occupy valleys.
- Structural relief along major strike-slip faults is inconsistent in that structurally high areas alternate repeatedly across the faults.
- Splay, parallel, and conjugate faults may occur adjacent to or diverge from the principal wrench-fault zone, forming anastomosing or horsetail fault patterns.
- *En echelon* structures may develop on either side of the principal or secondary strike-slip fault zone, forming at an oblique angle to the zone.
- Lateral offset or bending of structural, natural, or man-made features may be visible across the fault.

- Transpression or transtension along a wrench-fault zone may be recognized by the dominance of contractional or extensional structures, respectively.

These criteria define distinguishing surface characteristics of wrench-fault assemblages that differentiate them from other styles of deformation. As shown in this examination, remote sensing data can be used in practical geologic interpretation of structures and structural styles. The approach is to determine the diagnostic geometric characteristics of individual structural elements, and avoid detailed identification and mapping of every linear and curvilinear feature on these data that may or may not be related to geologic structures. The type, orientation, and distribution of these elements are then mapped and analyzed to establish a structural style. With this approach, a better understanding of regional as well as individual structures in both well-mapped and frontier areas can be developed. Remote sensing data can present a complimentary view in regional geologic analysis.

REFERENCES CITED

Babcock, E. A., 1974. Geology of the northeast margin of the Salton trough, Salton Sea, California. Geol. Soc. America Bull., 85:321-332.

Burgmann, R., 1991. Transpression along the southern San Andreas fault, Durmid Hill, California. Tectonics, 10:1152-1163.

Christie-Blick, N., and K.T. Biddle, 1985. Deformation and basin formation along strike-slip faults, *in* K.T. Biddle and N. Christie-Blick, eds., Strike-slip deformation, basin formation, and sedimentation.Soc. Econ. Paleont. Miner., Spec. Publ. 37:1-34.

Corona, F. V., 1993. Recognition of wrench-fault systems, *in* F.V. Corona, F.F. Sabins Jr. and E.G. Frost, fieldtrip leaders, The San Andreas Fault System: Ninth Thematic Conf. Geologic Remote Sensing, Pasadena, California:32-63.

Corona, F. V., S.F. Krupicka, G.T. Ririe and E.A.E. Johnson, 1991. The structural framework of the Imperial Valley area, southeastern California, derived from Landsat and image-enhanced potential field data. San Diego, Geol. Soc. America, Abs. with Programs, 23(5):A91.

Corona, F. V., F.F. Sabins Jr., and E.G. Frost, fieldtrip leaders, 1993. The San Andreas Fault System. Ninth Thematic Conf. Geologic Remote Sensing, Pasadena, California: 210 p.

Crowell, J. C., 1962. Displacement along the San Andreas fault, California. Geol. Soc. America Spec. Paper, 71: 61 p.

Crowell, J. C., and A.G. Sylvester, eds., 1979. Tectonics of the junction between the San Andreas fault system and the Salton trough, southeastern California - a guidebook. Dept. of Geol. Sci., Univ. California Santa Barbara: 193 p.

Dibblee, T. W., Jr., 1977. Strike-slip tectonics of the San Andreas fault and its role in Cenozoic basin evolvement, *in* T.H. Nilsen, ed., Late Mesozoic and Cenozoic sedimentation and tectonics in California. Bakersfield, California, San Joaquin Geol. Soc:26-38.

Elders, W. A., 1979. The geological background of the geothermal fields of the Salton trough, *in* W.A. Elders, ed., Geology and geothermics of the Salton trough. Geol. Soc. America Guidebook, Fieldtrip No. 7:1-19.

Harding, T. P., 1974. Petroleum traps associated with wrench faults. Amer. Assoc. Petrol. Geologists Bull., 58:1290-1304.

___, 1990. Identification of wrench-faults using subsurface structural data: criteria and pitfalls. Amer. Assoc. Petrol. Geologists Bull., 74: 1590-1609.

Harding, T. P., and J.D. Lowell, 1979. Structural styles, their plate-tectonic habitats, and hydrocarbon traps in petroleum provinces. Amer. Assoc. Petrol. Geologists Bull., 63:1016-1058.

Lowell, J. D., 1990. Structural styles in petroleum exploration. Oil & Gas Consultants International Publications, Tulsa, Oklahoma, 3rd printing: 470 p.

Hill, D. P. 1977., A model for earthquake swarms. Jour. Geophys. Res., 82:1347-1352.

Hutton, L. K., L.M. Jones, E. Hauksson and D.D. Given, 1991. Seismotectonics of southern California, *in* D.B. Slemmons, E.R. Engdahl, M.D. Zoback and D.D. Blackwell, eds., Neotectonics of North America. Boulder, Colorado, Geol. Soc. America, Decade Map, 1:133-152.

Lachenbruch, A. H., J.H. Sass and S.P. Galanis Jr., 1985. Heat flow in southernmost California and the origin of the Salton trough. Jour. Geophys. Res., 90:6709-6736.

Lonsdale, P., 1989. Geology and tectonic history of the Gulf of California, *in* E.L. Winterer, D.M. Hussong and R.W. Decker, eds., The Eastern Pacific Ocean and Hawaii. Geol. Soc. America, The Geology of North America, N:499-521.

Reading, H. G., 1980. Characteristics and recognition of strike-slip fault systems, *in* P.F. Ballance, P. F. and H.G. Reading, Sedimentation in oblique-slip mobile zones. Intl. Assoc. Sediment., Spec. Pub, 4:7-26.

Sabins, F. F., 1967. Infrared imagery and geologic aspects. Photogrammetric Engineering, 29:83-87.

Sharp, R. V., 1982. Tectonic setting of the Imperial Valley region, *in* The Imperial Valley, California, earthquake of October 15, 1979. U.S. Geol. Survey Prof. Paper, 1254:5-14.

Sibson, R. H., 1987. Earthquake rupturing as a mineralizing agent in hydrothermal systems. Geology, 15:701-704.

Sylvester, A. G., 1988. Strike-slip faults. Geol. Soc. America Bull., 100:1666-1703.

Sylvester, A. G., and R.R. Smith, 1976. Tectonic transpression and basement-controlled deformation in San Andreas fault zone, Salton trough, California. Amer. Assoc. Petrol. Geologists Bull., 60:2081-2102.

Wilcox, R. E., T.P. Harding and D.R. Seely, 1973. Basic wrench tectonics. Amer. Assoc. Petrol. Geologists Bull., 57:74-96.

The Salton Trough Rift

MICHAEL A. McKIBBEN *Department of Earth Sciences, University of California, Riverside CA 92521*

ABSTRACT

The Salton Trough rift is manifested geomorphically as the Imperial Valley in southern California and the Mexicali Valley in northern Baja California. These valleys are major areas for agriculture, game fish, and waterfowl migration and management. Major nonrenewable resources include metallic minerals (primarily gold) and industrial minerals (primarily gypsum and aggregate). Two of the world's largest liquid-dominated geothermal energy fields are located in the rift: the Salton Sea field in California and the Cerro Prieto field in Mexico. The Salton Trough is an active continental rift, underlain by a fragmented oceanic ridge spreading system into which has been deposited the delta of the Colorado River. Deposition of the delta has significantly influenced the character of mineralization in the rift. The combination of magmatic heat sources, thick porous sediments, tectonic activity, and saline lakes has provided a unique environment for the accumulation and movement of metalliferous hydrothermal brines.

TECTONIC EVOLUTION OF THE GULF OF CALIFORNIA AND SALTON TROUGH

The Salton Trough (Fig. 1) is located within a unique tectonic transition zone between the divergent tectonics of the East Pacific Rise (which dominate the Gulf of California) and the strike-slip tectonics of the San Andreas fault system (which dominate California) (Fig. 2). Presently, Baja California and the portion of California west of the modern San Andreas fault system are part of the Pacific plate, moving northwest relative to the North American plate.

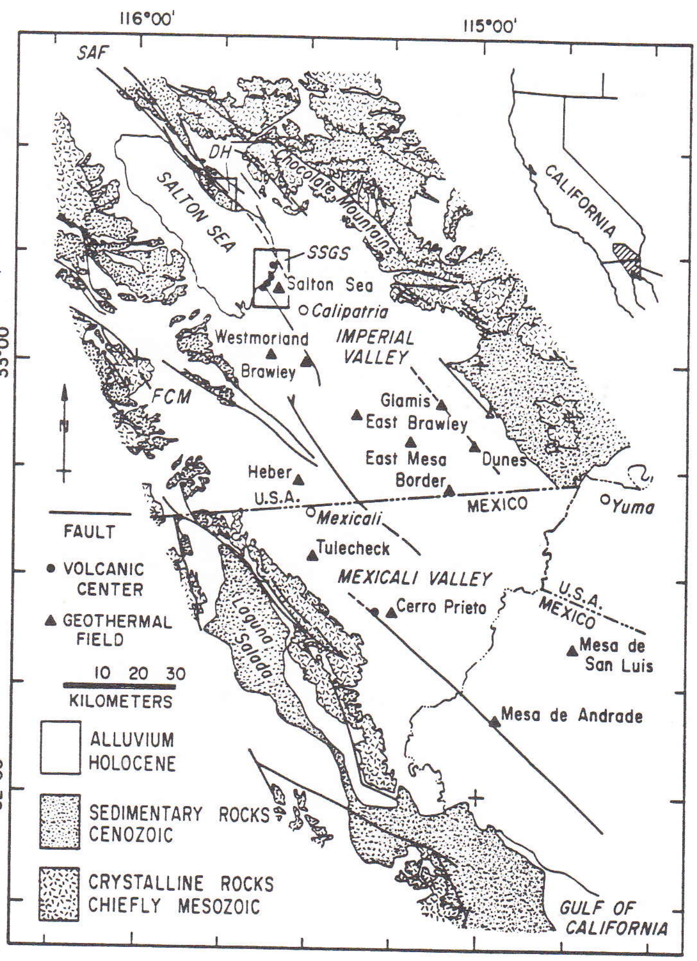

Figure 1. Map of the Salton Trough, showing features discussed in the text. SAF=San Andreas fault, SSGS=Salton Sea Geothermal System, FCM=Fish Creek Mountains, DH=Durmid Hills.

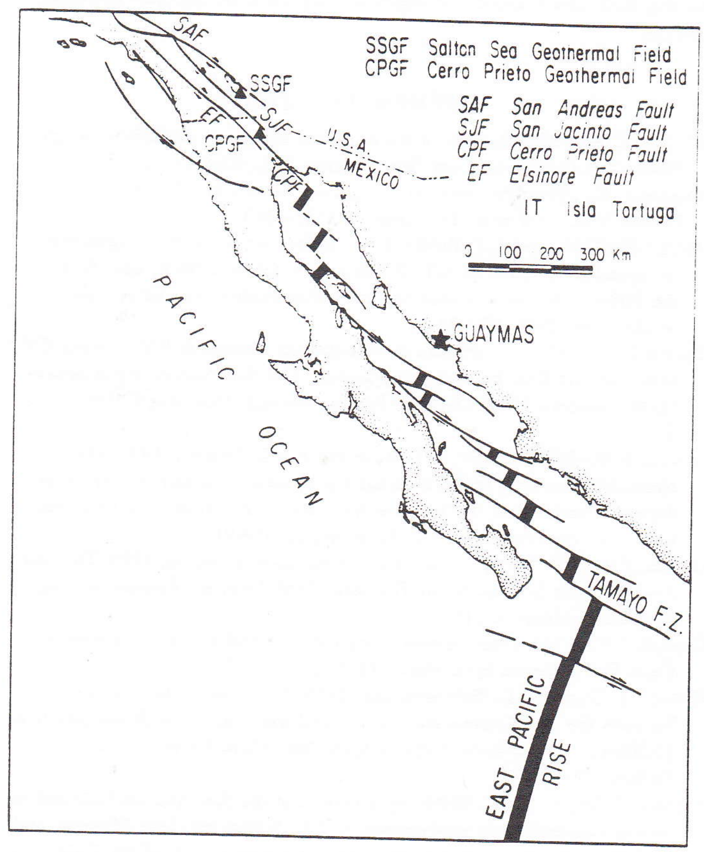

Figure 2. Map showing plate tectonic features of Southern and Baja California.

Comprehensive reviews of the regional Tertiary geologic evolution can be found in Elders and others (1972), Elders (1979), Fuis and others (1982) and Lonsdale (1989). Prior to the end of the Miocene, the area corresponding to the Gulf of California largely consisted of an andesitic volcanic arc overlying the zone of subduction of the Farallon plate under the North American continent. Near the end of the Miocene, the spreading center separating the western Farallon plate from the eastern Pacific plate was obliquely subducted under the North American continent. This resulted in a complex series of tectonic changes that essentially "captured" Baja California and part of southern California, rafting them away from the North American plate (Lonsdale, 1989).

The environment for formation of the modern Gulf of California and Salton Trough was set at about 12 Ma, when subduction ceased and an inland belt of east-west extension, alkali basalt volcanism, and subsidence and basin sedimentation was initiated. Marine evaporites in the Fish Creek Mountains (Fig. 1) and marine sediments in the Yuma Basin may have formed by early incursion of seawater into these proto-Gulf structures. The shear zone comprising the principal tectonic boundary between the Pacific and North American plates appears to have shifted about 250 km inland into this weakened belt by about 6 Ma, and the opening of the modern Gulf of California and Salton Trough began.

Because of the 10-20° angle between the shear zone and the relative motions of the pacific and North American plates, the Gulf of California and Salton Trough are characterized by oblique rifting that is distinct from more typical styles of continental rifting (Lonsdale, 1989). The modern tectonics are dominated by a series of *en echelon* transform faults connecting spreading center fragments (Fig. 2).

It appears that the highest intensity modern hydrothermal systems tend to occur in sediment-filled pull-apart basins (rhombochasms) overlying these spreading center fragments (e.g. Salton Sea, Cerro Prieto, Guaymas Basin) (Fig. 3). These systems exhibit high heat flow, strong gravity and magnetic anomalies, and often have surface manifestations such as Quaternary volcanoes and mud pots.

Lower intensity hydrothermal systems such as Dunes, Heber and East Mesa (figs. 1, 3), and their fossil analogs such as the Modoc

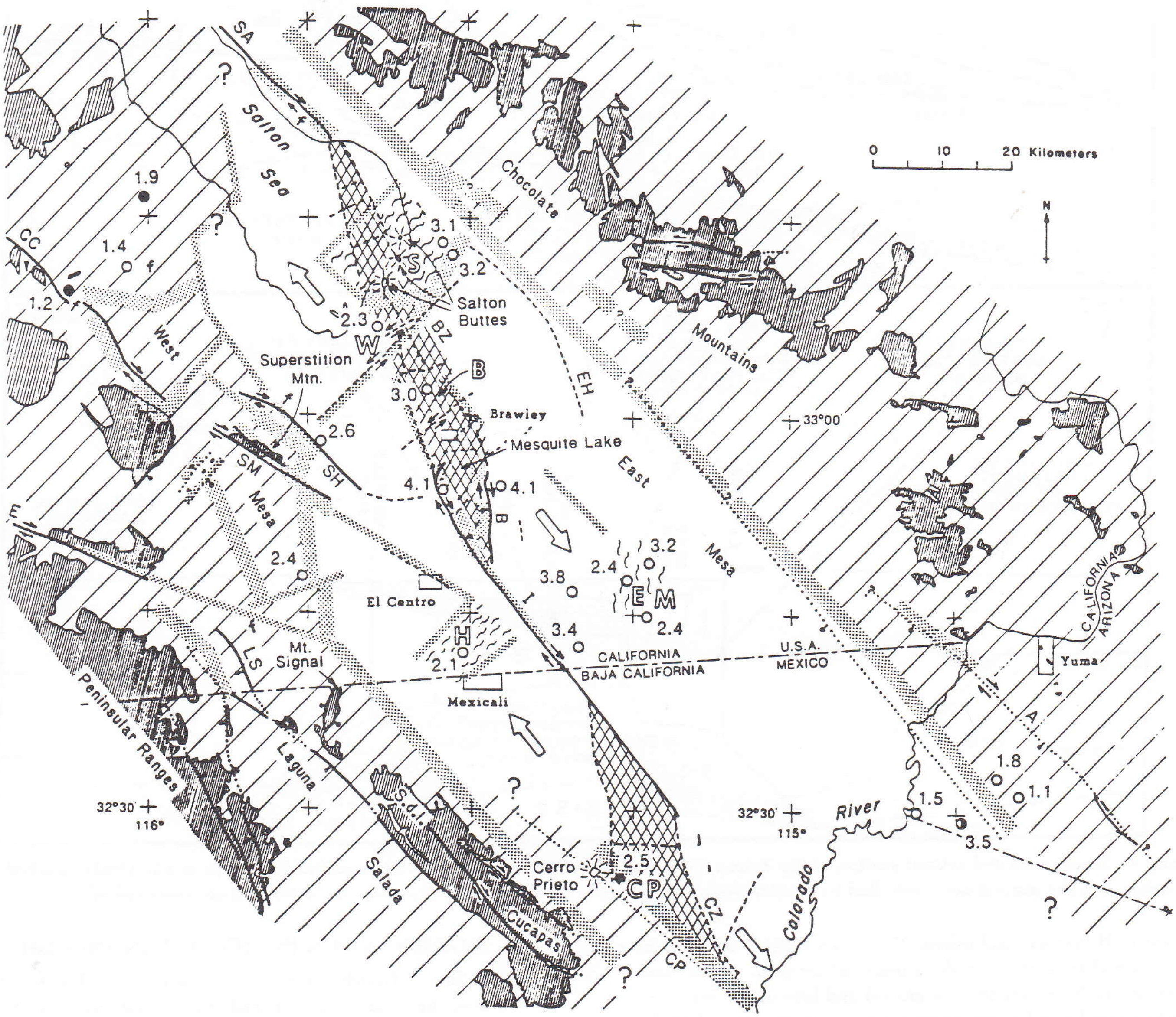

Figure 3. Structure and tectonic summary map of Salton Trough (Figure 6 from Fuis and Kohler, 1984). Circles denote wells with depths in km: open circles penetrated only Cenozoic sedimentary rocks, filled circles penetrated crystalline rocks. Outcrops of pre-Cenozoic crystalline basement are indicated by closely spaced lines; inferred extent of crystalline basement beneath Cenozoic sedimentary rocks is indicated by widely spaced lines. Zones with high (greater than 16%) gradient in depth to basement are indicated by stippled bands of different lengths. "f" refers to areas of Cenozoic folding and/or reverse faulting. Geothermal fields are indicated by block letters:S=Salton Sea, W=Westmorland, B=Brawley, H=Heber, EM=East Mesa, CP=Cerro Prieto. Seismic zones are crosshatched: BZ=Brawley seismic zone, CZ=Cerro Prieto seismic zone. Wavy lines indicate apparent basement shallowing under geothermal fields. Large open arrows indicate direction of spreading in Brawley and Cerro Prieto spreading centers.

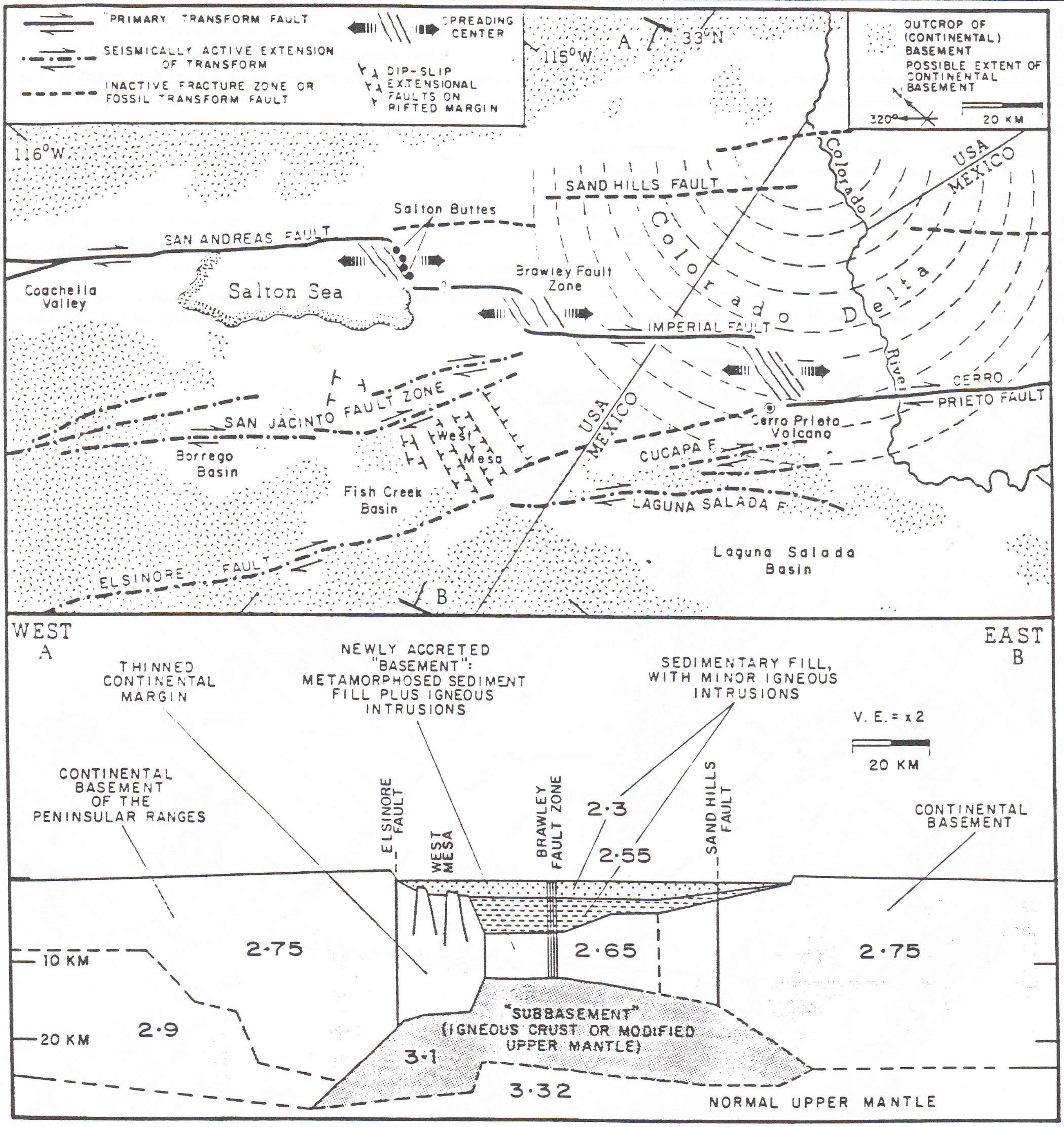

Figure 4. Sketch map and crustal section of the Salton Trough (Fig. 6 from Lonsdale, 1989, modified from Fuis et al., 1982). Dashed boundaries in the section are controlled by gravity modeling only (not by refraction). Numbers are estimated densities (g/cm³).

Prospect (Hillemeyer and others, 1991; Van Buskirk and McKibben, this volume) tend to occur along more rift-marginal normal and strike-slip faults, where shallow ground and lake waters are conductively heated above basement highs. In the case of Modoc, structural control along reactivated portions of an older rhombochasm may have been important. Typically these systems have little surface expression and only moderate geophysical signatures. Some are gold-bearing.

SEDIMENTATION IN THE SALTON TROUGH

As the Salton Trough has opened, it has been filled with sediment derived from the delta of the Colorado River. The river has been building its delta from the east into the trough since about 5 Ma, and sedimentation has apparently kept pace with subsidence. Beginning about 4 Ma the delta had prograded southwestward (transaxially) across the Salton Trough (Fig. 4), so that no marine sediments younger than this are found in the now hydrologically closed northern trough (Winker and Kidwell, 1986). Since then, waters of the Colorado River have alternately flowed north and south through time, resulting in the repeated generation and desiccation of freshwater lakes (collectively termed Lake Cahuilla) in the northern

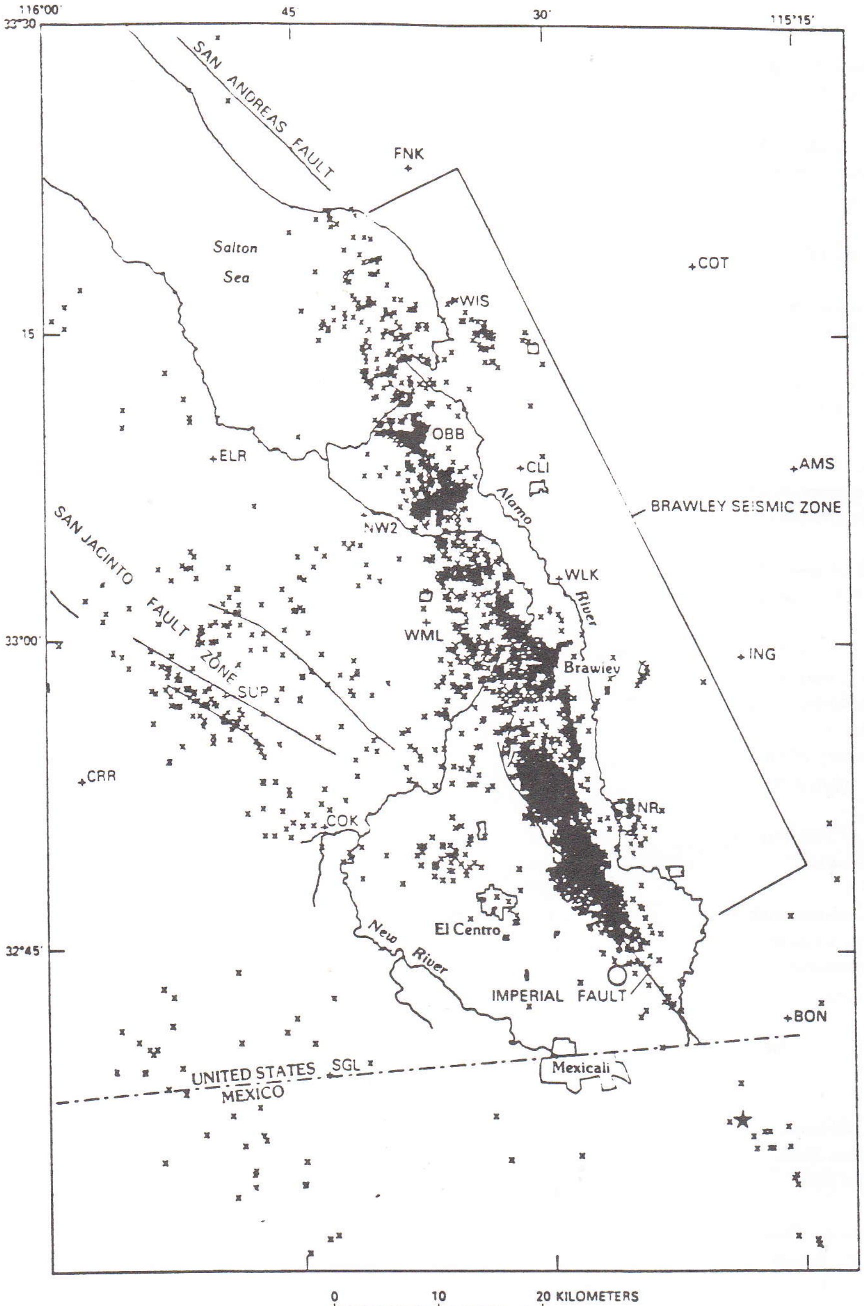

Figure 5. Seismicity of Imperial Valley, from Johnson and Hill (1982, Figure 7). Shown are all epicenters with horizontal location errors less than 2.5 km (A- and B- quality solutions) for interval June 1973 through November 1978. Circle north of Mexicali marks instrumental epicenter of 1940 Imperial Valley earthquake , dot at left edge of 1942 Superstition Mountain earthquake (M_L = 6.5), and star in lower right corner of 1979 Imperial Valley earthquake. Letters refer to station localities in southern California seismic network.

trough. This lacustrine evaporitic environment has dominated Pliocene and Quaternary sedimentation in the northern trough, resulting in the downward percolation and accumulation of saline formation brines ("rift basinal brines") which characterize the Salton Sea and Brawley geothermal systems (McKibben and others, 1988; Osborn and others, 1988; Williams and McKibben, 1989).

Crustal spreading and accompanying subsidence continues in the central part of the trough, where sediments accumulate at rates of 2-3 mm/yr. Along the margins of the trough, equivalents of these young sediments are being uplifted near strike-slip faults. For example, in the Durmid Hills east of the Salton Sea (Fig. 1) (Babcock, 1974), movements along the San Andreas fault have exposed tightly folded but unmetamorphosed Pleistocene lacustrine evaporite sediments. These sediments are laterally equivalent to undeformed metasediments found at depths of 2 km in the Salton Sea geothermal field (Herzig and others, 1988), where they have been metamorphosed into greenschist and amphibolite facies hornfelses. This contrast in the deformation and metamorphism of stratigraphically equivalent sediments reflects the rapid and diverse tectonics of the rift.

DEEP STRUCTURE OF THE TROUGH

Fluvial and lacustrine sediments have been penetrated in the central part of the northern trough by drilling to depths of at least 4 km. Seismic refraction measurements (Fuis and others, 1982) suggest that north of the present delta apex, about 4 km of sediments overlie about 10 km of "basement" crustal rocks, which may consist of metamorphosed post-middle Miocene sediments (Fig. 4). Because sediments may have been densified by hydrothermal metamorphism, however, seismic distinctions between metasediments and mafic intrusions related to the crustal spreading may be difficult. Dikes and sills of MORB-type basalt and diabase are encountered in several geothermal wells at depths of 2-4 km (Elders, 1979; Herzig and Elders, 1988). A high-velocity "subbasement" layer at least 10 km thick lies beneath the 14-15 km of sediments; it may be an igneous crustal layer (Fuis and others, 1982) or altered upper mantle (Nicolas, 1985).

Quaternary rhylitic domes near the Salton Sea contain xenoliths of granitic rocks, but recent Sr isotopic data and U-Pb age dates on zircons indicate ages of less than 100,000 years (Herzig and Jacobs, 1991). These are thus cognate xenoliths related to the rhyolitic domes. There is no evidence for significant amounts of older granitic continental crust underlying the central part of the Salton Trough.

SEISMIC ACTIVITY

Five major earthquakes have occurred in the Salton Trough this century (Fig. 5) (Ellsworth, 1990). The Cerro Prieto fault ruptured in November, 1915 (magnitude 7.1), resulting in a steam eruption at Volcano Lake near the fault's northern terminus. The fault moved again in December, 1934 (magnitude 7.0). In May, 1940, the Imperical Valley earthquake (magnitude 7.1) generated a surface rupture at least 60 km long, showing a peak right-lateral offset of 7 m at the U.S.-Mexico border. This quake resulted in the discovery of the Imperial fault (Fig. 4). In October, 1979 the northern part of this fault moved again (magnitute 6.5) with 30 km of surface rupture and 1 m of strike-slip offset. The Superstition Hills fault moved in November, 1987 (magnitude 6.6), rupturing along its entire length with offset along numerous conjugate faults at its northern terminus. A distinct pattern of shallow (<7 km) microearthquake swarms, probably caused by dike intrusions, can be distinguished from deeper shocks related to regional strike-slip motions (Hill and others, 1990).

REFERENCES CITED

Babcock, E.A., 1974. Geology of the northeast margin of the Salton Trough, Salton Sea, California. Geological Society of America Bulletin, 85:321-332.

Elders, W.A., 1979. The geological background of the geothermal fields of the Salton Trough, *in* Geology and geothermics of the Salton Trough, W.A. Elders, ed. University of California, Riverside, Campus museum contribution, 5:1-19.

Elders, W.A., R.W. Rex, T. Meidav, P.T. Robinson, and S. Biehler, 1972. Crustal spreading in southern California. Science, 178:15-24.

Ellsworth, W.L., 1990. Earthquake history, 1769-1989, *in* The San Andreas fault system, California. U.S. Geological Survey Professional Paper, 1515:153-188.

Fuis, G.S. and others, 1982. Crustal structure of the Imperial Valley region, *in* The Imperial Valley, California earthquake of October 15, 1979. U.S. Geological Survey Professional Paper, 1254:25-49.

Fuis, G.S. and W.M. Kohler, 1984. Crustal structure and tectonics of the Imperial Valley region, California, *in* The Imperial Basin - tectonics, sedimentation and thermal aspects, C.A. Rigsby, ed. Soc. Econ. Paleont. Mineral., Pacific section:1-13.

Herzig, C.T. and W.A. Elders, 1988. Igneous rocks in the State 2-24 research borehole, Salton Sea scientific drilling project, California, U.S.A. Journal of Geophysical Research, 93:13069-13080.

Herzig, C.T. and D.C. Jacobs, 1991. Late Cenozoic basalt magmatism in the Salton Trough: implications for tectonic development, *in* The diversity of mineral and energy resources of southern California, M.A. McKibben (ed). Society of Economic Geologists, Guidebook Series, 12:104-116.

Herzig, C.T., J.M. Mehegan and C.E. Stelting, 1988. Lithostratigraphy of an active pull-apart basin: Salton Sea Scientific Drilling Project. Journal of Geophysical Research, 93:12969-12980.

Hill, D.P., J.P. Eaton and L.M. Jones, 1990. Seismicity, 1980-86, *in* The San Andreas fault system, California. U.S. Geological Survey Professional Paper, 1515:115-152.

Hillemeyer, F.L., M.D. Johnson and R.R. Kern, 1991. Geology, alteration and mineralization of the Modoc hot springs gold prospect, Imperial County, California, *in* The diversity of mineral and energy resources of southern California, M.A. McKibben (ed). Society of Economic Geologists, Guidebook Series, 12:139-156.

Johnson, C.E. and D.P. Hill, 1982. Seismicity in the Imperial Valley, *in* The Imperial Valley, California earthquake of October 15, 1979. U.S. Geological Survey Professional paper, 1254:15-24.

Lonsdale, P., 1989. Geology and tectonic history of the Gulf of California, chp. 26 *in* The Eastern Pacific Ocean and Hawaii, E.L. Winterer, D.M. Hussong and R.W. Decker, eds. Geological Society of America, The Geology of North America, N:499-521.

McKibben, M.A., A.E. Williams, and S. Okubo, 1998. Metamorphosed Plio-Pleistocene vaporites and the origins of hypersaline brines in the Salton Sea geothermal system, California: fluid inclusion Evidence. Geochimica et Cosmochimica Acta, 52:1047-1056.

Nicolas, A., 1985. Novel type of crust produced during continental rifting. Nature, 315:112-115.

Osborn, W.L., M.A. McKibben and A.E. Williams, 1988. Formation, diagenesis and metamorphism of lacustrine sulfacts under high geothermal gradients in an active continental rift zone. Geological Society of America Abstracts with program, 20(7):51.

Williams, A.E. and M.A. McKibben, 1989. A brine interface in the Salton Sea geothermal system, California: fluid geochemical and isotopic characteristics. Geochimica et Cosmochimica Acta, 53:1905-1920.

Winker, C.D. and S.M. Kidwell, 1986. Paleocurrent evidence for lateral displacement of the pliocene Colorado River delta by the San Andreas fault system, southeastern California. Geology, 14:788-791.

THIS ARTICLE AND ACCOMPANYING FIGURES WERE ABSTRACTED FROM *THE DIVERSITY OF MINERAL AND ENERGY RESOURCES OF SOUTHERN CALIFORNIA*, MICHAEL A. MCKIBBEN, ED., © 1991, SOCIETY OF ECONOMIC GEOLOGISTS, GUIDEBOOK SERIES, VOL. 12.

The Modoc Fossil Hot Spring Deposit

M. C. VAN BUSKIRK and M. A. McKIBBEN *Department of Earth Sciences, University of California, Riverside CA 92521*

ABSTRACT

The Modoc deposit is a recently discovered gold-bearing, hot-spring type sinter deposit located in the Salton Trough. The deposit is structurally controlled by a northeast-striking, southeast-dipping fault through which geothermal fluids rose, depositing silica and gold in sheeted veins and sinter. Jurassic crystalline rocks and derived Plio-Pleistocene sediments in the hanging wall of the fault suffered widespread argillic alteration. Fluid inclusion and stable isotope data indicate that geothermal fluids were low-temperature, and possibly mixtures of various non-marine waters in the vicinity at that time.

INTRODUCTION

The Modoc Deposit, a gold-bearing fossil hot spring sinter, is located on the northwestern side of the Salton Trough (Fig. 1). The deposit was initially mapped and named by Dibblee (1954) as the Truckhaven Rhyolite. Later workers, however, recognized the deposit as a fossil hot springs system wherein geothermal fluids, percolating up through the Truckhaven fault zone, deposited silica and gold. In 1988, Fischer-Watt, a gold exploration group, found high gold values at the Modoc deposit and commenced an extensive exploration program.

GEOLOGY

The deposit is structurally controlled by the east-northeast striking, southeasterly dipping oblique-slip Truckhaven fault system which can be traced from near Travertine Rock to the head of Wonderstone Wash. Sediments derived from Jurassic granodiorites were deposited on the downdropped hanging wall of the growth (?) fault and later silicified by geothermal fluids percolating up through and laterally away from the fault. These silicified sediments form what now can be seen from Highway 86 as an extensive, flat-lying sinter. Evidence that the sinter was a surface feature may be seen in the fossilized reeds and filamentous algae that can be found there.

MINERALIZATION

The Truckhaven fault zone was the site of repeated brittle fracturing and multiple stages of mineralization. This episodic activity is indicated today by silicified breccias, crustiform banded and sheeted veins, and stockwork veins consisting of microcrystalline quartz, locally with a few volume percent pyrite, adularia and native gold or electrum. Gold values at the Modoc deposit locally reach grades as high as 1.4 ounces per ton (Hillemeyer and others, 1991). Large, late-stage, cross-cutting veins of hydrothermal carbonate minerals occur throughout the deposit and Travertine Rock itself may be a manifestation of this late-stage carbonate deposition.

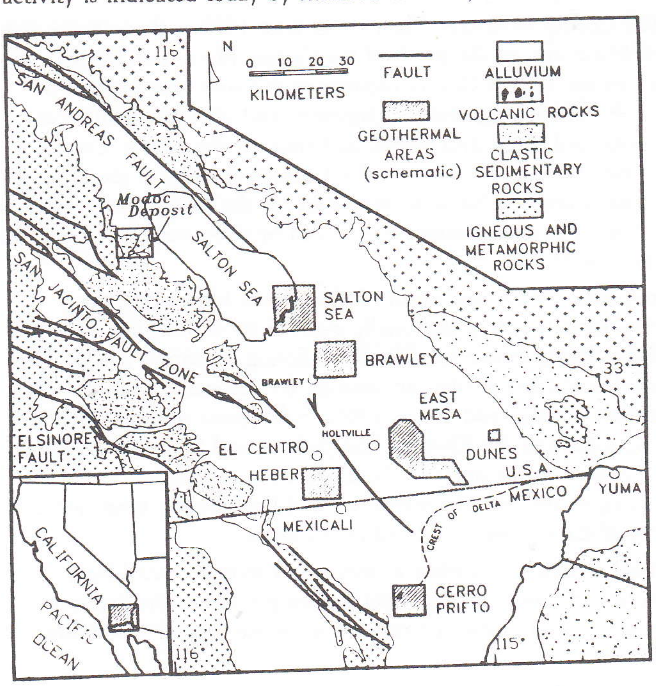

Figure 1. Location of study.

ALTERATION

Hydrothermal activity at the Modoc deposit, probably including boiling in the fault zone and shallow condensation of acidic steam, produced intense alteration which has argillized the conglomerates and sediments derived from Jurassic crystalline rocks in the Santa Rosa Mountains in the hanging wall, destroying all former textures. This widespread alteration is characterized by abundant kaolinite and can be easily seen from Highway 86 as a white, bleached zone.

FLUID INCLUSION AND STABLE ISOTOPE STUDIES

Fluid inclusion data indicate that silica minerals in the veins were deposited at temperatures averaging 160°C. Gold deposition appears to be associated with periods of high fluid discharge and associated shallow boiling. Therefore, among other theories, gold mineralization may have been caused by steepened pressure gradients in a rising fluid column capped by the sinter, lifting the boiling level to very near the surface.

Stable isotope and fluid inclusion data indicate that geothermal fluids were non-marine and may have been mixtures of meteoric water recharge, fossil rivers, or waters from ancient Lake Cahuilla (an intermittent lake that formed whenever the Colorado River broke through its delta to backfill the Salton Trough depression). One of Lake Cahuilla's prominent high water stand lines can be seen today passing under the Modoc deposit.

CONCLUSION

Because the Modoc deposit is a relatively young and well-preserved fossil hot spring sinter, it provides constraints on surface and near-surface paleoenvironments of mineral deposition. The Modoc deposit is important because it encourages exploration for other gold-bearing fossil hot-spring type deposits which may lie in the Salton Trough-Gulf of California rift setting.

REFERENCES CITED

Dibblee, T.W., 1954. Geology of the Imperial Valley region, California, *in* Jahns, R.H., ed., Geology of California. California Division of Mines Bulletin, 170(2):21-28.

Hillemeyer, F.L., Johnson, M.D., Kern, R.R., 1991. Geology, alteration and mineralization of the Modoc Hot Springs Gold Prospect, Imperial County, California, *in* McKibben, Michael A., ed., The diversity of mineral and energy resources of southern California. Society of Economic Geologists Guidebook Series, 12.

Fossil Mammals from the Imperial Formation (upper Miocene-lower Pliocene), Coyote Mountains, Imperial County, California

THOMAS A. DEMÉRÉ *Department of Paleontology, San Diego Natural History Museum, San Diego, CA 92112*

ABSTRACT

New discoveries of fossil mammals from the Latrania Sands of the Imperial formation include fragmentary remains of a camelid, a balaenopterid mysticete, and a sirenian. The only previous report of mammals from the Imperial formation was an odobenid walrus from the Coyote Mountain Clays. The occurrence of walrus, baleen whale, and sea cow in the Imperial formation is evidence of the successful invasion of the late Miocene–early Pliocene proto-Gulf of California by marine mammals.

INTRODUCTION

The Imperial formation of the Salton Trough is well known for its abundant and diverse assemblages of fossil marine invertebrates, most notably corals, molluscs, and echinoderms. Numerous reports have been published on these fossil groups (Kew 1914; Vaughan 1917; Hanna 1926; Stump 1972; Schremp 1981; Kidwell 1988). These reports document the Caribbean affinities of many of the invertebrate taxa; strong evidence for deposition of the Imperial formation prior to formation of the Isthmus of Panama during the Pliocene. Until the isthmus formed, a connection existed between the Caribbean Ocean and the eastern tropical Pacific. Crustal thinning and tectonics associated with passage of a triple-junction plate boundary (Atwater 1970) resulted in formation of a proto-Gulf of California (i.e., pre-rift), which evidently extended from tropical latitudes as far north as present-day Riverside County. The rich fossil invertebrate assemblages of the Imperial formation attest to the high biological diversity of the proto-Gulf.

Up to now, remains of fossil vertebrates were virtually unknown from the Imperial formation, with two exceptions. Hanna (1926) reported the occurrence of a single tooth of the white shark, *Carcharodon carcharius* from Garnet Canyon and Mitchell (1961) described the humerus of a fossil walrus, *Valenictus imperialensis* from Painted Gorge. Both of these occurrences were from deposits of the Imperial formation in the Coyote Mountains of western Imperial County, California. The present report describes additional fossil mammal remains recently collected from the Imperial formation as exposed in the central portion of the Coyote Mountains.

GEOLOGY

The geology of the Imperial formation has been described in several published reports and unpublished theses (Hanna 1926; Woodring 1931; Christensen 1957; Stump 1972; Bell-Countryman 1984). A number of stratigraphic schemes have been proposed, most of which are informal. A majority of workers recognize a lower sandstone and conglomerate unit and an upper claystone and siltstone unit. The name Latrania Sands is typically applied to the lower sandstone and conglomerate unit (Hanna 1926; Stump 1972; Powell 1986; Kidwell 1988), while the terms Burrobend member (Stump 1972; Powell 1986) and Coyote Mountain Clays (Hanna 1926; Bell-Countryman 1984) are most often associated with the upper claystone and siltstone unit. For the purposes of this report the name Coyote Mountain Clays will be used for the upper claystone and siltstone unit. The Latrania Sands are both non-marine and marine in origin, while the Coyote Mountain Clays are considered to be primarily marine.

The Latrania Sands in the Coyote Mountains have a maximum thickness of approximately 150 m (Stump 1972) and are divisible into a basal non-marine sequence of interbedded reddish-brown, cobble and boulder conglomerates (fanglomerates) and poorly sorted coarse-grained sandstones, gradationally overlain by a marine sequence of interbedded gray, well sorted, medium-grained, massive and bioturbated, micaceous sandstones; gray, fine-grained laminated and cross-stratified, micaceous sandstones; and bioclastic sandstones. In the central Coyote Mountains the lower non-marine sequence varies from 0 to 50 m thick and is interpreted to have been deposited as a wedge of coarse clastic debris in alluvial fans along a rugged and embayed coastline (Bell-Countryman 1984). The upper marine sequence ranges up to 60 m thick and was deposited in littoral to subtidal environments (Bell-Countryman 1984).

In the central Coyote Mountains the lower conglomerate and coarse sandstones of the Latrania Sands are often seen to lie directly on metamorphic basement rocks, except where relief on the basement buttress unconformity was sufficient to allow the upper marine sandstone sequence to overstep the conglomerates to lie directly on the basement rocks. Kidwell (1988) provides an excellent description of the composition and origin of the bioclastic sandstones of the Latrania Sands.

The Coyote Mountain Clays are at least 1300 m thick in the Fish Creek Mountains to the north of the Coyote Mountains (Stump 1972). In the central Coyote Mountains this rock unit consists of yellowish, massive, gypsiferous claystones and siltstones with local, well cemented oyster and pecten bioherms. In the central Coyote Mountains the contact between the Latrania Sands and the Coyote Mountain Clays is difficult to determine, as the two units are often in fault contact or their contact is obscured by slope wash or Pleistocene pediment surfaces.

In Carrizo Wash, just north of the Coyote Mountains, the Imperial formation is gradationally overlain by sedimentary rocks of the Palm Spring formation. The Palm Spring formation has yielded diverse assemblages of Blancan through Irvingtonian terrestrial vertebrates (Downs and White 1968). Subsequent transtensional faulting related to the Elsinore, San Jacinto, and San Andreas fault zones resulted in the uplift of the Coyote Mountains and the splintering of the Imperial formation and Palm Spring formation into a series of isolated and deformed fault blocks.

Fossil mammals described in this report were collected from bioclastic sandstones in the upper marine portion of the Latrania Sands as exposed in the central portion of the Coyote Mountains.

GEOLOGIC AGE

The age of the Imperial formation is not well defined and published discussions variously place it in the late Miocene (Powell 1986), and/or early Pliocene (Stump 1972; Ingle 1974; Johnson and others 1983), and/or late Pliocene (Powell 1986). Biostratigraphic correlations are complicated by the occurrence of tropical and subtropical molluscan taxa that are not found in the well-calibrated Neogene marine deposits of coastal southern California. Radiometric dates for the Imperial formation are not available. Johnson and others (1983) offer an age estimate of 4.3 Ma (early Pliocene) for the Imperial formation based upon paleomagnetic correlations. These authors also suggest that marine deposition could have begun as early as 5.5 Ma (late Miocene) in the Salton Trough.

Ingle (1974) reported foraminferal assemblages from the Imperial formation at Fish Creek Wash, north of the Coyote Mountains. He concluded from the fossils that deposition of the preserved section probably began in the early Pliocene (zone N19). Ingle (1974) went on to suggest that considerable section (and time) was probably missing from the base of the formation here, based upon the occurrence of upper bathyal and shelf foraminifers in the basal Imperial formation. This proposed hiatus is supported by Quinn and Cronin (1984:76), who reported that only the "middle" and "upper" members of the Imperial formation occur in the Fish Creek Wash section.

The occurrence of *Carcharodon carcharius* (=*C. arnoldi* and *C. sulcidens*) in the basal marine Latrania Sands as exposed in the central Coyote Mountains (Hanna 1926) has some biostratigraphic significance. This species seems to have had its stratigraphic first appearance in the California Tertiary in latest Miocene time (Hemphillian North American Land Mammal Age equivalent (personal observation).

Powell (1986) correlated the lower portion of the Imperial formation (the Latrania Sands) with the Capistrano formation (upper Miocene - lower Pliocene) and the upper portion of the formation (Coyote Mountain Clays) with the San Diego formation and Niguel formation (upper Pliocene). The Capistrano formation has yielded vertebrate fossils that suggest correlation with the Hemphillian NALMA, latest Miocene. The San Diego formation has yielded vertebrate fossils suggesting correlation with the Blancan NALMA (late Pliocene).

Summarizing these data suggests that the Imperial formation ranges in age from late Miocene (6-7 Ma) to late Pliocene (2-3 Ma).

METHODS

From 1985 to 1988, field crews from the San Diego Natural History Museum conducted reconnaissance geologic mapping and fossil prospecting in the central portion of the Coyote Mountains. This work was supported in part by a grant from the El Centro Office of the Bureau of Land Management. The impetus for this work was the discovery of cetacean fossils in the area by Mr. Andrew Gale and Ms. Pamela Mahon of San Diego. During the field work stratigraphic sections were measured and described and representative collections were made of biostratigraphically significant fossil invertebrate taxa. Remains of fossil vertebrates were also collected in the course of this work. Although these remains are generally fragmentary they offer a preliminary view of the vertebrate fossil assemblage of the Latrania Sands of the Imperial formation.

FOSSILS

Vertebrate fossil remains collected from the Latrania Sands include bones and teeth of sharks, ray, bony fishes, sea turtle, walrus, sea cow, baleen whale, and camel. The present report will focus on the new fossil mammal remains. Also discussed is the holotype of *Valenictus imperialensis* Mitchell (1961), which was collected from the Coyote Mountain Clays as exposed in the western Coyote Mountains.

Order Carnivora
Suborder Pinnipedia
Family Odobenidae
Valenictus imperialensis Mitchell 1961

LACM (CIT) 3926, a nearly complete left humerus. Collected from LACM (CIT) locality 472 (Coyote Mountain Clays; Capote member of Christensen 1957, in Mitchell 1961:4). Features that are unique to the type humerus include its planar posterior shaft outline and its possession of an enlarged entepicondyle that is rounded and knob-like. Features shared with the modern walrus, *Odobenus*, include a greater tuberosity that is thickened and only slightly elevated above the capitulum; a deltopectoral crest that is broad and not developed as a sharply keeled ridge; and a deltoid tubercle located posterior to the deltopectoral crest as a distinct swollen area. Overall the humerus is relatively stocky compared to that of *Odobenus*, and the fossil walruses *Alachtherium* and *Imagotaria*.

Remarks: *Valenictus* is the only pinniped known from the Imperial formation and the only fossil marine mammal reported from the Coyote Mountain Clays. Although the species is based solely on the holotype humerus, the features described above clearly indicate that *Valenictus* was an odobenine walrus more closely related to modern *Odobenus* than to more generalized walruses such as *Imagotaria* or *Neotherium*. Repenning and Tedford (1977) referred a distal humeral fragment from the San Joaquin formation (USNM 13643) to this species, but further study has shown this specimen to be related to a new species of odobenine walrus from the upper Pliocene, San Diego formation (Deméré in prep.). In this paleontological light, *Valenictus* is seen as an endemic pinniped of the proto-Gulf.

Order Artiodactyla
Suborder Tylopoda
Family Camelidae

SDSNH 38345, a complete right scapula. Collected from SDSNH locality 3481 (Latrania Sands, 1.5 m above the base of the marine section). Overall the scapula is broad and triangular in shape, like *Camelops* (Webb 1965) and *Lama* and unlike the narrower scapulae of *Camelus*. The acromion process is missing, but the scapular spine is well preserved and extends distally to the distal portion of the neck of the scapula, near the coracoid process. The coracoid process is large and well preserved and separated from the lateral border of the glenoid cavity. The supraspinatus fossa widens proximally and is approximately one third the size of the large infraspinatus fossa. Distally, the supraspinatus fossa terminates at a point where the anterior border of the scapula joins with the scapular spine to form a continuous planar surface as in *Lama*. The infraspinatus fossa is broad and meets the flattened posterior border of the scapula at nearly right angles. On the medial surface of the scapula, a distinct ridge parallels the posterior border of the blade as in *Lama*. The maximum dorsoventral dimension is 365 mm, the estimated maximum proximal width is 260 mm, and the width of the glenoid cavity is 57 mm.

Remarks: This specimen represents the only terrestrial mammal known from the Latrania Sands. Morphologically, it compares favorably with scapulae of *Camelops* and *Lama*, although it is smaller than *Camelops* and larger than *Lama*. The occurrence of terrestrial vertebrates in marine deposits is rare but not unique. In this case it supports the hypothesis that the Latrania Sands were deposited in shallow marine, inner shelf depths, immediately adjacent to a rugged and embayed coastline (Bell-Countryman 1984; Kidwell 1988).

Order Cetacea
Suborder Mysticete
Family Balaenopteridae

SDSNH 26215, a fragmentary left dentary. Collected from SDSNH locality 3233 (Latrania Sands; approximately 30 m above the base of the marine section). The specimen preserves a 320 mm long section of the ramus just anterior to the mandibular foramen. Posteriorly, nearly the entire dorsoventral dimension (86 mm) of the ramus is preserved. The medial surface is planar, while the lateral surface is broadly concave, with the widest point (51 mm) occurring below the mid-line. The dorsal surface of the ramus is eroded to reveal a large, sandstone-filled, mandibular canal. Exiting from the mandibular canal, on the dorsolateral surface, is a smaller sandstone-filled canal that presumably connected with an external mental foramen. Posteriorly, on the dorsomedial side of the ramus are two sandstone-filled gingival foramina. Although the lateral and medial surfaces of the specimen are etched due to chemical weathering, they seem to lack the fibrous texture characteristic of dentaries of immature individuals.

Remarks: The planoconvex, cross-sectional shape (widest below the mid-line) of the specimen is characteristic of balaenopterid mysticetes (Deméré 1986). The dimensions of the specimen suggest that, when complete, the whole dentary was relatively small, approximately 1 m in length. Assuming a ratio of lower jaw to total body length for balaenopterids of 1:5, this Imperial formation whale was diminutive and only about 5 m in total length. This is probably close to the adult length based upon the apparent maturity of the bone surfaces on the referred dentary. Balaenopterid mysticetes have not been previously reported from Neogene deposits of the proto-Gulf.

Mysticeti indet.

SDSNH 46015, a partial anterior left rib preserving the proximal end and most of the shaft. Collected from SDSNH locality 3233 (Latrania Sands; approximately 30 m above the base of the marine section). The arc of the rib measures approximately 700 mm. The proximal end of the rib consists of the capitulum at the end of a long (100 mm) and slender neck. The tuberculum is missing. The shaft is flattened and broadly curved. At its widest point the shaft is 60 mm wide by only 11 mm thick.

Remarks: The morphology of the proximal end suggests that this is the 3rd, 4th, or 5th rib. Fusion of the capitulum to the neck indicates a mature individual. The size of the rib is compatible with the animal described above for the dentary fragment.

Order Sirenia
Family Dugongidae

SDSNH 46016, a fragmentary rib preserving only portions of the shaft. Collected from SDSNH locality 3762 (Latrania Sands; approximately 40 m above the base of the marine section). The cross-sectional dimensions of the fragments are 49 mm transversely and 67 mm anteroposteriorly.

SDSNH 46017, a fragmentary rib preserving only portions of the shaft. Collected from SDSNH locality 3763 (Latrania Sands; marine section). This specimen is smaller than SDSNH 46016, measuring 45 mm x 60 mm.

Remarks: The dense osteosclerotic interior of these rib fragments is characteristic of sirenian ribs. The dimensions of the rib fragments are greater than those of *Dusisiren jordani* as discussed by Domning (1978) and smaller than those of *Hydrodamalis cuestae* as discussed by Domning and Deméré (1984). This represents the first record of sirenians from the Imperial formation and from the proto-Gulf.

DISCUSSION

Although preservation of the fossil remains described here is fragmentary, the fossils nonetheless offer the first evidence of camel, baleen whale, and sea cow from the Latrania Sands of the Imperial formation. The occurrence of walrus, baleen whale, and sea cow in the area during Imperial formation time is not surprising. After all, similar taxa are known from contemporaneous deposits along the Pacific coast of Baja California and Alta California. What is surprising is the fact that remains have not been reported until now. This suggests the need for further prospecting and collecting of fossils.

As mentioned, the mysticete and sirenian material from the Latrania Sands is associated with richly fossiliferous bioclastic sandstones that contain a diverse assemblage of marine invertebrate taxa. In contrast, the walrus, *Valenictus* is associated with the low diversity oyster and pecten bioherms typical of the Coyote Mountains Clays. Previous authors have suggested that sedimentation rates were relatively low during deposition of the Latrania Sands as compared to the greater rates operating during accumulation of the Coyote Mountain Clays (Bell-Countryman 1984; Kidwell 1988). The effect of this increased turbidity (related to initiation of Colorado River deposition in the Salton Trough) on marine mammal diversity is unclear. Foraminiferal and ostracod assemblages (Ingle 1974; Quinn and Cronin 1984) suggest a shoaling paleobathymetric trend for the Imperial formation. Conceivably, if significantly shallower waters prevailed during deposition of the Coyote Mountain Clays, the range of such purely aquatic forms as the whales and sea cows could have been limited.

ACKNOWLEDGMENTS

Field work was supported through a contract with the Bureau of Land Management (BLM). Pat Welsh of BLM facilitated the contract. Richard Cerutti, Steve Walsh, Andrew Gale, and Pamela Mahon assisted in field reconnaissance and fossil collection.

REFERENCES CITED

Atwater, T. 1970. Implications of plate tectonics for the Cenozoic tectonic evolution of western North America. Geological Society of America Bulletin, 81:3513-3536.

Bell-Countryman, P. 1984. Environments of deposition, Pliocene Imperial formation, southern Coyote Mountains, Imperial County, California, *in* Rigsby, C. A. (ed.), The Imperial Basin-tectonics, sedimentation, and thermal aspects. Society of Economic Paleontologists and Mineralogists, Pacific Section:45-70.

Christensen, A.D. 1957. Part of the geology of the Coyote Mountain area, Imperial County, California. University of California, Los Angeles, Unpublished Master's Thesis: 188 p.

Deméré, T.A., 1986. The fossil whale, *Balaenoptera davidsonii* (Cope, 1872), with a preliminary taxonomic review of Neogene balaenopterids of the world (Cetacea: Mysticeti). Marine Mammal Science, 2:277-298.

Domning, D.P., 1978. Sirenian evolution in the north Pacific Ocean. University of California Publications in Geological Sciences, 118:1-176.

Domning, D.P. and T.A. Deméré, 1984. New material of *Hydrodamalis cuestae* (Mammalia: Dugongidae) from the Miocene and Pliocene of San Diego

County, California. San Diego Society of Natural History Transactions, 20(12):169-188. (with D.P. Domning)

Downs, T. and J.A. White, 1968. A vertebrate faunal succession in superposed sediments from late Pliocene to middle Pleistocene in California. XXIII International Geological Congress, 10:41-47.

Hanna, G.D., 1926. Paleontology of Coyote Mountains, Imperial County, California. California Academy of Sciences Proceedings, 4(14):51-186.

Ingle, J.C., Jr., 1974. Paleobathymetric history of Neogene marine sediments, northern Gulf of California, *in* G. Gastil and J.A. Lillegraven (eds.), Geology of Peninsular California. Pacific Section, American Association of Petroleum Geologists, 49th Annual Meeting:121-138.

Johnson, N.M., N.D. Opdyke, G.D. Woodard, P.K. Zeitler, E.H. Lindsay, 1983. Rates of late Cenozoic tectonism in the Vallecitos-Fish Creek basin, western Imperial Valley, California. Geology, 11:664-667.

Kew, W.S.W., 1914. Tertiary echinoids of the Carrizo Creek region in the Colorado Desert. University of California Publications in Geological Sciences Bulletin, 8:39-60.

___, 1920. Cretaceous and Cenozoic Echinoidea of the Pacific Coast of North America. University of California Publications in Geological Sciences Bulletin, 12:23-236.

Kidwell, S.M. 1988. Taphonomic comparison of passive and active continental margins: Neogene shell beds of the Atlantic Coastal Plain and northern Gulf of California. Palaeogeography, Palaeoclimatology, Palaeoecology, 63:201-223.

Mitchell, E.D. Jr., 1961. A new walrus from the Imperial Pliocene of southern California: with notes on odobenid and otariid humeri. Los Angeles County Museum Contributions in Science, 44:1-28.

Powell, C.L., 1986. Stratigraphy and bivalve molluscan paleontology of the Neogene Imperial formation in Riverside County, California. San Jose State University, Unpublished Master's Thesis: 324 p.

Quinn, H.A. and T.M. Cronin, 1984. Micropaleontology and depositional environments of the Imperial and Palm Spring formations, Imperial County, California, *in* C.A. Rigsby (ed.), The Imperial Basin-tectonics, sedimentation, and thermal aspects, Society of Economic Paleontologists and Mineralogists, Pacific Section:71-85.

Repenning, C.A. and R.H. Tedford, 1977. Otarioid seals of the Neogene. U. S. Geological Society Professional Paper, 992:1-93.

Schremp, L.A., 1981. Archaeogastropoda from the Pliocene Imperial formation of California. Journal of Paleontology, 55:1123-1136.

Stump, T.E., 1975. Stratigraphy and paleontology of the Imperial formation in the western Colorado Desert. San Diego State University, Unpublished Master's thesis: 128 p.

Vaughan, T.W., 1917. The reef-coral fauna of Carrizo Creek, Imperial County, and its significance. United States Geological Survey Professional Paper, 98:355-386.

Webb, S. D., 1965. The osteology of *Camelops*. Bulletin of the Los Angeles County Museum, 1:1-54.

Woodring, W.P., 1931. Distribution and age of the Tertiary deposits of the Colorado Desert. Carnegie Institute of Washington Publication, 418:1-25.

Biostratigraphy and Magnetostratigraphy in the Southern Anza-Borrego Area

EVERETT H. LINDSAY and JOHN S. WHITE, *Department of Geosciences, University of Arizona, Tucson AZ 85721*

Geology of the Imperial Valley and surrounding area was mapped by T. Dibblee (1954). Dibblee mapped the light gray, poorly indurated silts and sands exposed in badlands and roadcuts to the north and west of the Salton Sea as the Palm Spring formation. Dibblee mapped the finer grained, poorly bedded sediments (that attain a thickness of about 2,000 m in the Borrego Badlands) as the Borrego formation, considering the Borrego formation a lacustrine facies of the more deltaic and fluvial Palm Spring formation. Later geologic studies in the Borrego Badlands were undertaken by Dick Merriam and students from USC, during the 1960's. Paul Remeika, a park ranger with training in geology at Anza-Borrego State Park has been mapping and studying the sediments in the Borrego Badlands since the early 1980s.

The Carrizo Badlands, south of the Pinyon-Vallecito Mountains and Fish Creek Mountains (about 16-20 miles south of Highway S22), has been the object of intensive paleontologic investigation for many of the last 30-40 years. Fossils from that area were brought to the attention of Ted Downs at the Los Angeles County Museum by Harley Garbani in 1952. Downs, Garbani, G. D. Woodard and John White collected from these deposits during the latter 1950's, through the 1960's and into the 1970's; Downs and White described the faunal sequence (Layer Cake, Arroyo Seco and Vallecito Creek faunas) in 1968. The work was continued in the late 1970's and 1980's by the late George Miller, formerly at the Los Angeles County Museum, and students from the Imperial Valley College at El Centro. Miller and colleagues at Borrego Springs were active in establishing the Anza-Borrego State Park Visitor Center in Borrego Springs where modern and fossil biota of the area are displayed. The vertebrate fossil collection assembled by Miller and colleagues from the Borrego Badlands and the Carrizo Badlands, housed at the Imperial Valley College Museum, were transferred in 1992 to Anza-Borrego Park Headquarters at Borrego Springs.

Fossil mammals from Coyote Creek Canyon, north of Borrego Springs, were brought to the attention of R.A. Stirton at UC Berkeley about 50 years ago. Stirton identified a hyaenoid dog in this sample and assigned the sample to Blancan land mammal age, based on stage of evolution of the dog. Later collections were made from Coyote Creek Canyon by Ted Downs of the Los Angeles County Museum and by George Miller and associates from Borrego Springs and Imperial Valley College. To our knowledge, all of the fossils from Coyote Creek Canyon are consistent with assignment to Blancan land mammal age, and the sediments should be equivalent, more or less, to those in the Borrego Badlands and the Carrizo Badlands.

Sediments that produced vertebrate fossils in the Carrizo Badlands and the Borrego Badlands, east of Borrego Springs, were named the Palm Spring formation by Woodring (1932). These deposits are underlain by and intertongue with the marine Imperial formation of Woodring (1932); they also intertongue with the Canebrake Conglomerate of Dibblee (1954) on the western side of the Carrizo Badlands. The Palm Spring formation is about 4100 m thick in the Carrizo Badlands and spans about 3 million years (about 1 Ma to 4 Ma); it is one of the thickest and most complete late Cenozoic terrestrial sedimentary sequences known in North America. As currently understood, the Palm Spring formation represents the early delta of the Colorado River (Johnson et al., 1983); details relating to detachment of the Baja peninsula, formation of the Gulf of California, tectonism, rotation and subsidence of the Salton Trough, along with shifts in rate of sediment accumulation are still equivocal. This area was tectonically active for at least 4 million years, and it continues to be tectonically active. All of which helps to expose more fossils, and renders correlation between fault blocks hazardous.

BIOSTRATIGRAPHY AND MAGNETOSTRATIGRAPHY

The problem of ordering fossil sites in the thick and well exposed Carrizo Badlands was solved by Ted Downs who plotted 210 stratigraphic levels (approximately 15 m in thickness) through the most fossiliferous part of the sequence, tied to distinctive topographic markers. Fossil sites could be traced along strike to the intersection with strata in the numbered sequence of Downs, and thereby placed into the biostratigraphic framework. Downs and White (1968) ordered 450 sites, placing over 5000 specimens in a biostratigraphic framework that allowed them to define three stratigraphically superposed local faunas: (in ascending order) the Layer Cake, Arroyo Seco, and Vallecito Creek local faunas. Layer Cake and Arroyo Seco faunas are correlated with Blancan land mammal age; Vallecito Creek fauna is correlated with Irvingtonian land mammal age.

Opdyke and others (1977) sampled the Palm Spring formation and upper part of the Imperial formation for paleomagnetism, using the biostratigraphic framework of Downs and White for stratigraphic control. They placed 150 paleomagnetic sites in the 4,000 m Carrizo Badland sequence to identify 12 magnetozones, and then correlated the magnetic sequence with the magnetic polarity time scale. The polarity sequence established by Opdyke and colleagues spans the upper Gilbert, the Gauss and the lower Matuyama magnetic chrons. Based on their correlations, the Palm Spring/Imperial contact is approximately below and adjacent to the Cochiti subchron in the Gilbert magnetic chron (4.0±Ma), the Layer Cake/Arroyo Seco boundary is approximately at the Gauss/Gilbert chron contact (3.4 Ma), and the Arroyo Seco/Vallecito Creek boundary is in the upper part of the Gauss magnetic chron (>2.5 Ma). The uppermost normal magnetozone is poorly defined; it could represent the Brunhes magnetic chron (ca. 0.73 Ma) or the Jaramillo subchron (ca. 0.9 Ma) in the Matuyama magnetic chron. Opdyke and colleagues also sampled the Borrego Badlands for paleomagnetism in hope of correlating sediments in the Borrego Badland and Carrizo Badland areas; unfortunately, they were unable to find a section in the Carrizo Badland area that was sufficiently long to permit the correlation. The Carrizo Badland area is intensely faulted and correlation between fault blocks was a greater problem than identification of remnant magnetic polarity.

Johnson and others (1983) resampled the stratigraphic sequence and extended it downward. They also dated a volcanic ash (2.3 ± 0.4 Ma) just below the top of the Gauss magnetic chron, which strengthened the correlations of Opdyke et al. (1977).

REFERENCES CITED

Dibblee, T.W., Jr., 1954. Geology of the Imperial Valley Region, California. California Division of Mines Bulletin, 170(II):21-28.

Downs, T. and J.A. White, 1968. A vertebrate faunal succession in superposed sediments from late Pliocene to middle Pleistocene in California. Proc. XXIII Int. Geological Congress, 10:41-47.

Johnson, N.M., C.B. Officer, N.D. Opdyke, G.D. Woodard, P.K. Zeitler, P.K. and E.H. Lindsay, 1983. Rates of late Cenozoic tectonism in the Vallecito-Fish Creek basin, western Imperial Valley, California. Geology, 11:664-667.

Opdyke, N.D., E.H. Lindsay, N.M. Johnson and T. Downs, 1977. The paleomagnetism and magnetic polarity stratigraphy of the mammal-bearing section of Anza-Borrego State Park, California. Quaternary Research, 7:316-329.

Late Pliocene and Pleistocene Cotton Rats in the Southwestern United States

ROBERT A. MARTIN *Department of Biology, Berry College, Mt. Berry, GA 30149*

Cotton rats of the genus *Sigmodon* are common runway-making, grassland grazing herbivores. Modern representatives of the species range in size from an average of about 58 g (*S. mascotenis*) to over 100 g (*S. peruanus*). They are found today mostly in oldfields and prairies, although in Mexico they are known to inhabit marginal habitats, such as lava fields, when more than one species is present. Like arvicolids and pocket gophers, they appear to be highly aggressive, and cotton rats are reputed to attack and kill other rodents in their environment.

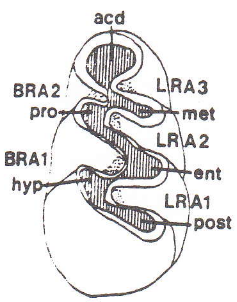

Fig. 1. Topography of a *Sigmodon hispidus* left first lower molar. BRA=buccal reentrant angle, LRA=lingual reentrant angle, acd=anteroconid, pro=protoconid, met=metaconid, hyp=hypoconid, ent=entoconid, post=posterior cingulum.

There is a marginal record of a modern species, *Sigmodon arizonae*, from a high elevation area at Needles, California: otherwise cotton rats are absent from the state. In times past, though, cotton rats were common in southern California, as their presence in the Vallecito-Fish Creek beds of the Anza-Borrego Desert attest.

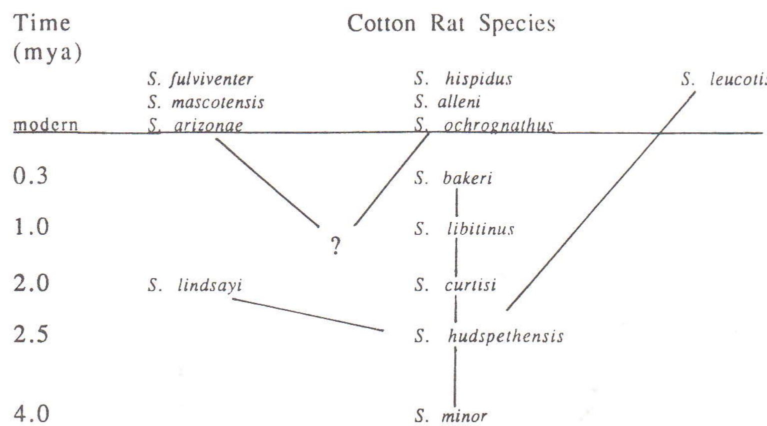

Fig. 3. Possible evolutionary scenario for the genus *Signodon*. Names of extinct species represent approximate first appearances, not full geological ranges (e.g., *S. minor* and *S. curtisi* coexisted during part of the late Blancan in southern Arizona; Curtis Ranch l.f., ca 1.88 mya).

These superposed beds document a considerable history of *Sigmodon* in southern California. *Sigmodon minor* (=*S. medius*) is a small species (ave. mass approx. 50 g in California) that ranged through the late Pliocene Layer Cake and Arroyo Seco faunal levels. A larger species, *S. lindsayi* (ave. mass approx. 77 g), apears in the early Pleistocene Vallecito Creek faunal zone (Martin and Prince, 1989). Illustrations of the dentitions of these species are provided in Figs. 1 and 2, with a brief list of distinguishing features. Although there is no record of both *S. minor* and *S. lindsayi* from the same stratigraphic level, this may be an artefact of sampling, and it is likely that both shared the same habitats in southern California for at least a brief period. I say brief because evidence suggests that cotton rat species are highly intolerant of one another, and small cotton rat species especially do not seem to have fared well over the long term.

Sigmodon minor or a related species apparently gave rise to a more advanced group of larger species including in North America the extinct *S. curtisi*, *S. libitinus*, *S. hudspethensis*, *S. lindsayi* and the extant *S. leucotis*. These species all possess three or occasionally four roots on the first lower molar (M_1) and a suite of other dental features. They were apparently mostly replaced in North through Central America by another cotton rat radiation, beginning probably during the late middle Pleistocene, of large species characterized by four well-developed roots on M_1. A modern member of this radiation, *S. arizonae*, seems to be hanging on in grassy swales along streams in the southern Arizona deserts and, as noted above, is the only

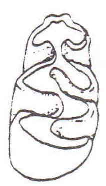

S. lindsayi
Acd M_1 extended labially & lingually
mcd on M_1 often bulbous
prd on M_1 often triangular
LRA2 on M_1 deep and anteriorly directed
M_1 with 3 or 4 roots
Mean length M_1 = 2.36 mm (2.15-2.74)

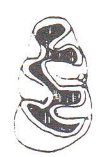

S. minor medius
Acd M_1 not extended labially or lingually
M_1 with 2, occasionally 3 (poorly developed), roots
Mean length M_1= 2.12 mm (2.03-2.24)

S. hispidus
Acd M_1 not extended labially or lingually
M_1 with 4 well-developed roots
Mean length M_1 = 2.44 mm (2.11-2.73)

S. mascotensis
Acd M_1 slightly extended labially
M_1 with 4 well-developed roots
Mean length M_1= 2.22 (2.18-2.25)

Fig. 2. Lower molars of four cotton rat species known as fossils from the Vallecito-Fish Creek beds or related to these species. The dentition of *S. arizonae* is not currently separable from *S. hispidus* with certainty (see Martin, 1979).

cotton rat that today reaches California. However, there is no clear tie of this species to any of the extinct taxa from southern California. Instead, the dentition of *S. lindsayi* shows some similarity to that of the living Jaliscan cotton rat, *S. mascotensis*, from southwestern Mexico. A possible phylogeny for the cotton rats is presented in Figure 3.

LITERATURE CITED

Martin, R.A., 1979. Fossil history of the rodent genus *Sigmodon*. Evolutionary Monographs, 2:1-36.

___, 1986. Energy, ecology and cotton rat evolution. Paleobiology, 12:370-382.

Martin, R.A. and R.H. Prince, 1989. A new species of early Pleistocene cotton rat from the Anza-Borrego Desert of southern California. Bull. Southern California Acad. Sci., 88:80-87.

The Borrego Local Fauna: Revised Basin-Margin Stratigraphy and Paleontology of the Western Borrego Badlands, Anza-Borrego Desert State Park, California

PAUL REMEIKA and GEORGE T. JEFFERSON *Anza-Borrego Desert State Park, Borrego Springs, CA 92004*

INTRODUCTION

The Borrego Local Fauna (BLF) (Remeika, 1992) is a diverse assemblage of primarily large terrestrial vertebrates recovered from the fluvial-floodplain syndepositional sedimentary sequence throughout the mid-Pleistocene Ocotillo formation (OF) (Remeika and Pettinga, 1991). Vertebrate-bearing strata (Table 1) exposed throughout the western-most half of the Borrego Badlands (BB) along the northwestern basin margin of the Borrego-San Felipe Basin (BSFB of Reynolds and Remeika, this volume) measures 377 m in thickness. Based on recent geologic mapping, the stratotype for the BLF has been located in the Arroyo Otro-Mammoth Cove sedimentary section, above and below the Ocotillo Rim and north of the left-lateral Inspiration Point fault (Remeika 1992, see Reynolds and Remeika, this volume). The BLF presently includes over 5 k specimens that represent 49 vertebrate taxa (Table 1). Within the region, the BLF most closely compares taxonomically with a similar age fauna recovered from the Coyote Badlands of the BSFB and Pauba formation, Riverside County (Reynolds and Reynolds, 1990; Reynolds and others, 1991) in the Murrieta area 90 km northwest of the BB.

Under the direction of C. Frick of the American Museum of Natural History (AMNH), G. Hazen first discovered vertebrate fossils in the BB in 1935. Field studies initiated in the 1970's by T. Downs and H. Garbani of the Natural History Museum of Los Angeles County (LACM), and continued during the late 1970's and 1980's by G. Miller of the Imperial Valley College Museum, and in the 1990's by P. Remeika, Anza-Borrego Desert State Park (ABDSP), have led to periodic recovery of significant vertebrate remains. Assemblages representing the BLF are presently housed in the AMNH, LACM, and in the Vertebrate Paleontology Collection of ABDSP.

GEOLOGIC SETTING

Fossiliferous basinal sediments of the OF exposed in the BB lie along the western-most edge of BSFB within the active seismogenic San Jacinto fault zone. These deposits record Neogene basin-margin deposition in response to a fault-induced subsiding structural trough situated between two parallel mountain ranges: the Santa Rosa Mountains to the northeast and Coyote Mountain to the northwest. Quaternary deformation has been dominated by NW-SE right-lateral strike-slip motion on the Clark and Coyote Creek faults and by NE-SW left-lateral cross-faults that display significant crustal shortening and rotation orthogonal to the main faults. Block rotation behavior has been discussed by Scheuing and others (1988) and Nicholson and Seeber (1989). Trends of *en echelon* fold axes imply progressive deformation of the sedimentary package by a complex basement-cover *decollement* (Pettinga, 1991).

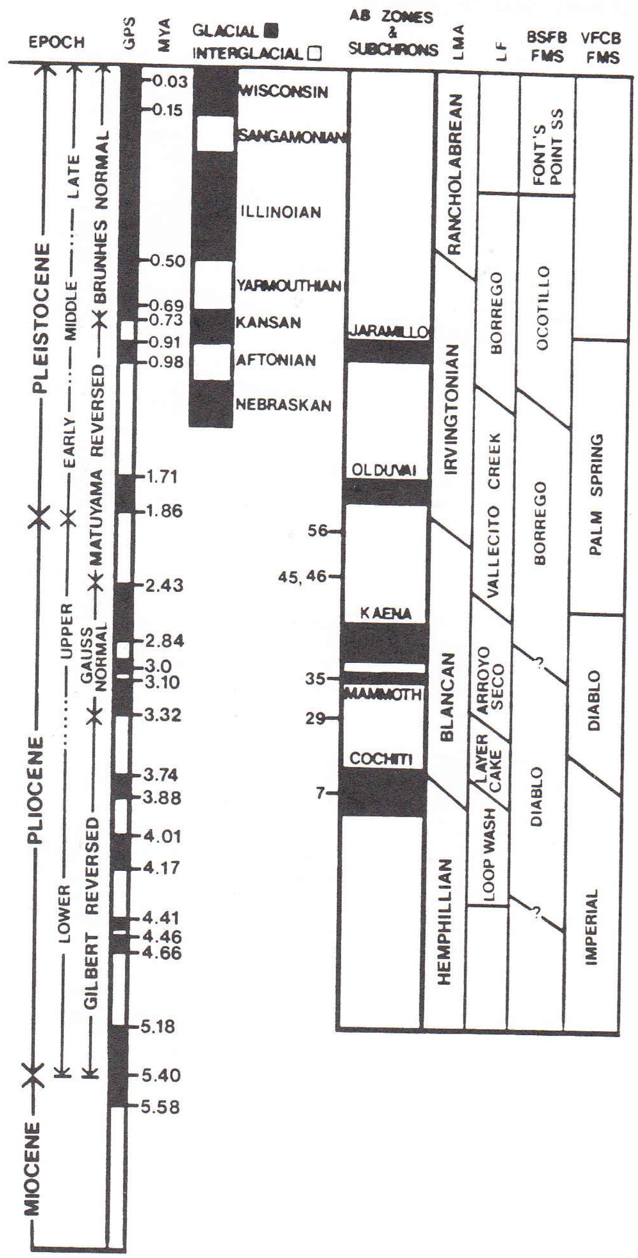

Figure 1. Diagrammatic magnetostratigraphy based on lithologic and biostratigraphic correlations between the Borrego-San Felipe and Vallecito-Fish Creek basins, ABDSP. Mod. fr. Remeika et al.(1988) and Opdyke et al.(1977); geomagnetic polarity timescale aft. Ryan (1973).

TABLE I. Composite taxonomic list of the Borrego Local Fauna.
Taxonomy follows Banks and others (1987) and Simpson (1945). Published faunal accounts include Howard (1963), Remeika (1992). Fish remains identified by M. Roeder (pers. comm. 1991) and equids by E. Scott (pers. comm. 1992). Extinct forms denoted by †.

Class Osteichthyes	
Order Teleostei	
Family Catostomidae	
Xyrauchen sp. cf. *X. texanus*	humpback sucker
? genus	minnows
Class Reptilia	
Order Chelonia	
Family Testudinidae	
? genus	tortoise
Family Emydidae	
Clemmys sp.	pond turtle
Class Aves	
Order Falconiformes	
Family Accipitridae	
Buteo sp.	hawk
Aquila sp.	eagle
Accipiter striatus	sharp-shinned hawk
A. cooperi	Cooper's hawk
Family Cathartidae	
Cathartes aura	turkey vulture
Family Anseriformes	
? genus	ducks
Order Ciconiformes	
Family Phoenicopteridae	
Phoenicopterus sp.	flamingos
Family Strigiformes	
Tyto alba	barn owl
Class Mammalia	
Order Edentata	
Family Megalonychidae	
Megalonyx jeffersonii†	ground sloth
Family Megatheriidae	
Nothrotheriops sp. cf. *N. shastense* †	small ground sloth
Order Lagomorpha	
Family Leporidae	
Sylvilagus audubonii	desert cottontail
Lepus sp. cf. *L. californicus*	jackrabbit
Order Rodentia	
Family Sciuridae	
Ammospermophilus leucurus	antelope ground squirrel
Family Geomyidae	
Thomomys sp.	pocket gopher
Geomys sp.	pocket gopher
Family Heteromyidae	
Dipodomys sp.	kangaroo rat
Family Cricetidae	
Sigmodon hispidus	cotton rat
Peromyscus maniculatus	white-footed mouse
Neotoma lepida	wood rat
Microtus californicus	California meadow vole
Order Carnivora	
Family Mustelidae	
Taxidea taxus	badger
Family Ursidae	
Arctodus sp. †	short-faced bear
cf. *Ursus* sp.	black bear
Family Canidae	
Canis dirus †	dire wolf
C. latrans	coyote
Family Felidae	
Felis rufus	bobcat
F. concolor	mountain lion
Panthera atrox †	North American lion
Smilodon gracilis †	gracile sabertooth cat
S. fatalis †	California sabertooth cat
Order Proboscidea	
Family Elephantidae	
Mammuthus columbi †	columbian mammoth
M. imperator †	imperial mammoth
Order Perissodactyla	
Family Equidae	
Equus bautistensis †	Bautista horse
E. (Dolichohippus) enormuus †	giant Anza-Borrego zebra
Equus (*Dolichohippus*) sp. †	small zebra
Equus sp. ? *E. hemionus* †	half ass
Order Artiodactyla	
Family Camelidae	
Camelops huerfanensis †	camel
Camelops sp. †	camel
Gigantocamelus sp. †	giant camel
Hemiauchenia sp. †	llama
Family Antilocapridae	
Capromeryx sp. †	small prongbuck antelope
Tetrameryx sp. †	4-tyned prongbuck antelope
Family Cervidae	
Odocoileus sp.	mule deer
Family Bovidae	
Ovibovini	muskoxen
Euceratherium sp. †	shrub-oxen

STRATIGRAPHY AND AGE

The OF is composed primarily of locally derived fluvial and lacustrine deposits (Anza-Borrego Group of Reynolds and Remeika, this volume). Four genetically interrelated sedimentary depositional subenvironments that are typical of topographically low basin centers have been stratigraphically delineated. In ascending order they include, (1) alluvial fan sediments (Mammoth Cove Sandstone Member) (MCSM), (2) lacustrine claystones (Arroyo Otro Claystone) (AOC), (3) playa margin deposits (Inspiration Wash Member) (IWM), and (4) playa basin deposits (Las Playas Member, new name) (LPM). The MCSM consists of a 74 m thick megasequence of locally derived, subaqueously deposited distal alluvial fan sediments that interfingers with extraregional lacustrine claystones (Borrego formation, Colorado River Group of White and others, 1991). This stratigraphic relationship is exposed in the deposits beneath Font's Point in the southeastern portion of the Badlands. The fresh water AOC, totaling 87 m in thickness, is stratigraphically discontinuous pinching out both to the east and west as exposed in Arroyo Otro and Inspiration Wash. The 216 m thick IWM is laterally widespread and consists of interstratified fluvial-floodplain and playa-margin deposits. These grade basinward, east into the LPM which is primarily composed of fine-grained sediments. Eastward at Valle Escondido, the IWM is laterally equivalent to the informal Short Wash Member of Pettinga (in press).

Fossil localities are concentrated north of Dump Wash, within alluvial fan/fluvial deposits (MCSM) of local provenance that crop out between Tumbleweed Wash and Two-sloth Wash. Above the Ocotillo Rim, strata of the MCSM, AOC, and IWM are folded and faulted and the section is repeated in exposures across Arroyo Otro and Inspiration Wash. To the east, floodplain deposits (IWM) grade laterally into lacustral playa deposits (LPM) between Inspiration Wash and Font's Wash. Vertebrate fossils only occur in thin, 2-3 m, sandstone interfluves within the lacustrine sediments. In the BB, the OF is overlain by unfossiliferous alluvial plain-braided fluvial deposits of the late Pleistocene Font's Point Sandstone.

Based on the preliminary magnetostratigraphic work of Scheuing and others (1988), and Bogen and Seeber (1986), the OF ranges in age from 1.25 to 0.37 Ma BP (Figure 1). This period is correlative with the Irvingtonian and earliest Rancholabrean Land Mammal Ages (Savage, 1951; Woodburne, 1987). Distal fan deposits within the basal MCSM span the Matuyama reversed magnetochron, and range in age from 1.25 to about 0.90 Ma BP. The geomagnetic event within the lower IWM probably represents the Jaramillo normal magnetosubchron which ranges from 0.98 to 0.91 Ma BP. The remaining IWM and LPM are magnetically normal and probably represent the Brunhes normal magnetochron. The Matuyama/Brunhes geomagnetic boundary is marked by the presence of the Bishop Tuff (Izett, 1981; Sarna-Wojcicki and others, 1984). This ashfall tuff occurs above the level of the Jaramillo event within the lower portion of the IWM. In the nearby Coyote Badlands it has been tentatively chemically correlated with the Fryant Ash member of the Bishop series dated at about 0.62 Ma BP (Sarna-Wojcicki, pers. comm., 1984).

TABLE II. Stratigraphic distribution of selected mammalian taxa within members of the Ocotillo formation, Borrego and Coyote Badlands.

Explanation: CB = Coyote Badlands; IWM = Inspiration Wash Member; LC = lacustrine claystone member; LPM = Las Playas Member; MCSM = Mammoth Cove Sandstone Member.

TAXON	MCSM	LC	IWM	LPM	CB
Megalonyx jeffersonii	■				■
Nothrotheriops sp. cf. *N. shastense*	■		■	■	■
Sylvilagus sp.	■				
Lepus californicus	■	■	■	■	
Taxidea taxus	■	■			
Arctodus sp.	■		■		■
Ursus sp.	■	■			
Canis latrans	■	■			
Canis dirus					■
Felis rufus	■	■	■		
Panthera atrox	■				■
Smilodon gracilis					■
Smilodon fatalis					■
Mammuthus imperator	■				
Mammuthus columbi	■		■	■	■
Mammuthus sp.	■	■	■		■
Equus bautistensis	■		■		■
Equus enormuus	■				■
Equus hemionus	■				■
Equus sp.	■	■		■	
Camelops huerfanensis		■			
Camelops sp.	■	■	■	■	■
Gigantocamelus sp.		■	■	■	
Hemiauchenia sp.	■		■		■
Capromeryx sp.			■		■
Tetrameryx sp.					■
Odocoileus sp.	■		■	■	■
Ovibovini	■				
Euceratherium sp.	■				■

BIOSTRATIGRAPHY

The BLF (Table 1) is based primarily on fragmentary postcranial remains, however, a few articulated specimens have been recovered. Species of *Mammuthus*, *Equus*, and *Camelops* are the most abundantly represented mammalian taxa. Both large and small carnivores are represented but the materials are diagnostic only to generic level. Together with the large herbivores that include a relatively balanced representation of grazers, browsers and mixed feeders (Akersten and others, 1984; Jefferson, 1988), they suggest an open, savanna-like environment with permanent water and scattered gallery forests. Aquatic vertebrates (Table 1) record the presence of marshy lacustrine habitats, which may have been locally ephemeral. Assemblages from each of the described, fossiliferous members of the OF (see Table 2) are discussed below.

Although many of the taxa from the MCSM are shared with the Blancan-Irvingtonian age Vallecito Creek Local Fauna from the Vallecito Badlands (Downs and White, 1968) of the Vallecito-Fish Creek Basin (VFCB) (White and others, 1991), the presence of *Mammuthus imperator*, *Equus bautistensis*, and *Camelops huerfanensis* clearly indicates an Irvingtonian Age. A partial, about 60% complete skeleton of *M. imperator* was recovered from the upper part of this unit (Miller and others, 1991). Microvertebrates are relatively rare in this portion of the OF.

As well as the more common taxa (Table 2), the AOC assemblage includes the humpback sucker *Xyrauchen* sp. cf. *X. texanus* and *Accipiter striatus*, the sharp-shinned hawk. A camelid trackway has been found here that is comparable to the ichnogenus *Pecoripeda* (*Ovipeda*) sp. cf. *Camelops* sp. from Camel Ridge in the Vallecito Badlands (Stout and Remeika, 1991). In addition to the taxa listed in Table 2, the following lower vertebrates and birds have been recovered from the IWM: *Xyrauchen* sp. cf. *X. texanus*, *Clemmys* sp., *Buteo* sp., *Aquila* sp., and *Tyto alba* (Table 1). The IWM assemblage is closely comparable to that recovered from the Coyote Badlands (Table 2), 16 km northwest of the BB. Similar stratigraphic sections that include the Bishop Tuff are present in both areas, suggesting that they have been right-laterally displaced at least 16 km along the Coyote Creek fault. At Valle Escondido, strata high in the section are especially rich in microvertebrates. The fragmentary remains include *Lepus* sp. cf. *L. californicus*, *Ammospermophilus leucurus*, *Thomomys* sp., *Dipodomys* sp., *Sigmodon hispidus*, *Peromyscus maniculatus*, *Neotoma lepida*, and *Microtus californicus*. The arvicoline rodent *M. californicus* (Zakrzewski pers. comm., 1988), and *S. hispidus* are evolved forms that index the Irvingtonian LMA (Repenning and others, 1987; Kurten and Anderson, 1980). Vertebrate remains within this unit (Table 2) occur in interbeds of fluviatile sandstone. Near the top of the section, these strata occur above the Bishop Ash, and may span the Irvingtonian-Rancholabrean LMA boundary.

In summary, within ABDSP, faunal correlations between vertebrate-bearing strata in the VFCB and BB (Figure 1) record a continuous succession of vertebrate fossil assemblages ranging from the latest Hemphillian through earliest Rancholabrean ages. The stratigraphic ranges of *Mammuthus imperator* (MCSM) and *M. columbi* (MCSM-LPM) (Table 2) document only one example of faunal change (Downs and White, 1968) within the record.

ACKNOWLEDGEMENTS

R. E. Reynolds and E. Scott of the San Bernardino County Museum reviewed the manuscript and provided helpful comments and suggestions.

LITERATURE CITED

Akersten, W.A., T.M. Foppe, and G.T. Jefferson, 1984. New source for dietary data from large extinct herbivores. Quaternary Research, 30(1):92-97.

Banks, R.C., R.W. McDiarmid, and A.L. Gardner, 1987. Checklist of Vertebrates of the United States, the U.S. Territories, and Canada. United States Department of the Interior, Fish and Wildlife Service, Resource Publication, 166:1-79.

Bogen, N.L., and L. Seeber, 1986. Neotectonics of rotating blocks within the San Jacinto fault zone, southern California. Abstract. Eos, 67:1200.

Downs, T., and J.A. White, 1968. A vertebrate faunal succession in superposed sediments from late Pliocene to middle Pleistocene in California, *in* Tertiary/Quaternary Boundary, International Global Congress, Prague, 23(10):41-47.

Howard, H.H., 1963. Fossil birds from the Anza Borrego Desert. Los Angeles County Museum Contributions in Science, 73:1-33.

Izett, G.A., 1981. Volcanic ash beds: recorders of upper Cenozoic silic pyroclastic volcanism in the western United States. Journal of Geophysical Research, 86(B11):10200-10222.

Jefferson, G.T., 1988. Late Pleistocene large mammalian herbivores: implications for early human hunting patterns in southern California. Bulletin of the Southern California Academy of Sciences, 87(3):89-103.

Kurten, B., and E. Anderson, 1980. Pleistocene mammals of North America. Columbia University Press, New York: 442 p.

Miller, G.J., P. Remeika, J.D. Parks, B.W. Stout, and V.E. Waters, 1991. A preliminary report on half-a-million-year-old cutmarks on mammoth bones from the Anza Borrego Desert Irvingtonian. Imperial Valley College Museum Society Occasional Papers, 8:1-47.

Nicholson, C., and L. Seeber, 1989. Evidence for contemporary block rotation in strike-slip environments: examples from the San Andreas fault system, southern California, *in* Paleomagnetic rotations and continental deformation, C. Kissel and C. Laj (eds). Kluwer Academic Publishers:247-280.

Opdyke, N.D., E.H. Lindsay, N.M. Johnson, and T. Downs, 1977. The paleomagnetism and magnetic polarity stratigraphy of the mammal-bearing section of Anza-Borrego Desert State Park, California. Quaternary Research. 7:316-329.

Pettinga, J.R., 1991. Structural styles and basin margin evolution adjacent to the San Jacinto fault zone, southern California. Abstracts with Programs, Geological Society of America Annual Meeting, San Diego, California:A257.

Remeika, P., 1992. Preliminary report on the stratigraphy and vertebrate fauna of the middle Pleistocene Ocotillo formation, Borrego Badlands, Anza-Borrego Desert State Park, California. Abstracts of Proceedings, 6th Annual Mojave Desert Quaternary Research Symposium, San Bernardino County Museum Quarterly, 39(2):25-26.

Remeika, P., I.W. Fischbein, and S.A. Fischbein, 1988. Lower Pliocene petrified wood from the Palm Spring formation, Anza-Borrego State Park, California, *in* Review of palaeontology and palynology, 56:183-198.

Remeika, P., and J.R. Pettinga, 1991. Stratigraphic revision and depositional environments of the middle to late Pleistocene Ocotillo Conglomerate, Borrego Badlands, Anza-Borrego Desert State Park, California. Symposium on the Scientific Value of the Desert, Anza-Borrego Foundation, Borrego Springs, California, Abstract:13.

Repenning, C. A., E.M. Browers, L.O. Carter, L. Marincovich Jr., and T.A. Ager, 1987. The Beringian ancestry of *Phenacomys* (Rodentia; Cricetidae) and the beginning of the modern Arctic Ocean borderland biota. United States Geological Survey Bulletin, 1687:1-31.

Reynolds, R.E., and R.L. Reynolds, 1990. Irvingtonian? faunas from the Pauba formation, Temecula, Riverside County, California, *in* Abstracts and proceedings, 1990 Mojave Desert Quaternary Research Symposium, J. Reynolds (ed). San Bernardino County Museum Association Quarterly, 37(3,4):37.

Reynolds, R.E., R.L. Reynolds, and A.F. Pajak III, 1991. Blancan, Irvingtonian, and Rancholabrean(?) Land Mammal Age faunas from western Riverside County, California, *in* Abstracts and Proceedings, 1991 Mojave Desert Quaternary Research Symposium, J. Reynolds (ed). San Bernardino County Museum Association Quarterly, 38(3,4):37-40.

Ryan, W.B.F., 1973. Paleomagnetic stratigraphy. In Initial Reports of the Deep Sea Drilling Project, LEG XIII, 2, W.B.F. Ryan and K.H. Hsu (eds). United States Government Printing Office, Washington, D.C.:1380-1386.

Sarna-Wojcicki, A.M., H.R. Boweman, C.E. Meyer, P.C. Russell, M.J. Woodward, G. McCoy, J.J. Rowe Jr., P.A. Baedecker, F. Asaro, and H. Michel, 1984. Chemical analyses, correlations, and ages of upper Pliocene and Pleistocene ash layers of east-central and southern California. United States Geological Survey Professional Paper, 1293:1-40.

Savage, D.E., 1951. Late Cenozoic vertebrates of the San Francisco Bay region, California. University of California Publications Department of Geological Sciences, 28(10):215-314.

Scheuing, D.F., L. Seeber, K.W. Hudnut, and N.L. Bogen, 1988. Block rotation in the San Jacinto fault zone, southern California. American Geophysical Union, Abstracts to Meetings.

Simpson, G.G., 1945. The principles of classification and a classification of mammals. American Museum of Natural History Bulletin, 85:1-350.

Stout, B.W., and P. Remeika, 1991. Status report on three major camelid track sites in the lower Pliocene delta sequence, Vallecito-Fish Creek Basin, Anza-Borrego Desert State Park, California. Symposium on the Scientific Value of the Desert, Anza-Borrego Foundation, Borrego Springs:9.

White, J.A., E.H. Lindsay, P. Remeika, B.W. Stout, T. Downs, and M. Cassiliano, 1991. Society of Vertebrate Paleontology field trip guide to the Anza-Borrego Desert. Society of Vertebrate Paleontology 51st Annual Meeting, San Diego: 23 p.

Woodburne, M.O., 1987. Cenozoic mammals of North America. University of California Press, Berkeley: 336 p.

Razorback Sucker (*Xyrauchen*) Fossils from the Anza-Borrego Desert and the Ancestral Colorado River

J.D. STEWART, *Vertebrate Paleontology, Natural History Museum of Los Angeles County, Los Angeles CA 90007*
MARK A ROEDER, *Paleontology, San Diego Natural History Museum, P.O. Box 1390, San Diego CA 92112*

ABSTRACT

The first documentation of fossil *Xyrauchen* indicates that a major fluvial-tributary system of the ancestral Colorado River flowed into the Borrego Badlands during at least part of the Pleistocene period (Ocotillo formation). *Xyrauchen* is also present in the lower Pliocene Diablo Formation in and around the San Felipe Hills.

Few fossil fresh water fishes are known from the ancestral Colorado River drainage. *Xyrauchen texanus*, the razorback sucker or humpback sucker (Fig. 1), is one of the fishes endemic to the Colorado drainage and one of the largest catostomid fishes from North America. The historic range of *Xyrauchen* is entirely within the Colorado River drainage (Lee and others, 1980), where it is limited to the Colorado River and major tributaries such as the Gila and Green rivers. *Xyrauchen* is a large fish (up to 1 m) relative to other North American fresh water fishes. It was once a major food source for Native Americans living along the Colorado River. Because of manipulation of the water flow of the lower Colorado River, this fish is now an endangered species in California (McGinnis, 1984).

Minkley, Hendrickson, and Bond (1986:581) mentioned that one of us (MAR) had identified a "well-preserved Pleistocene fossil *Xyrauchen* from the Colorado Desert west of the Salton Sea." This is the only published reference to a fossil record of the genus to date. The specimen in question, SBCM A768-1, was collected by Ruth Coyle on the north side of the San Felipe Hills near the western boundary of Imperial County and north of State Highway 78, an area originally mapped as part of the Palm Spring formation by Dibblee (1954). In 1991, Remeika recognized that these beds are not genetically synonymous with the Palm Spring formation that is restricted in outcrop to the Vallecito Badlands of Anza-Borrego Desert State Park (ABDSP). To establish appropriate nomenclature and stratigraphic control, Remeika (1991) and Remeika and Lindsay (1992) named the informal Diablo formation for Colorado River-derived fluvial sandstones deposited as part of the deltaic plain of the Colorado Rivera long the western side of the Salton Trough region of southern California. Remeika (pers. comm.) states that this *Xyrauchen* specimen (SBCM A768-1) is of early Pliocene age, demonstrating that the large river-adapted lineage of *Xyrauchen* extends back more than three million years.

The San Felipe Hills specimen consists of a foot long skeleton preserved inside an oval-shaped arenitic sandstone concretion. The specimen was donated to the San Bernardino County Museum by Ruth Coyle. According to Paul Remeika of the Anza-Borrego State Park, the lithology of the concretion appears to be from ancestral Colorado River-derived sediments of the Diablo formation (Pliocene) and not from the lacustrine Borrego formation. The specimen, which is nearly complete, is being studied by Dr. Kenneth Gobalet, California State University, Bakersfield, and Mark Roeder. Because of the completeness of the specimen, it may be possible to determine whether this specimen represents an earlier species of this genus, or extends the range of *Xyrauchen texanus* to early Pliocene times.

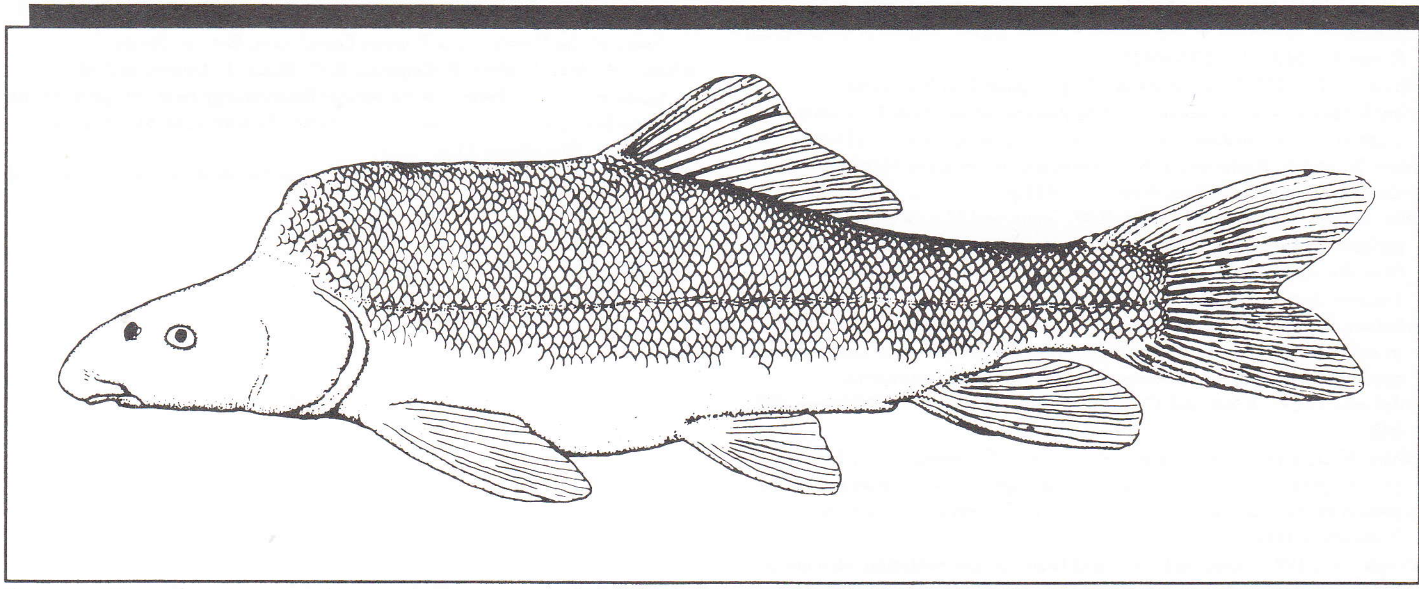

Figure 1. *Xyrauchen texanus*, the razorback sucker, exhibits the unusual hump characteristic of a few of the large Colorado River fish species.

Table I. LACM specimens of *Xyrauchen texanus* from the Borrego Badlands

LACM Locality	Formation	Member	Specimen Number	Elements
4123	Ocotillo Fm		118500	fish fragments including left half of autogenous neural arch of third vertebra of *Xyrauchen*
4124	Ocotillo Fm	Inspiration Wash Mbr	130319	L quadrate, partial L operculum, neural complex, centrum, parapophysis, R 1st pectoral fin ray
6763	Ocotillo Fm	Inspiration Wash Mbr	130322	Neural complex, part, predorsal, centrum
6775	Ocotillo Fm		135364	Neural complex
67113	Ocotillo Fm	Los Playas Mbr	130320	Neural complex
			130321	Neural complex
			135427	Abdominal vertebra, rib, L pectoral fin ray, R half autogenous neural arch of 3rd vertebra

Even though SBCM A768-1 is of Pliocene age, Pleistocene specimens of *Xyrauchen* do exist. Six specimens in the Natural History Museum of Los Angeles County (LACM) (LACM 130319, 130320, 130321, 130322, 135364, 135467) from the Ocotillo Formation are assigned to *Xyrauchen texanus*.

The osteological nomenclature employed here follows that of Nelson (1948). The Weberian apparatus of *Xyrauchen* is most like those of the Catostomini and Erimyzonini, in that the neural spine of the third vertebra does not participate in the posterior margin of the neural complex (Nelson, 1948). In *Catostomus*, the posterior border of the neural complex is very attenuate and dorso-posteriorly directed. Furthermore, at least two vertebral neural arches behind the neural complex support the neural complex in *Catostomus*. In *Xyrauchen*, however, the supraneural is oriented directly above vertebrae one through four. The neural arch of the fourth vertebra is inclined slightly forward to reach the neural complex, and the fifth vertebra extends its neural arch considerably forward to effect this contact. A large supraneural is sutured to the posterior side of the neural complex, and that supraneural also has a smaller supraneural sutured to its posterior side. Unlike the condition in *Catostomus*, a great deal of the neural complex and its attached supraneural extend above the neural arches of vertebrae four and five.

The most easily identified skeletal element of *Xyrauchen* in collections from the Borrego Badlands is the neural complex of the Weberian apparatus (see Table 1 for complete listing). This element and the two enlarged supraneurals of the Weberian apparatus are the osteological basis of the conspicuous hump of *Xyrauchen*. Five specimens of the neural complex are represented from four Borrego Badlands localities in the LACM collections. A fifth locality produced a fragment of the modified pleural rib of the fourth centrum. None of the specimens can be distinguished from those elements of *Xyrauchen texanus*. All are from large individuals, well in excess of 50 cm standard length (comparison to LACM 43613-1).

The Ocotillo formation is composed of locally-derived sediments (Remeika, 1991; Remeika and Jefferson, this volume), and probably does not represent Colorado River sediments *per se*. These sediments more probably represent a Colorado River tributary system; the fossils of large *Xyrauchen* indicate that the tributary was sizeable. The estimated age of the Ocotillo Formation in the Borrego Badlands spans approximately 0.37—1.25 Ma (Remeika and Jefferson, this volume). This may or may not include some sediments of the Rancholabrean North American Land Mammal (NALM) Age. The Irvingtonian/Rancholabrean NALM Age boundary is not well dated or agreed upon. Estimates for the age of the boundary range from 0.2–0.55 Ma (Lundelius and others, 1987). Regardless, the bulk of the Ocotillo formation was deposited within the Irvingtonian NALM Age. A volcanic ash in the upper part of the Inspiration Wash member is thought to be correlated with the Bishop Tuff (Remeika, 1992). A potassium/argon date is pending for that ash. The most reliable K-Ar dates and the average zircon fission-track age for the Bishop Tuff are each approximately 0.74 Ma (Izett and others, 1988). According to Remeika (pers. comm.) some of the localities that produced the LACM specimens lie above this tuff, and some lie below.

ACKNOWLEDGEMENTS

We wish to thank Ruth Coyle for recognizing the importance of the San Felipe Hills specimen and donating it to the San Bernardino County Museum. Robert Reynolds (SBCM) brought the specimen to our attention. Dr. William Minkley of Arizona State University gave us comparative material of *Xyrauchen texanus*. Paul Remeika generously supplied information on the stratigraphy of the Anza-Borrego Desert State Park and adjacent areas. Dr. Robert Lavenberg (LACM) gave us access to ichthyological collections in his care. Dr. John M. Harris critically read this manuscript.

REFERENCES

Dibblee, T.W. Jr., 1954. Geology of the Imperical Valley region, California. California Division of Mines Bulletin, 170 (II,2):21-28, pl. 2: generalized geologic map of Imperial Valley region, California, scale 1 inch = 6 mi.

Izett, G.A., J.D. Obradovich and H.H. Mehnert, 1988. The Bishop Ash Bed (Middle Pleistocene) and some older (Pliocene and Pleistocene) chemically and mineralogically similar ash beds in California, Nevada, and Utah. U.S. Geological Survey Bulletin 1675: 37 p.

Lee, D.S., C.R. Gilbert, C.H. Hocutt, R.E. Jenkins, D.E. McAllister, and J.R. Stauffer Jr., 1980. Atlas of North American freshwater fishes. Raleigh, 867 p.

Lundelius, E.L Jr., T. Downs, E.L. Lindsay, H.A. Semkin, C.S. Churcher, C.R. Harrington, G.E. Schultz, and S.D. Webb, 1980. The North American Quaternary sequence, *in* Cenozoic mammals of North America, M.O. Woodburne (ed). Berkeley, University of California Press:211-235.

McGinnis, S.M., 1984. Freshwater fishes of California. Berkeley, University of California Press: 316 p.

Minkley, W.L., D.A. Hendrickson, and C.E. Bond, 1986. Geography and western North American freshwater fishes: description relationships to intracontinental tectonism, *in* Zoogeography of North American freshwater fishes, C.H. Hocutt and E.O. Wiley (eds). New York, Wiley and Sons:519-613.

Moyle, Peter B., 1976. Inland fishes of California. Berkeley, University of California Press: 405 p.

Nelson, E.M., 1948. The comparative morphology of the Weberian apparatus of the Catostomidae and its significance in systematics. Journal of Morphology, 83:225-251.

Remeika, P., 1991. Formation status for the Diablo Red Beds; differentiating between Colorado River affinities and the Palm Spring formation, *in* Symposium on the scientific value of the desert, J. Rickard (ed). The Anza-Borrego Foundation, Desert Symposia.

___, 1992. Preliminary report on the stratigraphy and vertebrate fauna of the Middle Pleistocene Ocotillo formation, Borrego Badlands, Anza-Borrego Desert State Park, California. Abstracts of Proceedings, 6th Annual Mojave Desert Quaternary Research Symposium, San Bernardino County Museum Association Quarterly, 39(2):25-26.

Remeika, P. and G.T. Jefferson, 1993. The Borrego local fauna: revised basin-margin stratigraphy and paleontology of the western Borrego Badlands, Anza-Borrego Desert State Park, California. this volume.

Remeika, P. and L. Lindsay, 1992. Geology of Anza-Borrego: edge of creation. Dubuque, Kendall/Hunt Publ. Co., Sunbelt Publication California Desert Natural History Guide: 208 p.

Smith, G.R., 1978. Biogeography of intermountain fishes, *in* Intermontain biogeography: a symposium, K.T. Harper and J.L. Reveal (eds). Great Basin Naturalist Memoirs, 2:1-268.

Pegmatites in the Chihuahua Valley Region

AL ORDWAY *Research Associate, Department of Earth Sciences, San Bernardino County Museum, Redlands CA 92374*

Gem quality minerals and unusual mineral assemblages are found in pegmatite dikes along Highway 79 in the northern Peninsular Ranges of Riverside and San Diego counties.

Beauty Peak. The Pawnee Mine, north of Oak Grove, contains specimens of scheelite in garnet skarn, is on the southerly slope of Beauty Peak. For several years it was worked for tungsten.

Lost Valley Truck Trail. Several pegmatites cut across the Lost Valley Truck Trail about two miles north of the highway. Two of the larger pegmatites were prospected for colored tourmaline with minimal results. Schorl was the common pocket tourmaline with rare occurrences of aquamarine and morganite beryls. Farther north a small prospect next to the road produced several pounds of small aquamarine crystals and a few specimens of columbite.

Chihuahua Valley. Chihuahua Valley, an east-west trending depression along the Hot Springs fault, lies at an elevation of approximately 4200' and is bordered by tonalite and granodioritic intrusives of the California Batholith. The higher peaks to the north are comprised of older, Paleozoic metamorphic rocks. Pegmatite dikes have penetrated the igneous and metamorphic rocks and are probably the youngest recognized intrusives in this region. They occur as small lenses a few inches thick to more massive dikes several feet thick and several hundred feet in length.

Despite the great abundance of pegmatite dikes, only the Blue Lady Mine and an unnamed prospect have produced specimens of interest, including cassiterite and apatite. The Blue Lady is noted for its dark blue tourmaline, tons of quartz crystals, cassiterite, and a few morganite beryls of a color unequaled by any other worldwide occurrence. An unnamed prospect, consisting of three tiny pegmatites, was encountered during development for housing in the flatlands of the Chihuahua Valley. Specimens, though very few, consisted of apatite, beryl and herderite.

Metamorphic Zone. North of the Chihuahua Valley, bordering and within Riverside County, is a zone of higher peaks comprised entirely of Paleozoic metamorphic rocks. Pegmatites here are generally smaller and fewer than in the Chihuahua Valley, but several outcrops have produced a few specimens of beryl and herderite. A single prospect named the Blue Chihuahua Mine received world recognition for its abundance of exceptionally fine crystallized herderite. This mine also produced good specimens of topaz and schorl.

Pegmatite Minerals near Aguanga

DANA GOCHENAUR *Gochenaur Minerals, Santa Ana CA*

Southeast from Temecula, the terrain along Highway 79 becomes increasingly rugged with the appearance of granitic mountains with a wide variety of minerals. The area has mines famous for their gem minerals: topaz, tourmaline, beryl, and quartz. Crystals in granitic rock of this type are found in coarse-grained bodies called pegmatites. The crystals can be encased ("frozen") or in cavities ("pockets").

One group of mines northeast of Aguanga along Highway 371 is near Cahuilla Mountain. This mining district was first developed in the late 1890s by Burt Simmons, an early settler of Oak Grove, San Diego County. Bert sold the best mine to A.E. Fano in 1905. This mine has had several periods of activity. Initially, during its heyday, the "Fano" produced pink and blue tourmaline for the gem trade. The claims were patented in 1914 and became private property. Nothing is known about production until the early 1950s when some fine golden beryl and large smoky quartz crystals were reported. Falling into obscurity, the mine languished through the 1970s.

In the spring of 1980 the old "Fano" was opened for leasing by a new owner. After the general cleanup of the old workings, the first specimens found were some spectacular "frozen" green beryls, some weighing several kilograms. Next came the first big find, a pocket containing over fifty gem beryls in blue, green and yellow, some attached to smoky quartz or albite feldspar. A typical pocket was lined with quartz and feldspar, filled with mud and loose crystals, usually muscovite mica, smoky quartz, and albite and, with luck, black tourmaline or beryl. Rare minerals including cassiterite and mangano-columbite are found in well-formed crystals.

The next ten years saw a variety of beautiful gem and mineral specimens, the most notable being beryl and lustrous black tourmaline crystals on quartz or albite. Many of these specimens can be seen at the San Bernardino County Museum.

In the early part of this century, Burt Simmons explored much of southern California, locating deposits in both Riverside and San Diego counties. Two of Burt's finds were near Sunshine Summit on Aguanga Mountain, just south of the Palomar Observatory. Named the Mountain Lily claims, they were reached after a long and difficult climb by mule. Only small amounts of tourmaline were found, and the two claims were sold in 1902. Sometime after 1909 the property was renamed the Emeralite 1 and 2 by John W. Ware. The pegmatites are horizontal, one on the crest and the other just down the hill. Both have many small pockets with quartz and feldspar. With increased production, several hundred pounds of blue and green topaz were reported. Another important discovery was tourmaline in vivid colors of blue, blue-green and green, highly sought after as gemstones.

The mines were developed further in the 1950s by Norm Dowson who also found "nile-green" tourmaline and fine blue topaz. Today the mine on the crest is called the Ware and the lower mine is the Maple-lode. These mines have produced many fine minerals and gemstones, such as clear and smoky quartz, green apatite, and pink, blue and green beryl. Specimens from this locality can be seen in California museums and across the country. A large blue topaz weighting 12 ounces is in the collection of the California Institute of Technology. The Palomar Truck Trail runs through both properties, but permission is needed to enter these privately-owned properties.

Rodents and Rabbits from the Temecula Arkose

ROBERT E. REYNOLDS and RICHARD L. REYNOLDS, *Division of Earth Sciences, San Bernardino County Museum, Redlands CA 92374*

ABSTRACT

The Tertiary Temecula Arkose underlies an unnamed sandstone and the Pauba Formation in the Elsinore fault zone. The age of the Temecula Arkose was considered to be early Pliocene (Blancan LMA) based upon vertebrate fossils. An age of 4.5 m.y. was assigned on the basis of *Neotoma (Paraneotoma) sawrockensis* in the formation near Radec. This paper discusses additional small vertebrates of early Blancan LMA from the section between Radec and Vail Lake. The minimum age of the fauna is important because it provides constraints on structural and landslide events associated with the Lancaster fault in the Aguanga basin.

GEOLOGIC BACKGROUND

The Elsinore fault zone trends northwest parallel to the San Jacinto fault from Santa Ana Canyon south to the Yuha Desert near the California-Mexico border, approximately 128 miles (Rogers, 1965). The Agua Caliente fault zone runs along the east side of the Elsinore fault zone from Temecula to the southern Borrego Badlands, a distance of 64 miles. Sediments filling the Elsinore trough south of Lake Elsinore were first described in print by Mann (1955) and in somewhat greater detail by Kennedy (1977). Based on fossil vertebrates and the presence of the Bishop Ash, a late Pleistocene age was suggested for the Pauba Formation, early Pleistocene for the "unnamed sandstone" formation, and late Pliocene Blancan Land Mammal Age (LMA) for the Temecula Arkose (Kennedy, 1977; Golz and others, 1977). Examination of a wood rat, *Neotoma (Paraneotoma) sawrockensis*, allowed Repenning (1987: fig. 8.1) to suggest an age of 4.5 m.y. for the Temecula Arkose at Radec.

PALEONTOLOGIC LOCALITIES

Golz and others (1977) reported vertebrate faunas (Table I) from the vicinity of Pechanga (west), Vail Lake (central), and Radec (east) in outcrops of Temecula Arkose. They note the specimens from Radec are 20 m lower in the section than the Vail Lake and Pechanga localities when measured from the top of the tuffaceous sandstone facies. However, using conservative attitudes shown in the geologic map of Mann (1955), it appears that the Radec locality (SBCM 5.2.16) is 70 m below the Shamrock locality (SBCM 5.2.6), while the Butterfield Valley locality (SBCM 5.2.51) is 200 m higher than Shamrock and the Vail Lake locality (SBCM 5.2.1) is 100 m higher still. Although Mann (1955:11) states, "A detailed stratigraphic study of the Temecula Arkose would be impossible because of poor exposures, a paucity of traceable lithologic units, and highly complex faulting," further detailed field investigations would help clarify stratigraphic relationships of the localities.

SMALL VERTEBRATES

The faunas from Vail, Butterfield, Shamrock and Radec contain taxa previously unreported from the Temecula Arkose that are considered to be Hemphillian LMA holdovers. These include *Calomys gidleyi, Cupidinimus* cf. *C. bidahokiensis*, and *Prothomomys warrensis*.

Hemphillian indicator taxa

Calomys gidleyi was previously recognized in California from the late Hemphillian Warren fauna (May, 1982) and the Kern River formation (Reynolds,1990; Reynolds and Czaplewski, 1989). *Cupidinimus* sp. cf. *C. bidahokiensis* is known from the Hemphillian LMA of northeastern Arizona (Baskin, 1979; Barnosky, 1986). *Prothomomys warrensis*, possibly ancestral to *Thomomys*, was described by May (1982) from the Late Hemphillian Warren fauna west of Mojave, Kern County, California.

The presence of *Copemys vasquezi, Peromyscus valensis* and *?Copemys* sp. suggests faunas in which *Peromyscus* is developing from ancestral *Copemys* with forms that are transitional between the two referred to as *?Copemys*. *Copemys vasquezi* from the late Hemphillian of eastern Arizona is discussed by Jacobs (1977). One of the latest *Copemys* species is from Verde, Arizona (Czaplewski, 1990).

Blancan indicator taxa

Indicators of the Blancan LMA include *Calomys arizonae* and *Onychomys gidleyi*. Carleton and Eshelman (1979) provide measurements and discussion of the *O. leucocaster* group and synonomize *O. larrabeei* with *O. gidleyi*. The *O. gidleyi* from Radec compares well with Blancan I and II forms of *O. gidleyi*. *Calomys arizonae* is distinguished from *C. gidleyi* by the teardrop-shaped M/1 with shallowly bifurcate anteroconid. *C. arizonae* is known from the Verde locality, Arizona (Czaplewski, 1990), which is earliest Blancan II (Repenning, 1987).

Geomyidae

Three gophers appear to be present in the section between Radec and Vail Lake. They include *Prothomomys warrensis* (May 1982), known by distinctive $dP/_4$s and the round configuration of $P^4/_4$ protocone/id. The other common gopher is *T. gidleyi* (Wilson, 1933; Gufstafson, 1978), with a triangular protocone/id of $P^4/_4$. A third specimen is a relatively complete skull with incisors, premolars and molars. The upper premolars have a protocone with a "rhomboid" occlusal configuration that is somewhat similar to *T. bottae* but is distinct from *T. gidleyi* and *Prothomomys warrensis*.

Cricetidae

Czaplewski and Repenning recognize early Blancan *Sigmodon* from Radec (Czaplewski, 1987). The *S. medius* from Radec measures close in length and crown height to *S. minor medius* from the Rexroad fauna (Martin and Prince, 1989) of Blancan II LMA, 3.8 Ma (Repenning, 1987). It is somewhat higher-crowned than the Verde form (Czaplewski, 1987). In addition to two major roots, the lower first molars from Radec consistently have one strong and one weak accessory root. *Prosigmodon* spp. from Verde and Chihuahua have a single accessory root on M_1. *Sigmodon medius* (Czaplewski, 1987) from Verde has no accessory roots. *S. minor* specimens (Martin, this volume) from locations including Borchers, Kansas, and southeastern Arizona (Tomida, 1987) all have a single accessory root. The relationship of size, cusp morphology, and presence of accessory rootlets of the specimens of *Prosigmodon* (Verde), *Sigmodon medius* (Radec), and *S. lindsayi* (Vallecito, California) (Martin and Prince, 1989) should be examined. The presence of accessory roots may not

Table 1. Vertebrate taxa reported from three localities in the Temecula Arkose by Golz and others (1976)

	Pechanga	Vail Lake	Radec
Chelonia	■	■	■
Iguanidae			■
Anguidae			■
Talpidae			■
Xenarthra (size of *Nothrotheriops*)			■
Hypolagus cf. *H. limnetus*	■		■
Hypolagus cf. *H. regalis*			■
Sciuridae			■
Perognathus			■
cf. *Dipodomys*			■
Neotoma			■
Sigmodon			■
Cricetinae (sm)			■
Rodentia	■		
Canis (size of *C. latrans*)			■
Taxidea			■
Felis			■
Lynx?			■
Proboscidea			■
Equus	■	■	■
Nannippus	?	■	
Camelops?			■
Lamini			■
Camelidae		■	
Odocoileus			■
Tetrameryx			■

be an advanced characteristic but may fluctuate through populations.

Neotoma (Paraneotoma) sp. occurs at all the Temecula Arkose localities discussed here. *N. (P.) sawrockensis* was noted by Repenning (1987) from U.S.G.S. localities at Radec. The SBCM localities contain *N. (P.) sawrockensis* from the Vail, Butterfield and Shamrock localities. The Radec SBCM collections have no small wood rats similar in size to *N. (P.) sawrockensis*, but two large wood rats occur there. Both of the large Radec woodrats are approximately similar in molar occlusal dimensions and crown height. One has inflated, rounded tooth walls and an M_1 with dorso-ventrally shallow metaflexid (=antero lingual reentrant) that is lost in early wear. This form is referred to *N. (P.) quadriplicatus*.

The second wood rat from Radec has relatively straight-walled teeth and an M_1 with a dorso-ventrally deep metaflexid. Although similar in occlusal dimensions and crown height to *N. (P.) quadriplicatus* from the same site, this form is referred to *N. (P.) taylori* on the basis of the straight-walled teeth and morphology of the metaflexid. It is slightly smaller than *N. (P.) taylori* from the mid Blancan of southeast Arizona (Tomida, 1987). Because of the small size, the two species of wood rat at the SBCM Radec localities are considered to be ancestral to *N. (P.) taylori* and *N. (P.) quadriplicatus* that occur in the mid Blancan of southeastern Arizona.

Leporidae

The leporids of the Temecula Arkose are represented by a large, less common species and one or possible more abundant small species, all apparently *Hypolagus*. Golz, Jefferson and Kennedy (1977) referred these to *H. regalis* and *H. limnetus*, respectively. We recognize the large species as *H. vetus* and one of the small species as *H. edensis*.

The large species is represented at the Vail Lake locality by a P_3 and at the other localities by fragmentary material. Morphologically, this specimen must be referred to *H. vetus*. Measurements (3.5 x 3.0 mm) of this specimen fall within the large end of *H. vetus* measurements and are near the mean for *H. gidleyi* (White, 1987). White (1987) reexamined the *H. regalis* material and referred it to *H. vetus* because of similarity to specimens from Anza Borrego, California, and Thousand Creek, Nevada. Although *H. vetus* and *H. gidleyi* are similar in P_3 morphology, *H. vetus* appears to be geographically restricted to areas west of the Rocky Mountains in Hemphillian times and to California and Baja California in Blancan times. Its larger relative, *H. gidleyi*, is restricted to New Mexico and Texas in the Hemphillian but reached Washington and Idaho in the Blancan LMA.

P_3s referable to *H. edensis* are present at the Vail Lake and Butterfield localities. All upper teeth in the four localities which can be assigned to a small leporid appear to have uncrenulated hypostria. The association of upper teeth lacking crenulated anterior borders of the reentrants and P_3s referable to *H. edensis* is not unique to the Temecula Arkose localities. The Warren local fauna from the Horned Toad Hills (May, 1982) and the Kern River local fauna in the San Joaquin Valley (Wilson, 1937) are other examples. White (1987) synonymized *Hypolagus edensis* Frick 1921 and *Hypolagus limnetus* Gazin 1934 because both are distinguished from all other species of *Hypolagus* by the presence of a deep and smooth-sided anteroexternal reentrant on the P_3. In *H. limnetus* the interior hypostria on upper molariform teeth is "well crenulated" (Dawson, 1958). The type of *H. edensis* is a fragmentary dentary with P_3-M_1 (Frick, 1921). Regardless of whether or not the upper teeth in question belong to *H. edensis*, as is likely, or to an unnamed species, the generic diagnosis of *Hypolagus* may need to be emended to include varieties lacking crenulations in the upper molariform teeth should this prove to be the case in all stages of wear.

BIOSTRATIGRAPHY

In the Temecula Arkose section between Radec and Vail Lake, Hemphillian holdovers are common. Six Hemphillian taxa appear low in the section at Radec and Shamrock, while only two Hemphillian taxa appear at Butterfield and Vail, higher in the section. The presence of *Cupidinimus bidahociensis* and *Prothomomys warrensis* are significant range extensions.

Blancan rodent indicator species also appear low in the section at Radec and Shamrock. These include *Onychomys gidleyi*, *Neotoma (Paraneotoma) sawrockensis* and *Calomys arizonae*. Their presence

Table 2. Rabbits & rodents from the Temecula Arkose. H=Hemingfordian LMA indicator; B=Blancan LMA taxon

Taxon	Vail	Butterfield	Shamrock	Radec
Hypolagus sp. cf. *H. edensis*	■	■		
Hypolagus sp. (sm)	■	■	■	■
Hypolagus sp. cf. *H. vetus*	■			
Neotoma (Paraneotoma) quadriplicatus (sm)				■
Neotoma (Paraneotoma)? nr. *taylori*				■
N. (P.) sawrockensis	B	B	B	
Prothomomys sp. (lg) cf. *warrensis*	H	H	H	H
Thomomys sp. cf. *T. gidleyi*		B	B	
Thomomys sp. cf. *T. bottae*			■	
Perognathus sp.	■			■
Cupidinimus sp. (lg) cf. *bidahociensis*			H	H
Calomys sp. nr. *gidleyi*	H		H	
Calomys arizonae				B
Copemys vasquezi			H	H
?Copemys				H
Peromyscus valensis			H	H
Sigmodon minor medius				B
Onychomys gidleyi				B
? *Paronychomys* sp.			■	■

suggests that the fauna represents Blancan I and II of Woodburne (1987) and corresponding with Repenning's (1987 and pers. comm. to R.E. Reynolds) assessment of earliest Blancan age, around 4.5 Ma. Because of the diversity of small mammals in addition to the presence of *Equus* (s.l.), *Nannipus* and other large mammals, it holds promise for further biostratigraphic resolution as well as for tephrochronologic and magnetostratigraphic interpretation.

LANDSLIDES

The Oak Mountain landslide complex is described by Hart (1991) as a group of coalescing gabbroic slides 4.8 km wide and 800 m long. It is unusual in the Peninsular Range in that "deep-seated landslides involving large volumes of unweathered gabbroic rocks are rare." (Hart, 1991:349). The landslide complex is exposed along the trace of the Lancaster fault on the north side of Vail Lake Valley. The gabbroic debris apparently came from sources on Oak Mountain, north of the Lancaster fault, and extended south to the vicinity of Vail Dam, blocking the basin. Hart indicates that the Oak Mountain landslide complex overlies and thus is younger than the 4.5 Ma Temecula Arkose. This may indicate that the Lancaster fault has been active within the last 4 million years.

LITERATURE CITED

Baskin, J.A., 1979. Small mammals of the Hemphillian age White Cone local fauna, northeastern Arizona. Journal of Paleontology, 53(3):695-708.

Barnosky, A.D., 1986. New species of the Miocene rodent *Cupidinimus* (Heteromyidae) and some evolutionary relationships within the genus. Journal of Vertebrate Paleontology, 6(1):46-64.

Carleton, M.D. and R.E. Eshelman, 1979. A synopsis of fossil grasshopper mice, genus Onychomys, and their relationships to recent species. University of Michigan Mus. Pale., Papers on Paleontology, 21:1-63.

Czaplewski, N.J., 1987. Sigmodont rodents (Mammalia; Muroidea; Signodontinae) from the Pliocene (Early Blancan) Verde Formation, Arizona. Journal of Vertebrate Paleontology, 7(2):183-199.

___, 1990. The Verde Local Fauna: small vertebrate fossils from the Verde Formation, Arizona. SBCM Assoc. Quarterly, 37(3):1-39.

Dawson, M.R., 1958. Later Tertiary leporidae of North America. University of Kansas Paleontological Contributions: Vertebrata 6:1-75.

Frick, C., 1921. Extinct vertebrate faunas of the badlands of Bautista Creek and San Timoteo Cañon, southern California. Univ. California Publications, Bulletin Dept. Geology, 12(5):277-424.

Gazin, C.L., 1934. Fossil hares from the late Pliocene of southern Idaho. U.S. Nat'l Mus. Proc., 83(2976):111-121.

Golz, D.J., G.T. Jefferson, and M.P. Kennedy, 1977. Late Pliocene vertebrate fossils from the Elsinore fault zone, California. J. Paleo. 51(4):864-866.

Gustafson, E.P., 1978. The vertebrate faunas of the Pliocene Ringold formation, south-central Washington. Mus. Nat. Hist. Univ. Ore., 23:1-62.

Hart, M.W., 1991. Landslides in the Peninsular Ranges, southern California, *in* Geological excursions in southern California and Mexico, M.J. Walawender and B.B. Hanan, eds. Guidebook, 1991 Annual Meeting Geological Society of America, San Diego:372-377.

Jacobs, L.L., 1977. Rodents of the Hemphillian age Redington Local Fauna, San Pedro Valley, Arizona. Journal of Paleontology, 51(3):505-519.

Kennedy, M.P., 1977, Recency and character of faulting along the Elsinore fault zone in southern Riverside County, California. California Division of Mines and Geology Special Report, SR 131:1-12, scale 1:24,000.

Mann, J.D., 1955, Geology of a portion of the Elsinore fault zone, California. California Division of Mines and Geology Special Report, 43:1-22, 2 pls.

Martin, R.A. and R.H. Prince, 1989. A new species of early Pleistocene cotton rat from the Anza-Borrego desert of southern California. Bulletin So. Calif. Acad. Sci., 8(2):80-87.

May, S.R., 1982. Geology and mammalian paleontology of the Horned Toad Hills, Mojave Desert, California. Univ. Calif., Riverside, MA thesis: 290 p.

Repenning, C. A., 1987. Biochronology of the microtine rodents of the United States, pp 236-268, *in* Cenozoic mammals of North America (M.O. Woodburne, ed.) University of California Press:xvi + 336 p.

Reynolds, R.E., 1990. Paleontologic monitoring and salvage, Sycamore Cogeneration Project, Oildale, Kern County, California. Redlands, San Bernardino County Museum, unpubl. technical report SCSC 0213 for Sycamore Cogeneration Company, Bakersfield: 222 p.

Reynolds, R.E. and N.J. Czaplewski, 1989. A Hemphillian LMA fauna from the Kern River formation, California, *in* Abstracts of Papers, 49th Annual Meeting, Society of Vertebrate Paleontology. J.Vert. Paleo, 9(3)36A.

Rogers, T.H., 1965. Geologic map of California, Santa Ana sheet, scale 1:250,000. California Division of Mines and Geology, Regional Map Series.

Tomida, Y., 1987. Small mammal fossils and correlation of continental deposits, Safford and Duncan basins, Arizona, U.S.A. Tokyo, National Science Museum:x-141.

White, R.W., 1937. The Archaeolaginae (Mammalia, Lagomorpha) of North America, excluding *Archaeolagus* and *Panolax*. Journal of Vertebrate Paleontology, 7(4):425-450.

Wilson, R.W., 1933. A recent fauna from Later Cenozoic beds of southwestern Idaho. Contrib. Paleontology, Carnegie Inst. Wash. Publ, 449:117-135.

___, 1937. New middle Pliocene rodent and lagomorph faunas from Oregon and California. Carnegie Inst. Washington Pub., 487:1-19.

Woodburne, M.O., 1987. Cenozoic mammals of North America. Berkeley, University of California Press.

Harlan's Ground Sloth, *Glossotherium harlani*, from Pauba Valley, Riverside County, California

H. GREGORY McDONALD *Hagerman Fossil Beds National Monument, P.O. Box 570, Hagerman ID 83332*

ABSTRACT

Harlan's ground sloth, *Glossotherium harlani*, is reported for the first time from the Pleistocene Pauba formation (Rancholabrean?), Riverside County. Its presence at the Pauba Mesa site in Pauba Valley fits the pattern of other known Late Pleistocene (Rancholabrean) localities for the species in the state. Its distribution was confined primarily to the lowlands and coastal region along the western margin of the state.

INTRODUCTION

Although the best record of the extinct Harlan's ground sloth, *Glossotherium harlani*, is from the asphalt deposits of Rancho La Brea, this species ranged throughout the state of California and is present in many faunas of Rancholabrean age. It is currently known from 61 localities in 26 counties (Table 1). Recent work in the Pauba formation by the staff of the San Bernardino County Museum (SBCM) has resulted in the recovery of a diverse fauna including the first record of this ground sloth from the formation.

LOCALITY AND GEOLOGY

The Pauba Mesa locality is east of Interstate 15 between Pauba Road and Highway 79 that runs through Pauba Valley east of Temecula, in sections 8 and 9, T.8S R.2W, SBB&M (Pechanga 7.5' quad, Riverside County). The *Glossotherium* was recovered from two localities, SBCM 05.006.390 and SBCM 05.006.391, about 1/4 mile apart. This places it in the Elsinore fault zone southeast of Temecula.

The Pauba formation consists of fine-grained silty sands. It unconformably overlies an unnamed sandstone and lies below Pleistocene old alluvium.

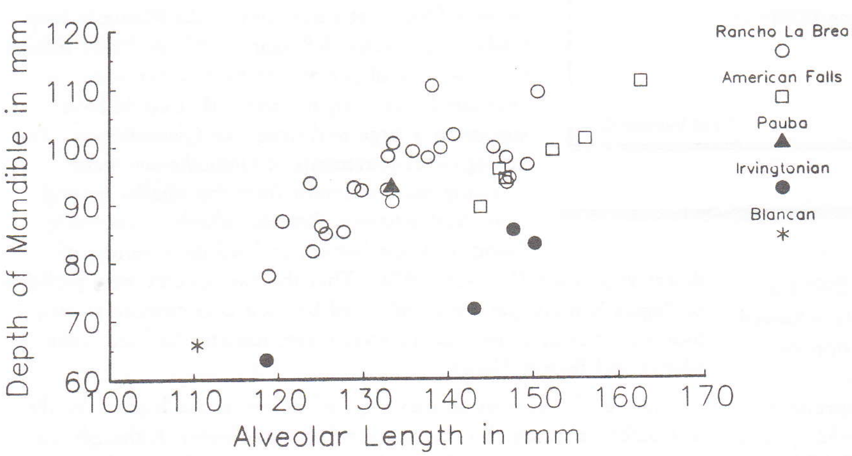

Figure 1. Scatter diagram showing relationship of depth of mandible and alveolar length of the mandible in *Glossotherium harlani*.

MATERIAL

Two individuals of *Glossotherium harlani* from the Pauba Mesa locality were recovered, represented by the following specimens:

SBCM 05.006.390
- SBCM A2658-1, ventral portion of skull
- SBCM A2658-6, right mandible
- SBCM A2658-4, right ulna
- SBCM A2658-2, right femur
- SBCM A2658-3, left pelvis half

SBCM 05.006.391
- SBCM A2658-5, complete mandible

Although not closely associated, the material from SBCM 05.006.390 appears to represent one individual; the second individual is represented by the mandible from SBCM 05.006.391. All material is housed in the vertebrate paleontology collections of the San Bernardino County Museum.

AGE OF THE FAUNA

The Pauba Fauna includes one species of land snail, one species of fish, a toad, pond turtle, two species of snake, two rabbits, a shrew, six rodent species, two species of horse, deer, pronghorn, llama, camel, mastodon and mammoth (Reynolds and Reynolds, 1990; Reynolds, Reynolds and Pajak, 1991). *Glossotherium harlani* can now be added to this diverse assemblage. A Late Irvingtonian to Early Rancholabrean age for the fauna was postulated by Reynolds and Reynolds (1990) based on the presence of *Microtus californicus* and *Mammuthus* sp. cf. *M. imperator*.

McDonald (in press) has documented the size increase in *Glossotherium* from the Blancan to the Rancholabrean and based on this trend in size and changes in mandibular proportions has suggested that the approximate age of a fauna can be determined. Measurements of the Pauba Mesa *Glossotherium harlani* were compared to those of individuals of *G. harlani* from the early Irvingtonian Leisey Site 1A Florida (1.7±0.35 myr, Webb and others, 1989) and individuals from American Falls Reservoir, Idaho (ca. 100,000 yr BP) and Rancho La Brea (>40,000 yr BP) (Fig. 1). The mandible from the Pauba Mesa specimen falls into the size range and proportions of the late Rancholabrean sample from Rancho La Brea rather than the earlier and smaller Irvingtonian population. Based on these criteria a younger age for

Table I. Rancholabrean LMA occurrences of *Glossotherium* in California, arranged by county. USNM=U.S. National Museum; LACM=Los Angeles County Museum of Natural History

Alameda
Alameda Canal (Jefferson 1991)
Alameda Tube Excavation (Jefferson 1991)
Delta Mendota (Jefferson 1991)
Doolan Canyon (Jefferson 1991)
Oakland Coliseum (Jefferson 1991)
Rodeo Station #2 (Jefferson 1991)
Rodeo Station #1 (Harris 1985)
Shattuck Ave #1 (Jefferson 1991)

Contra Costa
Alamo Creek #2 (Jefferson 1991)
Antioch #2-3 (Savage 1951)
Bulls Head (Savage 1951)
Cameo Acres (Jefferson 1991)
Hwy 40 #1 (Jefferson 1991)
Hipparion Point #2 (Jefferson 1991)
Martinez (Stock 1925)

El Dorado
Hawver Cave (Stock 1918)

Kern
Maricopa (LACM collections)
McKittrick (Stock 1925)

Kings
Dudley Ridge (Jefferson 1991)
Tulare Lake (Harris 1985)

Los Angeles
Century Blvd/Van Ness (Jefferson 1991)
Harbor Fwy & 112-113th (Jefferson 1991)
La Brea & San Vicente (Jefferson 1991)
Los Angeles Brick Yard (Jefferson 1991)
L.A. Harbor Berth 128 (Miller, 1971)
Naval Housing Unit (Jefferson 1991)
Palos Verdes Hills (Langenwalter 1975)
Rancho La Brea (Jefferson 1991)
San Fernando Dam (Jefferson 1991)
Woodland Hills (Jefferson 1991)

Marin
Hamlet Station (Jefferson 1991)

Merced
Merced River #1 (Jefferson 1991)

Orange
Bolsa Chica State Park (Jefferson 1991*)
Costeau Pit (Miller 1971)
Imperial Hwy La Habra (Miller 1971)
Salt Creek Labuna Niguel (Jefferson 1991)
San Clemente (Jefferson 1991)

Riverside
Carbon Cnyn Wastewater, Chino (Reynolds & Reynolds 1991)
Pauba Mesa (this paper)

Sacramento
Sac'to Sports Stadium (Jefferson 1991)
Teichert Gravel Pit (Harris 1985)

San Bernardino
Lake Manix (Jefferson 1987)

San Francisco
Twin Peaks Tunnel (Stock 1925)
Pacific St. San Francisco (Stock 1925)

San Luis Obispo
Diablo Canyon (Jefferson 1991)
Pecho Creek (Jefferson 1991)

San Mateo
Mussel Rock #2 (Savage 1951)

Santa Barbara
Los Alamos (Jefferson 1991)
Point Concepcion (Stock 1925)
Point Sal (Jefferson 1991)

Santa Clara
Mountain View Dump (Jefferson 1991)
Vet Hosp Matadero Cr (Jefferson 1991)

Santa Maria
Lompoc-Vandenburg (USNM humerus cast)

Siskiyou
Yreka (Jefferson 1991)

Solano
Suisun Slough (Jefferson 1991)

Sonoma
McGrew's Ranch, Petaluma (Savage 1951)
Crandall (Jefferson 1991)
Petaluma (Stock 1925)

Stanislaus
Brant Ranch (Jefferson 1991)

Ventura
Brea Canyon, Simi (Jefferson 1991)

Yolo
Steven's Creek Bridge (Jefferson 1991)

Yuba
Marysville (Stock 1925)

* not Ventura Co.

the fauna than that postulated by Reynolds and Reynolds (1990) is suggested. However, it is possible that *G. harlani* had already achieved its maximum size by the Irvingtonian-Rancholabrean transition ca. 500,000 yrs BP. As can be seen from Figure 1, specimens from American Falls Reservoir, Idaho fall into the size range of specimens from Rancho La Brea. Recent work by Scott and others (1982) places the age of the American Falls Fauna around 100,000 yrs BP. This suggests that it may not be possible to distinguish between early and late Rancholabrean individuals using size as the only criteria. This pattern may be further complicated by a positive Bergman's response in *Glossotherium*. As can be seen in Figure 1, individuals from the more northern American Falls fauna tend to be larger than those found at Rancho La Brea. Additional samples of *Glossotherium* from localities of known age will be required to improve the resolution of this technique and to determine when *Glossotherium harlani* achieved its maximum size and the relationship of that size to geography.

More important are the relative dimensions of the alveolar length of the mandible and the depth of the ramus. The depth of the ramus in Irvingtonian specimens of *Glossotherium* is relatively shallower than in Rancholabrean specimens. In this respect the Pauba specimen more closely resembles individuals from Rancho La Brea than specimens of Irvingtonian age.

Recent C^{14} analysis on a peat layer apparently located below the Pauba Mesa fauna provides two dates: 33,470±710 YBP (Beta 89730) and >40,300 YBP (Beta 39731) (Beta Analytic, October 1990). These dates are consistent with a late Rancholabrean LMA implied by the morphometrics of the *Glossotherium*.

DISTRIBUTION OF *GLOSSOTHERIUM* IN CALIFORNIA

Although *Glossotherium* is widely distributed latitudinally in California and its range extends into the surrounding states of Oregon, Nevada and Arizona, the greatest concentration of sites in California are coastal or in lowlands near the coast (Figure 2). The Pauba Mesa record fits this pattern. *Glossotherium* was also reported from the Carbon Canyon Wastewater Facility, Chino, San Bernardino County by Reynolds, Reynolds and Pajak (1991). The specimen this record is based upon is the distal end of a right femur (SBCM A2362-1).

Stock (1925) considered *Glossotherium* to be indicative of grassland and open habitat and the species distribution within the state seems to fit Stock's interpretation. Even the one record from the Mojave Desert, at Pleistocene Lake Manix (Camp Cady Local Fauna, Jefferson, 1987) probably reflects the existence of permanent fresh water and associated lake margin habitat that could have supported a large herbivore like *Glossotherium*. The ecological requirements of *Glossotherium* were certainly quite different from the smaller ground sloth *Nothrotheriops shastense* which is commonly found in desert habitat and fed on a variety of desert vegetation (Hansen, 1978). That the two species were probably ecologically incompatible is indicated by their cooccurence at only four localities in California: Hawver Cave, Rancho La Brea, Lake Manix and Suisun Slough.

Hawver Cave, with an elevation of 393 m, is the highest locality in California at which *Glossotherium* has been found. Although the highest elevational record for *Glossotherium* in California, this locality is still low topographically compared to much of the eastern portion of the state. Despite the apparent restriction of *Glossotherium* to lower elevations in California, it has been found at higher elevations in other states. It is known from American Falls Reservoir, Idaho at

1340 m and Silver Creek, Utah, the highest known locality with *Glossotherium*, at an elevation of 1950 m. However, both the Idaho and Utah localities are considered to be Sangamon in age and the presence of *Glossotherium* at higher elevations during an interglacial may reflect either a milder temperature regime that facilitated an elevational expansion of its range or the expansion of suitable habitat to higher elevations.

SUMMARY

The recent recovery of *Glossotherium harlani* from the Pauba formation expands our knowledge of the diversity of the fauna. *Glossotherium* increases in size from the Blancan to the Rancholabrean and the Pauba Mesa *Glossotherium* is consistent in size with late Rancholabrean populations, such as at Rancho La Brea. However, samples of *Glossotherium harlani* from the earlier American Falls fauna indicates *Glossotherium* had already reached its maximum size by this time. Larger samples from sites of known age are required to refine this approach.

Glossotherium harlani is known from more localities of Rancholabrean age in California than either *Nothrotheriops shastense* or *Megalonyx jeffersonii*. These localities are concentrated along the western margin of the state in the lowlands and near the coast and probably reflect the distribution of grasslands and open habitat during the late Pleistocene.

ACKNOWLEDGEMENTS

I would like to thank Bob Reynolds of the San Bernardino County Museum who suggested this project, provided access to the specimens and supported it in numerous ways.

REFERENCES CITED

Jefferson, G.T., 1987. The Camp Cady Local Fauna: paleoenvironment of the Lake Manix Basin. San Bernardino County Museum Association Quarterly, 34(3,4):3-35.

___, 1991. A catalogue of late Quaternary vertebrates from California: part two, mammals. Natural History Museum Los Angeles County Technical Reports, 7:129 p.

Hansen, R.M., 1978. Shasta ground sloth food habits, Rampart Cave, Arizona. Paleobiology, 4:302-319.

Harris, A.H., 1985. Late Pleistocene vertebrate paleoecology of the west. Austin, University of Texas Press: 293 p.

Langenwalter, P.E., 1975. Chordates: the fossil vertebrates of the Los Angeles and Long Beach harbors, Los Angeles County, California. Marine studies of San Pedro Bay, California, part 9, Paleontology, D.F. Soule and M. Oguri, eds. Allan Hancock Foundation and Sea Grants Programs, University of Southern California, publication USC-SG-4-75:36-54.

McDonald, H.G. (in press). Gravigrade Xenarthrans from the Middle Pleistocene Seisey Shell Pit 1A, Hillsborough County, Florida. Bulletin of the Florida Museum of Natural History.

Miller, W.E., 1971. Pleistocene vertebrates of the Los Angeles basin and vicinity (exclusive of Rancho La Brea). Los Angeles County Museum Science Series, 10: 124 p.

Reynolds, R.E. and R.L. Reynolds, 1990. Irvingtonian? faunas from the Pauba formation, Temecula, Riverside County, California. Abstracts of proceedings, 1990 Mojave Desert Quaternary Research Symposium, Redlands, J. Reynolds, ed. San Bernardino County Museum Association Quarterly, 37(2):37.

___, 1991. The Pleistocene beneath our feet: near-surface Pleistocene fossils in inland southern California basins. San Bernardino County Museum Association Quarterly, 38(3,4):41-43.

Reynolds, R.E., R.L. Reynolds and A.F. Pajak III, 1991. Blancan, Irvingtonian, and Rancholabrean(?) land mammal age faunas from western Riverside County, California. San Bernardino County Museum Association Quarterly, 38(3,4):37-40.

Savage, D.E., 1951. Late Cenozoic vertebrates of the San Francisco Bay region. University of California Publications, Bulletin of the Department of Geological Sciences, 28(10):215-314.

Scott, W.E., K.L. Pierce, J.P. Bradbury and R.M. Forester, 1982. Revised Quaternary stratigraphy and chronology in the American Falls area, southeastern Idaho, *in* Cenozoic geology of Idaho, B. Bonnichsen and R.M. Breckenridge, eds. Idaho Bureau of Mines and Geology Bulletin, 27:581-595.

Stock, C., 1918. The Pleistocene fauna of Hawver Cave. University of California Publications, Bulletin of the Department of Geological Sciences, 10(24):461-515.

___, 1925. Cenozoic gravigrade edentates of western North America with special reference to the Pleistocene Megalonychinae and Mylodontidae of Rancho La Brea. Carnegie Institue of Washington Publications, 331: 206 p.

Webb, S.D., G.S. Morgan, R.C. Hulbert Jr., D.S. Jones, B.J. MacFadden and P.A. Mueller, 1989. Geochronology of a rich Early Pleistocene vertebrate fauna, Leisey Shell Pit, Tampa Bay, Florida. Quaternary Research, 32:96-110.

Refined Chronologic Resolution of the San Timoteo Badlands, Riverside County, California, and Tectonic Implications: A Prospectus

L. BARRY ALBRIGHT and MICHAEL O. WOODBURNE, *Department of Earth Sciences, University of California, Riverside CA 92521*

INTRODUCTION

The San Timoteo Badlands, in Riverside County, California, includes a thick sequence of Plio-Pleistocene non-marine sedimentary rocks. These deposits are ideally situated both spatially and temporally for refined geochronological studies relating to slip history along strands of the San Andreas fault system and uplift initiation of the eastern Transverse Range. Over the next few years, personnel from the University of California, Riverside, the San Bernardino County Museum, the University of Florida, and the United States Geological Survey will join in a combined effort to fully characterize the stratigraphy of the Badlands sequence in an attempt to accurately date the tectonic, sedimentologic, and biologic phenomena recorded within these deposits. Detailed geologic mapping and precise stratigraphic control of the vertebrate fossils contained within should permit the development of a refined biostratigraphy. The biostratigraphy, when coupled with the local magnetic polarity signature, can be correlated to the Magnetic Polarity Time Scale to provide a high resolution chronologic framework. Radioisotopic data will be included to provide additional age control provided datable tuffaceous horizons can be located. The project, therefore, plans to set into motion a point recognized by Reynolds and Reeder (1986)—that a refined temporal framework of the San Timoteo Badlands will provide a data base allowing detailed evaluation of various physical phenomena that occurred in the region during the time the sediments are thought to have been deposited.

BACKGROUND

Geology

The San Timoteo Badlands include approximately 12,000 feet of continental sedimentary rocks that have been folded into a shallow, northwest-plunging anticline as a result of their position between the San Bernardino Mountain segment of the San Andreas fault to the northeast and the San Jacinto fault to the southwest. The stratigraphically lowest sedimentary rocks include reddish, coarse-grained arkosic sandstones with clasts indicating derivation from Peninsular Range Province basement highs such as Mount Eden (Matti and Morton, 1975). These beds have variably been referred to as the Potrero Creek deposits (Frick, 1921), the Red Bed Member of the Mt. Eden Formation (Fraser, 1931), the Jackrabbit Sandstone plus the "lower member of the Mt. Eden Formation" (English, 1953), and "unit 1" (Matti and Morton, 1975; Rees and others, 1987) (Fig. 1). Overlying this arkose is the Mt. Eden Formation which includes a lower calcareous siltstone member with prominent limestone horizons, a middle layer of dark shales, and a well indurated, laminated, fine-grained sandstone member with soft sediment structures and ripple marks. This unit includes the Middle and Upper Members of the Mt. Eden Formation of English (1953); Unit 2 of Matti and Morton (19750; and Units 2 and 3 of Rees and others (1987). The Mt. Eden Formation is likely lacustrine in origin. Beginning above this unit are the fluviatile deposits of the San Timoteo Formation. The San Timoteo Formation, as used here, is equivalent to Matti and Morton's (1975) Units 3 and 4, and to Unit 4 of Rees and others (1987). Alternating beds of sandstones, conglomerates, and reddish-brown paleosols with distinct pedogenic carbonate horizons characterize this unit. Clast composition indicates derivation from the Transverse Ranges tectonic province (Matti and Morton, 1975). The boundary between the Mt. Eden and San Timoteo formations represents the transition from subaqueous to subaerial basin infilling. Excellent exposures perpendicular to the axis of the anticline occur along the Jack Rabbit Trail and Route 60.

Paleontology

In 1916-1917, Childs Frick launched a paleontological reconnaissance of the San Timoteo Badlands as part of an extensive University of California study on the "geologic and faunal history of the Pacific coast. . . " (Frick, 1921:279). In this early study of the San Timoteo Badlands, numerous vertebrate fossils were collected from several localities; Frick determined that they were of Pliocene age. Very few subsequent paleontological studies have been conducted and no attempts have been made to develop a detailed chronostratigraphic characterization of the two recognized formations. May and Repenning (1982) were the first to apply modern geochronologic tools there, noting the importance of the deposits insofar as they could provide a temporal framework for the timing of San Andreas slip histories and Transverse Range uplift. They concluded that the fauna from the lower unit of the Badlands sequence, the Mt. Eden Formation, was between 5.4 and 5.0 m.y. based on the stage of evolution of a microtine rodent coupled with the paleomagnetic signature of the sediments from which the rodent fossils were recovered. Reynolds and Reeder (1991) provided a general overview of the lithology, structure, and paleontology of the Badlands, and added further constraints on the age of the sequence. Based on mammal fossils from three local faunas found in the upper part of the San Timoteo Formation, Reynolds and Reeder (1991) concluded that deposition continued until approximately 1.3 Ma. A faunal list of these three local faunas (El Casco, Shutt Ranch, and Olive Dell) was also provided. The above studies indicate that the deposits of the San Timoteo Badlands are amenable to both biostratigraphic and magnetostratigraphic analysis.

SIGNIFICANCE

The report of microtine rodent fossils by May and Repenning (1982) and Reynolds and Reeder (1991) is particularly encouraging with respect to the development of a high resolution biostratigraphy for the San Timoteo Badlands. Such development is probable because microtine rodents are both fast evolving and geographically widespread—two necessary criteria for the construction and correlation of such a biostratigraphic scheme. More importantly, the San Timoteo Badlands sequence spans an interval of time over which

Figure 1. Stratigraphic divisions in the San Timoteo badlands

<table>
<tr><th>Frick (1921)</th><th>Fraser (1931)</th><th colspan="2">English (1953)</th><th>Matti & Morton (1975)</th><th>Rees et. al. (1987)</th></tr>
<tr><td rowspan="2">SAN TIMOTEO FM</td><td rowspan="4">MT. EDEN FM</td><td colspan="2" rowspan="2">SAN TIMOTEO FM</td><td>UNIT 4</td><td rowspan="2">UNIT 4</td></tr>
<tr><td>UNIT 3</td></tr>
<tr><td rowspan="2">EDEN FM</td><td rowspan="3">MT. EDEN FM</td><td>Upr Mbr</td><td rowspan="2">UNIT 2</td><td>UNIT 3</td></tr>
<tr><td>Mdl Mbr</td><td>UNIT 2</td></tr>
<tr><td rowspan="2">POTRERO CREEK DEPOSITS</td><td rowspan="2">RED BED MEMBER</td><td>Lwr Mbr</td><td rowspan="2">UNIT 1</td><td rowspan="2">UNIT 1</td></tr>
<tr><td colspan="2">JACKRABBIT SANDSTONE</td></tr>
</table>

these rodents rapidly diversified, and over which a number of important allochthonous immigrations were recorded (Repenning, 1987). Utilizing these "events," Repenning (1987) defined a total of ten mammal ages extending over the last six million years. He was also able to calibrate many of these events using K-Ar dates, magnetic polarity reversals, tephrochronology, and climatic interpretations. The power of such a a biochronology is in the resolution attainable.

> With a diagnostic fossil microtine fauna it is possible to tell time at any point in the last 5 Ma [in North America] with a minimum precision of 270,000 years. This, coupled with a minimal paleomagnetic determination, can easily reduce the uncertainty to 150,000 years (Repenning, 1987:252).

Thus, an age interpretation based on microtine rodent faunas can provide a more accurate age estimate than can a K-Ar date, given the analytical precision of the latter. The paucity of potentially radioisotopically datable tuffaceous horizons (preliminary field reconnaissance has failed to locate volcanic tuffs of the quality necessary for radioisotopic analysis) should, therefore, pose no problem for the construction of an accurate and precise chronologic framework with which regional biologic and geologic hypotheses can be tested. Particular emphasis, therefore, will be placed on locating sites in the field which harbor the greatest potential for recovering rodent remains. Previous workers (R. Reynolds, perc. comm. 1992) have determined that paleosols are just such high potential horizons and, fortunately, the San Timoteo Badlands are punctuated with many.

The sediments of the San Timoteo Badlands were deposited during a critical interval of time with respect to the tectonic history of southern California. They also span nearly all of the time over which Repenning's (1987) rodent ages extend. They are immedately adjacent to the San Bernardino Mountains which were rising during this period, but they include a variety of rock types that indicate the basin was filled from additional sources. Furthermore, they occur in the only exposed depositional basin strategically located between the San Bernardino Mountain segment of the San Andreas fault and the San Jacinto fault strand of the San Andreas fault system. Recent studies on stress changes caused by the June, 1992 Landers and Big Bear earthquakes indicate that these two fault strands now constitute the most dangerous segments of the San Andreas fault system in southern California (Jaumé and Sykes, 1992; Stein and others, 1992). Therefore, the development of a high resolution biostratigraphic and magnetostratigraphic framework for the Badlands will permit precise definition of past tectonic events of the region and it will provide for a comparison of the timing of faunal changes in other stratigraphic sections of similar age in the southwestern United States.

REFERENCES CITED

English, H.D., 1953. The geology of the San Timoteo Badlands, Riverside County, California. Unpublished Masters Tehsis, the Claremont Graduate School: 99 p.

Fraser, D.M., 1931. Geology of the San Jacinto quadrangle. California Journal of Mines and Geology, 27(4):494-540.

Frick, C., 1921. Extince vertebrate faunas of the badlands of Bautista Creek and San Timoteo Canon, southern California. University of California Publications, Bulletin of the Department of Geology, 12(5):277-424.

Jaumé, S.C. and L.R. Sykes, 1992. Changes in state of stress on the southern San Andreas fault resulting from the California earthquake sequence of April to June 1992. Science, 258:1325-1328.

May, S.R. and C.A. Repenning, 1982. New evidence for the age of the Mount Eden fauna, southern California. Journal of Vertebrate Paleontology, 2(1):109-113.

Matti, J.C. and D.M. Morton, 1976. Geologic history of the San Timoteo Badlands, southern California. Geological Society of America, Abstracts with Programs, 7(3):344.

Rees, R. M. Sullivan, G. Van and P. Sadler, 1987. Preliminary investigation of the lithostratigraphy of the southeastern San Timoteo Badlands, Riverside Co., S. California. GSC 120 Report, University of California, Riverside, Department of Earth Sciences: 16 p.

Repenning, C.A., 1987. Biochronology of the microtine rodents of the United States, *in* Cenozoic mammals of North America: geochronology and biostratigraphy, M.O. Woodburne (ed). Berkeley, University of California Press:236-268.

Reynolds, R.E. and W.A. Reeder, 1986. Age and fossil assemblages of the San Timoteo Formation, Riverside County, California, *in* Geology around the margins of the eastern San Bernardino Mountains, M.A. Kooser and R.E. Reynolds (eds). Publications of the Inland Geological Society, 1.

___. 1991. The San Timoteo Formation, Riverside County, California, *in* Inland Southern California: the last 70 million years, M.O. Woodburne, R.E. Reynolds and D.P. Whistler (eds). Redlands, San Bernardino County Museum Association Quarterly, 38(3,4):44-48.

Stein, R.S., G.C.P. King and J. Lin, 1992. Change in failture stress on the southern San Andreas fault system caused by the 1992 Magnitude=7.4 Landers earthquake. Science, 258:1328-1332.

Soil Development in the Northern Part of the San Timoteo Badlands, San Bernardino and Riverside Counties, California

K. L. KENDRICK *Dept. of Earth Sciences, University of California, Riverside CA 92521*
L.D. McFADDEN *Dept. of Geology, University of New Mexico, Albuquerque NM 87131*
D.M. MORTON *U.S. Geological Survey, University of California, Riverside CA 92521*

ABSTRACT

The degree of soil development associated with geomorphic surfaces in San Timoteo and Reche Canyons near the San Jacinto fault in the San Timoteo badlands is comparable to that of nearby, dated soils and allows correlation of the surfaces. Twenty soil profiles have been described and sampled, including four surface soils and two buried soils associated with surfaces in San Timoteo Canyon (Q1-Q4), and two surface soils associated with two surfaces in Reche Canyon (Q2, Q3). Soil development indices based on field descriptions, as well as laboratory analysis provide a basis for comparison of these soils to each other and to dated chronosequences at Cajon Pass, Merced and Anza.

The soils in the San Timoteo badlands region record a complex tectonic and climatic history. Evidence for this includes the presence of buried soils, the tilting and warping of both buried and surface soils, calcium carbonate coatings on manganese oxide and clay films, and the presence of silica cementation of soils in Reche Canyon, but not in the adjacent San Timoteo Canyon. The San Timoteo badlands include preserved surfaces intermediate in soil development to those at Cajon Pass, and do not preserve a record of the major Late Pleistocene to Early Holocene aggradational event observed elsewhere in the region.

In spite of the variability of the surfaces in the study area, soil development is similar to that of soils at other sites. With time the profiles develop progressively thicker argillic horizons, and increase in soil rubification, total mass of clay and crystalline iron oxides, and

Figure 1. An aerial view to the north in San Timoteo Canyon. Surface Q1 is visible on the left side of the photo, near the top. Surface Q2 is centered in the photo, and Q3 is in the upper part, on the right side. ***Photo by Carol Prentice, U.S.G.S.***

content and thickness of clay films. The composition and content of iron species in soils of the San Timoteo study area are similar to nearby sites, including the Cajon Pass chronosequence (McFadden and Weldon, 1987), Little Tujunga Canyon, Arroyo Seco Canyon, San Gabriel River, Day Canyon, Duncan Canyon, and the San Gorgonio Wash (McFadden, 1982; McFadden and Hendricks, 1985).

With increasing soil age, there is an increase in the ratio of dithionite-extractable iron to total iron, a decrease in the ratio of ferrous to ferric iron, and a decrease in the ratio of oxalate- to dithionite-extractable iron, though all these trends are more subdued in the San Timoteo study area than elsewhere in the region. These patterns suggest that the slightly lower precipitation in the San Timoteo badlands may be responsible for decreased silica leaching, and increased formation of more poorly crystalline iron species. The higher silica activity could also be responsible for a slower transformation of ferrihydrite to hematite, and the shift in the maximum content of oxalate-extractable iron towards older soils.

Weighted means of soil development indices and rubification index values are used to compare the soils of this study to those at Cajon Pass, Merced and Anza. A wide range of age estimates are determined using the maximum limits of these values, and result in 27.5–305 ka for Q1, 67–570 ka for Q2, and 305-700 ka for Q3 and Q4. Best estimates of age are determined by directly correlating soils with the same degree of soil development between this study and the closest dated chronosequence, Cajon Pass. This method constrains the time of formation of the Q1 surface to between 27.5–67 ka and the Q2 surface to 43–67 ka, and does not change the age estimates of the older surfaces.

Distinctive clast assemblages, identified by Morton and Matti (1993), are present along a limited section on the northeast side of the San Jacinto fault, and are preserved on two surfaces within Reche Canyon, on the southwest side of the fault. Subsequent displacement along the fault has resulted in offsets of approximately 1 and 4 km (Morton and Matti, 1993). Age estimates based on comparisons of soil development allow us to better constrain these offsets, with resulting slip rates of 7–13 mm/yr since the formation of Q3, and 13–26 mm/yr since the formation of Q2.

REFERENCES CITED

McFadden, L.D., 1982. The impacts of temproal and spatial climatic changes on alluvial soils genesis in southern California. PhD thesis, University of Arizona Dept. Geosciences: 430 p.

McFadden, L.D. and D.M. Hendricks, 1985. Changes in the content and composition of pedogenic iron oxyhydroxides in a chronosequence of soils in southern California. Quaternary Research, 23:189-204.

McFadde., L.D. and R.J. Weldon, 1987. Rates and processes of soil development in Cajon Pass, California. Geological Society of America Bulletin, 98: 280-293.

Morton, D.M. and J.C. Matti, 1993. Tectonic synopsis of the San Gorgonio Pass and San Timoteo Badlands areas, southern California. Redlands, San Bernardino County Museum Association Quarterly, 40(2):3-14.

SAN BERNARDINO COUNTY MUSEUM ASSOCIATION
INFORMATION FOR AUTHORS

The San Bernardino County Museum Association publishes articles and monographs on subjects pertaining to the cultural and natural history of San Bernardino County and surrounding regions. We welcome submissions of such manuscripts.

Subject Matter: articles and monographs pertaining to San Bernardino County, inland Southern California, and surrounding regions, in history, anthropology, archaeology, paleontology, mineralogy, zoology, botany, ornithology, and related disciplines. Manuscripts considered for *Quarterly* publication should be written toward the well-educated non-specialist. Technical research will also be considered for publication. All manuscripts should reflect original work which furthers knowledge in their fields.

Format: Two clear copies of the manuscript must be submitted to the Editorial Board with a letter of transmittal requesting that the manuscript be considered for publication and that it is not presently under consideration elsewhere. Manuscripts should be typewritten, double-spaced, on one side only of 8.5x11" paper. Ample margins should be allowed for editing comments. The first page should contain the title and author(s) name, address, and telephone number. The author's last name and page number should appear at the top of each following page. Include COPIES of figures, tables, and photographs. Do not send original photographs or figures with your initial submission.

Style: Authors should follow the standards for footnotes, citations, headings, and other conventions as applicable to their discipline. The Editorial Board suggests the following:

Anthropology/Archaeology: Society of American Archaeology *(American Antiquity)*
History: American Historical Association *(American Historical Review)*
Geology: Geological Society of America (GSA *Bulletin)*
Paleontology: Society of Vertebrate Paleontology *(Journal)*
Biological Sciences: American Institute of Biological Sciences (eg. *Journal of Entomology)*

Authors should be aware of and avoid inappropriate gender-biased language. The Editor is available for consultation on matters of style, format, and procedures.

Review: Manuscripts will be considered by the Editorial Board of the Museum Association Publications Committee, and will be reviewed by outside experts. Manuscripts may be accepted, provisionally accepted, or be found unsuitable for publication by the Association. Provisional acceptance may include suggestions for revisions. Very lengthy or profusely-illustrated monographs that are otherwise acceptable for publication may require outside funding to help defray publishing costs. Manuscripts will be copy edited after acceptance.

Attachments: Original or equivalent photographs will be required for publication. Photographs should be black-and-white, glossy finish, of good quality and contrast. Figures and drawings should be in India ink or equivalent on white paper or film; PMT's are acceptable. Captions should be submitted on separate pages, double-spaced, and referenced to their accompanying figures. Photographs should be marked lightly in pencil on the back border with the author's name and figure number. Authors are encouraged to submit accepted manuscripts on DOS-compatible disks in addition to paper copy.

Responsibilities: The author has the primary responsibility for the correctness and reasonableness of his or her information, arguments, and presentation. In submitting a manuscript for consideration, the author assures the Editorial Board that the manuscript is an original work and does not infringe upon the rights of previous authors or publishers.

Address queries and manuscripts to:
The Editor
San Bernardino County Museum Association
2024 Orange Tree Lane, Redlands CA 92374

San Bernardino County Museum Association
2024 Orange Tree Lane
Redlands, California 92374

BULK RATE
U.S. POSTAGE
PAID
Permit No. 1677
San Bernardino, CA